

Power Generation Assets

Energy Constraints, Upper Bounds and Hedging Strategies

DISSERTATION

zur Erlangung des akademischen Grades

doctor rerum politicarum

(Dr. rer. pol.)

im Fach Wirtschaftswissenschaften

eingereicht an der

Wirtschaftswissenschaftlichen Fakultät

Humboldt Universität zu Berlin

von

Herr Dipl. Wi.-Ing. Thomas Enge

geboren am 18.06.1976 in Frankfurt am Main

Präsident der Humboldt Universität zu Berlin:

Prof. Dr. Dr. h.c. Christoph Marksches

Dekan der Wirtschaftswissenschaftlichen Fakultät:

Prof. Oliver Günther, Ph.D.

Gutachter:

1. Prof. Dr. Kurt Helmes

2. Prof. Dr. Andreas Brandt

eingereicht am: 30.06.2010

Tag der mündlichen Prüfung: 20.09.2010

Abstract

The overall topic of this thesis is the valuation of power generation assets under energy and risk constraints. Our focus is on the modeling aspect i.e. to find the right balance between accuracy and computational feasibility. We define a new not yet investigated unit commitment problem that introduces an energy constraint to a thermal power plant. We define a continuous stochastic dynamic program with a nested mixed integer program (MIP). We introduce a fast implementation approach by replacing the MIP with an efficient matrix calculation and use principal component analysis to reduce the number of risk factors. We also provide a fast heuristic valuation approach for comparison. As both models can only provide lower bounds of the asset value, we investigate the theory of upper bounds for a proper validation of our power plant results. We review the primal dual algorithm for swing options by Meinshausen and Hambly and in particular clarify their notation and implementation. Then we provide an extension for swing options with multiple exercises at the same stage that we developed together with Prof. Bender, University of Braunschweig. We outline Prof. Bender's proof and describe the implementation in detail. Finally we provide a risk analysis for our thermal power plant. In particular we investigate strategies to reduce spot price risk to which power plants are significantly exposed. First, we focus on the measurement of spot price risk and propose three appropriate risk figures (*Forward delta* as opposed to Futures delta, *synthetic spot delta* and *Earnings-at-Risk*) and illustrate their application using a business case. Second we suggest risk mitigation strategies for both periods, *before* and *in* delivery. The latter tries to alter the dispatch policy i.e. pick less risky hours and accept a (desirably only slightly) smaller return. We introduce a benchmark that weighs risk versus return and that we will call *EaR-efficient* option value. We propose a mitigation strategy for this benchmark that is based on quantile regression. It defines a price interval for executing an individual swing right and is therefore very well suited for real world applications. In case of an American option we are able to show EaR-efficiency of our strategy in particular for a changing risk profile of the underlying price (altering volatility). Finally, we investigate hedging strategies before the delivery period as a function of the maximum available energy. In particular, we look at a hedge for the spot price risk of the power plant using a swing option. We propose a heuristic based on our synthetic spot deltas to find the relevant parameters of the swing option (number of swing rights and swing size) for a given upper generation amount.

Zusammenfassung

Wir betrachten die Einsatzplanung (Unit Commitment Problem) für ein thermisches Kraftwerk mit zusätzlicher Energieebenenbedingung. Dazu definieren wir ein stochastisches dynamisches Programm (SDP) mit stetigem Zustandsraum und integriertem gemischt-ganzzahligem Programm (MIP). Wir stellen einen effizienten Algorithmus vor zur Lösung des MIP über eine Matrixmultiplikation und verwenden eine Hauptkomponentenanalyse zur Reduzierung der Dimension des Preisvektors. Außerdem liefern wir zum Vergleich des SDP eine vereinfachte Regel zur Energieallokation. Zur Beurteilung der Güte der Ergebnisse betrachten wir als nächstes obere Grenzen. Für eine vereinfachte Modellierung des Kraftwerks als Swing Option mit Mehrfachausübung auf derselben Stufe bestimmen wir formal eine solche obere Grenze. Abschließend untersuchen wir Strategien zur Vermeidung des Spotpreisrisikos, dem das Kraftwerk aufgrund der Nichtspeicherbarkeit von Strom besonders ausgesetzt ist. Zunächst konzentrieren wir uns auf die Messung des Spotpreisrisikos und stellen drei neue Maße vor (Forward Delta, Synthetisches Spot Delta und Earnings-at-Risk). Danach präsentieren wir Strategien zur Risikoreduzierung vor und während der Lieferperiode. Im zweiten Fall wird versucht, durch einen neuen Produktionsplan das Risiko mehr als den Gewinn zu senken. Wir schlagen dazu einen Referenzwert vor, den wir EaR-effizienten Optionswert nennen und in eine neue Erzeugungspolitik basierend auf Quantil-Regression einfließt. Die Politik beschreibt ein Preisband innerhalb dessen ein beobachteter Preis zur Ausübung eines Swing-Rechts führt. Für den Fall der amerikanischen Option können wir EaR-Effizienz mit dieser Strategie nachweisen. Abschließend betrachten wir die Absicherung des Kraftwerks vor der Lieferung durch gezielten Verkauf einer Swing Option. Wir stellen eine Heuristik basierend auf unserem synthetischen Spot Delta vor, um Swinghöhe und -anzahl effizient zu finden.

Acknowledgement

Several people directly and indirectly contributed to the accomplishment of this thesis. First and foremost I would like to thank my supervisor Prof. Dr. Kurt Helmes for his support and particular his patience in times when progress was rather slow. He did not only give me the freedom, but also the space to realize my ideas. He provided me with a great working environment despite the fact that I was only an external PhD student. Many thanks go therefore also to Andrea Häußler and the entire staff of the department of Operations Research who treated me like a true colleague and member of the team.

In addition, I would like to thank Prof. Dr. Christian Bender for his friendly support and in particular his mathematical contribution to the theory of upper bounds for swing options. I was able to visit him twice and our discussions were always fruitful and inspiring.

My special thanks also go to my co-supervisor Prof. Dr. Andreas Brandt for his helpful remarks and continuous support during the last stage of the thesis.

For my wife Swetlana

Contents

1. Introduction	1
2. Upper Bounds for Swing Options	5
2.1. Basic Model	7
2.2. Upper Bound for American options	12
2.3. Upper Bounds for Swing Options	15
2.4. Upper Bounds for Swing Options with Volume Constraint	19
2.5. Numerical Examples	23
2.6. Directions for Further Research	28
3. Risk Management	31
3.1. Introductory Example	31
3.2. Hourly Forward Curve Engineering	41
3.3. Risk Measures	46
3.3.1. Future Delta	47
3.3.2. Forward Delta	48
3.3.3. Volumetric Delta	50
3.3.4. Synthetic Spot Delta	51
3.3.5. Earnings-at-Risk	53
3.3.6. Replacement Risk and Total Option Value	56
3.4. Risk Controlling	58
3.4.1. EaR Sensitive Control	61
3.4.2. Quantile Regression	64
3.4.3. Dynamic Swing Caps	68
3.5. Directions for Further Research	78
4. Power Generation Assets	81
4.1. Power Plant Characteristics	85
4.2. Electricity Prices: A Real World Example	87
4.2.1. Parameter Estimation	88
4.2.2. Price Generation	94
4.3. Valuation without Energy Constraints	94
4.3.1. MIP Reformulation	98
4.3.2. Bellman Iteration	99
4.3.3. Principal Component Analysis	101
4.3.4. Numerical Results	105
4.4. Valuation with Energy Constraint	110
4.4.1. MIP Reformulation	113
4.4.2. Bellman Iteration	114
4.4.3. Numerical Results	117
4.4.4. Heuristic Solution	125
4.5. Hedge Analysis	131
4.6. Directions for Further Research	143

A. Selected Source Code	147
A.1. Volumetric Swing Option	147
A.2. Risk adjusted Option Exercise	150
A.3. MIP Reformulation	152
A.3.1. Schedule Enumeration	152
A.3.2. Matrix Representation	155
A.4. Power Plant Valuation	158
A.4.1. No Energy Constraint - Discrete Model	158
A.4.2. Energy Constraint - Continuous Model	162
B. Volumetric Swing Option - Further Examples	171
C. Price Path Samples	173
D. Profit and Loss Distribution of Hedged Power Plant	175

List of Figures

2.1. Illustration for the computation of the marginal martingales	17
2.2. Computation of the marginal martingales in case of swing option with volume constraints	22
2.3. Indicator functions for different exercise rights	24
2.4. Sequence of stopping times for two and three swing rights	25
2.5. 99 % Marginal duality gap (99 % confidence level) across 100 exercise rights (unit vs. volume constraint)	28
3.1. Power plant and Future schedule on Tuesday for $\alpha_0 > 1$	37
3.2. Electricity Price Models	42
3.3. Price Forward Curve Construction	42
3.4. Relation between Future, Forward and spot price.	45
3.5. Cash flow vs. spot price deviations approximated via the spot delta for the synthetic product "Hour 9-11".	52
3.6. Earnings-at-Risk for option seller and buyer	55
3.7. Business Case: Trading unit as 'Man-in-the-Middle'	57
3.8. Overview of risk measures with applications in electricity models	59
3.9. Benchmark for a risk sensitive policy	62
3.10. Cash flow histogram for single exercise (risk and non-risk adjusted)	74
3.11. Upper and lower price threshold for each stage	75
4.1. Seasonal patterns vs. actual electricity prices in 2003 to 2007	89
4.2. Seasonal pattern vs. historical price for a weekday in July 2007	90
4.3. Seasonal pattern vs. historical price for a weekday in October 2007	90
4.4. Volatility on weekdays from log returns (P1) vs. prices (P2)	91
4.5. Volatility on weekends from log returns (P1) vs. prices (P2)	92
4.6. Correlation on weekdays between neighboring prices	93
4.7. Correlation on weekdays between neighboring prices	93
4.8. The simulated price on top of the season and Forward price	95
4.9. Sub matrix of Λ for $t_{\text{on}} = 12$ and $t = -10$	98
4.10. Matrix E	98
4.11. The optimal schedules for the Future price and hourly PFC	107
4.12. The optimal schedules for two specific price scenarios.	108
4.13. Profit-energy curve $\mathbb{L}\hat{z}_d^i$ for a single weekday in March 08 (K=70) with fixed grid and quadratic approximation	118
4.14. Parameter pairs $(a_{1,D-1}, \alpha_{D,0})$ for all three strikes at $D = 30$	119
4.15. Parameter pairs $(a_{1,D-1}, \alpha_{D,1})$ for all three strikes at $D = 30$	119
4.16. Parameter pairs $(a_{1,D-1}, \alpha_{D,2})$ for all three strikes at $D = 30$	119
4.17. Production as a function of the first PC a_1 and available energy W_d	121
4.18. Profit Energy Curves for all price scenarios.	122
4.19. Upper and lower bound option values, C_0^f and C_0 for all three strikes.	123
4.20. Forward iteration with 3 out-of-sample data sets.	126
4.21. Power plant valuation with $t_{\text{on}} = 12$ and $t_{\text{off}} = 8$ and L622 for the SDP.	130

4.22. Power plant valuation with $t_{\text{on}} = 6$ and $t_{\text{off}} = 4$ and L723 for the SDP.	130
4.23. Forward deltas for all three valuation models and strikes	132
4.24. Spot deltas calculated via SDP and total information.	136
4.25. Profit and loss histogram for 70 % of total energy \overline{W}_0	141
C.1. Mean reverting prices around $x_0 = 1$	173
C.2. Hourly electricity prices for March 08 with weekend and weekday day types .	174
D.1. Profit and loss histogram for 70 % of total energy \overline{W}_0	175

List of Tables

2.1. Select Papers for Lower Bound Valuation Models	5
2.2. Selected Papers for Upper Bound Valuation Models	6
2.3. Swing option with unit constraint	25
2.4. Swing option with volume constraint	27
3.1. Risk figures before and in delivery	39
3.2. Risk figures for $(1 - \beta) = 30\%$ before and in delivery (in EUR)	39
3.3. Future delta	48
3.4. Future delta (Normalized Spot Prices)	48
3.5. Forward Delta	49
3.6. Volumetric Delta	51
3.7. EaR vs. VaR	54
3.8. Earnings-at-Risk	55
3.9. Total Option Value (1%, 5%, 30% uncovered spot exposure)	58
3.10. Average R^1 and R^2 statistic for different probabilities β and strikes K (American option).	66
3.11. R^1 statistic 1 % and 99 % probability.	66
3.12. R^1 statistic for 30 % and 70 % probability.	67
3.13. Impact of risk adjusted policy on total option value	72
3.14. Impact of risk adjusted policy on price scenarios with altering volatility ($\beta = 1\%$)	73
3.15. Buyer's and seller's total option value (risk and non-risk adjusted)	76
3.16. As Table 3.15 but based on price scenarios with altering volatility	77
4.1. Selected generation asset valuation literature (Part 1)	82
4.2. Selected generation asset valuation literature (Part 2)	83
4.3. Mean-reversion vector κ	91
4.4. Percentage of the total variance explained by the new factors.	102
4.5. Contained information and correlation of the first three principal components with respect to each individual hour by weekday and weekend	104
4.6. Value of the Power Generation for March 08 in mio EUR.	106
4.7. Option values in EUR and EUR/MWh for different max energy levels (Backward Iteration)	124
4.8. Option values in mio EUR relative to $\overline{\overline{W}}_0$ (forward iteration with new price scenarios)	129
4.9. MW deltas for different upper energy bounds relative to $\overline{\overline{W}}_0$ and strike $K = 50$ EUR	133
4.10. MW deltas for different upper energy bounds relative to $\overline{\overline{W}}_0$ and strike $K = 70$ EUR	134
4.11. MW deltas for different upper energy bounds relative to $\overline{\overline{W}}_0$ and strikes $K = 90$ EUR	134
4.12. EaR values in multiples of 100,000 EUR	140

B.1. Swing Option with Volume Constraint ($\mu = 0.1$)	171
B.2. Swing Option with Volume Constraint ($\mu = 0.1, K = 1$)	172

Abbreviations and Symbols

i.i.d.	independent identically distributed
itm	in-the-money ($K = 0$ and $K = 50$)
atm	at-the-money ($K = 1$ and $K = 70$)
otm	out-of-the-money ($K = 2.5$ and $K = 90$)
ACF	accumulated cash flow
K	strike
MIP	mixed integer linear program
PC	principal component (see section 4.3.3)
PFC	Price Future Curve (usually in hourly granularity)
SDP	Stochastic Dynamic Programming Model according to equation 4.47
EaR	Earnings-at-Risk
VaR	Value-at-Risk
C_0	option value i.e. expectation of value function V_t at initial stage $t = 0$
I	unity vector
I	maximum number of price scenarios
$q_\beta(X)$	β -quantile of distribution for random variable X
V_t	accumulated cash flow from t to $T - 1$
Y_t	approximated continuation value at stage t in context of Bellmann equation
Z_t	cash flow at stage t
$ \mathbb{T} $	total number of items in set \mathbb{T}
*	component-wise vector multiplication
\simeq	substitution

1. Introduction

The main objective of this thesis is the development of models and the implementation of related algorithms for the valuation and risk management of thermal power plants under energy constraints. Different to the long term valuation we are not interested in the investment of a new power plant that would need to take into account construction costs and the long term evolution of prices and exogenous factors like political and environmental implications or the impact of increasing deregulation. Instead we want to focus on existing power plants and assess their profit and loss for a regular balance sheet period i.e. a year. For this purpose we are rather interested in the operations of a power plant and want to find the best generation schedule that maximizes the profit, but at the same time keeps potential losses small.

We define a new not yet investigated unit commitment problem that introduces an energy constraint to a thermal power plant. Energy constraints are well-known in context of hydro plants where the water reservoir can be translated into an energy constraint. In the last three to five years green energy initiatives like CO₂ certificate trading and installation of large wind mill parks implicitly impose energy constraints on thermal power plants as well. Wind energy varies heavily with weather conditions and therefore causes imbalances in the grid that need to be compensated by so called *spinning reserve energy*. Power plant owners are legally obliged to withhold this extra energy or buy it from another utility. Both, the pricing of CO₂ allowances and spinning reserve energy requires the calculation of the marginal energy cost of a power plant and thus entail an energy constraint in related valuation models. From a technical perspective the dispatch decision of a thermal power plant with known fuel and electricity price is a mixed integer problem (MIP). Integer variables are required to model different running modes (start-up, shut-down, cooling, running, ...). Integer problems, however, are computationally expensive, in particular in conjunction with a risk analysis like the calculation of the profit and loss distribution of the generation schedule which requires multiple recalculations and hence re-optimizations for different price scenarios. An energy variable additionally expands the decision space and explains why this type of unit commitment problem was not yet investigated. We deliberately decided to use a real world power plant profile for our investigation as we did not want to compromise on the numerical complexity.

Our basic framework is stochastic dynamic programming in conjunction with Monte-Carlo regression by Longstaff and Schwartz (see section 2.1). This type of model was investigated by Meinshausen and Hambly [50] in context of swing options. Swing options are the simplest representation of a power plant with energy constraints. They are basically American options with multiple exercises (swings) for a predefined period (delivery period) and thus their total exercise profile resembles a dispatch schedule. We tailor the Meinshausen and Hambly model to our power plant by first moving from an hourly to a daily energy allocation (decision stage) reflecting more appropriately the real world information flow (the next 24 hourly prices are usually traded on the day ahead market). We replace the original single price variable by a vector of 24 correlated hourly price processes. Running the Longstaff-Schwarz regression on the full price vector is numerically infeasible and requires to preprocess the price vector first. Therefore we investigate algorithms to reduce the price dimension and in particular apply principal component analysis (PCA). Indeed we find a compact representation of the vector by a single factor (see Table 4.5). As a second modification to the basic model, we introduce a nested mixed integer problem to compute the dispatch schedule within each day

for a given price vector. A fast algorithm for the MIP is crucial for the overall performance of the asset valuation as it has to run for each price scenario separately. We are able to reduce the MIP to a simple matrix multiplication (see section 4.3.1 and 4.4.1) which significantly reduces the computation time (up to 25 times faster). The core idea is the separation of the hourly dispatch schedule into its on/off sequence plus the actual volume profile on top of it. This interpretation helps us to further simplify the stochastic program by considering only the relevant schedule candidates for the valuation (see Table 4.6). This concept even allows for a third and final modification of the basic model to a *continuous* stochastic dynamic program despite the formal integer constraints for the on- and off-times of the power plant (see equation 4.47). We compare our results with an upper bound calculation based on full price information (deterministic dynamic programming) and a heuristic with a simplified rule for the daily energy allocation that does not require any estimation of the continuation value (see equation 4.71). The heuristic imposes a higher/less likely exercise price the smaller the remaining available energy amount becomes. The heuristic reveals a good performance compared to the stochastic and deterministic model (see Figure 4.21) in case of long on- and off-times, while the stochastic model prevails for shorter on- and off-times (see Figure 4.22).

The comparison of the three option values reveals the lack of a benchmark/reference value for a proper model validation and motivated us to investigate the theory of upper bounds. The current literature does not provide theoretical results for real options that go beyond American option like contracts. Therefore we reduce the complexity of our power plant model back to a swing option i.e. our basic model by Meinshausen and Hambly for which the two authors presented also an upper value. However, the notation in their paper is incomplete and therefore partially misleading. For this reason, we rephrase their main result and in particular specify their index definition more precisely which is critical to the entire algorithm (see equation 2.30). We go through the algorithm step by step and stress potential pitfalls (see equation 2.35 to 2.38). Next, we move one step towards our actual power plant model. Recall that we defined daily rather than hourly decision stages. Generating power on several hours during the same day is similar to exercising an option multiple times. For this reason we investigate a swing option with multiple exercises at the same stage. Together with Prof. Bender (University of Braunschweig) who provides the formal proof [8] we work out an extension of the Meinshausen and Hambly result (see equation 2.43). This thesis focuses on the implementation aspect and describes the algorithm in detail (see equation 2.50 to 2.53). We show that the gap between lower and upper bounds of multiple vs. single exercises is similar in size (see Table 2.4 and Figure 2.5).

Besides the focus on the modeling and implementation aspect of thermal power plants with energy constraints and the investigation into their upper bounds, this thesis also contributes new insights into the important topic of spot price risk in electricity markets. A generation schedule with its hourly changing volume profile cannot be entirely hedged on the Future market where only block peak and base contracts (identical hourly capacity throughout the entire delivery period of the same price band) are traded. Individual hourly volume deviations from the peak and base energy need to be bought and sold on the day ahead market in order to meet the actual production/demand. This spot market, however, reveals a high volatility and spikes due to sudden power plant outages and changes in weather. In particular the introduction of further wind energy to the overall generation mix will increase the volatility of the spot market. Therefore the management of the spot price risk to hedge the asset values will draw more and more attention in the future. We start our analysis with the construction of an hourly price Forward curve that anticipates the spot price behavior for a longer future time period. Based on this hourly curve we propose three new spot price risk measures: Forward delta, synthetic spot price delta and Earnings-at-Risk (see section 3.3.2, 3.3.4 and 3.54). They deliberately relate to the two most accepted and widely used risk

measures i.e. delta (first derivative of the option value with respect to the underlying) and Value-at-Risk (quantile of the profit and loss distribution) as we want these new figures to be suitable for real world applications. The latter will be motivated with a business case in section 3.3.6 where we impose a risk fee (spread) on the real option value to compensate the potential replacement risk i.e. the cost for delivering very high prices (option seller) or the loss by exercising low prices (option buyer). The example proposes this spread-adjusted option premium as a reference price for an internal pricing scheme when transferring risk from/to a trading unit within a utility company. The trading entity of a large utility corporation usually acts as an interface between the outside world (retail and trading markets) and the internal units (generation) and especially serves as a risk hub within the entire organization. Internal prices are therefore important to quantify and track the risk transfer within the corporation.

In addition to the mere measurement of spot price risk we also investigate exercise strategies that should prevent a large exposure to this type of risk. We differentiate between strategies within and before the generation period. Strategies *before delivery* look for appropriate hedging portfolios while strategies *within delivery* try to alter the dispatch policy (pick less volatile hours). The latter will automatically entail a reduction in expected profits i.e. option value. We therefore propose an adequate relation of risk vs. return that we call EaR-efficient option value (see section 3.4.1). The core idea is that an efficient strategy in our sense should overcompensate the potential loss in profit with savings in the replacement risk fee as introduced in our business case. For this investigation we need to reduce the complexity of the model and simplify our power plant model again to a swing option contract. We provide a heuristic that meets our benchmark in case of an American option, in particular for a varying risk profile of the underlying price where a risk sensitive policy becomes most beneficial (see Table 3.14). Our heuristic is based on quantile regression (see equation 3.73) as it fits very well into our Longstaff-Schwarz regression framework. We also investigate the heuristic for swing options (see equation 3.84) and show that it meets our benchmark at least in relative terms (see Table 3.15).

We also investigate appropriate hedging strategies before delivery where we will focus again on the complete power plant model. In particular we look at a hedge portfolio of our power plant and a swing option and are interested in the number of swing rights and swing size of the swing option (see equation 4.81). We present a heuristic that is based on our synthetic spot delta definition to approximate optimal swing option parameters (see equation 4.88). We are able to show that the heuristic provides a hedge whose remaining risk is only slightly higher, but is computationally less expensive than the optimal hedge that we found by enumerating across all swing option parameters (see Table 4.12).

This thesis is organized in three main chapters. The first chapter introduces our basic valuation framework that we use throughout the thesis and covers the upper bound theory for the swing option. The second chapter contains our risk management analysis including the price forward curve design, the definition of our three new risk measures, the related notion of EaR efficiency illustrated with the aforementioned business case and the investigation of risk adjusted exercise policies. The last and largest chapter focuses on the actual modeling of our thermal power plant with energy constraint and the hedge analysis using swing options. Each chapter starts with a review of relevant papers, then introduces the theoretical framework and presents our new concepts before it focus on the numerical results. We conclude each chapter with an outlook on further research. The Appendix provides further numerical results and illustrations as well as a commented list of selected code sections that explain specific implementation aspects of the individual algorithms. The complete source code can be found on the CD attached to the hard covered version of this thesis.

2. Upper Bounds for Swing Options

In this first chapter we want to investigate upper bounds for the value of power generation assets as power plants are called in a real option framework. The valuation of power plants is usually complex due to their operational constraints. Therefore most models only provide a lower bound for the true value. For this reason we have to compromise on the technical restrictions of a power plant and can only start with a fairly simple representation of a generation asset as a swing option. We will give a detailed description of a swing option in the following section, but already want to emphasize two main properties that qualify swing options for our analysis. First, they are very similar to American options which allows us to start our investigation from this well known option framework. Second, they are a first approach to model operational constraints as their ability for multiple exercises throughout a specific time period reflects the power plant's flexibility in generating electricity for a certain delivery period. In particular the number of exercises allows to impose an upper energy bound and energy restrictions for thermal power plants are the overall topic of this thesis.

Lower Bound Models	Description	Literature
Stochastic Dynamic Programming	Regression	Carriere, Tsitsiklis and van Roy Longstaff Schwarz Glasserman, Yu Tompaidis, Yang
	Grid, Meshs	Bally, Printemps Hambly, Howison, Kluge
	Tree, Forest	Kaminsky Jaillet, Ron, Tompaidis Bally, Pages, Printemps
Continuous Stochastic Impulse Control	Solving system of inequalities	Dahlgren
Exercise Boundary by Simulation	Sequential solving of equilibrium conditions	Ibanez, Zapatero
Policy Improvement	Direct approximation of Snell envelope	Kolodko, Schoenmakers
	Extension for multiple stopping problems	Schoenmakers, Bender

Table 2.1.: Select Papers for Lower Bound Valuation Models

The investigation of lower bounds for American style contingent claims has a long tradition starting from Cox's et al. binomial lattices [20]. He suggested a solution scheme based on stochastic dynamic programming (SDP) which is still the most popular approach to find optimal stopping times. Kaminski [40] was one of the first who extended the idea for multiple exercise rights creating a forest of lattices. Thus, each exercise right is represented by a separate tree and the backward iteration moves through this forest to find the option value. Later Jaillet et al. [37] specifically investigated electricity contracts and defined mean-reverting trees that are more appropriate for electricity prices as we will later see in section 2.1. Especially for underlyings with higher dimension the tree approach becomes infeasible and Monte-Carlo simulation helps to discretize the price domain more easily. The description of the transition probability, however, becomes more difficult. One approach is quantization. Hence, the price

domain will be discretized into buckets with an associated bucket representative and bucket probability usually calculated via the average and frequency of the related cash flows falling into the specific bucket. The bucket design (grid size and number) is a trade off between accuracy and computational cost. Bally et al. [4] develop a probabilistic method to find the right grid size and investigate convergence of the option values with respect to the grid structure. Glasserman and Broadie [13] investigate a mesh method to describe the transition probabilities. Hambly et al. [32] calibrate the grid to electricity Forward prices and value electricity swing options. By far the most popular combination of SDP's backward iteration with forward based MC simulation is the regression technique by Carriere [16], Tsitsiklis and Van Roy [63], and Longstaff and Schwarz [47]. This is also the approach that we will mainly use in this thesis and that will be described in the next section. Glasserman and Yu [30] refer to the Longstaff-Schwarz algorithm as "Regression Later" indicating that the regression is based on the next stage information whereas they investigate "Regression Now" that uses the information of the current stage as an input for the regression. Tompaidis and Yang [61] provide a good overview of relevant regression methods in context of backward dynamic programming.

Alternatives to dynamic programming try to approximate the exercise boundary directly i.e. the price level that indicates an option exercise when exceeded by the current price. Dahlgren [21] looks at a continuous model and tries to find those thresholds by solving variational inequalities in context of continuous stochastic impulse control. The method does not require Monte Carlo simulation and therefore provides stable results. On the other hand it is not designed for higher dimensional underlyings (Dahlgren uses a single risk factor). Ibanez [36] investigates multidimensional options and therefore relies again on Monte-Carlo simulation. He iteratively solves equilibrium conditions based on simulated sample points to find the exercise boundary along the entire holding period. Kolodko and Schoenmakers [46] provide an iterative method that they call *policy improvement* which is also based on Monte-Carlo simulation. However, compared to dynamic programming fewer calculations of the conditional expectation are required. Bender and Schoenmakers [9] extend the approach for multiple exercise rights.

Upper Bound Models	Description	Literature
Duality Approach	Additive method	Haugh Kogan, Rogers
	Multiplicative method	Jamshidian
	Primal-dual algorithm of additive method	Andersen, Broadie
	Regression Later	Glasserman, Yu
	Hedge portfolio, buyer's/seller's option	Joshi
	Regression estimator for Martingale to prevent nested MC	Bender, Schoenmakers, Belomestny
Regression via consumption process	Iterative generation of lower and upper bounds	Milstein, Belomestny

Table 2.2.: Selected Papers for Upper Bound Valuation Models

A straightforward procedure to compute upper bounds is the valuation with full information i.e., loosely speaking, all future outcomes of the random variable are known. We will also rely on this procedure for our more complex models in chapter 2 and 3. The reason is that the theory of upper bounds for real options is still at an early stage mainly focusing on American

options as the basis theory for more exotic options. Rogers [57] developed a dual approach to find an upper value for an American option and Haugh and Kogan [33] independently developed a similar method for Bermudan options. They reformulate the maximization of the expected cash flows in terms of a minimization problem. Rogers' duality is called the *additive* method as it relies on the Doob-Meyer decomposition that separates the cash flow process of the Snell Envelope into a sum of two processes involving a martingale. We will describe the idea in detail later in this chapter. Jamshidian [38] instead presents a multiplicative decomposition that describes the cash flow in terms of a dominating numeraire. Consequently, the maximum of a ratio rather than a sum has to be computed. Jamshidian also needs to address specifically the issue of potential zero numeraires and therefore provides two versions of his formula for positive and semi-positive options. Joshi [39] rephrases both methods in terms of a hedging problem where the martingale and the new numeraire respectively serve as a hedge portfolio. We will come back to this idea later in this chapter. Glasserman and Chen [18] examined whether the additive or multiplicative method produces better upper bounds with no clear answer. We will focus on the additive method and in particular we will look at an implementation algorithm by Andersen and Broadie [2] that makes use of the optimal policy for the lower bound calculation and is therefore called the *primal-dual algorithm*. We will see that the main challenge lies in the computational complexity of the algorithm as the estimator for the martingale requires nested Monte-Carlo simulations. Broadie and Cao [12] therefore only recently presented further improvements to the algorithm like sub optimality checking and collecting paths. The latter allows to skip the computation for selected paths (boundary distance grouping). Bender, Schoenmakers and Belomestny [6] show for a Bermudian option that in case of Brownian motion for the price process the martingale can be estimated without nested simulations. Belomestny, Milstein and Spokoiny [7] examine yet another description of the cash flow. They use the Riesz decomposition which allows to separate an American option into a European part plus a consumption process. In this way they can construct iteratively a sequence of increasing lower and decreasing upper bounds. However, similar to the primal-dual algorithm each iteration requires a rather expensive calculation.

Meinshausen and Hambly [50] extended Rogers' dual result for the case of swing options. Bender and Wang [10] presented another derivation of the same result that will help us to define the upper bound for yet another extension of the swing option. We will call it swing option with *volume constraint*. It allows for multiple exercises at the same stage. Before we look at this kind of option in section 4 we review the lower bound valuation for a swing option in section 1. In section 2 we will look at the upper bound for American options and describe Rogers' approach in detail. Section 3 will focus on the upper bound for the regular swing option. Finally we provide numerical results in section 5 and will conclude this chapter in section 6 with an outlook for further research.

2.1. Basic Model

Before we start with the upper bound models, we will first present a lower bound value for we will later see that the lower bound is an input to the upper bound algorithm. Technically a swing option is a generalization of an American and Bermudian option. The option holder has the right to buy (call) or sell (put) the underlying for a predefined price (strike) at predefined dates. The main difference to a Bermudian option is the right for multiple exercises (each at a different date). The term *swing* refers to the option's origin in the energy industry. The swing option is an instrument to describe the generation flexibility of a power plant or storage capability of a gas storage facility. Altering or *swinging* the electricity output (the underlying of the swing option) from a low or zero level to a max level is the technical interpretation of

an option exercise. In context of a power plant these exercise decisions have to be made on an hourly basis resulting in a daily production schedule. Thus, the swing option is a simplified model of a power plant. The contract is usually restricted to a certain maximum energy production. In the simplest version the total energy production is a multiple of a single exercise. Then, the maximum energy constraint of the power plant for a specific delivery period translates directly to a maximum number of exercise rights.

We will look at a swing option with single exercise per hour first. We choose the valuation model by Meinshausen and Hambly [50] and make it our basic model not only for this chapter, but this entire thesis. This is in particular true for all variable declarations. Multiple exercise rights are labeled with $n \in \{1, \dots, N\}$. The exercise period is $t = 0, \dots, T$ and we calculate the option value at $t = 0$ i.e. the beginning of the delivery period where the random price $X_0 = x_0$ is known. Hence, we have $T+1$ possible exercise times. The payoff function $Z_t = (X_t - K)^+ = \max(X_t - K, 0)$ is the classical contingent claim of a call option with strike K . The underlying price process $\{X_t\}_t$ is a Markov chain with discrete time steps that generates a filtered probability space $(\Omega, \mathcal{F}, \{\mathcal{F}_t\}_{t=0}^T, \mathbb{P})$. We will write \mathbb{E} for expectation with respect to \mathbb{P} and $\mathbb{E}(\cdot | \mathcal{F}_t)$ for the conditional expectation at time t . Throughout this entire thesis we will ignore discounting. First, we describe the option value in terms of a stopping problem where $\tau_k := \tau_k(t, n)$ is the k -th stopping time in the discrete time period $\{t, t+1, \dots, T\} \cup \infty$ that we forecast with known price information up to t with n exercise rights still available. As not all swings need to be exercised we differ between the first l swings that will be actually exercised. If $l = n$ or $l = 0$ then all respectively no swings will be taken otherwise all $l+1, \dots, n$ swings will not be executed and therefore we set $\tau_k := \infty$ for $k > l$. Hence, we define the set of admissible policies as finite sequences of stopping times $\pi_t(n)$

$$\Pi_t(n) = \left\{ (\tau_n, \dots, \tau_1) \left| \begin{array}{l} \forall k = 1, \dots, l \quad 0 < l \leq n : \tau_k < \tau_{k-1} < \dots < \tau_1, \tau_k \in \{t, t+1, \dots, T\}, \\ \forall k = l+1, l+2, \dots, n \quad 0 \leq l < n : \tau_k := \infty \end{array} \right. \right\}, \quad (2.1)$$

We additionally set $Z_\infty := 0$. We denote with $\pi_t^*(n) = (\tau_n^*(t, n), \dots, \tau_1^*(t, n)) \in \Pi_t(n)$ the intermediate optimal sequence of stopping times that maximizes the expected profit over all sequences of stopping times for the remaining exercise period $[t, t+1, \dots, T]$ given the current price $X_t = x_t$, i.e. the solution of

$$C_t^*(x_t, n) = \sup_{\pi_t(n) \in \Pi_t(n)} \mathbb{E}^{(\pi_t(n))} \left[\sum_{k=1}^n Z_{\tau_k(t, n)} | X_t = x_t \right], \quad (2.2)$$

where $\mathbb{E}^{(\pi_t(n))}[\dots]$ stands for the expectation under the Markov chain that follows the policy $\pi_t(n)$. In particular we denote with $n = N$ and $t = 0$, i.e. $\pi_0(N)$, the sequence of stopping times from the beginning of the exercise period with N exercise rights available. Then $\pi_0^* = (\tau_N^*(0, N), \dots, \tau_1^*(0, N)) \in \Pi_0(N)$ is the optimal sequence of stopping times that maximizes the expected profit for the entire exercise period

$$C_0^*(x_0, N) = \sup_{\pi_0(N) \in \Pi_0(N)} \mathbb{E}^{(\pi_0(N))} \left[\sum_{k=1}^N Z_{\tau_k(0, N)} | X_0 = x_0 \right]. \quad (2.3)$$

Note the descending order of stopping times in terms of the exercise rights which Hambly et al. find via a Bellman iteration. The corresponding backward iteration motivates to count the remaining rather than the used number of exercise rights. Therefore the stopping times are defined in the same declining order and stand for the second dimension of the state space. The first dimension of the state space is the price X_t . The value function $C_t^*(x, n)$ is the value

of an option that would be newly issued at t with n remaining exercises up to T and would observe the current price x . The value function can be calculated via the Bellman equation

$$C_t^*(x, n) = \max_{a \in A(n)} \{Z_t(x, a) + \mathbb{E}[C_{t+1}^*(X_{t+1}, n - a) | X_t = x]\} \quad t = 0, \dots, T \quad (2.4)$$

where $C_{T+1}^*(X_{T+1}, n) := 0$ for $n=1, \dots, N$. The corresponding dynamic program is defined as follows

$$\begin{aligned} \text{state : } & (x, n) \quad x: \text{ current price, } n: \text{ remaining number of swings} \\ \text{action : } & a \in A(n) = \{0, \min(n, 1)\} \quad \text{exercise yes (1) or no (0)} \\ \text{transition : } & \{x, n\} \longrightarrow \{y, n - a\} \\ \text{marginal profit : } & Z_t(x, a) := (x - K)^+ a \\ \text{value function : } & C_t^*(x, n) \\ \text{continuation value : } & Q_{t+1}^*(x, n) := \mathbb{E}[C_{t+1}^*(X_{t+1}, n) | X_t = x], \end{aligned} \quad (2.5)$$

where x, y are realizations of the random price variables X_t, X_{t+1} . X_t and X_{t+1} are linked by the transition law (see equation 2.7). Note that the continuation value $Q_{t+1}^*(x, n)$ is the *expected* option value at the *next* stage $t + 1$ conditional on the current price x . For the remaining part of this entire thesis we introduce a more compact description of the dynamic program and rewrite the previous two equations as

$$\begin{aligned} C_t^*(X_t, n) &= \max_{a \in A(n)} \{Z_t(X_t, a) + \mathbb{E}[C_{t+1}^*(X_{t+1}, n - a) | X_t]\} \quad t = 0, \dots, T \\ \text{state : } & (X_t, n) \quad X_t: \text{ current price, } n: \text{ remaining number of swings} \\ \text{action : } & a \in A(n) = \{0, \min(n, 1)\} \quad \text{exercise yes (1) or no (0)} \\ \text{transition : } & \{X_t, n\} \longrightarrow \{X_{t+1}, n - a\} \\ \text{marginal profit : } & Z_t(X_t, a) := (X_t - K)^+ a \\ \text{value function : } & C_t^*(X_t, n) \\ \text{continuation value : } & Q_{t+1}^*(X_t, n) := \mathbb{E}[C_{t+1}^*(X_{t+1}, n) | X_t]. \end{aligned} \quad (2.6)$$

We can derive the relevant transition probabilities required for computing the conditional expectation of the continuation value from the dynamic of the price process. Hambly et al. define the log price as a mean-reverting process, $t=0, \dots, T$

$$\ln X_{t+1} = (1 - \kappa)(\ln X_t - \mu)\Delta t + \mu\Delta t + \sigma\epsilon_t \quad \epsilon_t \sim N(0, 1), \quad (2.7)$$

where $\{\epsilon_t\}_t$ are independent. We apply a discrete model with $\Delta t = 1$ and receive the distribution $\ln X_{t+1}$ given X_t as if $X_t = x$

$$\ln X_{t+1} \sim \mathbb{N}\left((1 - \kappa)(\ln X_t - \mu) + \mu, \sigma^2\right). \quad (2.8)$$

Formally the backward iteration of a dynamic program contradicts with the Forward iteration of a Monte-Carlo simulation. Longstaff and Schwarz [47] address this conflict and in particular discovered that for numerical efficiency rather than approximating the value function over the entire domain it is sufficient to approximate the continuation value only. They do so by relating the continuation value at time t to the corresponding accumulated cash flows (ACF)

$$V_t^*(X_t, n) := \sum_{k=1}^n Z_{\tau_k^*(t,n)}, \quad (2.9)$$

where $\tau_k^*(t, n) \in \pi_t^*(n)$ (see context of equation 2.1). To be precise Longstaff and Schwarz assume that an individual realization of the continuation value $Q_{t+1}(x_t^i, n)$ is close to the average of all ACFs $V_{t+1}^*(x_{t+1}^j, n)$ with realized prices x_{t+1}^j generated from x_t^i according to equation 2.7¹

$$Q_{t+1}^*(x_t^i, n) \approx \frac{1}{J} \sum_{j=1}^J V_{t+1}^*(x_{t+1}^j, n). \quad (2.10)$$

The numerical procedure can only approximate the optimal continuation value Q_t^* by Y_t and ACF V_t^* by \underline{V}_t (see following definitions). The continuation value will be approximated with a linear combination of basis functions

$$Y_{t+1}(X_t, n) := \sum_{r=1}^R \alpha_{r,n,t} \Psi_{r,n}(X_t) \approx Q_{t+1}^*(X_t, n). \quad (2.11)$$

The relevant coefficients $\alpha_{r,n,t}$ for the basis functions $\Psi_{r,n}$ will be computed by regressing the pairs $(X_t, \underline{V}_{t+1}(X_{t+1}, n))$. Note that at each stage t the regression needs to be performed N times (for each exercise opportunity $n = 1, \dots, N$ separately). Once, we have approximated the continuation value with a functional description Y_{t+1} we are able to approximate the best action $\hat{a}^*(X_t, n)$ which we then use to update \underline{V}_t from \underline{V}_{t+1}

$$\begin{aligned} \hat{a}^* &:= \hat{a}^*(X_t, n) := \arg \max_{a \in A(n)} \{Z_t(X_t, a) + Y_{t+1}(X_t, n - a)\} \\ \underline{V}_t(X_t, n) &:= Z_t(X_t, \hat{a}^*) + \underline{V}_{t+1}(X_{t+1}, n - \hat{a}^*). \end{aligned} \quad (2.12)$$

Then we can approximate the actual option value $C_0^*(x_0, N)$ with the average over $i = 1, \dots, I$ realizations of the approximated ACF at $t = 0$

$$\underline{C}_0(x_0, N) \approx \frac{1}{I} \sum_{i=1}^I \underline{v}_0^i(N). \quad (2.13)$$

Let us briefly summarize the backward algorithm for the approximation:

1. Generate $i = 1, \dots, I$ price scenarios x_t^i with $t = 1, \dots, T$ starting at x_0 .
2. Start at last stage T and initialize all N ACFs with the immediate payoff $\underline{V}_T(X_T, 1) = \dots = \underline{V}_T(X_T, N) = Z_T = (X_T - K)^+$.
3. For $t = T-1, \dots, 1$
 - a) Run regressions on the pairs $(X_t, \underline{V}_{t+1}(X_{t+1}, n))$, that is one regression for each number of exercise rights $n = 1, \dots, N_{t+1}$ with $N_{t+1} = \min\{T-t, N\}$ separately. This will lead to N_{t+1} function approximations of the continuation value $Y_{t+1}(X_t, n)$ with $n = 1, \dots, N_{t+1}$. Set $Y_{t+1}(X_t, n) := Y_{t+1}(X_t, N_{t+1})$ for $n = N_{t+1} + 1, \dots, N$.

¹Throughout this entire thesis we will represent realizations of random variables with small letters plus an exponent i indicating the i -th individual scenario e.g. x_t^i . For function values on realized random variables we will additionally skip the random parameter e.g. $v_t^i(\dots) := V_t(x_t^i, \dots)$.

- b) Store the coefficients $\alpha_{r,n,t}$ with $n = 1, \dots, N_{t+1}$. They implicitly define our exercise policy for the forward iteration at step t .
 - c) Find the best action a according to equation 2.12 and compute the ACF of the current stage $\underline{V}_t(X_t, n)$ for $n = 1, \dots, N_{t+1} + 1$. Set $\underline{V}_t(X_t, n) := \underline{V}_t(X_t, N_{t+1} + 1)$ for $n = N_{t+1} + 2, \dots, N$.
4. Finally we receive $i = 1, \dots, I$ ACFs $v_0^i(n)$ for each of the $n = 1, \dots, N_0$ exercise rights. Averaging the scenarios for each right n according to equation 2.13 returns N swing option values $\underline{C}_0(x_0, n)$.

The coefficients $\alpha_{r,n,t}$ are necessary for the forward iteration. They allow us to approximate the continuation value for any new set of prices on every stage t and any number of remaining exercises n . We can also define the marginal continuation value

$$\begin{aligned}\Delta Q_{t+1}^*(X_t, n) &:= Q_{t+1}^*(X_t, n) - Q_{t+1}^*(X_t, n-1) \\ \Delta Y_{t+1}(X_t, n) &:= Y_{t+1}(X_t, n) - Y_{t+1}(X_t, n-1),\end{aligned}\tag{2.14}$$

which describes the expected additional option value of the n -th exercise right in $t+1$ given today's price X_t . Recall that the approximated continuation value $\Delta Y_{t+1}(X_t, n)$ is our vehicle to find the next optimal exercise time $\tau_n(t+1, n)$. Therefore we can use the marginal continuation value to define an indicator function that tells us at each stage t whether to exercise the n -th option or not

$$l_t(X_t, n) := \begin{cases} 0 & Z_t(X_t, 1) < \Delta Y_{t+1}(X_t, n) \\ 1 & Z_t(X_t, 1) \geq \Delta Y_{t+1}(X_t, n). \end{cases}\tag{2.15}$$

As our value function is monotonous due to the structure of the Bellman iteration we can directly derive a threshold price $\underline{X}_{t,n}$ if the nature of our basis functions $\Psi_{r,n}$ allows to solve Y_{t+1} for X_t

$$l_t(X_t, n) := \begin{cases} 0 & X_t < \underline{X}_{t,n} \\ 1 & X_t \geq \underline{X}_{t,n}. \end{cases}\tag{2.16}$$

In short, the forward iteration runs as follows

1. Generate a new set of I price paths starting from x_0 and ending at final exercise date T .
2. For each path i
 - a) Find the earliest stage t where $l(x_t^i, N)$ indicates exercise. This is τ_N^i . Store cash flow $z_{\tau_N}^i$.
 - b) Continue at $t := \tau_N + 1$ and look for the earliest stage t where $l(x_t^i, N-1)$ indicates exercise. This is τ_{N-1}^i .
 - c) Repeat step (2.b) until you reached T or all remaining options $n = 1, \dots, N-2$ are exercised.
 - d) Sum the cash flows $z_{\tau_n}^i$ along each path i for all exercised options $n = 1, \dots, N$. This is $\underline{v}_0^i(N)$.
3. Average all $\underline{v}_0^i(N)$ to retrieve $\underline{C}_0(x_0, N)$.

As the forward iteration relies on the policy approximation of the backward calculation it can only provide a lower bound. We need to accept that some of our approximated optimal actions \hat{a}^* might be wrong (i.e. \hat{a}^* says exercise, but the true a^* does not or vice versa) and thus exercise at less valuable hours. Still, the forward iteration can be used to quickly compute a new option value for a small change in the initial start price x_0 . Larger deviations of the start price x_0 require a new approximation of the exercise policy and hence a new run of the backward iteration. The exact interval around x_0 where the initial policy still approximately holds true mainly depends on the underlying price process. The investigation of this interval in our specific situation would be a topic for further research.

2.2. Upper Bound for American options

In order to compare different valuation schemes and in particular to assess their accuracy an upper bound as a benchmark is required. Usually the straightforward approach is to allow for perfect foresight. Then all price scenarios are known beforehand and we can translate the stochastic into a deterministic valuation scheme. The resulting option value is an upper bound, but it could certainly be significantly above the true option value. Therefore we look for models that produce tighter upper bounds. We start our investigation for American options first and describe Rogers' duality approach [57] with Andersen and Broadie's [2] specific implementation.

The pricing problem of a single exercise right is a special case of our basic model in equation 2.6. We only need to reduce the number of exercise rights to 1 and can write the initial stopping problem

$$\text{Primal: } C_0^*(x_0, 1) = \sup_{\tau} \mathbb{E}_0 [Z_{\tau}], \quad (2.17)$$

with $\tau := \tau_1(0, 1) \in \{0, 1, \dots, T\}$ and $\mathbb{E}_0[\cdot] := \mathbb{E}[\cdot | X_0 = x_0]$. Haugh and Kogan [33] and Rogers [57] independently proposed a dual formulation of this lower bound model that at the same time serves as an upper bound. The definition requires the introduction of a martingale process $\{M_t\}_t$

$$\text{Dual: } C_0^*(x_0, 1) = \inf_{\{M_t\}_t \in \mathbb{M}_0} \left\{ M_0 + \mathbb{E}_0 \left[\max_{t \in \mathbb{T}} (Z_t - M_t) \right] \right\}, \quad (2.18)$$

where \mathbb{M}_0 is the set of all martingales with $M_0 := C_0^*(x_0, 1)$ and $\mathbb{T} := \{0, \dots, T\}$. Comparing equation 2.17 and 2.18 we can see that a martingale process $\{M_t\}_t$ will be introduced within the expectation and the order of taking the expectation and finding the supremum is switched around. Taking the expectation of the maxima resembles a situation of perfect foresight/ full information and provides an intuitive explanation that equation 2.18 is an upper bound. The dual problem can be interpreted as a lookback option with the option payoff Z_t being the state variable and the martingale M_t being the floating strike. Joshi [39] interprets the primal problem in equation 2.17 as the view of an option buyer. He needs to find the supremum of the cash flow Z_{τ} over all stopping times since he can choose when to exercise. The dual problem, on the other hand, represents the hedging situation of an option seller. We explained already that, when ignoring the martingale M_t for a moment, then the right side in equation 2.18 describes the situation of maximal foresight. This is the worst case scenario for the option seller and would mean that the buyer happens to exercise at the highest price which has a non-zero probability if he picks an exercise right randomly. Now, Joshi looks at M_t to be the value of a hedge portfolio consisting of the option itself and a bond. The seller initially buys one unit of the option to be hedged ($M_0 = C_0^*(x_0, 1)$) and follows the optimal

exercise strategy. If the buyer does so too, then the hedge will perfectly offset the buyer's option. But if the buyer does not follow the optimal exercise strategy, then the seller is always ahead. If the buyer exercises and the seller does not, then the option value is greater than the exercise value and the seller makes extra money and puts this money into a bond. If the seller exercises and the buyer does not, then the seller can buy a new unexercised option at a lower price. Hence the hedge portfolio M_t is always larger or equal to the current cash flow Z_t which explains that equation 2.18 holds true. Haugh and Kogan provide a different access to their equation. They show that the upper bound will exactly match the option value if M_t is set to the martingale component of the optimal value function

$$C_t^*(X_t, 1) = M_t^* - A_t^*, \quad (2.19)$$

where A_t^* is an increasing process following the Doob-Meyer decomposition. Then $A_0^* = 0$ and the optimal martingale $M_0^* = C_0^*(x_0, 1)$. Inserted into equation 2.18 we receive

$$C_0^*(x_0, 1) \leq C_0^*(x_0, 1) + \mathbb{E}_0 \left[\max_{t \in \mathbb{T}} (Z_t - C_t^*(X_t, 1) - A_t^*) \right] \leq C_0^*(x_0, 1), \quad (2.20)$$

where the additional inequality on the right side holds true because $C_t^*(X_t, 1) \geq Z_t$ and $A_t^* \geq 0$. In practice we usually do not know the true value function process $C_t^*(X_t, 1)$. Therefore we need to approximate M_t^* via a good approximation $\hat{C}_t(X_t, 1)$. This leads us back to our lower bound calculation. To clearly separate lower from upper bound values we will use an overline, e.g. $\overline{C}_0(x_0, 1)$, to mark upper bound figures like we use an underline for lower bound figures. We will use the corresponding \underline{M}_t of our lower bound calculation as our best estimate for M_t^* . Replacing the optimal option value $C_0^*(x_0, 1)$ with the lower bound approximation $\underline{C}_0(x_0, 1)$ leads to the error D_0 resulting from the approximated solution of the dual problem

$$\overline{C}_0(x_0, 1) := \underline{C}_0(x_0, 1) + \mathbb{E}_0[\max_{t \in \mathbb{T}} (Z_t - \underline{M}_t)] = \underline{C}_0(x_0, 1) + D_0. \quad (2.21)$$

Andersen and Broadie show that the martingale process $\{M_t\}_t := \{\underline{M}_t\}_t$ can be iteratively determined²

$$\begin{aligned} M_t &= M_{t-1} + \underline{C}_t(X_t) - Q_t(X_{t-1}) \\ Q_t(X_{t-1}) &:= \begin{cases} \mathbb{E}[\underline{C}_t(X_t)|X_{t-1}] & l_{t-1}(X_{t-1}) = 1 \\ \underline{C}_{t-1}(X_{t-1}) \approx Y_t(X_{t-1}) & l_{t-1}(X_{t-1}) = 0, \end{cases} \end{aligned} \quad (2.22)$$

for $t = 2, \dots, T$ with $M_0 = \underline{C}_0(x_0, 1)$ and $M_1 = \underline{C}_1(X_1)$. Thus, the martingale is the cumulative sum of value function differences at each stage. It is the difference between the individual value function $\underline{C}_t(X_t)$ and the expected value function $Q_t(X_{t-1})$ conditional on the previous stage. $Q_t(X_{t-1})$ has two different expressions dependent on whether the option was exercised at the previous stage or not. If it was not ($l_{t-1} = 0$), then the value function of the previous stage represents our expectation of the future exercise $Q_t(X_{t-1}) = \underline{C}_{t-1}(X_{t-1})$. If it was ($l_{t-1} = 1$), then we need to simulate a situation where the option was not exercised at $t-1$ and estimate the value of a new option that would be issued the next stage $Q_t := \mathbb{E}[\underline{C}_t(X_t)|X_{t-1}]$. In both cases we need to calculate the value function $\underline{C}_t(X_t)$ and $\underline{C}_{t-1}(X_{t-1})$. Formally we would need to apply the forward iteration from the previous section and would require to

²For the remaining part of this section we skip the underline for the martingale as in our context the term martingale is always the specific martingale that relates to the lower bound approximation. We also ignore the number of exercises as the American option by design only provides a single exercise right, i.e. $C_t(X_1) := C_t(X_1, 1)$, $Y_{t+1}(X_t) := Y_{t+1}(X_t, 1)$, etc.

scan the entire remaining time domain $\{t, \dots, T\}$ at every stage t and trajectory i until our indicator function l_t of equation 2.15 signals exercising. This is certainly too time consuming. In particular if we consider that the calculation of the expectation in case of $l_{t-1} = 1$ can only be approximated via a nested Monte Carlo loop starting from X_{t-1} . This additional simulation at every stage and state requires a faster approximation of the lower bound value $\underline{C}_t(X_t)$. We therefore only look at the cash flow of the current stage and compare it to our approximated continuation value $Y_{t+1}(X_t)$. We interpret the latter as our best estimate for the value of a future exercise from t to T ³

$$\underline{c}_t^i \approx \max \left\{ z_t^i, y_{t+1}^i \right\}. \quad (2.23)$$

In case of no exercise $z_t^i < y_{t+1}^i$, we approximate the lower bound value with the continuation value $\underline{c}_{t-1}^i \approx y_t^i$ as indicated in equation 2.22. Likewise we estimate the conditional value function $\mathbb{E}[\underline{C}_t(X_t)|X_{t-1}]$. Within a nested Monte-Carlo loop we will generate a new set of prices \tilde{x}_t^j starting from x_{t-1}^i and calculate the value function as above. Then we will use the sample mean to approximate the expectation

$$\mathbb{E}[\underline{C}_t(X_t)|X_{t-1}] \approx \frac{1}{J} \sum_{j=1}^J \underline{c}_t^j. \quad (2.24)$$

In this way we can reduce the nested price paths to a single time step. This certainly improves the calculation time. In this way we can compute all martingales according to equation 2.22 and calculate the individual upper value functions \bar{c}_0^i whose average is our estimator for the upper bound

$$\begin{aligned} \bar{c}_0^i &= \max_{t \in \mathbb{T}} (z_t^i - m_t^i) \\ \bar{C}_0(x_0) &\approx \frac{1}{I} \sum_{i=1}^I \bar{c}_0^i. \end{aligned} \quad (2.25)$$

In short, the algorithm for the upper bound of an American option runs as follows:

1. Generate I price paths starting from x_0 . For each price path $i = 1, \dots, I$:
 - a) Set $M_0 = C_0(x_0)$ and $m_1 = \underline{c}_1^i$.
 - b) For each stage $t = 2, \dots, T$:
 - i. Compute $\underline{C}_t(x_t^i) = \max\{z_t^i, y_{t+1}^i\}$ using our estimates $\alpha_{r,n,t}$ for the continuation value.
 - ii. If $l_{t-1}^i = 0$, then set $q_{t-1}^i = \underline{c}_{t-1}^i$, else
 - A. Generate another set of J prices \tilde{X}_t starting from x_{t-1}^i .
 - B. For each sub path \tilde{x}_t^j compute the value function $\underline{c}_t^j = \max(z_t^j, y_{t+1}^j)$ by again using our estimates $\alpha_{r,n,t}$.
 - C. Average these value functions to receive an estimator for $\mathbb{E}[\underline{C}_t(X_t)|x_{t-1}^i]$.
 - iii. Compute martingale m_t^i according to equation 2.22.
 - c) Compute individual upper bounds $\bar{c}_0^i = \max\{z_t^i - m_t^i\}$

³For the remaining part of this chapter we will abbreviate $z_t^i(\cdot) := Z_t(x_t^i, \cdot)$, $y_t^i(\cdot) := Y_t(x_{t-1}^i, \cdot)$ and $c_t^i(\cdot) := C_t(x_t^i, \cdot)$.

2. Average all individual upper bounds according to equation 2.25 to receive an estimate for the upper bound of the option value $\bar{C}_0(x_0)$.

Finally we should mention that due to the underlying Monte-Carlo simulation both numerical procedures for the lower and upper bound cannot guarantee true lower and upper bounds for all possible price paths. An unusual price path under the approximated optimal exercise policy might return a supposedly lower bound that actually lies above and then consequently the related upper bound will be below the optimal value. This is also true for all extensions of this primal-dual method that we present in the upcoming sections.

2.3. Upper Bounds for Swing Options

So far, we looked at an upper bound for an option with a single exercise. In order to understand the extension for multiple exercises we should think of the value contribution of every extra exercise right to be similar to an additional American option value. Intuitively, we could then apply Rogers' duality on the *marginal* value of the n-th exercise right of a swing option

$$\Delta C_t^*(n) := C_t^*(X_t, n) - C_t^*(X_t, n-1). \quad (2.26)$$

Meinshausen and Hambly [50] prove that this intuition is correct

$$\Delta C_0^*(n) = \inf_{\pi_0(n-1)} \inf_{\{M_t\}_{t \in \mathbb{M}_0}} \left\{ M_0 + \mathbb{E}_0 \left[\max_{t \in \mathbb{T} \setminus \{\tau_{n-1}, \dots, \tau_1\}} (Z_t - M_t(n)) \right] \right\}, \quad (2.27)$$

with $\mathbb{T} = \{0, \dots, T\}$ and $\tau_k := \tau_k(0, n-1)$, $k = n-1, \dots, 1$. Then $\{M_t(n)\}_t$ is the marginal martingale process for the n-th exercise right. Note the definition of the domain space for the maximization that only considers not yet exercised stages up to n-1. Accordingly, the additionally introduced infimum is defined over all policies with n-1 exercise rights $\pi_0(n-1)$ (see also equation 2.1). Equation 2.27 does not only require the knowledge of the stopping times $\tau_k(0, n-1)$, $k = 1, \dots, n-1$, but also of all marginal martingales in $t = 1, \dots, T$ and $n = 1, \dots, N$. Meinshausen and Hambly derive that analogously to the American option it is again the martingale component $M_t^*(n)$ of the optimal (marginal) value function $\Delta C_t^*(n)$ that attains the infimum. Furthermore the authors show that this martingale can be derived recursively similar to the case of the American option. They present an extension of the Andersen and Broadie iterative method in order to use again the lower bound approximation $\underline{M}_t(n)$ and $\Delta \underline{C}_t(n)$ as our best guess for M_t^* and $\Delta C_t^*(n)$. This leads to the duality gap $\Delta D_0(n)$

$$\Delta \bar{C}_0(n) := \Delta \underline{C}_0(n) + \mathbb{E}_0 \left[\max_{t \in \mathbb{T} \setminus \{\tau_{n-1}, \dots, \tau_1\}} (Z_t - \underline{M}_t(n)) \right] = \Delta \underline{C}_0(n) + \Delta D_0(n), \quad (2.28)$$

and thus to the upper bound value of the total swing option

$$\bar{C}_0(x_0, N) = \sum_{n=1}^N \Delta \bar{C}_0(n). \quad (2.29)$$

The decisive extension of the iteration in equation 2.22 is the introduction of the index k to find the martingales $M_t(n)$. Meinshausen and Hambly define k as the largest natural number with $t \leq \tau_k$ and $0 \leq k < n$. Recall that $\tau_k(0, n-1)$ is the optimal stopping time of the k-th

exercise right for a swing option with $n - 1$ (!) exercise rights available at $t = 0$ ⁴

$$\begin{aligned}
 M_t(n) &= M_{t-1}(n) + \underline{\Delta C}_t(X_t, k + 1) - \underline{\Delta Q}_t(X_{t-1}, k + 1) \\
 \underline{\Delta Q}_t(X_{t-1}, k + 1) &:= \begin{cases} \mathbb{E}[\underline{\Delta C}_t(X_t, k + 1)|X_{t-1}] & l_{t-1}(X_{t-1}, k + 1) = 1 \\ \underline{\Delta C}_{t-1}(X_{t-1}, k + 1) \approx \underline{\Delta Y}_t(X_{t-1}, k + 1) & l_{t-1}(X_{t-1}, k + 1) = 0 \end{cases} \\
 l_{t-1}(X_{t-1}, k + 1) &:= \begin{cases} 1 & Z_{t-1}(X_{t-1}) \geq \underline{\Delta Y}_t(X_{t-1}, k + 1) \\ 0 & \text{otherwise.} \end{cases}
 \end{aligned} \tag{2.30}$$

The definition of the iteration for computing the martingale process in conjunction with the option exercise process l_t is analogous to equation 2.22. It is even identical to equation 2.22 in case of $n=1$. Now it only applies for the marginal instead of the total figures. As the authors do not elaborate the formulas and algorithm in detail, especially their sub indices are not thoroughly applied and therefore cause confusion, we give a detailed description of the method in the next paragraphs. In context of the current stage t , $\tau_k(0, n - 1)$ is the next available stopping time from t onwards in the sequence of optimal stopping times according to $\pi_0(n - 1)$ (see also equation 2.1). So, we do not look at the local policy $\pi_t(n - 1)$, but always at the global one $\pi_0(n - 1)$. Also, the local maximum number of exercise rights n during the marginal martingale calculation should not be confused with the global number of exercise rights N of the entire swing option (see also discussion around Figure 2.4). These martingales will then be used to calculate the expectation in equation 2.27 and henceforth $\bar{C}_0(x_0, N)$. Note that $M_t(n)$ is a random variable. Thus $M_t(n)$ varies with every realized path. We therefore rewrite the previous two equations in terms of realizations of the random price variable and the approximation of the lower bound values with the help of our estimates for the continuation value. For $l_{t-1}(X_{t-1}, k + 1) = 1$, this is

$$\begin{aligned}
 m_t^i(n) &= m_{t-1}^i(n) + \underline{c}_t^i(k + 1) - \underline{c}_t^i(k) - \mathbb{E}[\underline{C}_t(X_t, k + 1)|x_{t-1}^i] + \mathbb{E}[\underline{C}_t(X_t, k)|x_{t-1}^i] \\
 &\approx m_{t-1}^i(n) \\
 &\quad + \max \left[z_t^i + y_{t+1}^i(k), y_{t+1}^i(k + 1) \right] - \max \left[z_t^i + y_{t+1}^i(k - 1), y_{t+1}^i(k) \right] \\
 &\quad - \frac{1}{J} \sum_1^J \max \left[Z_t(\tilde{x}_t^j) + Y_{t+1}(\tilde{x}_t^j, k), Y_{t+1}(\tilde{x}_t^j, k + 1) \right] \\
 &\quad + \frac{1}{J} \sum_1^J \max \left[Z_t(\tilde{x}_t^j) + Y_{t+1}(\tilde{x}_t^j, k - 1), Y_{t+1}(\tilde{x}_t^j, k) \right],
 \end{aligned} \tag{2.31}$$

where \tilde{x}_t^j are simulated prices with start value x_{t-1}^i according to equation 2.7. And for $l_{t-1}(X_{t-1}, k + 1) = 0$ this is

$$\begin{aligned}
 m_t^i(n) &= m_{t-1}^i(n) + \underline{c}_t^i(k + 1) - \underline{c}_t^i(k) - \underline{c}_{t-1}^i(k + 1) + \underline{c}_{t-1}^i(k) \\
 &\approx m_{t-1}^i(n) \\
 &\quad + \max \left[z_t^i + y_{t+1}^i(k), y_{t+1}^i(k + 1) \right] - \max \left[z_t^i + y_{t+1}^i(k - 1), y_{t+1}^i(k) \right] \\
 &\quad - y_t^i(k + 1) + y_t^i(k).
 \end{aligned} \tag{2.32}$$

Comparing equations 2.31 and 2.32 we see that $\underline{c}_{t-1}^i(k + 1)$ and $\underline{c}_{t-1}^i(k)$ will be replaced by $y_t^i(k + 1)$ and $y_t^i(k)$ as in the latter case there was no exercise on the previous stage and

⁴Again we skip the underline for \underline{M}_t for better readability.

hence $z_{t-1}^i = 0$. The two previous equations apply for $t = 2, \dots, T$. For $t = 0$ and $t = 1$ we have $m_0^i(n) = 0$ and $m_1^i(n) = \Delta c_1^i(n)$. For $t = T$ we set $Y_{T+1} := 0$ and consequently we get $Y_T(k) = Z_T$ for $k > 1$. Then, for $k > 1$ almost all terms cancel out and we receive $m_T^i(n) = m_{T-1}^i(n)$. For $k = 0$ we have $Y_t(0) = 0$ for $t = 1, \dots, T$ and we receive the same result as for the American option

$$m_T^i(n) := \begin{cases} m_{T-1}^i(n) + z_T^i - y_T^i(1) & l_{T-1}^i = 0 \\ m_{T-1}^i(n) + z_T^i - \frac{1}{J} \sum_{j=1}^J Z_T(x_T^j) & \text{otherwise.} \end{cases} \quad (2.33)$$

Once we have computed the marginal martingales for the n -th exercise right along all hours t , we compute the individual upper bound $\Delta \bar{c}_0^i(n)$ and approximate the expectation in equation 2.27 via averaging the individual upper bounds

$$\begin{aligned} \Delta \bar{c}_0^i(n) &= \max_{t \in \mathbb{T} \setminus \{\tau_{n-1}^i, \dots, \tau_1^i\}} (z_t^i - m_t^i(n)) \\ \Delta \bar{C}_0(n) &\approx \frac{1}{I} \sum_{i=1}^I \Delta \bar{c}_0^i(n). \end{aligned} \quad (2.34)$$

The domain space for the maximization \mathbb{T} shrinks with increasing exercise rights n as all previous stopping times will be extracted first. Recall that the sequence of stopping points⁵ $\tau_1^i(0, n-1), \dots, \tau_{n-1}^i(0, n-1)$ changes with every price scenario i . Let us illustrate the entire calculation with an example. We assume that our swing option has a time horizon of 12

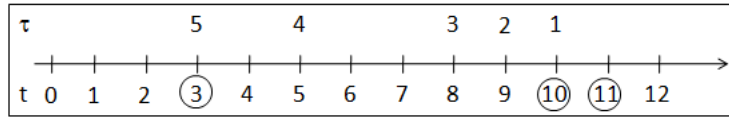


Figure 2.1.: Illustration for the computation of the marginal martingales

stages and a max number of $N = 10$ exercise rights. We further assume that we already ran a backward iteration and therefore can compute an approximation for all continuation values $Y_t(n)$ for all $t = 0, \dots, 12$ and $n = 1, \dots, 10$. Now, we want to compute the upper bound for the marginal option value of the 6-th exercise right for the first price trajectory $\Delta \bar{c}_0^1(6)$. Hence, we use our optimal policy of the lower bound calculation to find the first five(!) stopping points for our price scenario 1. This is $\pi_0^1(5)$ which is presented in Figure 2.1. From now on we skip the index 1 indicating realizations of price path 1 ($x := x^1, z := z^1, \dots$) for readability. Note that the stopping points are always in strict descending order with respect to the remaining exercise rights. Now, we want to present the calculation of the 6th martingale $m_t(6)$ for three different stages $t = 3, 10$ and 11 . At $(t = 3)$ the largest k is still the max number of 5 exercise rights like for any hour $t \leq 3$. As $l_2(6) = 0$ we compute

$$\begin{aligned} m_3(6) &= m_2(6) + \Delta c_3(6) - \Delta y_3(6) \\ &= m_2(6) + \max [z_3 + y_4(5), y_4(6)] - \max [z_3 + y_4(4), y_4(5)] - y_3(6) + y_3(5). \end{aligned} \quad (2.35)$$

⁵We declare a stopping *point* $\tau_k^i(t, n)$ as the realization of a stopping *time* $\tau_k(t, n)$ for a specific price path i .

At ($t = 10$) the largest available number of exercises is 1 with $\tau_1 = 10$. This time the exercise of option ($k + 1 = 2$) occurs at the previous stage $l_9(2) = 1$ and thus

$$\begin{aligned}
 m_{10}(6) &= m_9(6) + \Delta c_{10}(2) - \mathbb{E}[\Delta C_{10}(X_{10}, 2)|x_9] \\
 &\approx m_9(6) + \max[z_{10} + y_{11}(1), y_{11}(2)] - \max[z_{10}, y_{11}(1)] \\
 &\quad - \frac{1}{J} \sum_1^J \max[Z_{10}(\tilde{x}_{10}^j) + Y_{11}(\tilde{x}_{10}^j, 1), Y_{11}(\tilde{x}_{10}^j, 2)] \\
 &\quad + \frac{1}{J} \sum_1^J \max[Z_{10}(\tilde{x}_{10}^j), Y_{11}(\tilde{x}_{10}^j, 1)],
 \end{aligned} \tag{2.36}$$

where \tilde{x}_{10}^j are simulated prices with start value x_9^i according to equation 2.7. At ($t = 11$) all options are already exercised ($k=0$) and therefore the martingale value of the first ($k+1=1$) exercise right will be computed. We have to take into account that the first exercise right was executed at the previous hour $l_{10}(1) = 1$

$$\begin{aligned}
 m_{11}(6) &= m_{10}(6) + \Delta c_{11}(1) - \mathbb{E}[\Delta C_{11}(X_{11}, 1)|x_{10}] \\
 &= m_{10}(6) + \max[z_{11}, y_{12}(1)] - \frac{1}{J} \sum_1^J \max[Z_{11}(\tilde{x}_{11}^j), Y_{12}(\tilde{x}_{11}^j, 1)],
 \end{aligned} \tag{2.37}$$

where \tilde{x}_{11}^j are simulated prices with start value x_{10}^i according to equation 2.7. Likewise we compute $m_t(6)$ for all other t . Next, we calculate the upper marginal value function $\Delta \bar{c}_0(6)$. For $n = 6$ we need to ignore the stopping points τ_1 to τ_5 and can only look for the maximum at the states 0,1, 2, 4, 6, 7, 11 and 12

$$\Delta \bar{c}_0(6) = \max_{t \in \{0,1,2,4,6,7,11,12\}} (z_t - m_t(6)). \tag{2.38}$$

The same way we proceed with all other scenarios 2,...,I. Then we can approximate the marginal upper option value according to equation 2.34. Likewise, we proceed with all other exercise rights $n = 1, \dots, 12$. Again, recall that for every price trajectory and intermediate number of exercise rights n there will be a separate sequence of stopping points and hence a new Figure 2.1. Let us summarize the algorithm:

1. Run a backward iteration to determine the coefficients for all approximated continuation values $\alpha_{r,n,t}$ according to equation 2.12.
2. Generate I new price paths.
3. For each exercise right $n = 1, \dots, N$:
 - a) For each price path $x_t^i, i = 1, \dots, I$:
 - i. Find the stopping points $\pi_0^{*,i}(n-1) = \{\tau_{n-1}^i(0, n-1), \dots, \tau_1^i(0, n-1)\}$ for all ($n-1$) exercise rights in a forward iteration (set $\pi_0^{*,i}(0) = \{\}$).
 - ii. Set $m_1^i(n) = \Delta c_1^i(n)$ and $m_0^i(n) = 0$.
 - iii. For each stage $t = 2, \dots, T$:
 - A. Find in $\pi_0^{*,i}(n-1)$ the highest exercise right k whose stopping point $\tau_k^i(0, n-1)$ lies within the remaining delivery period from t to T (set $k = 1$ for $\pi_0^{*,i}(0)$).
 - B. Check whether the ($k+1$)-th option was exercised at the previous stage ($l_{t-1}^i(k+1) = 1$).

- C. if it was, then generate another set of J prices \tilde{x}_t^j starting from x_{t-1}^i and calculate $m^i(n)$ according to equation 2.31
 - D. if it was not ($l_{t-1}^i(k+1) = 0$), then calculate $m^i(n)$ according to equation 2.32 without any extra loop
 - iv. Compute the upper value functions $\Delta \bar{c}_0^i(n)$ according to equation 2.34, do not forget to skip all stopping points from $\pi_0^{*,i}(n-1)$.
 - b) Average all $\Delta \bar{c}_0^i(n)$ to retrieve an estimate for the marginal upper option values $\Delta \bar{C}_0(n)$.
4. Sum up all marginal option values for the total upper option value $\bar{C}_0(x_0, N)$.

2.4. Upper Bounds for Swing Options with Volume Constraint

So far, our swing option could be used to model a power plant with a single or no production unit per day. In practice, however, a power plant can produce several units per day where the max number of daily units can vary over time. An off-peak swing contract for instance can produce 12 hours on weekdays and 24 hours on weekends. While the price actually also changes with every extra production hour, we want to start simpler and assume a fixed average off-peak price per unit on the same day. Then this off-peak option could produce one 12-hour block on weekdays and two 12-hour blocks on weekends. We want to call this option a swing option with *volume constraint*. This new constraint translates into a regular swing option, but with multiple exercises at the *same* stage.

The main difference to our basic model from section 2.1 is the extension of the action space that allows to choose between 1 and up to U_t exercises per stage as long as the remaining number of swings allows so. Note that U_t is deterministic, but can vary over time as required by our off-peak swing option example. Before we look at the upper bound, let us first formally describe the optimal stopping problem. We define the set of admissible policies as

$$\begin{aligned} \Pi_0(N) &:= \Pi_0(N, \{U_t\}_{0 \leq t \leq T}) \\ &:= \left\{ (\tau_N, \dots, \tau_1) \left| \begin{array}{l} \tau_N \leq \tau_{N-1} \leq \dots \leq \tau_1, \\ \sum_{k=1}^N \mathbb{I}_{t=\tau_k} \leq U_t, t = 0, \dots, T, \\ \tau_k \in \{0, \dots, T\} \cup \infty \end{array} \right. \right\}, \end{aligned} \quad (2.39)$$

with $\tau_k := \tau_k(0, N)$ and \mathbb{I} being the indicator function. We look for the policy $\pi_0^*(N) \in \Pi_0(N)$ that will return the maximum expected cash flow

$$C_0^*(x_0, N) = \sup_{\pi_0(N) \in \Pi_0(N)} \mathbb{E}^{(\pi_0(N))} \left[\sum_{k=1}^N Z_{\tau_k} | X_0 = x_0 \right], \quad (2.40)$$

where $\mathbb{E}^{(\pi_0(N))}[\dots]$ stands for the expectation under the Markov chain that follows the policy $\pi_0(N)$. Furthermore we set the cash flow for $\tau_k = \infty$ to $Z_\infty := 0$. We can use a slight modification of our stochastic dynamic program to find the right stopping times. Again, the value function $C_t(X_t, n)$ is the value of an option that would be newly issued at t with current price X_t and n remaining exercise rights. Whereas the continuation value Q_{t+1} is the

expected option value at the next stage $t + 1$ conditional on today's price

$$\begin{aligned}
 C_t^*(X_t, n) &= \max_{a_t \in A_t(n, U_t)} \{Z_t(X_t, a) + \mathbb{E}[C_{t+1}^*(X_{t+1}, n - a) | X_t]\} \quad t = 0, \dots, T \\
 \text{state : } &(X_t, n) \quad n: \text{remaining number of swings} \\
 \text{action : } &a \in A_t(n, U_t) = \{0, 1, \dots, \min(n, U_t)\} \quad \text{number of exercises} \\
 \text{transition : } &\{X_t, n\} \longrightarrow \{X_{t+1}, n - a_t\} \\
 \text{marginal profit : } &Z_t(X_t, a) := (X_t - K)^+ a \\
 \text{value function : } &C_t^*(X_t, n) \\
 \text{continuation value : } &Q_{t+1}^*(X_t, n) := \mathbb{E}[C_{t+1}^*(X_{t+1}, n) | X_t],
 \end{aligned} \tag{2.41}$$

where $C_{T+1}^*(X_{T+1}, n) := 0$ for $n = 1, \dots, N$. As a brief side note we want to remark that if the allowed number of exercises is constant over time i.e. $U_1 = U_2 = \dots = U_T = U$, then the value function at each stage is equivalent to U options that can be exercised once at a time

$$C_t^*(X_t, n) - C_t^*(n - U) = U \cdot (C_t^*(X_t, n) - C_t^*(X_t, n - 1)). \tag{2.42}$$

Let us now return to the upper bounds. Intuitively, the swing option with volume constraint should only require a relaxation of the search domain for the stopping points. Recall that in the unit constraint case the stopping points of all exercised swings will be deleted from the domain space, i.e. $\mathbb{T} \setminus \{\tau_{n-1}, \dots, \tau_1\}$ with $\mathbb{T} := \{0, \dots, T\}$. The new domain definition for finding the n -th stopping time \mathbb{T}_{n-1} instead contains, loosely speaking, all still exercisable stages from $t = 0$ to T after $n-1$ options were already exercised under the volume constraint U_t . Any stage t will only be entirely excluded from the domain if U_t exercises already occurred at that very stage. This intuition is correct and we receive

$$\begin{aligned}
 \Delta C_0^*(n) &= \inf_{\pi_0(n-1)} \inf_{\{M_t\}_{t \in \mathbb{M}_0}} \left\{ M_0 + \mathbb{E}_0 \left[\max_{t \in \mathbb{T}_{n-1}} (Z_t - M_t(n)) \right] \right\} \\
 \mathbb{T}_n &= \mathbb{T} \setminus \left\{ t_i \in \mathbb{T} : \sum_{j=1}^n \mathbb{I}_{\{\tau_j = t_i\}} = U_{t_i} \right\},
 \end{aligned} \tag{2.43}$$

with $\Delta C_0(n)$ as defined in equation 2.26 and $\tau_j := \tau_j(0, n - 1)$. However, the proof that equation 2.43 actually truly holds is not straightforward. For the detailed proof we refer to Bender [8] who will publish a detailed version in one of his upcoming papers. We only want to present the rational behind the proof and provide first numerical results.

The core idea of the proof is to rewrite the swing option value in terms of a sum of American options. Then we can apply the Andersen and Broadie primal-dual algorithm for each individual American option to come up with a total upper bound for the swing option. For a better understanding of the new calculation method let us briefly recap our existing model. So far, we have built a stochastic dynamic program with a strict sequence of discrete time steps $t = 0, \dots, T$, each defined by a two dimensional state space consisting of the continuous price X_t and the discrete number of remaining exercise rights n . During the backward iteration we move stage by stage back from T to 0 and iteratively solve the Bellman equation for each 2-dimensional space in order to update our value function $\underline{C}_t(X_t, n)$.

Instead, Bender remains conceptually within the framework of a stopping problem. He thinks of a swing option as a sum of single stopping problems with the decisive difference that the domain of decision stages \mathbb{T}_n shrinks with every new option exercise. Let us first look at a single exercise. We find the first stopping time $\tau_1 := \tau_1(0, n)$ (possibly with the help of a stochastic dynamic program) and exercise. If U_{τ_1} is greater than 1 then the stage

will be valid for the next exercise as well and we will have still the entire domain available for the second exercise right. The stopping problem is identical to the first one and hence $\tau_2 := \tau_2(0, n) = \tau_1$. In short, we will execute at τ_1 as long as U_{τ_1} allows to do so. After U_{τ_1} exercises we will look at a new stopping problem where the new search domain will skip τ_1 : $\mathbb{T}_{n-U_{\tau_1}} := \mathbb{T}_n \setminus \{\tau_1\}$. We will find a new first stopping time τ_2 where we will exercise the next U_{τ_2} options. Afterwards we update our domain again $\mathbb{T}_{n-U_{\tau_1}-U_{\tau_2}} := \mathbb{T}_{n-U_{\tau_1}} \setminus \{\tau_2\}$ and repeat the previous steps until all N swing rights are exercised. Note that different to a regular forward iteration we always start the search for the next stopping time again at $t = 0$.

The proof needs to show that this iterative solving of American options in deed leads to the optimal swing option value. The derivation is based on induction. Finding the first stopping time is identical to solving the standard Snell envelope

$$C_0^*(x_0, 1) = \sup_{\tau_1} \mathbb{E}_0 [Z_{\tau_1}], \quad (2.44)$$

with stopping time $\tau_1 = \tau_1(0, N) \in \mathbb{T}_1$ with $\mathbb{T}_1 := \{0, 1, \dots, T\} \cup \infty$. For two exercise times, Bender proves that one of the two stopping times is identical to the single stopping time problem and that the second one can be found by solving the Snell envelope over the time domain that ignores τ_1

$$\begin{aligned} C_0^*(x_0, 2) &= \sup_{\tau_1, \tau_2} \mathbb{E}_0 \left[\sum_{k=1}^2 Z_{\tau_k} \right] \\ &= Z_{\tau_1^*} + \sup_{\tau_2} \mathbb{E}_0 [Z_{\tau_2}], \end{aligned} \quad (2.45)$$

with $\tau_1 := \tau_1(0, N) \in \mathbb{T}_1$ and $\tau_2 := \tau_2(0, N) \in \mathbb{T}_2$ with $\mathbb{T}_2 := \mathbb{T}_1 \setminus \{\tau_1^*\}$. Bender actually does not explicitly reduce the domain space, but works with a modified cash flow process $Z_t^{[\tau_1]}$ that penalizes payments at invalid stages

$$Z_t^{[\tau_1, \dots, \tau_n]} := \begin{cases} Z_t & \sum_{j=k}^n \mathbb{I}_{\{\tau_k=t\}} < U_t \\ -1 & \text{otherwise,} \end{cases} \quad (2.46)$$

with $\tau_k := \tau_k(0, N)$. Finally, Bender induces from n to $n+1$ and proves that equation 2.45 holds true for any N exercise rights

$$\begin{aligned} C_0^*(x_0, N) &= \sup_{\pi_0(N)} \mathbb{E}_0 \left[\sum_{k=1}^N Z_{\tau_k} \right] \\ &= \sum_{k=1}^{N-1} Z_{\tau_k^*} + \sup_{\tau_N} \mathbb{E}_0 [Z_{\tau_N}], \end{aligned} \quad (2.47)$$

where $\tau_N \in \mathbb{T}_N$ with $\mathbb{T}_N := \mathbb{T}_{N-1} \setminus \{\tau_{N-1}^*\}$ and exercise policy $\pi_0(N)$ as defined in equation 2.40. Hence, the swing option valuation can be separated in solving a chain of individual American style stopping problems with interdependent, but still individual search domains. Then the proof for the upper bound is straightforward. We simply apply Roger's duality on all individual stopping problems and the sum delivers the upper bound for the entire swing option. This procedure also works for the regular swing option with $U_t = 1$ for all t . A direct implementation of this new valuation method is not advisable. While it is appealing to rerun the same American-style valuation algorithm with every additional exercise right and only change the input data i.e the cash flow process $Z_t^{[\tau_n]}$, this procedure would not be valid. Recall that the sequence of actual stopping points $\pi_0^i(N)$ varies with every price path

i. Consequently, the same hour t will be a stopping point and thus be erased for only some scenarios dependent on individual price trajectories. Hence, each stage is not uniquely defined any more across all scenarios. Then, the pairs of current price and next hour's value function relevant for the LS regression are not well-defined any more. Then, the modified cash flow process can violate the Markov property and therefore the individual stopping times cannot be computed with dynamic programming any longer. However, as Bender's proof leads to the result in equation 2.43, we can start from our algorithm of the previous section. We only need to revise the domain space by the multiple exercise constraint U_t . Then we can use the approximated policy of our lower bound option in equation 2.41 to compute the upper bound. The computation of the marginal martingales and value functions follows the equations 2.30 to 2.32. The only minor adjustment is the definition of the indicator function that needs to take into account U_t before signaling an option exercise

$$l_t(X_t, k) := \begin{cases} 1 & Z_t(X_t) \geq \Delta Y_t(X_t, k) \wedge \sum_{j=1}^{k-1} \mathbb{I}_{\{\tau_j=t\}} < U_t \\ 0 & \text{otherwise.} \end{cases} \quad (2.48)$$

Also, the computation of the marginal upper value function needs to follow the new domain space

$$\begin{aligned} \Delta \bar{c}_0^i(n) &= \max_{t \in \mathbb{T}_{n-1}} (z_t^i - m_t^i(n)) \\ \Delta \bar{C}_0(n) &\approx \frac{1}{I} \sum_{i=1}^I \Delta \bar{c}_0^i(n), \end{aligned} \quad (2.49)$$

where \mathbb{T}_{n-1} is defined as in equation 2.43. Again, let us illustrate the marginal martingale computation. We extend our previous example by allowing 2 exercises at hour 5 and hour 9. Figure 2.2 presents a slight modification of Figure 2.1. The graph shows us again the stopping points of a single price path with 12 stages. This time we look at a swing option with volume constraint and therefore it is no surprise that we observe multiple stopping points at both hours 5 and 9. Recall that we found these stopping points using the policy $\pi_0^1(5)$ as we will compute again the 6th marginal martingale. The figure shows us the stopping points. We

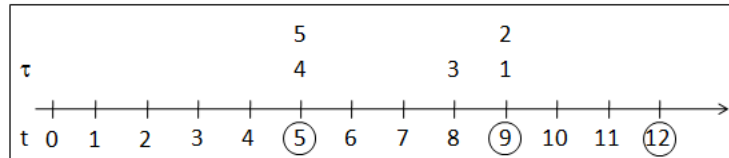


Figure 2.2.: Computation of the marginal martingales in case of swing option with volume constraints

will illustrate the computation at three different stages $t = 5, 9$ and 12 . Again, we will ignore the index $i = 1$ for indicating the realization of the first price scenario. At $(t = 5)$ the largest k is still 5 and consequently there cannot be any previous exercise ($l_4(6) = 0$)

$$\begin{aligned} m_5(6) &\approx m_4(6) + \Delta \underline{c}_5(6) - \Delta y_5(x_4, 6) \\ &= m_4(6) + \max[z_5 + y_6(5), 2z_5 + y_6(4), y_6(6)] \\ &\quad - y_5(6) + y_5(5). \end{aligned} \quad (2.50)$$

Note, that we have to consider the second exercise right ($2z_5$) at $(t = 5)$ when computing $\underline{c}_5(5)$ and $\underline{c}_5(6)$ for the marginal value functions $\Delta \underline{c}_5$. At $(t = 9)$ the largest available number

of exercises is also two ($U_9 = 2$) and this time the third swing was exercised on the previous stage ($l_8(3) = 1$)

$$\begin{aligned}
 m_9(6) &= m_8(6) + \Delta c_9(2) - \mathbb{E}[\Delta C_9(X_9, 2)|x_8] \\
 &\approx m_9(6) + \max[z_9 + y_{10}(1), 2z_9, y_{10}(2)] - \max[z_9, y_{10}(1)] \\
 &\quad - \frac{1}{J} \sum_1^J \max[Z_9(\tilde{x}_9^j) + Y_{10}(\tilde{x}_9^j, 1), 2Z_9(\tilde{x}_9^j), Y_{10}(\tilde{x}_9^j, 2)] \\
 &\quad + \frac{1}{J} \sum_1^J \max[Z_9(\tilde{x}_9^j), Y_{10}(\tilde{x}_9^j, 1)],
 \end{aligned} \tag{2.51}$$

where \tilde{x}_9^j are simulated prices with start value x_8^i according to equation 2.7. At ($t = 12$) all options are already exercised and there was no exercise on the previous stage ($l_{11}(1) = 0$). Hence, we get

$$\begin{aligned}
 m_{12}(6) &\approx m_{11}(6) + \Delta C_{12}(1) - \Delta y_{12}(1) \\
 &= m_{11}(6) + z_{12} - y_{12}.
 \end{aligned} \tag{2.52}$$

Likewise we compute $m_t(6)$ for all other t . Next, we derive the upper marginal value function $\Delta \bar{c}_0(6)$. For $n = 6$ we need to ignore the stopping points τ_1 to τ_5 . Compared to our previous example there are more valid stages to consider due to the multiple exercises. To be precise this is additionally $t = 4$ and $t = 10$

$$\Delta \bar{c}_0(6) = \max_{t \in \{0,1,2,3,4,6,7,10,11,12\}} (z_t - m_t(6)). \tag{2.53}$$

As this example illustrates the algorithm for the swing option with volume constraint is almost identical to the regular swing option. The single difference lies within the calculation of the marginal value function $\Delta C_t(n)$ that needs to take into account all possible exercises a_t on state $C_t(n)$ and $C_t(n-1)$. The relevant exercise right k for the marginal martingale at stage t is still the largest available exercise right from t onwards regardless whether there is a single or several exercises at t as illustrated for ($t = 5$). Hence, the extension is fairly simple and easier to implement than another proposal by Aleksandrov and Hambly [1]. They only recently presented a derivation of the upper bound of a swing option with volume constraints. They were not able to reuse the algorithm for the unit constraint case and rather extended the initial proof by Meinshausen and Hambly resulting in a comparably complex implementation.

2.5. Numerical Examples

For our numerical example we start with the same swing option setup that Meinshausen and Hambly [50] used for their illustrations. They investigate an in-the-money (itm) swing option with strike $K = 0$ and a single exercise right per hour. They defined a delivery period of $t = 0, \dots, 1000$ hours and allowed up to $N = 100$ swings. By setting the mean μ to zero they reduce their initial price process (see equation 2.7) to a discrete Ornstein-Uhlenbeck process with parameters

$$\sigma = 0.5, \quad \kappa = 0.9, \quad \mu = 0, \tag{2.54}$$

and $x_0 = 1$ (see Appendix C for sample paths). Meinshausen and Hambly rely on the Longstaff Schwartz algorithm and run a regular linear regression with the basis functions $\Psi_{1,n}(X_t) = 1$

and $\Psi_{2,n}(X_t) = X_t$

$$Y_{t+1}(X_t, n) := \alpha_{0,n,t} + \alpha_{1,n,t}X_t. \quad (2.55)$$

In order to obtain the lower bound, they use 1000 price scenarios to pre-calculate the parameters $\alpha_{r,n,t}$ necessary to approximate the optimal exercise policy. Figure 2.3 illustrates the resulting exercise policy by plotting the indicator functions according to equation 2.16 for various marginal swing rights. The shape of the functions along the timeline resembles

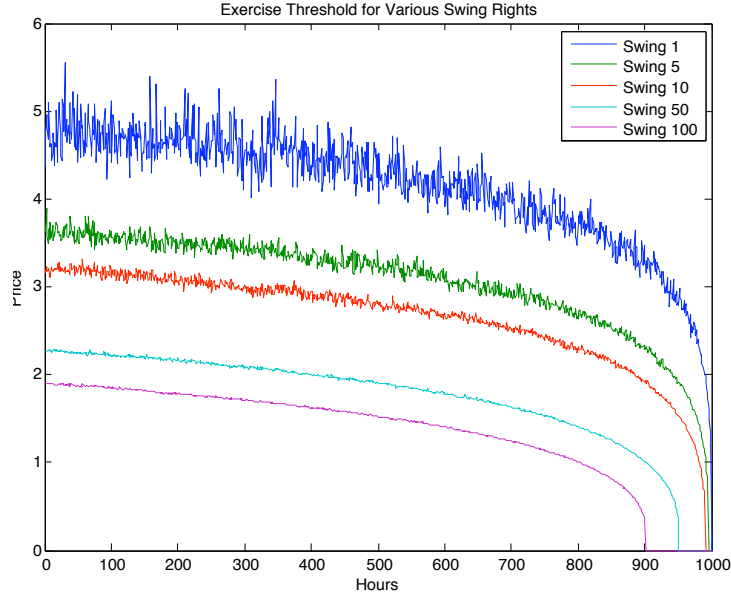


Figure 2.3.: Indicator functions for different exercise rights

a concave curve and reflects the intuitive decision rule that a smaller exercise price will be accepted the closer one gets to the final expiration. At the last delivery hour any price above 0 will be accepted for the first exercise right. The same argument explains the nested structure of the indicator functions which start at a lower price for every additional exercise right. The more rights are still available the smaller the price threshold for the next exercise. The indicator functions touch the timeline at that time step where the remaining number of hours is identical to the remaining number of swings. This is a technical side-effect resulting from the simulation (formally the threshold functions are smooth curves). Any swing right larger than the remaining time period is automatically expired and therefore the threshold is 0. We can also observe that the concave curve becomes smoother with increasing number of swings. High prices are rare and differ more in size than prices around the average (since $x_0 = 1$ and $\mu = 0$ the prices deviate around 1). Every swing right tries to capture the highest available price. Thus with every additional swing the remaining prices are more and more equal in size and therefore the jitter becomes weaker. Once the continuation values are approximated, the indicator functions and thus the set of stopping points $\pi_0^i(N)$ is fixed for one price scenario i . All swing options with intermediate upper swing number $n < N$ will be based on a subset of $\pi_0^i(N)$. However, their stopping sequence in declining order according to the Meinshausen and Hambly definition (see section 2.3) varies with every n . In other words, the same exercise hour for the same price path can be the first, second or n -th stopping point for different n . This is the very reason why we do not compute all N stopping points once for all n iterations of a single price path beforehand in our upper bound algorithm in section 2.3 and 2.4. Instead

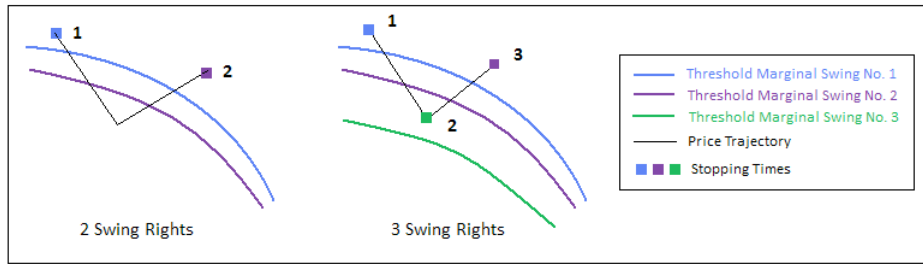


Figure 2.4.: Sequence of stopping times for two and three swing rights

we have to re-compute the new sequence of stopping points $\pi_0^i(n)$ with every intermediate maximum number of stopping rights n . We want to briefly illustrate the behavior with Figure 2.4. The left sub figure shows the exercise thresholds for two swing rights and the corresponding price path. The swings will be exercised once the price exceeds one of the thresholds. The marks on the trajectory indicate an exercise and the color corresponds to the threshold line that was the trigger. In the right sub figure we see the situation for three swing rights. Now there is an extra trigger line for the third swing right located below the other two as explained in the previous paragraph. The new marks on the price trajectory demonstrate that the threshold for the third marginal swing right now triggers the second stopping time. It also underlines that the initial two stopping times still belong to the optimal policy, only the sequence changes due to the additional swing right. In this case $\tau_2(0, 2) = \tau_3(0, 4)$.

Let us now return to the lower bound calculation. After the approximation of the continuation values Meinshausen and Hambly generate another 1000 price paths and apply their exercise policy in a forward iteration to receive the actual lower bound $\underline{C}_0(n) := \overline{C}_0(x_0, n)$. We follow exactly their approach. The second column of Table 2.3 shows our results for different numbers of initial swing rights n . These lower bound values differ from the results of Meinshausen and Hambly by less than $\pm 0.5\%$. Next, we compute the corresponding upper

n	$\underline{C}_0(n)$	$\Delta D_0(n)$	$[\underline{C}_0^{(99\%)}(n), \overline{C}_0^{(99\%)}(n)]$
1	4.777	0.004	[4.697 , 4.783]
2	9.029	0.022	[8.922 , 9.069]
3	13.051	0.028	[12.924 , 13.132]
4	16.842	0.024	[16.699 , 16.965]
5	20.463	0.033	[20.308 , 20.601]
10	37.346	0.023	[37.130 , 37.625]
15	52.668	0.028	[52.408 , 53.040]
20	66.981	0.022	[66.686 , 67.439]
30	93.670	0.020	[93.314 , 94.709]
40	118.452	0.015	[118.053 , 119.877]
50	141.799	0.039	[141.361 , 143.558]
60	164.044	0.012	[163.571 , 166.020]
70	185.414	0.021	[184.910 , 187.856]
80	205.983	0.036	[205.447 , 209.068]
90	225.876	0.021	[225.313 , 229.411]
100	245.154	0.032	[244.562 , 249.015]

Table 2.3.: Swing option with unit constraint

bounds for the swing option. Again we follow the setup by Meinshausen and Hambly and

use $I = 20$ price scenarios for the outer loop and $J = 50$ trajectories for the inner simulation. The third column presents the corresponding duality gaps of the marginal swing rights i.e. the difference of the upper and lower option value for the n -th marginal swing right $\Delta D_0(n) = \Delta \bar{C}_0(n) - \Delta \underline{C}_0(n)$. Let us first look at the duality gap for the American option ($n = 1$). With $\Delta D_0(1) = 0.004$ the gap is negligibly small which underlines the good approximation of the exercise policy and thus the efficiency of the Longstaff-Schwartz approximation procedure in case of an American option. Also note that the additional noise introduced by the nested loops does not have a significant numerical effect. However, the situation changes when we move to the swing option ($n > 1$). Already in case of two swings the duality gap increases from 0.004 to 0.022. At least for any further number of swings this gap does not increase any more, but varies between 0.015 and 0.039 with an average around 0.031 throughout all swing rights. Meinshausen and Hambly present similar results. Their total duality gap for 100 swings for instance is $248.63 - 245.157 = 3.47$ which breaks down to an average marginal duality gap of 0.0347 and lies within our computed ranges. There is no relation between gap size and number of swings. Our duality gap is rather stable around 0.025. We assume that the gap could be narrowed even further with a more refined set of basis functions $\Psi_{r,n,t}$ for the Longstaff Schwartz regression. Recall that we currently only apply linear regression.

The last column in Table 2.3 shows the upper and lower bound of the swing option not on the marginal, but on the total level. Hence, for $n = 30$, the marginal gap of the 30th swing right is 0.020 and the option value for all 30 swing rights varies between 93.314 and 94.709. These intervals are based on the $1 - \beta = 99\%$ confidence level. For the purpose of direct comparison we follow Meinshausen and Hambly's definition of the confidence interval $[\underline{C}_0^{(1-\beta)}(n), \bar{C}_0^{(1-\beta)}(n)]$. They apply the confidence level of a Normal distribution. The distribution of our value function is not necessarily Normal and the authors do not provide any other legitimation than the asymptotic convergence to the Normal distribution. They apply the two variances of the value functions for the lower and upper bound calculation separately

$$\begin{aligned}
 \underline{C}_0^{(1-\beta)}(n) &:= \underline{C}_0(x_0, n) - \beta \frac{\underline{\sigma}(n)}{\sqrt{I}} \\
 \bar{C}_0^{(1-\beta)}(n) &:= \bar{C}_0(x_0, n) + \beta \frac{\bar{\sigma}(n)}{\sqrt{I}} \\
 \underline{\sigma}(n) &\approx \sqrt{\frac{1}{I} \sum_{i=1}^I (v_0^i(n) - \underline{C}_0(n))^2} \\
 \bar{\sigma}(n) &\approx \sqrt{\frac{1}{I} \sum_{i=1}^I (\bar{c}_0^i(n) - \bar{C}_0(n))^2} \\
 \underline{C}_0(n) &\approx \frac{1}{I} \sum_{i=1}^I v_0^i(n) \\
 \bar{C}_0(n) &\approx \frac{1}{I} \sum_{i=1}^I \sum_{k=1}^n \Delta \bar{c}_0^i(k)
 \end{aligned} \tag{2.56}$$

where $\beta = \Phi^{-1}(1 - 0.01/2)$ is the quantile of the standard normal distribution, $\Delta \bar{c}_0^i(k)$ is defined in equation 2.34 and $v_0^i(n)$ is the ACF of a single path (see equation 2.9). Our confidence intervals are slightly larger than the ranges that Meinshausen and Hambly presented. We could only meet their figures if we increased the number of external scenarios from 20 to 200 which narrowed the volatility.

Finally we want to produce the same figures for the case of a swing option with volume

constraint. We return to our initial example of an off-peak swing option that allows to exercise the off-peak price twice on weekends since there are no peak hours. We introduce the number of maximum exercise rights U_t . Now we interpret each stage as days instead of hours and define $t = 1$ as Monday. Then, we set $U_t = 2$ for $t = 6, 7, 13, 14, \dots, 992, 993, 1000$ and everywhere else $U_t = 1$. Again, we pre-calculate the relevant parameters $\alpha_{r,n,t}$ to approximate the exercise policy by running our dynamic program in equation 2.41 on our first set of 1000 price scenarios. With our second set of 1000 trajectories we compute the lower bound value within a forward iteration (see second column of Table 2.4). By design, for a single right the values are identical to the unit constraint case. The more swing rights are available the more multiple exercises will occur and the higher the difference between unit and volume constraint swing options (compare second column of Tables 2.3 and 2.4). For two swings we start with a value difference of $9.15 - 9.029 = 0.121 \hat{=} 1.3\%$ and end with a spread of $258.706 - 245.154 = 13.55 \hat{=} 5.53\%$ for 100 rights. However, this effect might be even stronger in reality where weekend off-peak prices are higher than weekday off-peak prices. Then multiple exercises on weekends would occur even more often than in our example where the average price does not vary throughout the entire delivery period. In order to compute the marginal duality gap in

n	$\underline{C}_0(n)$	$\Delta D_0(n)$	$[\underline{C}_0^{(99\%)}(n), \overline{C}_0^{(99\%)}(n)]$
1	4.777	0.004	[4.697 , 4.783]
2	9.150	0.017	[9.028 , 9.288]
3	13.290	0.029	[13.144 , 13.414]
4	17.228	0.024	[17.057 , 17.372]
5	21.035	0.009	[20.844 , 21.242]
10	38.496	0.015	[38.239 , 39.141]
15	54.541	0.019	[54.227 , 55.184]
20	69.611	0.027	[69.251 , 71.245]
30	97.633	0.021	[97.202 , 98.882]
40	123.806	0.011	[123.316 , 125.965]
50	148.550	0.030	[148.009 , 151.008]
60	172.184	0.020	[171.602 , 174.815]
70	194.879	0.023	[194.258 , 197.948]
80	216.820	0.012	[216.161 , 220.088]
90	238.070	0.026	[237.376 , 241.198]
100	258.706	0.025	[257.981 , 262.018]

Table 2.4.: Swing option with volume constraint

the third column we apply the algorithm of the previous chapter. Like for the unit constraint swing option the duality gap does not significantly alter with more swing rights. If we compare the figures with the unit constraint case we can observe slightly smaller gaps. The average of the duality gap across all swing rights is still around 0.025, but the range is a bit smaller moving between 0.017 to 0.03. Consequently, the confidence intervals are smaller too. For 100 swing rights, for instance, the difference between the upper and lower bound is $262.218 - 257.981 = 4.237$ which is slightly smaller compared to the unit constraint case of $249.015 - 244.562 = 4.453$. We can only explain this improvement with a better approximation of the continuation values as less different exercise points and thus less LS regressions are necessary to return the total option value. But the small difference could very well be only noise in the data. We therefore take another look at the variation of the marginal duality gaps. Figure 2.5 compares the 99 % confidence level of the marginal duality gap between the unit and volume constraint case. For consistency, we used again 200 instead of 20 external scenarios. In both

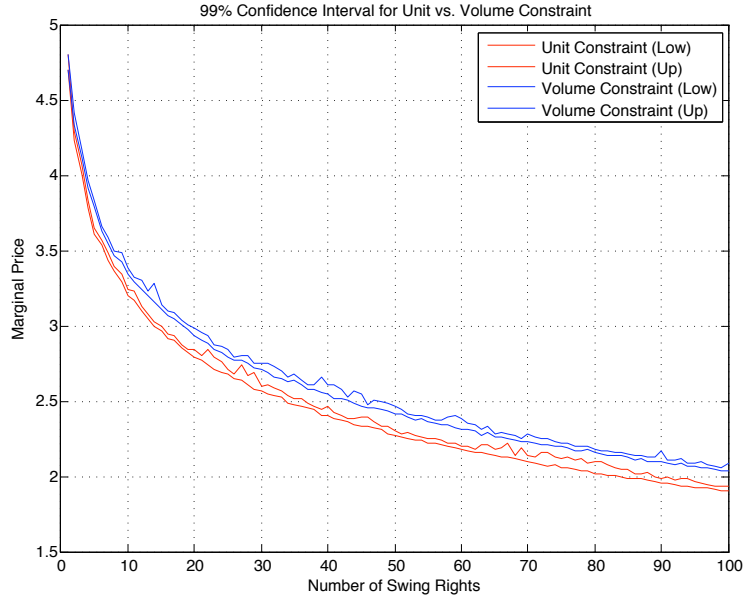


Figure 2.5.: 99 % Marginal duality gap (99 % confidence level) across 100 exercise rights (unit vs. volume constraint)

situations we observe a convex function as high prices will be exercised first. Not surprisingly the marginal swing values are higher in case of multiple exercises as higher prices can be executed more often. We can see that the lower bound of the confidence intervals are fairly smooth, almost like a straight line. The upper bound instead deviates more frequently for both type of swing options which we explain by the additional noise generated by the nested Monte-Carlo loop. Even though the bandwidth of the swing option with volume constraint seems to be slightly smaller, the deviation of the intervals across all swing rights is about the same size for both type of swing options. As a summary, we can state that the upper bound of the swing option with volume constraint is at least as accurate as the swing option with single exercises per stage. This observation is also true for different strikes and drift terms of the underlying price process (in Appendix B you will find two more examples: i) an atm option ($K=1$) and ii) drift term $\mu = 1$).

2.6. Directions for Further Research

Our results revealed that the duality gaps of a unit and volume constraint swing option are very similar in nature and scale. In both cases we observe a larger deviation of the upper bound value compared to the lower bound (see again Figure 2.5). The deviation is certainly induced by the nested loop. Improving the accuracy of the inner nested Monte-Carlo simulation would therefore be an immediate next step. First, it is worth investigating different basis functions other than the pure linear function that Meinshausen and Hambly suggested. In particular, the linear approach becomes problematic if the strike is non-zero. Then the payoff function Z is not linear any more for positive prices ($X_t \geq 0$). Second, one could try to reduce the amount of nested loops. Broadie [12] recently proposed several related adjustments to his algorithm for American options that are applicable for the swing option as well. Third, one could replace the nested loop entirely and estimate the martingale with the algorithm proposed by Schoemaker [6]. His algorithm is restricted to stochastic processes

based on Brownian motion, but it would still cover our mean-reversion price dynamics.

Our swing option with volume constraint is able to cover several extensions. An immediate next step towards a swing option with 24 exercises per day would look at a baseload swing option that can exercise twice a day. On weekdays the first swing would represent the production during peak hours with the average peak price. The second swing would stand for the off-peak hours with the average off-peak price. On weekends we would again allow to exercise the average off-peak price twice for the night and day hours. The upper bound for such a baseload option can be computed with our current model. One would only need to split the days in 2 half days representing the peak and off-peak hours and then apply the upper bound for the swing option with unit constraint. In a second step we could additionally allow to vary the generation amount during peak and off-peak hours. This extension can also be covered with our swing option with volume constraint. We would need to discretize the production amount into multiples of a predefined minimal energy size that would represent a single exercise. Then each half day would again allow multiple exercises of these energy buckets.

Recall that our objective is the investigation of power generation assets. The swing option was only meant as a first step towards a general upper bound calculation for power plants. Several further operational constraints need to be considered for a proper real option model of a power plant. A first important extension towards an upper bound value for a generation asset would be the introduction of on- and off-hours to the swing option. In context of optimal stopping times this would mean that a single stopping time would entail a subsequent row of n stopping times where n is the minimal number of running hours. We would call it a *swing option with time constraint*. The lower bound value can be computed via SDP. Compared to our existing model in equation 2.41 we only need to add another state dimension J for the running hours since the last start-up (see also section 4.3.2 for a detailed description of this extra operating state). Intuitively one would assume that our upper bound algorithm works analogously. Once we have computed the optimal lower bound policy we can define a new indicator function l_t that determines the exercise sequence for any new price path. Whenever l_t signals an exercise during the calculation of the marginal martingale, the computation of ΔQ_t would as usual trigger a nested loop and we would use the continuation values of our new SDP to quickly run the inner simulation. The trigger might become additionally dependent on the current run-time hours. An exercise that is mandatory to meet the minimum run-time might require a special treatment for the calculation of ΔQ_t . Still, we assume that a swing option with time constraint can rely on our existing primal-dual upper bound framework and only requires another modification of the domain space \mathbb{T} . A formal proof would certainly be an interesting next research topic.

3. Risk Management

In the previous chapter we focused on attaining the option value by maximizing the expectation of future cash flows and tried to find the corresponding optimal stopping times. In a complete market this is the preferred approach since we can always find a replication portfolio H that offsets the option exposure C completely: $C^{\text{com}} - H^{\text{com}} = 0$. In this way the option value C^{com} can be locked no matter how the prices are fluctuating. Therefore a natural replication portfolio for swing options would contain the products available at the electricity market i.e. Forwards, Futures and hourly spot contracts. However, the market for these products is illiquid. Hourly electricity is only traded on the day ahead market and monthly products go only half a year ahead. Furthermore the amount of energy traded on the Futures market is increasing, but still limited. Hence, we will see that the replication portfolio might fail to hedge the option entirely, especially for production periods with larger time horizons (>3 years). The incompleteness of the market asks for an additional risk premium that reflects the open gap ϵ due to the sub optimal hedge: $C^{\text{incom}} - H^{\text{incom}} - \epsilon = 0$. We want to work out the nature of this gap and define means to control this risk. This chapter is therefore divided into two parts. In the first section we analyze the origin of the market incompleteness in detail by investigating the different components of the electricity price. We start from the construction of an hourly price Future curve (PFC) and quantify the impact of individual price factors on the derivative value. We will also introduce two new risk measures: synthetic spot delta and Earnings-at-Risk. In the second part of this chapter we address to risk controlling in incomplete markets. We will define a risk adjusted option value and suggest appropriate exercise policies that lower the risk premium, but still achieve an adequate fair value. Based on this concept we will define a benchmark to compare different risk mitigation strategies. We will introduce a heuristic that delivers a strategy in favor of our benchmark and conclude this chapter with an outlook for further research.

3.1. Introductory Example

We want to motivate the objective of this chapter with an introductory example. Let us assume the following scenario: We are a dispatcher of a power plant on Monday, 29th June 09 and need to decide on the energy allocation for the remaining days in June i.e. for today and tomorrow. Our power plant can produce every day up to 1 MW and we are required to produce another 1 MW within the remaining two days. There are no marginal costs and no runtime constraints i.e. each day's production is only linked via the shared energy constraint. Today's spot price $X_0 = x_0$ is known to us. There is a Balance-of-Month June-09 Futures contract available to us with current price $G_0 = g_0$ that stands for the market's expectation of the average electricity price throughout the remaining delivery period in June which in our case is only today and tomorrow. If we buy the Future today, we commit to a margin payment tomorrow which is the difference between today's and tomorrow's Futures price. Tomorrow's spot price X_1 is not known to us. We therefore need to model future spot prices. In our example this is a combination of the Future price G_1 and a shift factor S_1 with random daily return rates $r_g \sim N(0, \sigma_g^2)$ and $r_s \sim N(0, \sigma_s^2)$. For illustration purposes we ignore correlation and normalization (see equation 3.32). Today's shift factor S_0 happens to be identical to our deterministic seasonal adjustment factor α_0 that reflects today's and tomorrow's day type (see

also discussion around equation 4.3). Usually the current (conditional) expectation of future spot prices will be plotted on a so called hourly price Future curve (PFC) $H_t := \mathbb{E}[X_t|G_0 = g_0]$ (see also equation 3.31). In particular we get $H_1 := \mathbb{E}[X_1|G_0 = g_0] = \alpha_0 g_0$. Let us summarize the parameter settings:

1. Two decision stages $t = \{0,1\}$ (Monday and Tuesday)
2. Marginal cost $K = 0$
3. Future price
 - a) today's Future price $G_0 = g_0$ is known
 - b) tomorrow's Future price G_1 is unknown
 - c) daily return rate $r_g = (G_t - G_{t-1})/G_{t-1} \sim N(0, \sigma_g^2)$
4. Spot prices
 - a) today's spot price $X_0 = x_0$ is known
 - b) today's and tomorrow's day type factors are known and identical $\alpha_1 = \alpha_0$
 - c) today's spot price component is identical to today's day type factor $S_0 := \alpha_0$
 - d) tomorrow's spot price is unknown $X_1 = S_1 G_1 = g_0 \alpha_0 (1 + r_g)(1 + r_s)$
 - e) daily return rate $r_s = (S_t - S_{t-1})/S_{t-1} \sim N(0, \sigma_s^2)$
5. Return rates are independent $Cov(r_s, r_g) = 0$
6. Mandatory remaining generation for June 09 $W_0 = 1$ MWh.
7. Daily maximum production $w_{0,1} = 1$ MWh.

Formally we can define a dynamic program where the state space has three dimensions: the spot price X_t , the Future price G_t and the remaining energy n (0 or 1 MWh). The marginal profit Z_t is identical to the current price X_t if 1 MWh will be produced. Otherwise it is zero. The action set A differs between no or 1 MWh energy production. The value function $C_t(X_t, G_t, n)$ is the value of a real option for the production period from t to T that would be newly issued at t given today's prices X_t, G_t and $n = 0,1$ MWh remaining energy. Likewise the continuation value Q_{t+1} is the expected option value given today's observed price on the shaped Future curve $X_t := S_t G_t$ and $n=0$ or $n=1$ MWh remaining energy. In order to find the best energy allocation and thus the real option value with 1 MWh remaining energy $C_0(x_0, g_0, 1)$ we can express the value function via the Bellman equation and find the maximum of today's versus tomorrow's production

$$\begin{aligned}
 C_t(X_t, G_t, n) &= \max_{a \in A(n)} \{Z_t(X_t, a) + \mathbb{E}[C_{t+1}(X_{t+1}, G_{t+1}, n - a)|G_t]\}, \quad t = 0, 1 \\
 \text{state : } (X_t, n) \quad n &\in \{0, 1\} \quad \text{remaining energy, 0 or 1 MWh} \\
 \text{action set : } a \in A(n) &= \{0, \min(n, 1)\} \quad \text{generate yes (1) or no (0)} \\
 \text{transition : } \{X_t, G_t, n\} &\longrightarrow \{X_{t+1}, G_{t+1}, n - a\} \\
 \text{marginal profit : } Z_t(X_t, a) &:= aX_t \quad \text{value of single day production} \\
 \text{value function : } C_t(X_t, n) & \\
 \text{continuation value : } Q_{t+1}(G_t, n) &:= \mathbb{E}[C_{t+1}(X_{t+1}, G_{t+1}, n)|G_t],
 \end{aligned} \tag{3.1}$$

where $C_2(X_2, G_2, n) := 0$ for $n=0,1$. Let us review the transition law in detail. G_1 is based on g_0 with distribution $G_1 \sim N(g_0, \sigma_g)$. The spot price X_1 instead does not rely on the previous

spot price x_0 , but on the current hourly price Future curve $\alpha_0 g_0$. Precisely speaking the transition law from Monday's to Tuesday's spot price only relies on the current Future price g_0 . This is why the continuation value $Q_{t+1}^*(G_t, n)$ is independent of X_t . From parameter setting 4d) we know that the Tuesday price X_1 is defined by a sum of normal and a product of two normal variables with zero mean. Its distribution can still be calculated analytically (see Springer [60]). Note that we do not use log returns. Thus, theoretically the Tuesday spot price X_1 could become negative for high volatilities σ_s and σ_g . In fact, this construction does reflect the real market situation. The European energy exchange accepts negative spot prices since 2008 and it occurred only recently during the Christmas holidays 2009 where wind energy drastically exceeded the demand (thus paying for delivering power to a counterparty can be cheaper than getting charged by the grid operator for exceeding schedule nominations). As we assume stochastic independence between S_t and G_t , the expectation of the Tuesday price is only dependent on the day type factor α_0 and we can simplify the Bellman equation to

$$\begin{aligned} C_0(x_0, g_0, 1) &= \max\{x_0, \mathbb{E}[C_1(X_1, G_1, 1)|G_0 = g_0]\} \\ &= \max\{x_0, \mathbb{E}[X_1|G_0 = g_0]\} \\ &= \max\{x_0, \alpha_0 g_0\}. \end{aligned} \tag{3.2}$$

Hence, we will produce tomorrow if our expectation of tomorrow's price as seen today on the shaped PFC is larger than today's spot price. Recall that this is the result of a merely risk neutral policy. Next, we want to take into account the associated risk as well. Now, let us assume that today's spot price is too small to afford a production today ($x_0 < \alpha_0 g_0$). Then we can rewrite the option value as

$$C_0(x_0, g_0, 1) := \alpha_0 g_0. \tag{3.3}$$

For the risk analysis we are not only interested in the expected value, but individual potential realizations of the option value. We therefore introduce the accumulated cash flow $V_0(x_0, g_0, 1)$ that has realizations $v_0^i(x_0, g_0, 1)$ for each price path $\{x_t^i\}_t$ separately. x_0 indicates that all price paths start from the same price x_0 and are generated for the *fixed* Future price g_0 . As we assume no exercise today there will only be a potential cash flow tomorrow and we can write

$$V_0(x_0, g_0, 1) = V_1(X_1, g_0, 1) := (1 + r_s)\alpha_0 g_0. \tag{3.4}$$

$V_1(X_1, g_0, 1)$ is the value of tomorrow's production assuming that there is no change in Future prices in between. Thus, this artificial value measures the impact of merely the spot price X_1 on the option value. The true option value for tomorrow will rely on both, a new spot and a new Future price X_1, G_1

$$V_1(X_1, G_1, 1) := \alpha_0 g_0(1 + r_g + r_s + r_g r_s). \tag{3.5}$$

Likewise we introduce

$$C_0(x_0, G_1, 1) := \alpha_0 g_0(1 + r_g) \tag{3.6}$$

to be the power plant value resulting from a mere Future price change. Now, we can start our risk analysis. First of all we can specify the total loss ℓ that is the difference between

tomorrow's potential cash flow $V_1(X_1, G_1, 1)$ and today's expected cash flow $C_0(x_0, g_0, 1)$

$$\begin{aligned}\ell &:= V_1(X_1, G_1, 1) - C_0(x_0, g_0, 1) = S_1 G_1 - \alpha_0 g_0 \\ &= g_0(1 + r_g)\alpha_0(1 + r_s) - \alpha_0 g_0 \\ &= g_0\alpha_0(r_g + r_s + r_g r_s).\end{aligned}\tag{3.7}$$

Due to the independence of r_s and r_g and the fact that both their means are zero, we can compute the standard deviation as follows

$$\sigma(\ell) = g_0\alpha_0\sqrt{\sigma_s^2 + \sigma_g^2 + \sigma_g^2\sigma_s^2}.\tag{3.8}$$

We want to quantify the total potential loss of the Tuesday production with the $(1-\beta)$ quantile $q_{1-\beta}(\ell)$ ¹ of the distribution of ℓ conditional on today's Future price g_0 , i.e. $\Phi(\ell|G_0 = g_0)$. However, we cannot conclude from the standard deviation on the quantile. Even though the returns r_s and r_g are normally distributed, the change in production value is not due to the product of r_s and r_g which is not normal. Again, we refer to Springer [60] for the analytical description of the distribution. The implementation of this analytical approach is rather cumbersome. For this reason, we will use Monte-Carlo simulation instead. This is also the framework that we will apply throughout the remaining chapters. Thus, we calculate the tails via simulation. The total loss $q_{1-\beta}(\ell)$ should not be confused with the Value-at-Risk figure which describes the loss resulting from *value* changes due to price changes of the underlying *tradable* products (see also related discussion in section 3.3.5). In our case the change of the real option value

$$\Delta C_0 := \Delta C_0(x_0, G_1, 1) := C_0(x_0, G_1, 1) - C_0(x_0, g_0, 1)\tag{3.9}$$

can only result from changes in the Future price $\Delta G_1 := G_1 - g_0 = g_0 r_g$

$$\Delta C_0(x_0, G_1, 1) = \alpha_0 g_0(1 + r_g) - \alpha_0 g_0 = \alpha_0 g_0 r_g.\tag{3.10}$$

This time the resulting marginal distribution is normal and we can calculate the VaR via the standard deviation

$$\text{VaR}_{1-\beta}(\ell) := q_{1-\beta}(\Delta C_0) = p_{1-\beta}\alpha_0 g_0 \sigma_g,\tag{3.11}$$

where $p_{1-\beta}$ is the percentile of the standard normal distribution with probability $1 - \beta$. Note, that the VaR does not consider any second order effect as it ignores the impact of the spot price that by definition is not tradable in advance. Next, we want to investigate the mere spot price risk i.e. *cash flow* changes due to spot price changes for the *fixed* Future price g_0

$$\begin{aligned}\Delta V_0 &:= \Delta V_0(x_0, g_0, 1) := V_0(x_0, g_0, 1) - C_0(x_0, g_0, 1) \\ &= V_1(X_1, g_0, 1) - C_0(x_0, g_0, 1) \\ &= \alpha_0 g_0(1 + r_s) - \alpha_0 g_0 = \alpha_0 g_0 r_s.\end{aligned}\tag{3.12}$$

This marginal distribution $\Phi(\Delta V_0|G_0 = g_0)$ ² is also normal and we use its $(1 - \beta)$ quantile $q_{1-\beta}$ to quantify the cash flow risk

$$q_{1-\beta}(\Delta V_0) = p_{1-\beta}\alpha_0 g_0 \sigma_s.\tag{3.13}$$

¹In this example we denote $q_{1-\beta}(x)$ to be the $(1-\beta)$ quantile of the distribution of the random variable x .

²We denote with $\Phi(X)$ the distribution law of the random variable X .

Note that both marginal distributions $\Phi(\Delta V_0|G_0 = g_0)$ and $\Phi(\Delta C_0|G_0 = g_0)$ do not cover the second order effect in equation 3.7 resulting from the product $r_g r_s$ which is only covered in the total loss $q_{1-\beta}(\ell)$. Now, that we quantified the risk of our power plant we want to investigate two hedge portfolios that are supposed to reduce this risk. We assume that we enter into these two hedge portfolios on Monday, i.e. *before* delivery ($t=0$) where G_1 is not known yet and will look at the impact not only before, but also *within* delivery ($t=1$) i.e. on Tuesday where $G_1 = g_1$ will be known. Both portfolios consists of our production value $C_0(x_0, g_0, 1)$ and a short position into the Future contract. They only differ in the amount to invest into the Future contract. Our first hedge portfolio will look at a so called *value* hedge as it intends to fix the production *value* as we see it on Monday. The relevant amount of Future contracts that we have to sell in order to offset the Tuesday production value due to Future price shifts is given by the so called *delta position* Δ^G . Formally, this is the first derivative of our production value with respect to the Future price

$$\Delta^G := \frac{\partial C_0(x_0, g_0, 1)}{\partial g_0} = \alpha_0. \quad (3.14)$$

As we own (are long) the power plant position we go short (sell) α_0 Future contracts. In the situation before delivery ($t=0$) our (value) hedge portfolio therefore looks as follows

$$H^{b, val} := H_0^{val}(x_0, g_0, 1) := C_0(x_0, g_0, 1) - \Delta^G g_0 = \alpha_0 g_0 - \alpha_0 g_0 = 0. \quad (3.15)$$

Thus, the value hedge perfectly offsets the option value, i.e. the expected cash flow as seen at $t = 0$. For a mere trading unit like a bank which will never let a position move into delivery by closing the position (i.e. selling the entire Tuesday production beforehand), the Future hedge is sufficient. Changes in the tradable part before delivery, i.e. only changes in the Future's price, will automatically be compensated. The bank can ignore the impact of the spot price X_1

$$\begin{aligned} \Delta H_G^{b, val} &:= H_1^{val}(x_0, G_1, 1) - H_0^{val}(x_0, g_0, 1) \\ &= (C_0(c_0, G_1, 1) - \alpha_0 G_1) - (C_0(c_0, g_0, 1) - \alpha_0 g_0) \\ &= \alpha_0 g_0(1 + r_g) - \Delta^G g_0(1 + r_g) - 0 \\ &= 0. \end{aligned} \quad (3.16)$$

Hence the VaR figure is zero

$$\text{VaR}_{1-\beta}^{b, val} := q_{1-\beta}(\Delta H_G^{b, val}) = 0. \quad (3.17)$$

However, the actual realization of the production value $V_1(X_1, G_1, 1)$ will usually differ from the expected value and we define the change in the hedge portfolio as the deviation of the actual realization $H_1(X_1, G_1, 1)$ from the production value before delivery $H_0(x_0, g_0, 1)$

$$\begin{aligned} \Delta H^{b, val} &:= H_1^{val}(X_1, G_1, 1) - H_0^{val}(x_0, g_0, 1) \\ &= V_1(X_1, G_1, 1) - \Delta^G G_1 - 0 \\ &= \alpha_0 g_0(1 + r_g + r_s + r_s r_g) - \alpha_0 g_0(1 + r_g) = \alpha_0 g_0(r_s + r_g r_s). \end{aligned} \quad (3.18)$$

Again, the distribution of the change in the hedge portfolio is not normal. At least, we can analyze the hedge effect via the standard deviation $\sigma(\Delta H^{b, val})$

$$\sigma(\Delta H^{b, val}) = \alpha_0 g_0 \sqrt{\sigma_s^2 + \sigma_g^2 \sigma_s^2}. \quad (3.19)$$

Obviously, the standard deviation could be reduced compared to the uncovered case in equation 3.8. Still, value changes due to spot price changes in first (r_s) and second order ($r_s r_g$) cannot be compensated with this type of hedge portfolio. In section 3.3.5 we will introduce an appropriate measure for this remaining risk called Earnings-at-Risk i.e. the $(1 - \beta)$ quantile of the distribution of cash flow changes after the Forward/Future hedge. In our example this is exactly the quantile of the change of our hedge portfolio

$$\text{EaR}_{1-\beta}^{b, \text{val}} := q_{1-\beta}(\Delta H^{b, \text{val}}). \quad (3.20)$$

Note that β is usually larger than 50%. Then, we look at the left tail of the distribution which is below zero. Hence, if we add the EaR number as a risk spread on top of the production value for Tuesday, then we penalize tomorrow's production and the Bellman equation from equation 3.2 changes as follows

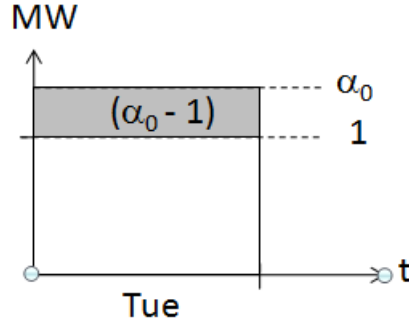
$$\hat{C}_0(x_0, g_0, 1) := \max\{x_0, \alpha_0 g_0 + \text{EaR}_{1-\beta}^{b, \text{val}}\}. \quad (3.21)$$

The choice of β defines the risk appetite of the dispatcher and makes future outcomes less valuable to him. In essence, the EaR figure is the amount of cash that can be potentially lost by significant changes in the spot price.

Our dispatcher also needs to take care of the situation *in delivery* i.e. on Tuesday (we label all corresponding figures with i). Let us still assume that our policy tells us to produce on Tuesday and we entered into a value hedge i.e. we sold Δ^G Future contracts to eliminate at least the Value-at-Risk. On Tuesday, we will sell the Future for g_0 , but need to buy another Δ^G MW on the spot market to meet the Future delivery. We also observe the new Future price $G_1 = g_1$ and need to pay or receive the difference to the Monday quote. In addition we sell our production amount of 1 MWh for the new spot price X_1 . Hence, the total cash flow in delivery looks as follows

$$\begin{aligned} H^{i, \text{val}} &:= H_1^{\text{val}}(X_1, g_1, 1) = V_1(X_1, g_1, 1) + \Delta^G(g_0 - X_1) + \Delta^G(g_1 - g_0) \\ &= V_1(X_1, g_1, 1) - \Delta^G(X_1 - g_1) \\ &= X_1 - \Delta^G(X_1 - g_1) \\ &= (1 - \Delta^G)X_1 + \Delta^G g_1. \end{aligned} \quad (3.22)$$

The fact that the Tuesday cash flow is the production of 1 MWh priced with the Tuesday spot price, hence, i.e. $V_1(X_1, g_1, 1) := X_1$ helps us to alternatively illustrate the previous equation with the energetic position. Recall that the offsetting position in the Future contract is $\Delta^G = S_0 = \alpha_0$. This is not 1 MWh as it should not compensate the energetic position, but the change in the generation asset value for Tuesday (we therefore called it a *value* hedge). Figure 3.1 illustrates the situation for $\alpha_0 > 1$. Thus, we produce 1 MW with our power plant, but sell α_0 MW for the price of g_1 to the market. Consequently we need to buy another $(\alpha_0 - 1)$ MW on the market to meet our volumetric obligation from the Futures contract. So, we need to accept a negative cash flow of $-(\Delta^G - 1)X_1 = (1 - \alpha_0)X_1$. Hence, the grey area is our remaining position that is exposed to the spot price only. Then, the change in the hedge portfolio in delivery can be described by the change of Tuesday's spot price ΔX_1 . We want to define the spot price change as the deviation from the initial expected spot price i.e. at $t = 0$. In our situation the expectation of the Tuesday spot price is only dependent on the


 Figure 3.1.: Power plant and Future schedule on Tuesday for $\alpha_0 > 1$

Future price g_0 .

$$\begin{aligned}\Delta X_1 &:= X_1 - \mathbb{E}[X_1|g_0] \\ &= X_1 - \alpha_0 g_0 \\ &= \alpha_0 g_0(1 + r_g + r_s + r_g r_s).\end{aligned}\tag{3.23}$$

Note the similarity to equation 3.12. In our specific case both equations are identical. For the general case we can at least state a close relation between the deviation of the spot price X_1 around its mean, i.e. the Future price g_0 , and the deviation of the cash flow $\Delta V_1(X_1, g_1, 1)$ around its mean, i.e. the production value $C_0(x_0, g_0, 1)$. We will make use of this analogy in section 3.3.2 and 3.3.4. Now, we can define the variance of the value hedge in delivery that is defined by mere changes in the spot price ΔX_1

$$\begin{aligned}\Delta H^{i, val} &:= H_1^{val}(\Delta X_1, g_1, 1) := (1 - \Delta^G)\Delta X_1 + \Delta^G g_1 \\ \sigma(\Delta H^{i, val}) &= |1 - \Delta^G| \alpha_0 g_0 \sqrt{\sigma_s^2 + \sigma_g^2 + \sigma_s^2 \sigma_g^2}.\end{aligned}\tag{3.24}$$

We can take the absolute term for $(1 - \Delta^G)$ as we take the square root of a squared term which stays positive. The stress factor α_0 is usually between 0.5 and 2 being greater than one during peak hours. Thus $0 \leq |1 - \Delta^G| \leq 1$ and the standard deviation in delivery reduces to exactly this fraction compared to the non-hedged figure before delivery (see equation 3.8).

Now, let us finally look at the second hedge portfolio that will guarantee the sale of our entire produced energy amount and is therefore called *volumetric* hedge. We sell the Tuesday production of 1 MWh on Monday for the Future price g_0 independent of the spot price. To be precise we only need to replace in equation 3.15 and 3.22 the Future delta Δ^G by the production amount, i.e. 1 MWh. Then the volumetric hedge before delivery looks as follows

$$\begin{aligned}H^{b, vol} &:= H_0^{vol}(x_0, g_0, 1) := C_0(x_0, g_0, 1) - g_0 = (\alpha_0 - 1)g_0 \\ \Delta H^{b, vol} &:= H_1^{vol}(X_1, G_1, 1) - H_0^{vol}(x_0, g_0, 1) \\ &= V_1(X_1, G_1, 1) - G_1 - (C_0(x_0, g_0, 1) - g_0) \\ &= \alpha_0 g_0(r_s + r_g + r_s r_g) - g_0 r_g \\ &= \alpha_0 g_0(r_s + (1 - \frac{1}{\alpha_0})r_g + r_s r_g) \\ \sigma(\Delta H^{b, vol}) &= g_0 \alpha_0 \sqrt{\sigma_s^2 + (1 - \frac{1}{\alpha_0})^2 \sigma_g^2 + \sigma_s^2 \sigma_g^2},\end{aligned}\tag{3.25}$$

which will very likely result in a higher standard deviation and thus probably in a higher EaR figure as well compared to the value hedge in equation 3.18 (for $\alpha_0 = 1$ both hedges would match). The volume hedge will also entail a VaR figure before delivery. Again, we only look at the value change contribution of the tradable product G, $\Delta H_G^{b,vol}$

$$\begin{aligned}\Delta H_G^{b,vol} &:= H_1^{vol}(x_0, G_1, 1) - H_0^{vol}(x_0, g_0, 1) \\ &= V_1(x_0, G_1, 1) - G_1 - (C_0 - g_0) \\ &= (1 + r_g)\alpha_0 g_0 - g_0(1 + r_g) - \alpha_0 g_0 + g_0 \\ &= g_0 r_g \left(1 - \frac{1}{\alpha_0}\right)\end{aligned}\tag{3.26}$$

The marginal distribution is normal and we can calculate the quantile analytically

$$\text{VaR}_{1-\beta}^{b,vol} := q_{1-\beta}(\Delta H_G^{b,vol}) = p_{1-\beta}\alpha_0 g_0 \left(1 - \frac{1}{\alpha_0}\right)\sigma_g.\tag{3.27}$$

During delivery, on the other hand, the volumetric hedge turns out to be quite efficient. Again we just replace Δ^G with 1 in equation 3.24 and observe no further spot price exposure as we sold the entire production beforehand

$$H^{i,vol} := H_1^{vol}(X_1, g_1, 1) = (1 - 1)V_1(X_1, g_1, 1) + 1 \cdot g_1 = g_1.\tag{3.28}$$

Hence, during delivery, there is no EaR as there is no spot price exposure left

$$\begin{aligned}\Delta H^{i,vol} &:= H_1^{vol}(\Delta X_1, G_1, 1) = 0 \\ \sigma \Delta H^{i,vol} &= 0 \\ \text{EaR}_{1-\beta}^{i,vol} &:= q_{1-\beta}(\Delta H^{i,vol}) = 0.\end{aligned}\tag{3.29}$$

Table 3.1 summarizes the results. It also adds a simplified EaR calculation labeled with a tilde (EaR) that ignores the product of r_g and r_s in equation 3.7. Then the sum of the remaining components is normally distributed and we can compute the quantile via the variance. The table emphasizes the trade-off between the risk exposure before and in delivery for both hedges. A volumetric hedge before delivery entails a higher VaR and a higher EaR compared to the value hedge. But during delivery it allows to eliminate EaR completely. The decision for one or the other is mainly driven by the difference of the two volatilities σ_s and σ_g . We will therefore continue with a numerical example to illustrate the effect. The June 09 Base contract at the EEX quoted for 33.75 EUR and we define all other parameters as follows:

$$g_0 = 33.75 \quad \sigma_g = 0.1 \quad \alpha_0 = 0.7 \quad \beta = 0.7\tag{3.30}$$

We choose a loss probability of $(1 - \beta) = 30\%$ to indicate that we are not completely risk averse (as would be the case for the regular VaR probabilities of 99% or 95%). Table 3.2 shows the corresponding risk figures for two different spot volatilities. The regular EaR figure was calculated with 50000 trials. As expected the analytical $\tilde{\text{EaR}}_\beta$ figures are smaller in absolute terms due to the missing second order effect. But even with a higher spot volatility the difference is almost negligible. This might change if we introduce a correlation between the spot and the Future price. We can also observe that both hedges have only minor influence on the spot price risk before delivery (e.g. $\text{EaR}_\beta(\Delta V_0) = -2.893$ EUR vs. $\text{EaR}_\beta(\Delta H^{b,vol}) = -2.422$ EUR and $\text{EaR}_\beta(\Delta H^{i,vol}) = -2.433$ EUR for $\sigma_s = 0.2$). Like in our example the volatility of spot price changes is usually significantly higher than of the Future's price and

	before delivery	in delivery
$\sigma(\ell)$	$\alpha_0 g_0 \sqrt{\sigma_s^2 + \sigma_g^2 + \sigma_s^2 \sigma_g^2}$	
$\text{VaR}_{1-\beta}(\ell)$	$p_{1-\beta} \alpha_0 g_0 \sigma_g$	
$\tilde{q}_{1-\beta}(\ell)$	$p_{1-\beta} \alpha_0 g_0 \sqrt{\sigma_g^2 + \sigma_s^2}$	
$q_{1-\beta}(\ell)$	numerical	
$\sigma(\Delta H^{val})$	$\alpha_0 g_0 \sqrt{\sigma_s^2 + \sigma_s^2 \sigma_g^2}$	$ 1 - \alpha_0 \alpha_0 g_0 \sqrt{\sigma_s^2 + \sigma_g^2 + \sigma_s^2 \sigma_g^2}$
$\text{VaR}_{1-\beta}^{val}$	0	$p_{1-\beta} 1 - \alpha_0 \alpha_0 g_0 \sigma_g$
$\tilde{\text{EaR}}_{1-\beta}^{val}$	$p_{1-\beta} \alpha_0 g_0 \sigma_s$	$p_{1-\beta} 1 - \alpha_0 \alpha_0 g_0 \sqrt{\sigma_s^2 + \sigma_g^2}$
$\text{EaR}_{1-\beta}^{val}$	numerical	numerical
$\sigma(\Delta H^{vol})$	$\alpha_0 g_0 \sqrt{\sigma_s^2 + (1 - \frac{1}{\alpha_0})^2 \sigma_g^2 + \sigma_s^2 \sigma_g^2}$	0
$\text{VaR}_{1-\beta}^{vol}$	$p_{1-\beta} \alpha_0 g_0 (1 - \frac{1}{\alpha_0}) \sigma_g$	0
$\tilde{\text{EaR}}_{1-\beta}^{vol}$	$p_{1-\beta} \alpha_0 g_0 \sqrt{\sigma_s^2 + (1 - \frac{1}{\alpha_0})^2 \sigma_g^2}$	0
$\text{EaR}_{1-\beta}^{vol}$	numerical	numerical

Table 3.1.: Risk figures before and in delivery

	$\sigma_s = 0.2$		$\sigma_s = 0.3$	
	before del.	in del.	before del.	in del.
$\sigma(\ell)$	5.304	5.304	7.504	7.504
$\text{VaR}_{1-\beta}^\ell$	-1.239	-1.239	-1.239	-1.239
$\tilde{q}_{1-\beta}^\ell$	-2.770	-2.770	-3.918	-3.918
$q_{1-\beta}^\ell$	-2.893	-2.893	-4.025	-4.025
$\sigma(\Delta H^{val})$	4.749	1.591	7.123	2.251
$\text{VaR}_{1-\beta}^{val}$	0.000	-0.372	0.000	-0.372
$\tilde{\text{EaR}}_{1-\beta}^{val}$	-2.418	-0.831	-3.717	-1.175
$\text{EaR}_{1-\beta}^{val}$	-2.422	-0.868	-3.731	-1.207
$\sigma(\Delta H^{vol})$	4.855	0.000	7.195	0.000
$\text{VaR}_{1-\beta}^{vol}$	-0.531	0.000	-0.531	0.000
$\tilde{\text{EaR}}_{1-\beta}^{vol}$	-2.534	0.000	-3.704	0.000
$\text{EaR}_{1-\beta}^{vol}$	-2.433	0.000	-3.732	0.000

 Table 3.2.: Risk figures for $(1 - \beta) = 30\%$ before and in delivery (in EUR)

therefore the Future fails to compensate the spot price risk no matter whether implemented as a volume or value hedge. An indication for the small EaR difference between the value and volume hedge before delivery is the variance. Both variances before delivery differ only by the term $(1 - \frac{1}{\alpha_0})^2 \sigma_g^2$. In our example this is $(1 - 1/0.7)^2 0.1^2 \approx 0.0018$ which is almost negligible compared to the dominating spot variance. Recall that the VaR figures merely show the impact of the Future price on the Tuesday production. Therefore, as expected, they are identical for changes in the spot price volatility. If we compare the sum of VaR and EaR before and in delivery, we can see that the volume hedge is by $|-0.53-2.433| - |-2.422| = 0.544$ EUR higher before delivery, but by $|0| - |-0.372 - 0.868| = -1.24$ EUR smaller in delivery compared to the value hedge. Hence, our dispatcher might favor the volume over the value hedge. Then, according to equation 3.21 he will produce on Monday instead of Tuesday if the current price x_0 is higher than $\alpha_0 g_0 + \text{EaR} = 0.7 \cdot 34 - 2.534 = 21.27$ EUR.

This example was meant to introduce the basic notion and relation between EaR, VaR, spot and Future price risk as well as value vs. volume hedge. It also illustrates that even in the simplest setup of a single period, two random variables and a static cash flow definition a proper analytical description is already beyond the straightforward calculation with normal distributions. Proceeding with the multi-period case and dynamic dispatch rules like in the subsequent sections the *general* production value and ACF become dependent on a vector δ covering of all relevant initial technical parameters, i.e. $C_0(x_0, g_0, \delta), V_0(x_0, g_0, \delta)$. Consequently we cannot describe the change in option value $\Delta C_0(x_0, g_0, \delta)$ and ACF $\Delta V_0(x_0, g_0, \delta)$ (see equation 3.9 and 3.12) analytically any longer, let alone their distributions. Therefore, for the remaining chapters, we will follow the basic idea of the Taylor series framework that describes small variations around an initial function value with a series of derivatives with respect to its function parameters. As we do not impose any restriction on the nature of $C_0(x_0, g_0, \delta)$ and $V_0(x_0, g_0, \delta)$ we cannot even be sure that their derivatives actually exist. In our specific example, we could at least calculate the first order derivative analytically with respect to the Future price (see equation 3.14). In section 3.3.1 we show how to calculate this derivative numerically. Similarly we will compute the sensitivity of $\Delta V_0(x_0, g_0, \delta)$ with respect to spot price path deviations around the fixed Future price g_0 (see sections 3.3.2 and 3.3.4).

Our example showed that we are not only able to calculate the associated risk of a dispatch decision, but are also able to let the risk impact the dispatch decision itself (see equation 3.21). The situation becomes more difficult in the multi-period setup where the current stage price will become unknown once we iterate one step back. In other words, the Monday price x_0 in equation 3.21 should also be penalized as it will become again a random variable X_0 once we iterate back to Sunday. Otherwise, we would tend to exercise right away and would pick less profitable hours. This will certainly reduce the potential losses. But in this way the expectation and thus the option value will shrink even more. We will investigate this conflict in more detail in section 3.4.3.

A multi-period decision problem will also result in a more elaborated generation schedule with on- and off-days and possibly varying volume profiles that cannot be hedged any longer in advance with a simple block production (in our example 1 MW flat throughout the delivery period) which in reality, however, is the only available product on the Future market. Consequently, a volume hedge, as efficient as it turned out to be in our example, is often not possible and some spot price risk remains. In the following two chapters we therefore investigate hedging strategies (sections 3.3.4 and 4.5) for this remaining spot price risk as well. But first, we describe the electricity price curve design and define the introduced risk figures in more detail.

3.2. Hourly Forward Curve Engineering

Since the deregulation of electricity markets about ten years ago, electricity price modeling became a popular research field. A profound risk management starts with the construction of the Forward curve. Generally speaking, this curve should incorporate all factors that impact the price. It is the foundation for any risk analysis and valuation. The price behavior can be described from two different directions. Macroeconomics uses equilibrium and game theory which try to explain price dynamics by the interaction of market participants and exogenous factors. In case of energy markets these are for instance weather, political implications (clean energy initiatives, deregulation, new pipelines, ...), etc. These models usually project trends or forecast prices on a larger scale (usually years) and are rather meant for strategic decision making. Our focus, however, is on trading and therefore we are rather interested in a short to mid term horizon with fine granularity down to an hourly level. This is rather a task for econometric models. They rely on plain time series of historic data and current prices only and try to identify the nature of the underlying dynamics using adequate tools from stochastic calculus. It is this characteristic of prices and in particular their underlying risk factors that we are interested in for our further analysis.

A good overview of recent econometric models for electricity prices can be found in [58]. The main characteristics of electricity prices are

- Hourly Granularity
- Mean-Reversion
- Seasonality
- High Volatility (time dependent or stochastic)
- Spikes

Seasonality results from the load demand that changes intra-day (worktime vs. freetime hours), intra-week (weekday, weekend) and intra-year (the four seasons) and are mainly driven by weather conditions. Mean-reversion is directly linked to seasonality as prices deviate, but tend to return to the seasonal shape. The deviation, though, can be very high. Due to its non-storability electricity prices have a strong fluctuation resulting in a high volatility. In case of shortages or oversupply prices can suddenly jump up or down from one hour to the next. Even negative prices can occur. That is the case if a utility registered more power supply with the grid operator than was actually used by his customers. Then the utility might be willing to pay another market participant for taking his power so that he can balance out his position. The grid operator's fee for stabilizing the grid despite the oversupply could be instead significantly higher.

Stochastic calculus provides various instruments to capture these electricity price characteristics. Figure 3.2 provides the most popular tools. Basically one can differ between jump diffusion, regime switching, autoregressive and n -factor models. Often one can find a combination of those. In particular the spikiness of electricity prices draws a lot of academic attention since this is a unique feature compared to other time series data in financial markets. A popular approach is to combine Merton's jump diffusion model [51] with strong mean-reversion in order to generate spikes. Deng investigated this approach in several papers, see [22] and references therein. Other authors like Bierbrauer et al. [11] describe the jumps with two mean-reverting processes that are linked via a probability transition matrix. This matrix describes the probability to stay and to shift between the two regimes/price processes. In fact, one can observe that a spike is often joined by a period of high volatility which in deed

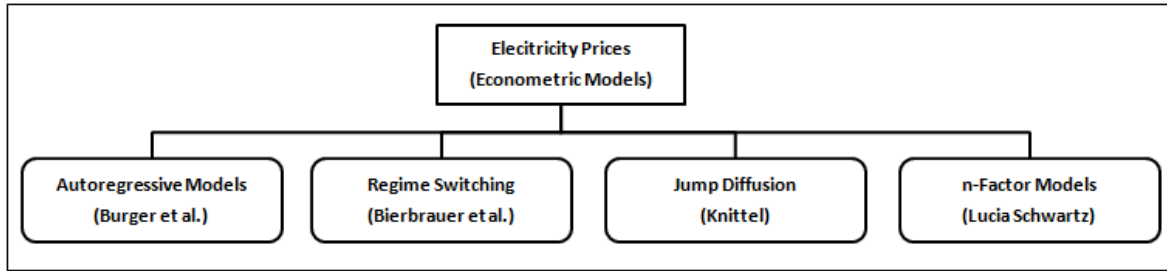


Figure 3.2.: Electricity Price Models

can be interpreted as a different price dynamics. Knittel et al. [42] approach this observation from a different angle by introducing a stochastic volatility model. In particular they use an EGARCH process which belongs to the family of autoregressive models. These kind of models are adequate to describe clustering of volatility. In general they differ between a long- and short-term volatility. This leads us to the last category of models we want to introduce which are the so called n -factor models. These models also differentiate between a long and a short term evolution, however, not for the volatility, but rather the price directly. In the simplest situation (1-factor model) the long-term drift can be described deterministically and only the short term fluctuations need a stochastic description. If the drift will be modeled as a nested stochastic process as well, then we talk about a 2-factor model. Lucia and Schwartz [47] investigated these two models for Nordpool electricity spot prices. Burger et al. [14] introduce the customer demand as a third factor to the spot price dynamics. In deed, merely looking at the correlation one can prove the strong interdependence between hourly prices and customer demand.

Independent from the specific selection of one of the presented stochastic processes, there is a standard approach on the general price modeling framework. It basically consists of two steps. First, one needs to generate a forward curve from the observable monthly, quarterly and yearly Futures prices. Then one imposes day types to create hourly shapes resulting in the so called hourly price Future curve (PFC). This curve represents the expectation of the hourly spot prices. Finally a spot price process will be added that describes the hourly random behavior. This is where the different price process models make a difference. Figure

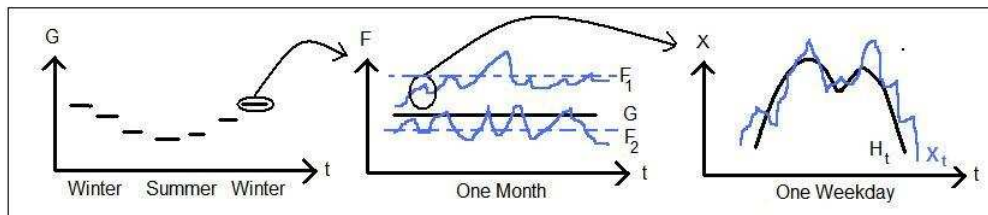


Figure 3.3.: Price Forward Curve Construction

3.3 illustrates the construction of the PFC in more detail. The first picture to the left shows the Forward curve with its monthly seasonal shape across the year. Monthly prices are not available for this long time period and need to be constructed from quarterly and yearly Forward and Futures prices via non-arbitrage relations (so called bootstrapping).

Both contract types, Forwards and Futures, provide a flat delivery schedule (e.g. 1 MW per hour) for a specific price band (usually base or peak) and delivery period (monthly, quarterly and yearly). Futures are officially quoted by the exchange and are mainly financial contracts with daily marking to market and margin payments. Hence, there is no discounting.

Forward contracts are bilateral trades with physical settlement. They provide the same delivery structure, but usually on a larger scale (e.g. the exchange only offers the next 8 months, while the OTC market offers monthly contracts for at least the next 12 months). Forward contracts settle against the average of the historical spot prices for the relevant delivery period. The Futures represent the *expected average* spot price instead. At the European Energy Exchange (EEX) a Future contract is also traded during delivery. Within the delivery period the Futures price is an average of the historical prices from the beginning of the month up to today and the expected price for the rest of the month. On the last delivery day the Futures and Forward prices match. Picture 2 illustrates their relation. It shows two individual hourly spot price trajectories. The dotted lines represent the average price of each trajectory. These are two realizations of the Forward price. The bold line in between is the expectation of both Forwards i.e. the Future price.³

The *hourly* PFC $\{H_t\}_t$ describes the expected spot price at a future time t conditional on today's Futures prices G_0^j (with $j = 0, \dots, J$ number of Futures) by applying *deterministic* scaling factors α_t to create an hourly shape that reflects the different seasonalities (working/non-working hours, weekday/weekend, summer/winter). These factors incorporate statistical information about historical electricity prices, but also external data like current temperature and water levels in reservoirs. Each Future price G_0^j is only valid for a certain future time period $\mathbb{T}^j = \{t_0^j, \dots, T^j\}$. Note that \mathbb{T}^j is a set of not necessarily subsequent hours. A peak Future contract, for instance, will skip the off-peak hours between 20:00 and 8:00. We therefore set $j := j(t)$ to automatically pick the relevant Future j for hour t , i.e. the contract with the relevant delivery period where the current hour t falls into. The spot price risk, however, is originated in individual hourly fluctuations. It therefore requires yet another *random* factor S_t that stresses the PFC on an hourly basis to generate the hourly electricity price $X_t := X_t(S_t, G_0^j)$ (see also the most right picture of Figure 3.3). From now on, we address to S_t as the *spot price component* of the electricity price. It is a stress factor with a mean of 1 and an hourly changing variance. The following equation also introduces the normalization factor η_j that we will explain in equation 3.32

$$\begin{aligned} X_t(S_t, G_0^j) &= S_t \alpha_t G_0^j \eta_j \\ H_t(G_0^j) &:= \mathbb{E}[X_t | G_0^j] = \mathbb{E}[S_t] \alpha_t G_0^j \eta_j = \alpha_t G_0^j \eta_j. \end{aligned} \tag{3.31}$$

Note that in the previous equation we implicitly assume independence between S_t and $G_0^{(0)}$. Hence a shift in the Futures price $\Delta G_0^j = G_0^j + h$ for sufficiently small h acts like a change in spot price level (the entire PFC within period \mathbb{T}^j moves up or down). Formally each spot hour should be treated as an own contract and hence an own risk factor since each hour is traded individually on the day ahead market at the exchange. We will come back to this notion in section 3.3.4. Equation 3.31 introduces the normalization factor η_j . Normalization is one method to handle the fact that there is no unique probability measure for risk neutral pricing in electricity markets since power is not storable and hence cash and carry arbitrage fails. The latter assumes that the expectation of a future spot price is equal to the current spot price compounded with the risk free interest rate r i.e. $\mathbb{E}[X_t | X_0 = x_0] = x_0 e^{rt}$. Instead, in electricity markets one assumes that the price of a Future G_0^j reflects the current expectation

³In reality Forward and Future do not have the straightforward relation. This standard modeling approach ignores that the Forward price additionally incorporates the impact of discounting (monthly vs. daily margin payments) and credit spreads (counterparty risk in bilateral trades).

of the average future spot prices for the corresponding delivery period \mathbb{T}^j

$$\begin{aligned} \mathbb{E} \left[\frac{1}{|\mathbb{T}^j|} \sum_{t \in \mathbb{T}^j} X_t \mid G_0^j = g_0^j \right] &\stackrel{!}{=} g_0^j \\ &\frac{1}{|\mathbb{T}^j|} \sum_{t \in \mathbb{T}^j} \alpha_t \eta_j g_0^j \stackrel{!}{=} g_0^j \\ &\Rightarrow \eta_j = \frac{1}{|\mathbb{T}^j|} \sum_{t \in \mathbb{T}^j} \alpha_t, \end{aligned} \quad (3.32)$$

where $|\mathbb{T}^j|$ stands for the number of hours in set \mathbb{T}^j . If the adjustment factors α_t are already normalized then the normalization factor η_j is 1. There is a separate normalization factor for each Future price G_0^j . Note that X_t is automatically normalized if H_t is since S_t has a mean of 1. Finally, we want to describe the relation between the Forward and the Future price. The Forward price F_0^j is the *average* price across all hours of the associated delivery period $\mathbb{T}^j = \{t_1^j, \dots, T^j\}$. It is therefore also called the *delivery price*

$$F_0^j = \frac{1}{|\mathbb{T}^j|} \sum_{t \in \mathbb{T}^j} X_t. \quad (3.33)$$

From equation 3.32 and 3.33 we can derive the following relation

$$g_0^j = \mathbb{E}[F_0^j \mid G_0^j = g_0^j]. \quad (3.34)$$

So we can think of the Forward price to be an individual realization of the delivery price whereas the Future price is the *expected* delivery price. Figure 3.4 illustrates this mechanism. The graph shows the first ($j=0$) Future G^0 of the entire production period. In this example we look at a base contract that delivers power at every hour, hence \mathbb{T}^0 consists of subsequent hours $\{t_0^0, t_0^0 + 1, \dots, T^0\}$. In our example in chapter 4 this will be March, hence we have $\mathbb{T}^0 := \{1 \text{ March } 00:00, \dots, 31 \text{ March } 23:59\}$. We also assume that today $t=0$ is the first hour of the first day of the Future's delivery period, hence $t_0^0 := 0$. We observe the spot price x_0 and the Future price g_0^0 . Furthermore the graph shows two sample spot price paths $\{x_t^1\}_t$ and $\{x_t^2\}_t$ starting from the known price x_0 . The average price of these two trajectories $f_0^{0,1}$ and $f_0^{0,2}$ we declared to be two realizations of the Forward price F_0^0 . If we had only two price scenarios, then the normalization would make sure that the average of both forward prices will be again the Future price indicated in the graph by the similar distance of the two Forward prices (dashed lines) from the Future price (solid line), one time below and the second time above the current Future price. Note that we found a similar relation in section 2.1 between the individual cash flow $V_0^*(x_0, N)$ of a generation schedule and the corresponding *expected* cash flow $C_0^*(x_0, N)$, i.e. the swing option value. We will make use of this analogy in section 3.3.2 and 3.3.4.

Now, let us illustrate the mechanism for our example of the previous chapter. For simplicity let us assume that there is only a single Future price $G_0 := G_0^0$ with $\mathbb{T}^0 := \mathbb{T}$ that we observe at the beginning of the corresponding delivery period i.e. $t_0^0 := t_0 := 0$. Then, let us try to identify the factors G_0 , α_t and S_t for our mean-reverting price process from equation 2.7 that we rename to \tilde{X}_t in order to prevent a potential confusion with our newly introduced price X_t from equation 3.31. We can write our former Ornstein-Uhlenbeck process as

$$\begin{aligned} \tilde{X}_t &= \tilde{X}_{t-1}^{(1-\kappa)} e^{\sigma \epsilon_t} \\ \epsilon_t &\sim N(0, 1), \end{aligned} \quad (3.35)$$

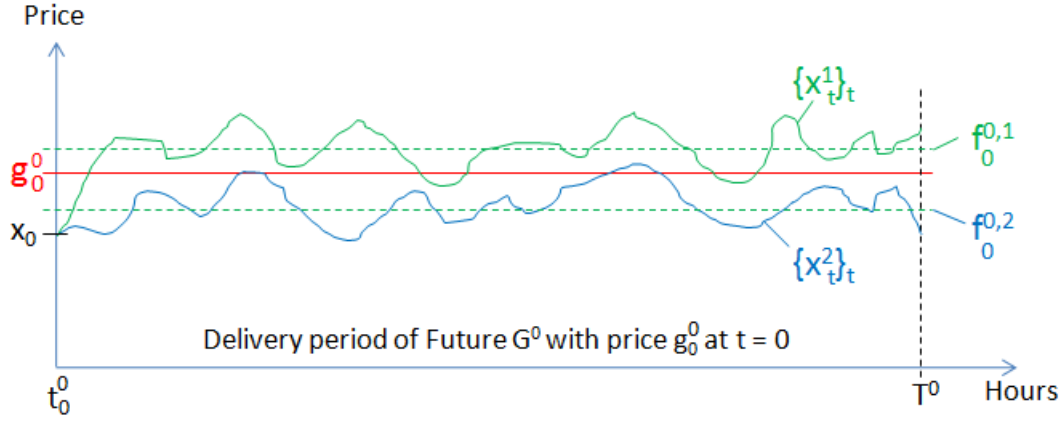


Figure 3.4.: Relation between Future, Forward and spot price.

where ϵ_t are i.i.d. If we rewrite

$$\tilde{X}_t = \frac{\tilde{X}_t}{\mathbb{E}[\tilde{X}_t]} \mathbb{E}[\tilde{X}_t], \quad (3.36)$$

we can express X_t from equation 3.31 in terms of \tilde{X}_t

$$\begin{aligned} X_t &= S_t \cdot \alpha_t \cdot G_0 \cdot \eta_0, \quad t = 1, \dots, T \\ X_t &= \left(\frac{\tilde{X}_t}{\mathbb{E}[\tilde{X}_t]} \right) (\mathbb{E}[\tilde{X}_t]) \cdot 1 \cdot \eta_0. \end{aligned} \quad (3.37)$$

Thus, we can set $S_t := \frac{\tilde{X}_t}{\mathbb{E}[\tilde{X}_t]}$ and $\alpha_t := \mathbb{E}[\tilde{X}_t]$. Note that indeed $\mathbb{E}[S_t] = 1$ as required. In this simple example the Future price is $G_0 = 1$ and the adjustment factor α_t is the expectation of each individual hourly price according to the Ornstein-Uhlenbeck process. The normalization factor η_0 becomes a function of the entire mean-reverting process $\{\tilde{X}_t\}_{t>0}$

$$\eta_0 = \eta_0(\{\tilde{X}_t\}_{t>0}) := \frac{1}{|\mathbb{T}|} \sum_{t \in \mathbb{T}} \mathbb{E}[\tilde{X}_t]. \quad (3.38)$$

So far we used 1000 time steps. Without loss of generality we now reduce the period to 720 reflecting the number of hours for a 30 day month. Furthermore we assume that there is a tradable Futures and Forward contract for that period. The average of the 720 prices of a single trajectory represents one possible outcome for the Forward price $f_0^i = 1/720 \sum_{t=1}^{720} x_t^i$, $i = 1, \dots, 1000$. Usually the price process would be normalized and the average of all Forward prices f_0^i should be again 1. The price process of our previous examples was not normalized therefore the normalization factor η_0 was not applied so far. Now, we want to create arbitrage free spot prices and compute the normalization factor according to equation 3.32. As $g_0 = 1$ we get

$$\eta_0 = \frac{1}{\frac{1}{720} \sum_{t=1}^{720} \left[\frac{1}{1000} \sum_{i=1}^{1000} x_t^i \right]} \quad (3.39)$$

and weigh each price of our price scenarios with this factor.

3.3. Risk Measures

In this section we want to quantify the *spot* price risk and propose two type of risk measures. First, a definition of spot price sensitivity suitable for numerical valuation models (see section 3.3.2 and 3.3.4) and second a quantile defined on a specifically tailored loss distribution (see section 3.3.5) that reflects the mere loss impact by spot price changes. In context of Taylor series expansion a sensitivity is the first derivative on an analytical function at a fixed function value with respect to one of the input parameters and thus describes small changes around the fixed function value by small shifts of the function's initial input parameters. In our situation the fixed function value was so far the swing option value for a fixed start price $X_0 = x_0$, i.e. $C_0^*(x_0, N)$. Recall that we could solve the underlying optimization problem only numerically and were only able to come up with an approximation $\underline{C}_0(x_0, N)$. So, in fact, we do not have a functional description of the true option value. This will be even more true if we move from the swing option to the more complex real option value of a power plant. The following sub sections will therefore propose appropriate sensitivity definitions for a numerical rather than analytical valuation framework. In section 3.2 we introduced a more general description of the price process and differed between the Future and a spot price component. As we want to look at the spot price risk only, we generate future spot prices for the *fixed* current Future price. For simplicity from now on we work with a single Future and Forward price only $F_0 := F_0^0, G_0 := G_0^0$, but our results apply for an entire term structure of Future prices $\{G_0^j\}_j$ as well. Hence, our currently observed Future price is $G_0 = g_0$. Hence, the known Future price g_0 becomes another input parameter of the real option. Additionally we introduce the parameter vector δ that covers individual technical constraints of a power plant⁴. So we generalize the swing option $C_0^*(x_0, N)$ to a real option $C_0^*(x_0, g_0, \delta)$. Accordingly we transform the definition of the ACF as well, i.e. we expand $V_0^*(x_0, N)$ to $V_0^*(x_0, g_0, \delta)$. Like for the swing option we can compute the optimal real option value $C_0^*(x_0, g_0, \delta)$ via the expectation of the optimal ACF $V_0^*(X_0, G_0, \delta)$ conditional on the current spot price $X_0 = x_0$ and Future price $G_0 = g_0$

$$C_0^*(x_0, g_0, \delta) := \mathbb{E}[V_0^*(X_0, G_0, \delta) | X_0 = x_0, G_0 = g_0]. \quad (3.40)$$

Now, we want to introduce $\Delta V_0^*(x_0, g_0, \delta)$ as the deviations of the individual cash flow realizations $V_0^*(x_0, g_0, \delta)$ from their mean, i.e. the real option value⁵

$$\Delta V_0^*(x_0, g_0, \delta) := V_0^*(x_0, g_0, \delta) - C_0^*(x_0, g_0, \delta). \quad (3.41)$$

Note that $\Delta V_0^*(x_0, g_0, \delta)$ must not be confused with changes $\Delta C_0^*(x_0, h, \delta)$ of the real option value itself i.e. changes of the *expected* cash flow that in our model can only result from small changes in spot price level i.e. the Future price $\Delta g_0 = g_0 + h$ with h sufficiently small

$$\Delta C_0^*(x_0, g_0, \delta) := C_0^*(x_0, g_0 + h, \delta) - C_0^*(x_0, g_0, \delta). \quad (3.42)$$

We will explain the difference between equation 3.41 and 3.42 in more detail in the subsequent sections. In practice, we do not know the true real option value $C_0^*(x_0, g_0, \delta)$ nor the related cash flows $V_0^*(x_0, g_0, \delta)$. Our numerical results therefore rely on our lower bound approximations. For this reason all our numerical examples in this chapter will work with $C_0(x_0, g_0, \delta)$

⁴See in particular section 4.5 for different implementations of vector δ .

⁵Recall that $V_0^*(x_0, g_0, \delta)$ is still a random number i.e. it has realizations for each price path $\{X_t\}_t$ separately. x_0 only indicates that all price paths start with the same price $X_0 = x_0$ and are generated from the same Future price g_0 .

and $V_0(x_0, g_0, \delta)$ instead of $C_0^*(x_0, g_0, \delta)$ and $V_0^*(x_0, g_0, \delta)$.⁶

3.3.1. Future Delta

To clarify the difference to our new sensitivity classical sensitivity definitions in section 3.3.2 and 3.3.4 we briefly recall the classical sensitivity definition, i.e.the Future delta Δ^G . It describes small changes of the real option value $\Delta C_0^*(x_0, g_0, \delta)$ around the initial contract value by small changes around the initial Future price $\Delta g_0 := g_0 + h$

$$\Delta C_0^*(x_0, g_0, \delta) = \Delta^G h + \epsilon_G, \quad (3.43)$$

with $\Delta C_0^*(x_0, g_0, \delta)$ as defined as in equation 3.42 and ϵ_G being the hedging error. Technically, the Future delta Δ^G is the first derivative of the real option value $C_0^*(x_0, g_0, \delta)$ with respect to the Future price. Usually this derivative cannot be computed analytically and rather requires a numerical approach. A commonly used method is the finite difference formula (see for instance [34])

$$\Delta^G = \frac{\partial C_0^*(x_0, g_0, \delta)}{\partial g_0} \approx \frac{C_0^*(x_0, g_0 + h, \delta) - C_0^*(x_0, g_0 - h, \delta)}{2h}, \quad (3.44)$$

with h sufficiently small. Recall that the previous equation assumes a single Future price g_0 . If the dispatch schedule covers $j=0, \dots, J$ Future delivery periods then the method involves a revaluation for each Future contract j on the PFC two more times and hence requires another two sets of price scenarios for each Future contract. A swing option for a yearly delivery, for instance, has exposure against 24 Future contracts (12 months base and peak) leading to a total of 48 recalculations of the option value. Obviously, this calculation is computationally expensive. There is a broad research for finding methods that speed up the calculation of Monte-Carlo greeks like variance reduction schemes (control variate techniques, stratified sampling, etc.) and quasi random sequences. A good overview can be found in Hull [34] and Glasserman [29]. We will not focus on the different delta calculations since they are well understood. We only want to mention one peculiarity of the delta interpretation in energy markets. Energy traders usually do not look at the mere Future delta, but rather on the *delta-weighted volume*. Since delta for a call option is between 0 and 1 being close to 0 if out of the money (otm) and close to 1 if in the money (itm), the delta can be interpreted as the probability of exercise. Hence, multiplying the delta by the total volume of the Future provides an indication of the energy contribution that can be expected from this option. For a swing option, however, where the Future price is not the true underlying of the option, this interpretation does not hold any longer. We want to illustrate the relation between delta and exercised energy by continuing with our example from the previous chapter.

We identified in equation 3.37 that our price scenarios from the previous chapter assume a Future price of 1. We apply the finite difference formula and use a deviation of 1 % from the initial Future price $g_0 = 1$ that is $h = 0.01$. In equation 3.44 we can generate the new up and down price scenarios by simply multiplying our existing spot scenarios with the new Future price: $X_t^u : X_t(S_t, g_0 + h) = 1.01X_t$, $X_t^d := X_t(S_t, g_0 - h) = 0.99X_t$ (recall that the change in the Future price results in an entire shift of all spot prices). For these two new sets of prices we compute the delta for 1, 360 and 720 swings. In our last chapter, we only investigated itm option values since the strike K was at 0 with the price deviating around 1. Now, we will investigate at the money (atm) ($K = 1$) and otm situations ($K = 2.5$) as well. Table 3.3

⁶We also skip the underline that we used in the previous chapter as from now on we will only look at lower bounds.

Swings	K	MWDelta [MW]	Delta [MWh]	K	MWDelta [MW]	Delta [MWh]	K	MWDelta [MW]	Delta [MWh]
1	0	0.0063	4.556	1	0.0064	4.6052	2.5	0.0060	4.331
360	0	0.7843	565.09	1	0.7701	554.48	2.5	0.1061	76.378
720	0	1.1358	817.81	1	0.7870	566.61	2.5	0.1061	76.378

Table 3.3.: Future delta

shows the regular option delta ("MWDelta" in MW) and the volume weighted delta ("Delta" in MWh). The former can be interpreted as the number of Future contracts a trader needs to buy/ sell in order to hedge his short/long position. In terms of a generation schedule it translates to a baseload schedule delivering MWDelta at each hour. The total energy of this schedule (delivery hours x hourly capacity) is identical to Delta (volume weighted delta) and therefore we assign the unit MWh. If we look at the single exercise with strike $K = 0$ we can see that Delta is more than four times the size of the exercisable energy amount (4.55 MWh instead of 1 MWh). Hence, the common interpretation of the delta to be the resulting energy of the option contract is misleading for swing options. For the itm option with full flexibility we would have expected that it will behave like a regular Future contract. All hours are in the money so they will all be exercised. In that situation we would expect a perfect hedge with a Future. Instead we observe still a higher energy delta: 817 MWh instead of 720 MWh. This is due to the fact that our price paths still follow our initial definition of the last chapter and hence are not normalized. The situation changes if we apply factor η_0 of equation 3.32. Table 3.4 presents the deltas for the normalized price scenarios. Now, we retrieve the desired result

Swings	K	MWDelta [MW]	Delta [MWh]	K	MWDelta [MW]	Delta [MWh]	K	MWDelta [MW]	Delta [MWh]
1	0	0.0056	4.0114	1	0.0058	4.1622	2.5	0.0051	3.6812
360	0	0.6910	497.51	1	0.5990	431.27	2.5	0.0583	41.943
720	0	1	720	1	0.5990	431.27	2.5	0.0583	41.943

Table 3.4.: Future delta (Normalized Spot Prices)

of 1 MW or 720 MWh respectively for the itm option with 720 swings. This option behaves almost like a regular European option on a Future contract with the typical MWDelta of 1 for itm, almost 0 for otm and around 0.5 for atm. Still, for 1 and 360 swings we observe higher deltas compared to a standard option on a Future. We will explain this behavior in the next section (see in particular equation 3.49).

3.3.2. Forward Delta

As we have seen in section 3.3.1 the Future delta can only cover changes of the *expected* cash flow by changes in the *expected* average spot price. However, as outlined in equation 3.41, we are rather interested in the impact of spot price changes only i.e. changes of the ACF around the real option value for a *fixed* Future price $G_0 = g_0$. We want to relate these individual cash flow deviations to the deviations of the individual spot price paths $\{X_t\}_t$ from their mean, i.e. the fixed Future prices g_0 (see also equation 3.31). Theoretically we could look at all hourly deviations $\Delta X_t := X_t - g_0$ separately, but in practice, we cannot hedge individual spot prices since there is no hourly Future contract. Then at least we want to hedge against the deviation of the *delivery* price, i.e. the average of all spot prices of the same price scenario along the delivery period (e.g. for a 30 days month these are 720 hourly prices). The individual delivery

price reflects the spot price behavior to a larger extent than the expected delivery price only. We can create this hedge with a Forward contract as this type of contract exactly settles against the delivery price for the specific delivery period.

Definition 3.3.1 (Forward Delta). *The Forward delta Δ^F is the slope parameter of a linear least-square regression⁷ to describe cash flow realizations $V_0^*(x_0, g_0, \delta)$ of a real option $C_0^*(x_0, g_0, \delta)$ with respect to Forward to Future price differences $(F_0 - g_0)$*

$$V_0^*(x_0, g_0, \delta) = C_0^*(x_0, g_0, \delta) + \Delta^F(F_0 - g_0) + \epsilon_F^*, \quad (3.45)$$

where x_0 is the current spot price, g_0 and F_0 are defined in equation 3.33 with $j = 0$, δ being a vector of further option parameters and ϵ_F^* is the residual.

The Forward delta measures the impact of Forward price deviations from the corresponding fixed Future price $F_0 - g_0$ on the ACF of a real option. Let us compute the Forward delta for our swing option example. We assume that the delivery period is covered by one Forward contract and we work only with normalized prices as motivated in the previous section. Table 3.5 shows the results. Like for the Future Delta we observe significantly higher energy

Swings	K	Option Value	Delta [MWh]	K	Option Value	Delta [MWh]	K	Option Value	Delta [MWh]
1	0	4.0114	8.7170	1	3.0142	8.4713	2.5	1.6041	8.4154
360	0	497.506	541.761	1	142.982	482.335	2.5	7.5946	66.7864
720	0	720	720	1	142.982	482.335	2.5	7.5946	66.7864

Table 3.5.: Forward Delta

deltas compared to the number of available swings. Some Forward Deltas are even higher than the ones we computed for the Futures. This behavior can be explained if we recall that the individual cash flows $V_0^*(x_0, g_0, \delta)$ are the result of applying the optimal exercise strategy on the associated price trajectory $\{X_t\}_t$. In context of a swing option we defined the optimal exercise strategy as $\pi_0^*(N)$ (see also equation 2.1) that we now want to interpret as an electricity schedule $\{L_t^*\}_t$ with

$$L_t^* := \begin{cases} L & t \in \pi_0^*(N) \\ 0 & \text{otherwise.} \end{cases} \quad (3.46)$$

where L is the fixed swing size in MW (1 MW in our example) that we apply at a stopping point $\tau_k^*(0, N) \in \pi_0^*(N)$. Therefore we can interpret each cash flow to be the value of a Forward contract with a specific load profile L_t^* and a fixed negative spread K on the Forward price

$$V_0^*(x_0, N) = \sum_{t=0}^T (X_t - K)L_t^* = \sum_{t=0}^T (X_t L_t^*) - K \sum_{t=0}^T (L_t^*), \quad (3.47)$$

with $V^*(x_0, N)$ defined in equation 2.9. The finite sequence $\{x_t^i, l_t^{*,i}\}_t$, i fixed, describes one possible price-schedule scenario for one realization of the Forward price $f_0^i = 1/T \sum_{t=0}^T x_t^i$. Similar to equation 3.31 we can express the spot price as a function of the Forward price by

⁷Throughout this entire thesis we only work with the estimator of the regression parameter that we calculated from concrete realizations $i = 1, \dots, I$ of the random value pairs $(F_t - g_0, V_t^*(x_t, g_0, \delta))$, i.e. of the Forward price and ACF. Therefore, whenever we use Δ^F in this thesis we actually refer to the estimator of the regression parameter that varies with every new data set unlike the true regression parameter.

introducing an individual shift \tilde{S}_t on the Forward price $X_t = \tilde{S}_t F_0$ ⁸. Thus, we can continue equation 3.47 with

$$V_0^*(x_0, N) = \sum_{t=0}^T (\tilde{S}_t L_t^*) F_0 - K \sum_{t=0}^T (L_t^*). \quad (3.48)$$

For each price path we know the individual ACF and Forward price and therefore can calculate for each path the derivative of the ACF with respect to the Forward price as

$$\frac{\partial v_0^{i,*}(x_0, N)}{\partial f_0^i} = \sum_{t=0}^T (\tilde{S}_t L_t^*). \quad (3.49)$$

This summation varies with every price trajectory and is not identical to the Forward delta Δ^F , but it will help to illustrate the mechanism. If \tilde{S}_t was always 1 then all hourly prices would match the Forward price F_0 and the previous equation would be at maximum the sum of all delivery hours times the swing size L ($\sum_{t=0}^T L_t^* = T \cdot L$). Of course, the optimal policy picks hours with high prices above F_0 i.e. $\tilde{S}_t > 1$ and then the sum can easily exceed the total number of swings (recall that Figure 3.1 illustrates this effect between value and volume hedge as well). We can see this effect most significantly for the single swing (American option). In order to hedge 1 MWh we need to invest more than 8 MWh in the Forward contract. For the single itm swing option the underlying is really merely one delivery hour. The fluctuation of a single hour can only hardly be represented by the Forward price i.e. the average spot price across the *entire* delivery period. The more swings are available the more the resulting schedule resembles a Forward contract. Already for 360 swings which represent half of the delivery period we can observe that the energy delta with 541 MWh is less than 50 % higher than the exercisable amount of 360. For the single option it was 800 % instead. For 720 swings and strike $K = 0$ the option behaves like a Forward. Then the option premium is simply the average of all Forward prices (this is 1 in our case) multiplied by the delivery hours i.e. 720.

3.3.3. Volumetric Delta

So far, we looked at value hedges that will offset changes in the power plant cash flow or expected cash flow. As illustrated in the introductory example in section 3.1 we do not only need to take care about the mere monetary value, but also about the physical energy that comes along with both the dispatch schedule and the hedging instrument. The *volumetric* hedge therefore seeks for compensating the energy resulting from the generation schedule by selling Forward contracts F_0 of the same total energy amount. In section 3.3.2 we explained that each individual cash flow $V_0^*(x_0, g_0, \delta)$ is the result of a specific price-schedule scenario $(x_t^i, l_t^i)_t$. Analogously, the pairs $(f_0^i, w^{*,i})$ describe one possible Forward price-energy scenario with $w^{*,i} := \sum_{t=0}^T l_t^{*,i}$. Note that in case of all $\tilde{S}_t = 1$ in equation 3.49, then w^* would be identical to the forward delta. This specific relation makes us interpret the produced energy amount as a sensitivity measure as well that we call volumetric delta. We therefore

⁸Note that $\tilde{S}_t \neq S_t$ for S_t is defined as a relative shift with respect to $H_t = \alpha_t G_0 \eta_0$ (see also equation 3.31) whereas \tilde{S}_t is a relative shift with respect to F_0 .

alternatively replace in equation 3.41 the Forward delta Δ^F with the volume delta Δ^w

$$\Delta^w := \mathbb{E} \left[\sum_{t=0}^T L_t^* \right] \approx \frac{1}{I} \sum_{i=0}^I \sum_{t=1}^T l_t^{*,i}$$

(3.50)

s.t.

$$V^*(x_0, g_0, \delta) = C^*(x_0, g_0, \delta) + \Delta^w(F_0 - g_0) + \epsilon_w^*,$$

with ϵ_w being the hedging error. We continue our example and add the volumetric delta for our three swing options. The volumetric delta gives a good indication how deep in-, out- or

Swings	K	MWDelta [MW]	Delta [MWh]	K	MWDelta [MW]	Delta [MWh]	K	MWDelta [MW]	Delta [MWh]
1	0	0.0014	1	1	0.0014	0.998	2.5	0.0013	0.94
360	0	0.5	360	1	0.4004	288.29	2.5	0.0191	13.733
720	0	1	720	1	0.4004	288.29	2.5	0.0191	13.733

Table 3.6.: Volumetric Delta

at-the-money a swing option really is. As we can see for $K = 2.5$, we would first think that the option is way out of the money. But there are single spot prices within the 720 hours that exceed the strike price nevertheless. Therefore we still expect almost the full energy amount to be exercised (0.94 MWh) for a single swing right. However, as soon as we add more swing rights, we quickly realize that not many spot prices can make it above $K = 2.5$ and therefore in average not more than 14 swings (13.73) will ever be exercised no matter whether we have 360 or 720 swings available.

3.3.4. Synthetic Spot Delta

The sensitivities we introduced so far are not able to capture the impact of individual hourly price fluctuations on the ACF. Even the Forward delta can only capture changes in the average spot price. A delta calculation should usually rely on the price of a tradable product. Then the delta tells us the amount to invest in this hedging product. Hourly spot price products, however, are only available on the day ahead market. However, the sensitivity of these quoted spot prices for tomorrow on the real option value of a monthly or even yearly production period is certainly negligible. We are rather interested in a spot sensitivity that captures an impact on the entire production period. A useful spot delta should also consider the effect of day types which could be viewed as separate products. The latter leads to the idea of treating hours of the same day type as one single artificial product p . We could treat, for example, hour 9 on weekdays as one separate contract. Then we implicitly assume that prices of hour 9 move Monday through Friday in parallel. We could also group neighboring hours together like hour 9-11 as long as these hours are sufficiently correlated. To be precise, we define the synthetic product price X_p as the average of the associated underlying spot prices X_t that belong to this product

$$X_p(\{X_t\}_t) := \frac{1}{|\mathbb{T}_p|} \sum_{t \in \mathbb{T}_p} X_t \quad \mathbb{T}_p \subset \{0, \dots, T\}.$$

(3.51)

Likewise we can define h_p as the average of the corresponding hourly curve adjusted prices h_t for a fixed Future contract $G_0 = g_0$

$$h_p(\{h_t(g_0)\}_t) := \frac{1}{|\mathbb{T}_p|} \sum_{t \in \mathbb{T}_p} h_t(g_0) \quad \mathbb{T}_p \subset \{0, \dots, T\}. \quad (3.52)$$

Now, we introduce a sensitivity measure in terms of the deviation of X_p from h_p which leads to the following definition:

Definition 3.3.2 (Synthetic Spot Delta). *The synthetic spot deltas Δ^p are the slope parameters of a P -dimensional linear least-square regression⁹ to describe cash flow realizations $V_0^*(x_0, g_0, \delta)$ of a real option value $C_0^*(x_0, g_0, \delta)$ with respect to spot price deviations X_p from the fixed hourly Future price curve h_p ; $p = 1, \dots, P$ are time buckets within the exercise period and X_p and h_p are the average price of the underlying spot prices X_t and Future prices h_t in time bucket p*

$$V_0^*(x_0, g_0, \delta) = C_0^*(x_0, g_0, \delta) + \sum_{p=1}^P \Delta^p (X_p - h_p) + \epsilon^*, \quad (3.53)$$

where x_0 is the current spot price, g_0 and F_0 are defined in equation 3.33 with $j = 0$, X_p and h_p are defined in equations 3.51 and 3.52, δ being a vector of further option parameters and ϵ^* being the residual.

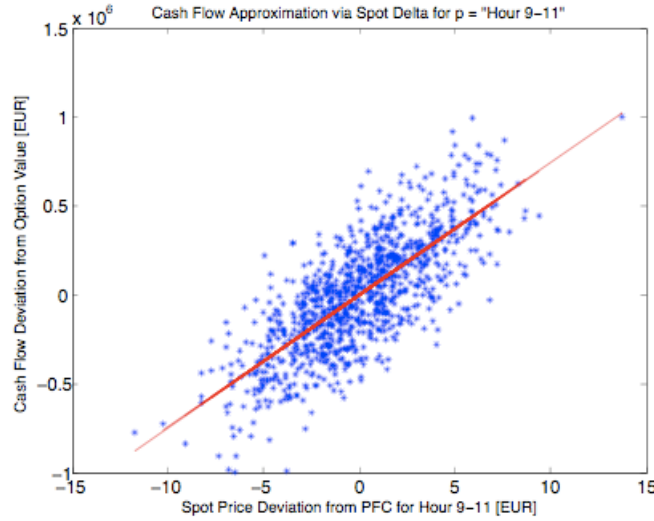


Figure 3.5.: Cash flow vs. spot price deviations approximated via the spot delta for the synthetic product "Hour 9-11".

Figure 3.5 presents an example taken from our numerical analysis in section 4.5 where we define $P = 4$ artificial products: "Hour 9-11", "Hour 12", "Hour 13-17", "Hour 18-20". The graph plots the spot price deviations of hours 9 - 11 from the hourly PFC, i.e. $(X_{9-11} - h_{9-11})$,

⁹Throughout this entire thesis we only work with an estimator of the regression parameter that we calculate from concrete realizations $i = 1, \dots, I$ of the random value pairs $(X_p - h_p, V_t^*(x_t, g_0, \delta))$, i.e. of the synthetic product price and ACF. Therefore, whenever we use Δ^p in this thesis we actually refer to the estimator of the regression parameter which varies with every new data set unlike the true regression parameter.

against deviations of the ACF from the real option value $\Delta V_0(x_0, g_0, \delta)^{10}$ for the delivery month of March. The cloud is based on 1000 spot price scenarios. In addition we see the approximation of this cloud via linear approximation using the synthetic spot delta Δ^{9-11} as the slope parameter. The graph illustrates the linear behavior of the cash flow deviations.

We interpret the coefficients Δ^p as the spot price sensitivity of the cash flows of the real option with respect to price shifts in the corresponding time window p . We will later call ϵ^* the open spot price exposure (see section 3.3.5). X_p is an average price of random spot prices and therefore is random as well whereas h_p is computed from the fixed (adjusted) Future price of the relevant delivery hours and therefore is non-random. Note that for $P = 1$ and $\mathbb{T}_1 = \{0, \dots, T\}$ we receive the Forward contract such that the Forward delta Δ^F is a special case of the more general synthetic spot delta definition Δ^p . As explained this artificial product does usually not exist in the market and cannot be immediately used for hedging. However, we will show that the spot delta figures will help us to find an appropriate swing option to hedge power plants with different technical and energetic constraints. We refer to section 4.5 for a more detailed numerical example where we analyze hedging instruments for power plants.

3.3.5. Earnings-at-Risk

In the last four sections we introduced linear hedging instruments and our examples illustrated that only in case of many exercise rights and low strikes the swing option can be efficiently hedged with Forwards and Futures. We identified significant basis risk since our hedging instruments only implicitly share the same underlying with the swing option. The Forward and Futures price simply cannot capture the individual spot price fluctuations. We recognized that the delta of our swing option did not behave like the delta of a standard European call option on an electricity Future. Now the question is how good are our hedges really. In other words, how should we quantify the remaining open exposure? Precisely speaking we are interested in the remaining exposure after applying a hedge i.e. the residual ϵ^* in equation 3.41. It represents the open spot price exposure. Now, we want to introduce *Earnings-at-Risk (EaR)* as an adequate risk measure for this spot price exposure. Terms like *Profit-at-Risk (PaR)* or *Cash-Flow-at-Risk (CFaR)* are often used in the same context. They all relate to the same concept that tries to capture the particular market risk of physical assets which is a combination of price and quantity risk that both determine the actual future cash flows/earnings. Our swing option model already covers the interdependence between price and quantity by the dispatch policy. Our EaR definition goes therefore one step further and additionally consider the hedge position:

Definition 3.3.3 (Earnings-at-Risk (EaR_β)). *Earnings-at-Risk is the β -quantile $q_\beta(\epsilon^*)^{11}$ of the distribution of residuals ϵ^* of a linear least square regression to describe individual cash flow deviations $V_0(x_0, g_0, \delta)$ from the expected cash flow (real option value) $C_0(x_0, g_0, \delta)$ with*

¹⁰To be precise, the values are taken from our stochastic dynamic programming (SDP) based power plant model $\mathbb{L}C_0^*(x_0, W_0)$ with total energy W_0 restricted to 70 % of the maximum producible energy \overline{W}_0 .

¹¹Throughout the entire thesis we only work with an estimator of the quantile $q_\beta(\epsilon^*)$. So instead of the probability distribution we rather use the frequency distribution that we generate from concrete realizations $i = 1, \dots, I$ of the random value pairs $(F_0 - g_0, V_t^*(x_t, g_0, \delta))$, i.e. of the Forward price and ACF. Therefore, whenever we use $q_\beta(\epsilon^*)$ in this thesis we actually refer to the estimator of the quantile using the frequency distribution which varies with every new data set unlike the true quantile based on the probability distribution.

respect to deviations of the Forward price F_0 from the fixed Future price g_0

$$\begin{aligned} \epsilon^* &:= V_0^*(x_0, g_0, \delta) - C_0^*(x_0, g_0, \delta) - \Delta^F(F_0 - g_0) \\ \text{and} \\ \beta &= \text{Prob}(\epsilon^* \leq q_\beta(\epsilon^*)). \end{aligned} \tag{3.54}$$

where x_0 is the current spot price, Δ^F is the Forward delta (see equation 3.45) and δ is a vector of further option parameters.

EaR is a risk figure for delivery based physical contracts. It describes the maximal loss in earnings of a Forward hedged dispatch schedule due to mere spot price and resulting quantity changes. We therefore also call ϵ^* the remaining open spot price exposure. Technically the definition is identical to VaR. However the main distinction lies in the different nature of the distributions which in return is the result of different time horizons. While the underlying distribution for VaR reflects a change in portfolio *value* and is usually generated by scaling the volatility of the portfolio's underlying market prices according to a short holding period (usually a day), the EaR distribution is rather shaped from *cash flows* that occur at different payment dates in the future, usually a complete balancing period i.e. a year. Hence, we need to evaluate the volatility at different future dates rather than just scaling the current one. That makes a significant difference. Table 3.7 provides a comparison of both risk measures.

Earnings-at-Risk	Value-at-Risk
EaR is a risk measure that quantifies the uncertainty of <i>delivery</i> contracts (physical positions).	VaR is a risk measure that quantifies the risk of a <i>trading</i> (financial) position.
EaR provides the max loss in <i>profit</i> during delivery.	VaR provides the max loss in <i>market value</i> within a specific holding period.
EaR measures risk against spot price changes.	VaR is measuring the risk against Forward Curve changes.
EaR requires to evaluate the risk factor at different future payment dates to generate the distribution.	VaR simply scales the risk factors' current volatility according to the holding period.

Table 3.7.: EaR vs. VaR

Depending on whether one is the buyer or the seller of a swing option either the left or the right tail of the distribution of ϵ^* represents a loss. The option holder is interested that the option value does not fall significantly below the initial premium that he has paid. Hence, he looks at the left tail: $q_\beta^B := q_\beta(\epsilon)$. The option seller instead is afraid of deep in the money situations ($V_0^*(x_0, g_0, \delta) \gg C_0^*(x_0, g_0, \delta)$) where delivering the power at a high price is expensive. Hence, for him the negative of the upside percentile $q_\beta^S := q_{1-\beta}(\epsilon)$ represents a loss.

Now, we return to our example and compute both tails before and after applying our hedges in order to assess their effectiveness. In our example we look at three swing options that cover a delivery period of one month. In particular we are interested in the comparison of the volumetric hedge versus the Forward hedge. As usual we work with our lower bound approximation $V_0 := V_0(x_0, N)$ and $C_0 := C_0(x_0, N)$. For our specific price process with a Futures price of 1 equation 3.54 reduces to $\epsilon_F = V_0 - C_0 - \Delta^F(F_0 - 1)$ and $\epsilon_w = V_0 - C_0 - \Delta^w(F_0 - 1)$ respectively. Table 3.8 presents the comparison for the quantiles of 1% and 99%. We added the (non-hedged) loss distribution $\ell = V_0 - C_0$ as a benchmark. First, we can see

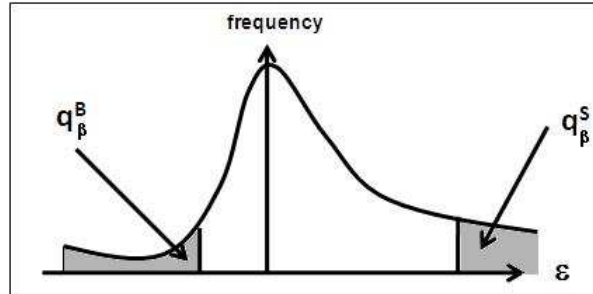


Figure 3.6.: Earnings-at-Risk for option seller and buyer

Swings	K	No hedge $q_{0.01}(\ell)$	Volume hedge $q_{0.01}(\epsilon_w)$	Forward hedge $q_{0.01}(\epsilon_F)$	No hedge $q_{0.99}(\ell)$	Volume hedge $q_{0.99}(\epsilon_w)$	Forward hedge $q_{0.99}(\epsilon_F)$
1	0	-2.1918	-2.1782	-2.0574	2.3814	2.3600	2.3530
1	1	-2.1947	-2.1912	-2.0951	2.4160	2.4185	2.3496
1	2.5	-1.6041	-1.6140	-1.6927	2.5570	2.5401	2.3771
360	0	-29.8809	-12.4935	-8.6047	31.0914	12.6469	8.3576
360	1	-25.9426	-12.6685	-9.0097	28.1081	14.2881	9.4357
360	2.5	-5.7408	-5.4910	-5.2904	7.9799	7.5767	6.6957
720	0	-37.1670	0.0	0.0	41.8404	0.0	0.0
720	1	-25.9426	-12.6685	-9.0097	28.1081	14.2881	9.4357
720	2.5	-5.7408	-5.4910	-5.2904	7.9799	7.5767	6.6957

Table 3.8.: Earnings-at-Risk

that the loss distribution is generally skewed to the right. The positive skewness increases the more the option goes out of the money (for $K = 0$ and 360 swings the left and right tail are almost equal in absolute terms: $q_{0.01}(\ell) = -29.9$ and $q_{0.99}(\ell) = 31.1$ opposed to $K = 2.5$ where the right quantile is larger: $q_{0.01}(\ell) = -5.7$ and $q_{0.99}(\ell) \approx 8$). The swing option tries to exercise high prices which results in a fatter right tail. Next, we can see that the Forward hedge prevails clearly the volumetric hedge throughout all strikes and swings. The gap is most obvious for 360 swings ($q_{0.99}(\epsilon_F) = 9.44$ vs. $q_{0.99}(\epsilon_w) = 14.29$ for $K = 1$). We can see that the quantiles are identical for 360 and 720 swings with $K = 1$ or $K = 2.5$. This is consistent with our results in table 3.5 where we recognized identical option values for these cases as well. Hence, the distributions are the same as in both cases less than 360 swings will be exercised. For $K = 0$ and 720 swings both the volumetric and Forward hedge offset perfectly changes in option value. This is what we expect since in this situation the swing option acts like a Forward. The opposite situation can be identified for the lower quantile of a single swing right with $K = 2.5$. The Forward hedge cannot compensate at all the few spot prices that do still exceed the strike. With $q_{0.01}(\epsilon_w) = -1.614$ and $q_{0.01}(\epsilon_F) = -1.6927$ vs. $q_{0.01}(\ell) = -1.60$, the supposed hedge even increases the risk.

3.3.6. Replacement Risk and Total Option Value

For our further analysis we want to focus on the following business case: A utility company is usually organized into three business units that are often even separate legal entities: a generation department, a trading unit and a retail branch (see also Figure 3.7). Before the deregulation of electricity markets retailers directly sold the power that the generation department delivered. With the rise of electricity exchanges and free floating electricity prices the utilities founded separate trading units. They reside in between the two other departments. The trading unit purchases the power from the generation unit and thus sells it to the retail unit. In between it manages the price risk by buying and selling power from/to the market. If it manages to sell the purchased production 1:1 then no risk resides within the trading department. However, generation output is way too large that it can be sold entirely to a single customer. It rather has to be sliced into smaller pieces. Often these deals are so called wholesale contracts where the customer can take as much electricity as he wants for a fixed price. On a smaller scale this is the classical household contract. In short, current generation and actual retail amount usually do not match, in particular not on the hourly level and the trading unit needs to fill the gap by buying/selling on the day ahead market. The trading unit can enter into Forward or Futures contracts on the OTC market or the exchange and lock the price if it does not want to be exposed entirely to the spot market. We learned in the last section, however, that this strategy does not provide a full hedge in most of the situations neither on the price nor on the volume. Hence, the trading unit needs to balance the remaining risk between the retail and generation unit. Now, we want to quantify an interval for the compensation fee for taking the price risk. This should provide a decision support for agreeing on an internal pricing scheme between business units. We will do so by using our swing option to model the generation as well as the retail side.

If we ignore the volume risk i.e. the fact that the demand is not only price driven but rather a risk factor on its own, then we can interpret a wholesale contract as a swing option that trading sells to retail. The contract allows to receive electricity for a fixed price every hour. On the opposite side trading buys the produced electricity from generation. In a first approach, we can interpret a power plant as an asset that has the flexibility to produce power for a fixed fuel price (i.e. the strike) or not. The number of swings reflects an energy limit that could be a CO_2 constraint for a thermal plant as well as a limited water reservoir of a hydro plant. In this specific setup the trading unit acts like a swing option buyer and option

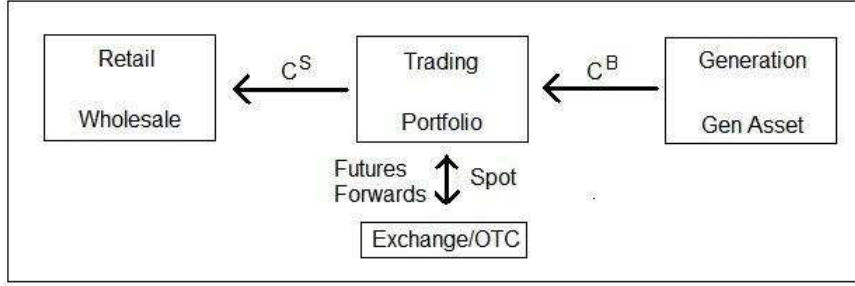


Figure 3.7.: Business Case: Trading unit as 'Man-in-the-Middle'

seller at the same time.

In the last section we introduced our definition of Earnings-at-Risk as the quantile of the loss distribution after a Forward/Future hedge. It therefore suits very well as a reference for the risk fee that the trading unit can ask for to finance the management of the price risk. Throughout this section we will use again the abbreviation $C_0 := C_0(x_0, N)$. Equation 3.55 presents the total option value for the seller and the buyer

$$\begin{aligned}
 C_\beta^B &:= C_0 + q_\beta(\epsilon) = C_0 + q_\beta^B(\epsilon) \\
 C_\beta^S &:= C_0 + q_{1-\beta}(\epsilon) = C_0 + q_\beta^S(\epsilon),
 \end{aligned}
 \tag{3.55}$$

where $q_\beta(\epsilon)$ is defined as in equation 3.54. Note that the previous equation also introduced new labels for the quantiles $q_\beta^B(\epsilon) := q_\beta(\epsilon)$ and $q_\beta^S(\epsilon) := q_{1-\beta}(\epsilon)$. C_β^B is the total option value that the trading unit accepts to pay to the power plant unit for the generated electricity (the trading unit is the buyer). Table 3.9 presents actual results for our three sample options and needs to be compared with the fair option values presented in Table 3.5. We could think of the three different strikes as marginal production costs of three different types of power plants. $K = 0$ would represent a power plant that is always itm like a nuclear plant. $K = 1$ represent atm power plants like a coal fired plant that needs to consider emission costs as well. $K = 2.5$ is a power plant that is only profitable for high price like a gas-fired peakload plant. The number of swings could model a shared power plant. 720 swings would represent the maximal output of the plant. Hence, 360 swings would represent a power plant that is shared between two owners. Especially in smaller East European countries power plants close to the border are shared between neighboring national utilities. Now, the trading unit asks for a discount on the fair value of the produced power to compensate for possible losses in case prices fall below the current price level when getting into delivery. The probability β describes the percentage of value losses that are not covered by the fee. Note that $\beta < 0.5$ and therefore $q_\beta(\epsilon)$ is negative and consequently we get $C_\beta^B < C_0$. So the risk fee makes the buyer's option cheaper. The higher β the less risk averse the trading unit is and henceforth the smaller the discount. We can see that a risk averse trading department would never invest in a small energy amount of a peakload plant (1 swing, $K = 2.5$). As Table 3.9 indicates the trading department would even ask for money (0.089 cents) to take over the risk of a remaining 1MW of production. The hedge obviously fails and it is cheaper not to hedge at all. Then the loss $q_\beta(V_0 - C_0) = -C_0$ is identical to the fair value as the smallest 1 % of all prices will lead to no exercise and the total option value is 0. For this reason we will later in this chapter (see Tables 3.13 and 3.14) replace this negative total option value by 0.

C_β^S is the seller option i.e. the total option value that trading sells to the retail department. As $\beta < 0.5$, we know that $q_{1-\beta}$ is positive and thus $C_\beta^S > C_0$. This additional spread on top of the fair value covers the replacement risk. This is the potential loss if the trading unit

Swings	K	$C_{0.01}^B$	$C_{0.01}^S$	$C_{0.05}^B$	$C_{0.05}^S$	$C_{0.3}^B$	$C_{0.3}^S$
1	0	1.9540	6.3644	2.6389	5.4376	3.6347	4.3515
1	1	0.9190	5.3638	1.7085	4.4531	2.6329	3.3562
1	2.5	-0.0886	3.9812	0.2333	3.0918	1.1847	1.9533
360	0	488.901	505.863	491.609	503.567	495.528	499.489
360	1	133.972	152.418	136.460	149.711	140.757	145.046
360	2.5	2.304	14.2903	3.5919	12.4253	5.9958	8.9053
720	0	720	720	720	720	720	720
720	1	133.972	152.418	136.460	149.711	140.757	145.046
720	2.5	2.304	14.2903	3.5919	12.4253	5.9958	8.9053

Table 3.9.: Total Option Value (1%, 5%, 30% uncovered spot exposure)

is forced to deliver electricity in hours when spot prices exceed the fixed retail price offered to external customers. Of course, C_{β}^S and C_{β}^B only define the lower and upper end of the internal pricing spectrum. If the trading department could realize the total option value on both sides it would receive a profit from the difference of the risk premia due to the skewness of the distribution ($q_{\beta}(\epsilon) \neq q_{1-\beta}(\epsilon)$). For instance buying half of a coal fired power plant (360 swings, $K = 1$) for $C_{0.01}^B = 134$ and selling it for $C_{0.01}^S = 152$ given a fair value of $C_0 = 143$ (see Table 3.5) would result in a comfortable profit of 18 despite of the same 1% remaining spot price risk. In case of a nuclear plant (720 swings, $K = 0$), as another example, the trading department can pass on 1:1 of the total energy to the market by selling Forwards and lock the value of 720 completely. Therefore there is no additional risk spread and the value has to be identical to the Forward value (contract price of 1 times 720 hours). The retail and generation department are aware of this entire mechanism as well. Hence, Table 3.9 might be a good reference for discussing appropriate internal prices.

3.4. Risk Controlling

In the previous chapter we focused on risk factors that are originated in price changes of tradable products and we gathered all further effects like second order sensitivities in the residual ϵ which we quantified using our EaR measure. Now, we want to go one step further and investigate how to manage and control this residual risk. We already explained that the Forward and Future delta divided by the contract hours for the associated delivery period (we called it "MWDelta") provide us with the number of Forwards to invest in for offsetting his current open exposure. We also presented situations where this hedge will be rather inefficient. One way to get rid off the remaining risk is to pass it on to another department or counterparty. We introduced the business case of a generation unit that transfers the spot exposure to the trading unit. We also suggested to ask for a risk premium to compensate potential losses of the inherent replacement risk. However, we saw that the risk spreads can be high and it is questionable whether these expensive fees can be achieved in reality. For this reason we want to investigate yet another alternative. Currently the exercise policy of our swing option model tries to pick the hours such that the expected payoff is maximized. Hours with high prices usually are a result of high volatility. Hour 12 on weekdays for instance is known for its frequent spikes. An optimal strategy would usually pick this hour by default. However, choosing hour 11 instead, which still promises high prices, but is less spiky, would result in a slightly smaller return, but also a thinner tail and thus a smaller risk premium $q_{\beta}(\epsilon)$. If the smaller risk premium more than compensates the decline in fair value, then hour 11 is the better choice. In other words, our third alternative tries to control the risk by

imposing a less risky exercise strategy. Therefore, we will introduce a risk constraint into our optimization procedure.

A risk measure ρ can be considered within the optimization in two ways. The first class of models introduces ρ as the objective function and henceforth defines an entirely new optimization model as it replaces the objective to maximize the generation asset value. Those models are usually minimization problems if they look merely at the risk functional. Alternatively the objective can balance between the maximization of payoffs Z and minimization of risk, so called *mean-risk models*. This can be achieved by either introducing a risk aversion factor γ that weights expectation vs. risk: $\gamma\mathbb{E}[Z] - (1 - \gamma)\rho(Z)$ as proposed by Markowitz [49] or by imposing a utility function U as introduced by the theory of von Neumann and Morgenstern [53]. It describes the risk aversion of the investor and usually also contains a calibration factor for the degree of risk aversion $U(\mathbb{E}[Z], \rho(Z), \gamma)$. The second class of models integrates the risk functional ρ into an existing optimization model as a further constraint with a predefined threshold, called *probabilistic* or *chance constraints* models. The decision on whether to apply a risk measure as an objective or as a constraint is often dependent on the type of risk measure itself. The individual mathematical characteristics of a specific measure determine the type of integration into an existing optimization problem in order to ensure a feasible solution scheme. Figure 3.8 illustrates this dependency in a matrix structure. While the columns represent the model class, the rows list the different risk measures. We can see that the rows are grouped by static and dynamic risk measures. The latter is a fairly new research field and describes a situation where the risk measure evolves over time, but still can be influenced by the decision maker. Shapiro et al. [59] provide a good overview of risk measures and adequate optimization algorithms. We will focus on applications to electricity markets and Figure 3.8 presents an overview of relevant papers. An evident first approach is

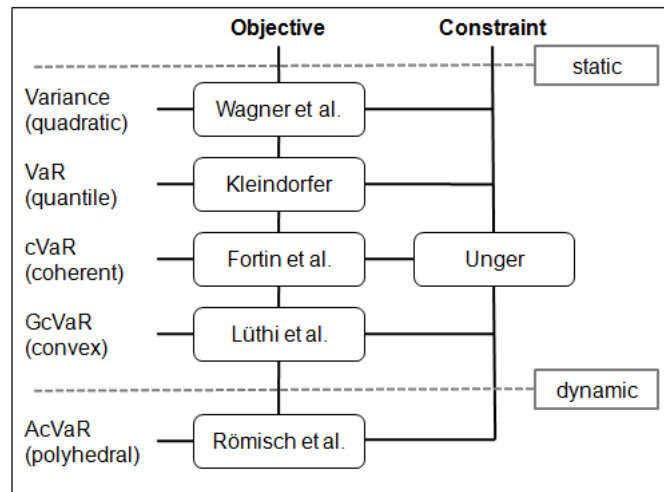


Figure 3.8.: Overview of risk measures with applications in electricity models

to apply the Markowitz model to power portfolio optimization. Wagner et al. [66] use the mean-risk model to find the best hedge of retail contracts (electricity contracts to customers with fixed price) with Forwards. Following the Markowitz model they use the variance as their risk measure and can therefore solve the problem via quadratic programming. This is actually only a vehicle to their original problem that tries to find a portfolio allocation which maximizes the cash flow for a given VaR boundary. Value-at-Risk is the second risk measure in the Figure 3.8 that we already discussed in context of section 3.54. For linear contracts and normally distributed prices the variance is sufficient to describe the tails and hence the

VaR. For this reason Wagner et al. could reformulate their problem in terms of the variance which introduces a quadratic expression into the objective function. Kleindorfer [41] uses the same approach to maximize a VaR constrained power portfolio consisting of a generation asset (simply modeled as fixed rate power contracts), daily put and call options, Forwards and wholesale power contracts (flexible volume at a fixed price). However, for a general distribution especially in a portfolio setting with multiple random variables and contracts the computation of VaR relies on Monte-Carlo simulation. This circumstance in combination with the non-subadditivity and non-convexity of VaR does not allow for using powerful and fast linear optimization techniques. Still VaR is widely accepted, understood and implemented in practice. Therefore one research direction started to look for similar measures that like VaR investigate the distribution tails and at the same time provide desired features like linearity for a feasible optimization scheme. One popular first result of this investigation is the definition of *conditional* Value-at-Risk $cVaR_\beta(Z)$ that is the expectation of a loss for only those cash flows Z that exceed the VaR value $cVaR_\beta(Z) = \mathbb{E}[Z|Z \geq VaR_\beta]$. Therefore cVaR is also known as *expected short-fall*. This definition of an expectation like measure ensures the linear property, a required feature for linear programming. In addition Rockafellar and Uryasev [56] reformulated cVaR as a linear programming problem whose dual representation leads to its computational ease. This new approach allows for introducing cVaR in broader optimization problems. Thus, cVaR can be used either as an objective or as a constraint. The latter was investigated by Unger [65] in the context of a power portfolio optimization. He maximizes the profit of a portfolio consisting of spot positions, Futures and swing options with respect to a cVaR threshold. Fortin et al. [27] analyzed investments in coal fired, biomass and wind power plants by minimizing a cVaR objective.

cVaR fails to differentiate among the severity of risky outcomes beyond the quantile. The probability mass could still be strongly bias and favor extreme events (i.e. probability mass at the far end of the tail) which cannot be covered by the mere conditional expectation. This shortcoming motivated a generalization of the underlying axiomatic framework. Pflug [54] showed that cVaR belongs to the class of coherent risk measures [3] if X is a discrete random variable. A coherent risk measure ρ_{ch} is a mapping: $X \xrightarrow{\rho_{ch}} \mathbb{R}$ with $X := X(\omega)$ being a random variable on the probability space (Ω, F, \mathbb{P}) having the mathematical desirable characteristics of being convex, monotone, translation invariant and positive homogeneous. In particular convexity ensures the subadditivity $\rho_{ch}(X + Y) \leq \rho_{ch}(X) + \rho_{ch}(Y)$ meaning that controlling the risk of subsidies X and Y via ρ_{ch} and adding them up will ensure an upper estimate of the total exposure measure in ρ_{ch} . Föllmer [26] investigated a relaxation of the coherent risk measure definition by ignoring the positive homogeneity which led to the definition of convex risk measures. Positive homogeneity assumes that risk grows proportional to the volume of a portfolio Z . However, if price liquidity cannot be assured which is typical for electricity markets due to the small number of producers then the exposure might grow faster than linear in traded energy amount. Lüthi [48] defines a convex cVaR measure that he calls *General cVaR* or $GcVaR_{\beta,L}(Z)$. The generalization is achieved by introducing the parameter L in the *cVaR* definition which allows for varying the measure between the regular cVaR and the maximal loss. In other words L enables to penalize large losses and hence account for a bias probability mass in the tail that cVaR cannot capture.

Still, *GcVaR* cannot overcome one more drawback of cVaR: it is only a static measure. In a multi-stage decision process like our option valuation, however, where the filtration of the price reveals statistical information of the future and knowledge of the past only in discrete time steps a risk measure that is based on a single set of stochastic data is not appropriate. Instead, a multi-period risk measure is required. Eichhorn et al. [24] suggest so called polyhedral risk measures. They are basically an extension of cVaR for the dynamic case. Hence, they can also

be expressed as optimal values of certain simple-structured stochastic minimization problems where the decision variables are defined on polyhedral cones which give this risk measure its name. It is rather a family of risk measures and Eichhorn presents several applications. One example is the average of cVaR measures calculated at several (not necessarily all) stages of the multi-period process (in Figure 3.8 denoted as *AcVaR*).

Returning to our initial objective of investigating risk sensitive exercise strategies a dynamic risk measure seems to be appropriate for our focus on swing options. A polyhedral risk measure like *AcVaR*, however, that averages intermediate cVaR results is rather problematic. Intermediate stages of the swing option optimization do not represent the entire option contract, but rather separate ones on shorter delivery periods. In our example we look at swing options for a one month delivery. Each stage of the dynamic program, however, can be interpreted as a separate valuation of a new option whose underlying is the remaining delivery period which grows from stage to stage. These options have different pay-offs and different distributions, in particular from the time step onwards where the delivery period exceeds the number of swing rights. Simply averaging the cVaR of these intermediate solutions will not reflect the overall cVaR let alone VaR of the option that one wants to reduce. In addition, we prefer a mere VaR based measure since it is more accepted in the market and fits better to our EaR based risk measure. In the next section we will therefore suggest an EaR based risk constraint for our purpose of risk controlling.

3.4.1. EaR Sensitive Control

In section 3.3.6 we introduced the total option value as the fair value plus or minus a risk spread dependent on whether one is the option buyer or seller. We explained that this value represents adequate lower and upper bounds for a risk adjusted swing option value. First, our risk spread is not based on mere variance like many risk-return models that fail to describe the behavior in the tails of non-normal distributions. This would have significantly reduced the spectrum of price processes for our option model. At the same time we introduced with EaR a risk measure that follows the popular concept of VaR. The option holder can express his risk aversion by choosing his acceptable loss probability. It states that $(1 - \beta)$ percent of the value fluctuations will be compensated by the extra spread either as a discount (buyer's option) or an extra fee (seller's option). We think that the percentile is a more intuitive way to capture the risk aversion of an investor compared to a utility function or a risk/return weighting factor. For this reason we will rely our benchmark for different risk controlling strategies on our total option value and introduce the following definition:

Definition 3.4.1 (EaR-Efficient Option Value). *An option value $\tilde{C}_\beta^e := \tilde{C}_\beta^e(x_0, g_0, \delta)$ is EaR efficient if the underlying exercise policy $\tilde{\pi}_0^*$ can reduce the risk premium measured as EaR $q_\beta(\tilde{\epsilon})$ with fixed $\beta < 0.5$ more than the inherent deduction in option value $\tilde{C}_0 := \tilde{C}_0(x_0, g_0, \delta)$ compared to a risk neutral valuation $C_0 := C_0(x_0, g_0, \delta)$ and $q_\beta(\epsilon)$*

$$\begin{aligned} \tilde{C}_\beta^e &:= \tilde{C}_0 + q_\beta(\tilde{\epsilon}) \\ \text{s.t.} & \\ C_0 - \tilde{C}_0^e &< q_\beta(\tilde{\epsilon}) - q_\beta(\epsilon), \end{aligned} \tag{3.56}$$

where x_0 is the current spot price, g_0 and F_0 are defined in equation 3.33 with $j = 0$ and $q_\beta(\epsilon)$ as described in equation 3.54.

Translated to our buyer's and seller's option we can write

$$\begin{aligned} C_0 - \tilde{C}_0 &< q_\beta^B(\tilde{\epsilon}) - q_\beta^B(\epsilon) \\ C_0 - \tilde{C}_0 &< q_\beta^S(\epsilon) - q_\beta^S(\tilde{\epsilon}). \end{aligned} \quad (3.57)$$

The quantiles of the seller's option $q_\beta^S(\epsilon)$ and $q_\beta^S(\tilde{\epsilon})$ are flipped as we look at the right tail (recall from equation 3.55 that $q_\beta^S := q_{1-\beta}$). A risk sensitive dispatch policy $\tilde{\pi}_0$ (from now on we mark risk sensitive values with a tilde) in the sense of definition 3.4.1 should raise the new buyer's total option value compared to C_β^B and lower the new seller's total option value compared to C_β^S to a more attractive sales price such that the inevitable reduction of real option value will be over-compensated by the mitigation in EaR (see equation 3.55 for the definition of $C_\beta^{B/S}$). The distribution of an EaR efficient option is tighter as shown in Figure 3.9. Let us illustrate this concept in context of our business case with our retail, trading and

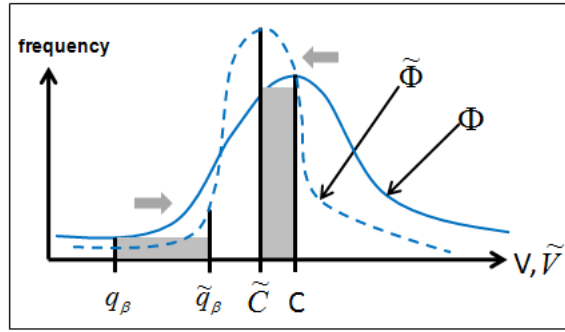


Figure 3.9.: Benchmark for a risk sensitive policy

generation unit. If the generation department could offer a production strategy that would lower the price risk and still assure an adequate return then the trading department will be willing to accept a smaller discount on the price for the generated electricity denoted as the new buyer's swing option \tilde{C}_β^B . The generation department in return could achieve a higher profit without increasing the risk for the entire organization. At the opposite side the trading unit could sell the risk sensitive policy as a swing option with special exercise conditions. Again, if those conditions still ensure a reasonable return and lower the risk fee at the same time, then the new lower option price \tilde{C}_β^S becomes more attractive to an industry customer and therefore the retail department would be willing to accept the price.

In case of our swing option with N exercise rights and initial price $X_0 = x_0$ we can write two optimization problems, for buyer and seller separately, that finds the most EaR efficient option value

$$\begin{aligned} \tilde{C}_0^{B,e}(x_0, N) &= \max_{\tilde{\pi}_B} \{ \tilde{C}_0(x_0, N) + q_\beta(\tilde{\epsilon}) \} \\ \tilde{C}_0^{S,e}(x_0, N) &= \max_{\tilde{\pi}_S} \{ \tilde{C}_0(x_0, N) - q_{1-\beta}(\tilde{\epsilon}) \}, \end{aligned} \quad (3.58)$$

with \tilde{C}_0 and $q_\beta(\tilde{\epsilon})$ as defined in equations 2.3 and 3.54 respectively and $\tilde{\pi}_{B/S} = \{ \tilde{\tau}_N^{B/S}(0, N), \dots, \tilde{\tau}_1^{B/S}(0, N) \}$ is a sequence of exercise times. The two equations penalize the swing option value with the EaR figure. Recall that the buyer's and seller's EaR are on opposite sides of the loss distribution which explains the change in sign. As the two equations stand for two separate optimization problems the resulting two optimal policies $\tilde{\pi}_B^*$ and $\tilde{\pi}_S^*$ might not be consistent. In other words, for the same hour one policy might exercise, but the other does

not. Translated to our business case we could imagine a situation where the retail department asks for power according to strategy $\tilde{\pi}_0^S$, but the trading unit cannot provide electricity from the generation department because it did not exercise his option according to $\tilde{\pi}_0^B$. Still this is not an issue, since the extra fee $q_\beta^S(\tilde{\epsilon})$ compensates the cost to buy the relevant power from the market. The same is true in the opposite direction where the trading unit exercises according to $\tilde{\pi}_0^B$, but the retail department does not. Then the trading unit might need to sell the power to a lower price to the market, but the compensation fee $q_\beta^B(\tilde{\epsilon})$ compensates the loss.

Let us now look at lower and upper bounds for these risk adjusted option values. The lower bound of these two optimization problems will be derived from the risk neutral policy according to equation 3.55. For $\tilde{C}_0^{B,e}$ this is immediately C_β^B as $C_0 + q_\beta$ happens to be the definition of the buyer's option (see equation 3.55). For the seller's option we get $C_0 - q_{1-\beta}^S = C_0 - q_\beta^S = C_0 - (C_\beta^S - C_0) = 2C_0 - C_\beta^S$. Thus, an EaR efficient buyer's and seller's option $\tilde{C}_\beta^{B/S,e}$ has to be above these values

$$\begin{aligned}\tilde{C}_\beta^{B,e} &\stackrel{!}{>} C_\beta^B \\ \tilde{C}_\beta^{S,e} &\stackrel{!}{>} 2C_0 - C_\beta^S.\end{aligned}\tag{3.59}$$

We can also provide an upper bound for the seller's option. Recall that we are actually interested in lowering the seller's option value C_β^S . Therefore an upper bound is more intuitive, especially for our numerical analysis in section 3.4.3. \tilde{C}_β^S becomes automatically cheaper due to the drop in fair value by $C_0 - \tilde{C}_0$. An efficient option value must be even cheaper by at least yet another $C_0 - \tilde{C}_0$ resulting from the reduction in the quantile $q_{1-\beta}(\tilde{\epsilon})$. Only then we have the desired compensation of risk vs. return

$$\tilde{C}_\beta^{S,e} \stackrel{!}{<} C_\beta^S - 2(C_0 - \tilde{C}_0).\tag{3.60}$$

We will use this benchmark in section 3.4.3. Formally, equation 3.58 introduces a quantile based measure in our initial optimization problem. Both summands, the fair value C_0 and the quantile $q_\beta(\epsilon)$, are linked by their common distribution. Usually the first summand reduces more relative to the second summand i.e. a mitigation in risk premium entails a declining fair value. Furthermore, the quantile is not a linear operator as discussed in section 3.4. Standard linear or dynamic programming are therefore not applicable. Another difficulty arises from the fact that ϵ is the remaining spot exposure after a Forward hedge which can only be calculated *after* the exercise strategy $\tilde{\pi}_B$ and $\tilde{\pi}_S$ is known. To illustrate the problem in context of our example, we need to assess the impact of each hour's dispatch decision on the Forward hedge that covers the entire delivery period. However, we can calculate the latter only *after* we know the entire schedule/option value. Thirdly, we need to compute the quantile *conditional* on today's price $X_0 = x_0$. Especially the latter motivated us to introduce a heuristic that is based on *quantile regression*. The heuristic will not work with the objective function in equation 3.58, but rather rely on a direct comparison with the risk neutral policy according to equations 3.59 and 3.60. The heuristic will still be based on our dynamic programming framework, but focus on a direct and permanent comparison of the expectation vs. the risk adjusted policy during each stage of the backward iteration. Before we lay out the heuristic in detail in section 3.4.3 we will briefly review the methodology of quantile regression and in particular look for a proper calibration of the respective regression function to our swing option framework.

3.4.2. Quantile Regression

The underlying idea of quantile regression is similar to linear regression. From linear regression we know that minimizing the sum of squared residuals provides the sample mean μ i.e. an estimate for the unconditional expectation

$$\mathbb{E}[V_{t+1}] \approx \arg \min_{\mu \in \mathfrak{R}} \sum_{i=1}^I (v_{t+1}^i - \mu)^2, \quad (3.61)$$

where $\{v_{t+1}^1, \dots, v_{t+1}^I\}$ are, in our context, the accumulated cash flows starting from the next to the last delivery hour T . Replacing the scalar μ by a parametric function $\mu(X_t, \gamma)$ with n -dimensional parameter vector γ allows to move from the estimate of the unconditional expectation $\mathbb{E}[V_{t+1}]$ to the *conditional* expectation $\mathbb{E}[V_{t+1}|X_t]$

$$\mathbb{E}[V_{t+1}|X_t] \approx \mu(X_t, \gamma^*) \quad (3.62)$$

where γ^* is the minimizer of

$$\min_{\gamma \in \mathfrak{R}^n} \sum_{i=1}^I (v_{t+1}^i - \mu(x_t^i, \gamma))^2. \quad (3.63)$$

We can apply a similar technique for the quantile. Just as we can define the sample mean as the solution to the problem of minimizing a sum of squared residuals, we can define an estimate for the median as the solution to the problem of minimizing a sum of absolute residuals

$$q^{0.5}(V_{t+1}) \approx \arg \min_{P \in \mathfrak{R}} \sum_{i=1}^I |v_{t+1}^i - P|. \quad (3.64)$$

The symmetry of the absolute value yields the median which is the 50% quantile. Koenker and Hallock [43] showed that *asymmetrically* weighted absolute residuals - giving different weights to positive and negative residuals - will yield the other quantiles

$$q^\beta(V_{t+1}) \approx \arg \min_{P \in \mathfrak{R}} \sum_{i=1}^I \rho_\beta(v_{t+1}^i - P), \quad (3.65)$$

where $\rho_\beta(z) = (\beta - I_{(-\infty, 0)}(z))z$ and I being the indicator function. Hence the weighting function ρ has a decreasing slope of $(\beta - 1)$ for negative z and an increasing slope of β for positive z . By definition the probability β is between 0 and 1. Now, we move again from the unconditional to the conditional quantile by introducing a parametric function $P(X_t, b)$ with n dimensional parameter vector b

$$q_{t+1}^\beta(V_{t+1}|X_t) \approx P(X_t, b^*) \quad (3.66)$$

where vector b^* is the minimizer of

$$\min_{b \in \mathfrak{R}^n} \sum_{i=1}^I \rho_\beta(v_{t+1}^i - P(x_t^i, b)). \quad (3.67)$$

As long as this function $P(x_t^i, b)$ is linear in x_t^i one can solve the previous equation with linear programming techniques to find the parameter vector b . Otherwise Koenker and Park [45]

developed an interior point method. Hunter and Lange [35] present a Majorize-Minimize method and provide a thorough comparison with the method by Koenker. We will focus on a linear approximation. Hence, our parametric function will be linear. Koenker [44] suggests a goodness of fit test that is similar to the R^2 statistic well known from linear regression to find an adequate number of degrees for the polynomial.

The classical R_t^2 statistic is a value between 0 and 1. The closer the value is to 1 the better the regression function explains the data cloud. Formally it is defined as follows

$$R_t^2 = 1 - \hat{S}_t / \tilde{S}_t, \quad (3.68)$$

where \hat{S}_t is the error sum of squared residuals that remain when subtracting the projected value $\mu(x_t^i, \gamma^*)$ from the real value v^i . \tilde{S}_t is the error sum of the squared residuals that result from subtracting the real value from the mean. Formally the mean can be approximated with a simplified linear regression that only uses a single parameter, i.e. the intercept, $\mu(x_t^i, \gamma) = \gamma_0$ as the basis function as we have seen in equation 3.61. Likewise we can define the R_t^1 statistic

$$\begin{aligned} R_{t+1}^1(\beta) &:= 1 - \hat{V}_{t+1}(\beta) / \tilde{V}_{t+1}(\beta) \\ \hat{V}_{t+1}(\beta) &:= \min_{b \in \mathbb{R}^{p+1}} \sum_{i=1}^N \rho_\beta \left(v_{t+1}^i - (b_0 + b_1 x_t^i + b_2 (x_t^i)^2 + \dots + b_p (x_t^i)^p) \right) \\ \tilde{V}_{t+1}(\beta) &:= \min_{b_0 \in \mathbb{R}} \sum_{i=1}^N \rho_\beta \left(v_{t+1}^i - b_0 \right). \end{aligned} \quad (3.69)$$

As \tilde{V}_{t+1} is the result of a minimization with only one parameter b_0 whereas \hat{V}_{t+1} can use all $p + 1$ parameters, it is immediately apparent that $\hat{V}_{t+1}(\beta) \leq \tilde{V}_{t+1}(\beta)$, thus $R_t^1(\beta)$ lies also between 0 and 1 and has the same interpretation as R_t^2 . Unlike R_t^2 , which allows to compare the relative success of two models for the conditional mean function in terms of residual variance, $R_t^1(\beta)$ can measure the relative success of two quantile regression models for a specific quantile in terms of an appropriately weighted sum of absolute residuals. Thus $R_t^1(\beta)$ constitutes a local measure of goodness of fit for a particular quantile rather than a global measure of goodness of fit over the entire conditional distribution like R^2 . In order to assess whether a set of estimated parameters b_p provides a good fit for the *entire* distribution one needs to compare the *processes* \hat{V}_{t+1} and \tilde{V}_{t+1} as processes of the quantile β . Koenker [44] investigates several different statistics like likelihood ratio tests and rank tests to allow for a formal test of hypothesis for these processes. We do not focus on these global tests since the local tests using the $R_t^1(\beta)$ statistic revealed already sufficient insights for our further analysis.

Table 3.10 presents the $R_t^1(\beta)$ statistic for the American option with different probabilities β and approximated with three different polynomials: a linear and quadratic function as well as a polynomial of third degree ($p=1,2,3$). We computed the R_t^1 statistic by running a quantile regression at each stage t on the pairs (X_t, V_{t+1}) . \bar{R}^1 in Table 3.10 is therefore the average across all 719 intermediate R_t^1 statistics

$$\bar{R}^1(\beta) := \frac{1}{T-1} \sum_{t=1}^{T-1} R_t^1(\beta). \quad (3.70)$$

The goodness of fit is always close to 0 and therefore rather poor. There are no significant improvements through higher degree polynomials. This weak performance let us question a linear approach for the quantile regression. However, the situation changes if one adds the

K	p	$\bar{R}^1(0.01)$	$\bar{R}^1(0.05)$	$\bar{R}^1(0.3)$	$\bar{R}^1(0.7)$	$\bar{R}^1(0.95)$	$\bar{R}^1(0.99)$	\bar{R}^2
0	1	0.007	0.003	0.001	0.001	0.003	0.010	0.001
0	2	0.012	0.005	0.002	0.002	0.005	0.016	0.001
0	3	0.016	0.007	0.002	0.002	0.008	0.022	0.001
1	1	0.014	0.006	0.002	0.002	0.007	0.024	0.003
1	2	0.024	0.012	0.004	0.004	0.014	0.039	0.003
1	3	0.034	0.017	0.006	0.006	0.020	0.053	0.003
2.5	1	0.057	0.056	0.040	0.047	0.145	0.155	0.056
2.5	2	0.123	0.122	0.088	0.097	0.249	0.260	0.056
2.5	3	0.188	0.187	0.137	0.146	0.339	0.349	0.056

Table 3.10.: Average R^1 and R^2 statistic for different probabilities β and strikes K (American option).

R_t^2 statistic for the conditional mean as a comparison. We computed the R^2 statistics of the classical Longstaff-Schwartz (LS) regression for the continuation value of all $t = 1, \dots, 719$ iterations. The table provides again the average \bar{R}^2 . Likewise, the results are rather poor despite of the good lower bounds we received with the same linear LS regression in the previous chapter. Apparently, even a coarse approximation according to the R^2 statistics can still lead to a good exercise policy. In order to assess whether this is also true for the R^1 statistic and the quantile regression, we compared directly the approximated quantiles with the ones taken from the histograms of our 1000 random realizations at each stage. Table 3.11 and Table 3.12 show that both are actually not too far off each other. Again we look at the American option for the three different strikes and the three degrees for the polynomial. We computed the quantiles for $\beta = 0.01, 0.3, 0.7$ and 0.99 . The third and seventh column

K	p	$\bar{q}^{0.01}$	$\bar{q}^{0.01}$	$\bar{q}_{\min}^{0.01}$	$\bar{q}_{\max}^{0.01}$	$\bar{q}^{0.99}$	$\bar{q}^{0.99}$	$\bar{q}_{\min}^{0.99}$	$\bar{q}_{\max}^{0.99}$
0	1	1.495	1.493	1.171	1.856	5.849	5.846	5.234	6.443
0	2	1.495	1.497	0.762	2.380	5.849	5.840	4.523	7.149
0	3	1.495	1.497	0.576	2.962	5.849	5.834	3.984	7.852
1	1	0.537	0.546	0.333	0.794	4.876	4.875	4.390	5.344
1	2	0.537	0.553	-0.019	1.337	4.876	4.862	3.603	5.996
1	3	0.537	0.554	-0.153	1.891	4.876	4.856	3.037	6.595
2.5	1	0.000	0.000	0.000	0.000	3.586	3.582	3.295	3.866
2.5	2	0.000	0.000	0.000	0.000	3.586	3.625	2.527	4.820
2.5	3	0.000	0.019	0.003	0.123	3.586	3.464	1.740	5.339

Table 3.11.: R^1 statistic 1 % and 99 % probability.

provide the unconditional quantile $q^\beta(V_t)$ with $V_t := V_t(X_t, 1)$ as defined in equation 2.12, i.e. we directly calculate the quantile from the ACF. To be precise \bar{q}_β is the average of these quantiles across all $t = 1, \dots, 719$ iterations. They are the benchmark to compare the other

columns with

$$\begin{aligned}
 \bar{q}^\beta &:= \frac{1}{T-1} \sum_{t=1}^{T-1} q^\beta(V_t) \\
 \bar{\hat{q}}^\beta &:= \frac{1}{(T-1) \cdot I} \sum_{t=1}^{T-1} \sum_{i=1}^I \hat{q}_t^i \\
 \bar{\hat{q}}_{\min}^\beta &:= \frac{1}{T-1} \sum_{t=1}^{T-1} \min_i[\hat{q}_t^i] \\
 \bar{\hat{q}}_{\max}^\beta &:= \frac{1}{T-1} \sum_{t=1}^{T-1} \max_i[\hat{q}_t^i] \\
 \hat{q}_{t+1}^i &:= Q_{t+1}^\beta(V_{t+1}|x_t^i) = \sum_{n=0}^N b_n(x_t^i)^n.
 \end{aligned} \tag{3.71}$$

Obviously the quantiles \bar{q}_β only change with the strike since they are computed directly from the empirical histogram of V_t . Column 4 and 8 are the average of the conditional quantiles across all scenarios and delivery hours $\bar{\hat{q}}^\beta$. In order to assess the impact of the averaging effect we also computed the minimum and maximum quantile across all scenarios for each hour separately ($\min_i[\hat{q}_t^i], \max_i[\hat{q}_t^i]$) and added their average across all iterations $\bar{\hat{q}}_{\min, \max}^\beta$ in columns 5, 6, 9 and 10. We can make two main observations in Table 3.11. First, we can see

K	p	$\bar{q}^{0.3}$	$\bar{\hat{q}}^{0.3}$	$\bar{\hat{q}}_{\min}^{0.3}$	$\bar{\hat{q}}_{\max}^{0.3}$	$\bar{q}^{0.7}$	$\bar{\hat{q}}^{0.7}$	$\bar{\hat{q}}_{\min}^{0.7}$	$\bar{\hat{q}}_{\max}^{0.7}$
0	1	3.100	3.099	3.013	3.206	3.748	3.748	3.658	3.856
0	2	3.100	3.099	2.882	3.327	3.748	3.748	3.548	3.985
0	3	3.100	3.099	2.804	3.466	3.748	3.748	3.407	4.096
1	1	2.102	2.104	2.035	2.187	2.754	2.756	2.680	2.845
1	2	2.102	2.104	1.904	2.313	2.754	2.756	2.560	2.980
1	3	2.102	2.104	1.844	2.453	2.754	2.756	2.421	3.095
2.5	1	0.675	0.680	0.640	0.722	1.371	1.379	1.334	1.428
2.5	2	0.675	0.682	0.543	0.837	1.371	1.374	1.193	1.556
2.5	3	0.675	0.693	0.491	1.002	1.371	1.373	1.043	1.685

Table 3.12.: R^1 statistic for 30 % and 70 % probability.

that the quantile domain $[\hat{q}_{\min}^\beta, \hat{q}_{\max}^\beta]$ increases with the degree of polynomials throughout all strikes. For $K = 0$, for instance, it almost doubles the size from $p = 1$ to $p = 3$ for $K = 0$. Table 3.10 reveals only a minor improvement of $\bar{R}^1(\beta)$ with increasing degree of polynomials. Hence, we cannot really deduce a better performance for polynomials with higher degrees. Second, we can observe that \bar{q}^β and $\bar{\hat{q}}^\beta$ are close to each other for $K = 0$ and the distance becomes larger the more the option gets out of the money. This is due to the fact that the LS regression suggests to only consider (x_t^i, v_{t+1}^i) pairs where x_t^i is in the money for only these prices are later relevant for the decision making. Recall that our price process fluctuates around 1. Thus, the higher K becomes, the less pairs enter the regression and hence the less accurate the results become. This is most obvious for $K = 2.5$ and $p = 3$ where $\bar{\hat{q}}^{0.01}$ is significantly higher than 0 which it should not as the smallest 1 % of all price scenarios will not lead to any option exercise. Comparing Table 3.11 with Table 3.12 we observe generally better results for $\beta = 0.3$. Obviously, more data points fall into these larger intervals that make an estimation more accurate.

3.4.3. Dynamic Swing Caps

In this section we want to introduce a heuristic that provides efficient policies in sense of equation 3.56. We want to focus on a dynamic hedging strategy *within* the delivery period giving direct decision support when to exercise a swing right in light of a risk constraint (this is different to a hedging strategy *before* delivery that usually focuses on buying/selling an adequate Forward contract to offset the position, see also our introductory example in section 3.1). Our main prerequisite for our heuristic is to stay within the dynamic programming framework. However, there is no straight-forward translation of our risk sensitive objective function in equation 3.58 into a value function that suits the Bellman iteration. Dynamic programming requires marginal intermediate results at each stage that sum up linearly to the overall optimal figure. The difficulty is threefold. First, it is not obvious how to compute the marginal quantile from one to the next stage based on the current action and price. The price at the current stage is known and henceforth there is no uncertainty and no distribution any longer. Second, even if we could compute intermediate quantiles, their summation would generally lead to a significant overestimation as correlation effects tend to keep the quantile of the overall distribution smaller than the sum of its parts. Third, we want to control the EaR exposure and therefore need to take into account the hedging effect as well. In this section we will propose a heuristic that will address these challenges. Let us look at the American option first.

As discussed in detail in chapter 2 the valuation of an American option results in at maximum one cash event $Z_{\tau_1^*(0,1)} := (X_{\tau_1^*(0,1)} - K)^+$ per scenario (see equation 2.3 with $N = 1$) and therefore there are no correlation effects for cash flows of the same path. Recall that the optimal policy states to exercise today's cash flow if it is above the expected value of the option for the remaining exercise period (continuation value) regardless how far it exceeds this value. However, exercising extremely high prices will make the right tail of the cash flow distribution $\Phi(Z_{\tau_1^*(0,1)})$ ¹² grow what the option seller in our example would like to avoid. Thus, in order to keep the distribution tight we should prevent to exercise and thus trigger a cash flow that falls beyond the upper quantile of the overall distribution. Our best guess on how this distribution will look like for the entire delivery period i.e. $\Phi(Z_{\tau_1^*(0,1)}) = \Phi(V_0^*(x_0, 1))$ is its interim evolution for any $t = 0, \dots, T-1$ represented by the intermediate distributions for the ACF from tomorrow onwards, i.e. $\Phi(Z_{\tau_1^*(t+1,1)}) = \Phi(V_{t+1}^*)$, with $V_{t+1}^* := V_{t+1}^*(X_{t+1}, 1)$ defined in equation 2.9 with $n=1$. We are mainly interested in the quantile and we will have a different expectation of this quantile if we observe a high instead of a low price today. To be precise we will look at the $(1 - \beta)$ -quantile *conditional* on the current price X_t that we denote as $q^{1-\beta}(Z_{\tau_1^*(t+1,1)}, X_t)$ and $q^{1-\beta}(V_{t+1}^*, X_t)$ respectively¹³

$$\begin{aligned} \beta &\approx \text{Prob} \left(Z_{\tau_1^*(t+1,1)} \leq q^{1-\beta}(Z_{\tau_1^*(t+1,1)}, X_t) | X_t \right) \\ \beta &\approx \text{Prob} \left(V_{t+1}^* \leq q^{1-\beta}(V_{t+1}^*, X_t) | X_t \right). \end{aligned} \tag{3.72}$$

This is where our quantile regression comes into play. From the pairs (X_t, V_{t+1}^*) we relate the current price to the quantile of the ACF of the next hour. To be precise we will apply

¹²We denote with $\Phi(X)$ the distribution law for the random variable X . Also recall our definition of stopping times $\tau_k(t, n)$ and related policies $\pi_t(n)$ in section 2.1.

¹³As we cannot guarantee the existence of this quantile in the general case we do not state strict equality for the probability β in the definition of the β -quantile.

equation 3.66 and use a polynomial approximation $P^{1-\beta}(X_t, b^*)$ to describe the quantile

$$q^{1-\beta}(V_{t+1}^*, X_t) \approx P^{1-\beta}(X_t, b^*) := \sum_{k=0}^K b_k^*(X_t)^k, \quad (3.73)$$

where vector $b^* := (b_0^* \dots b_K^*)'$ is the minimizer of

$$\min_{b \in \mathcal{R}^{K+1}} \sum_{i=1}^I \rho_{1-\beta} \left(v_{t+1}^i - P^{1-\beta}(x_t^i, b^*) \right). \quad (3.74)$$

I is 1000 in our numerical examples. Note that this quantile regression procedure is similar to the approximation of the continuation value $Q_{t+1}^*(X_t, 1)$ (see equation 2.10 with $n=1$). Recall from equation 2.11 that the approximated continuation value $Y_{t+1}(X_t, 1)$ allows to derive the threshold price that triggers an exercise. Analogously to equations 2.15 and 2.16 we can translate the approximated quantile $P_{t+1}^{1-\beta}$ from a *cash flow* threshold

$$l_t(X_t, 1) = \begin{cases} 0 & Z_t(X_t) > P^{1-\beta}(X_t, b^*) \\ 1 & Z_t(X_t) \leq P^{1-\beta}(X_t, b^*). \end{cases} \quad (3.75)$$

into an upper *price* threshold

$$l_t(X_t, 1) = \begin{cases} 0 & X_t > \overline{X}_t \\ 1 & X_t \leq \overline{X}_t. \end{cases} \quad (3.76)$$

So we do *not* allow an option exercise if the cash flow/price is *above* $P^{1-\beta}$ and \overline{X}_t , respectively. Theoretically we could add this upper line to our existing lower line exercise trigger resulting from the optimal exercise policy of the swing option (see again section 2.1). We could define this band as the new exercise strategy. However, our investigations revealed that this policy will not meet our benchmark in the sense of our definition 3.56 as the resulting option value $\tilde{C}_0^*(x_0, 1)$ ¹⁴ is much smaller compared to $C_0^*(x_0, 1)$ than the gain in the quantile. For this reason we have to run yet another optimization problem that finds a new lower exercise threshold given this quantile based upper bound defined by the risk neutral policy. We will call it the *risk-sensitive* optimization problem and we label all related figures with a tilde. Let us describe it in terms of a stopping problem.

Formally the new risk sensitive stopping time $\tilde{\tau}_1 := \tilde{\tau}_1(0, 1)$ needs to be linked to the risk neutral stopping time via the conditional quantile $q_{\tilde{\tau}}^{1-\beta}(Z_{\tilde{\tau}}^*, X_{\tilde{\tau}_1})$ such that $\tau_1^* := \tau_1^*(\tilde{\tau}_1 + 1, 1)$. Thus, our new risk sensitive optimization problem requires the calculation of the risk neutral policies $\pi_t^*(n)$ with $t = 0, \dots, T$ (see equation 2.1) and $n = 0, 1$ *beforehand*. We therefore add π as a left sub index to all figures that require the pre-calculation of $\pi_t^*(n)$. Consequently we denote the risk adjusted American option value as $\pi \tilde{C}_0^*(x_0, 1)$ and can write the following stopping problem

$$\pi \tilde{C}_0^*(x_0, 1) := \sup_{\tilde{\tau}_1} \mathbb{E}[\pi \tilde{Z}_{\tilde{\tau}_1}^\beta | X_0 = x_0], \quad (3.77)$$

where the cash flow $\pi \tilde{Z}_{\tilde{\tau}_1}^\beta$ is defined as follows

$$\pi \tilde{Z}_{\tilde{\tau}_1}^\beta := \begin{cases} Z_{\tilde{\tau}_1} & \text{if } Z_{\tilde{\tau}_1} \leq q^{1-\beta}(Z_{\tau_1}^*, X_{\tilde{\tau}_1}), \\ -c & \text{else,} \end{cases} \quad (3.78)$$

¹⁴We assign a tilde for any figures related to risk adjusted policies.

where $\tilde{\tau}_1 := \tilde{\tau}_1(0, 1)$ and $\tau_1^* := \tau_1^*(\tilde{\tau}_1 + 1, 1)$ and $Z_{\tau_1} := (X_{\tau_1} - K)^+$. We can also write the cash flow in terms of the ACF and the approximated quantile $P^{1-\beta}(X_t, b^*)$

$$\pi \tilde{Z}_t^\beta(X_t, \tilde{a}) := \begin{cases} \tilde{a} Z_t & \text{if } Z_t \leq P^{1-\beta}(X_t, b^*), \\ -c & \text{else,} \end{cases} \quad (3.79)$$

where $Z_t := (X_t - K)^+$. In case of an American option where the single cash flow is always greater equal to zero, $c = 1$ is already sufficient. The penalty term c applies whenever the cash flow $Z_{\tilde{\tau}_1}$ at the stopping point $\tilde{\tau}_1$ exceeds the conditional upper quantile. Then we can express the value function $\pi \tilde{C}_0^*(x_0, n)$ via the Bellman equation

$$\begin{aligned} \pi \tilde{C}_t^*(X_t, n) &= \max_{\tilde{a} \in A(n)} \left\{ \pi \tilde{Z}_t^\beta(X_t, \tilde{a}) + \mathbb{E} \left[\pi \tilde{C}_{t+1}^*(X_{t+1}, n - \tilde{a}) | X_t \right] \right\} \quad t = 0, \dots, T \\ \text{state : } (X_t, n) & \quad X_t: \text{ current price, } n=0,1: \text{ remaining number of swings} \\ \text{action : } \tilde{a} \in A(n) & := \{0, \min[1, n]\} \quad \text{exercise yes (1) or no (0)} \\ \text{transition : } \{X_t, n\} & \longrightarrow \{X_{t+1}, n - \tilde{a}\} \\ \text{marginal profit : } \pi \tilde{Z}_t^\beta(X_t, \tilde{a}) & \\ \text{value function : } \pi \tilde{C}_t^*(X_t, n) & \\ \text{continuation value : } \pi \tilde{Q}_{t+1}^*(X_t, n) & := \mathbb{E} \left[\pi \tilde{C}_{t+1}^*(X_{t+1}, n) | X_t \right], \end{aligned} \quad (3.80)$$

with $\pi \tilde{C}_{T+1}^*(X_{T+1}, n) := 0$ for $n = 0, 1$. Again, we will apply our Longstaff-Schwartz regression based valuation model to approximate the optimal action \tilde{a}^* with \hat{a}^* , the continuation value $\pi \tilde{Q}_{t+1}^*(X_t, n)$ with $\pi \tilde{Y}_{t+1}^*(X_t, n)$ and the optimal accumulated cash flow $\pi \tilde{V}_{t+1}^*$ with the lower bound $\pi \tilde{V}_{t+1}$. These approximations also imply an estimate of the penalty term or to be precise the conditional quantile $q^{1-\beta}(V_{t+1}^*, X_t)$ by $P^{1-\beta}(X_t, b^*)$

$$\begin{aligned} \hat{a}^* &= \arg \max_{\tilde{a} \in A(n)} \left\{ \pi \tilde{Z}_t^\beta(X_t, \tilde{a}) + \pi \tilde{Y}_{t+1}^*(X_t, n) \right\}, \\ \pi \tilde{V}_t(X_t, n) &= \pi \tilde{Z}_t^\beta(X_t, \hat{a}^*) + \pi \tilde{V}_{t+1}(X_t, n - \hat{a}^*) \\ \pi \tilde{Y}_{t+1}^*(X_t, n) &:= \sum_{\tilde{r}=0}^{\tilde{R}} \tilde{\alpha}_{\tilde{r}, t} X_t^{\tilde{r}}. \end{aligned} \quad (3.81)$$

For the approximation of the conditional quantile we rely on quantile regression that we introduced in the last section. Recall from equation 3.73 that $P^{1-\beta}(X_t, b^*)$ is not the quantile of our risk adjusted ACF \tilde{V}_{t+1} , but is calculated from the risk neutral ACFs V_{t+1} (remember that we denote a tilde to values of the risk sensitive model). In this way we capture the dependence of $\tilde{\tau}_1$ on τ_1^* of our stopping problem in equation 3.77. This mechanism reduces the accumulation effect of iterative tail cutting from stage to stage on the overall distribution of the final stage. The overall distribution and expectation would shrink drastically if each intermediate quantile relied on a previously cut distribution. It would not only generate a too defensive exercise policy and the loss in expected value would outnumber the gain in the tails. Also, the quantile of the distribution at the beginning of the backward iteration $q^{1-\beta}(\pi \tilde{V}_T, X_{T-1})$ would basically determine the shape of all subsequent distributions. Instead our benchmark in definition 3.4.1 demands a high expectation with a tight distribution. Hence, with every iteration we compute the quantile threshold from the distribution of our risk neutral ACFs according to our basic model in equation 2.6. Only cash flows that fall into the tail of this distribution will be rejected.

We want to point out that the new risk sensitive exercise policy $\tilde{\pi}_0^*(N)$ defines a threshold

that is always below the quantile based upper bound from equation 3.76. The lower bound is based on the continuation value and therefore relates to the mean of the ACF distribution $\Phi(\tilde{V}_{t+1}^*|X_t)$ while the upper bound stands for the upper quantile of the ACF distribution $\Phi(V_{t+1}^*|X_t)$. For small β the upper quantile $q^{1-\beta}$ usually lies above the mean for the same distribution. In our case we even have two distributions with $\tilde{V}_{t+1}^* < V_{t+1}^*$ in most cases. Thus, the distribution for the lower threshold has smaller realizations than the distribution for the upper threshold which is another indication that the policy $\tilde{\pi}_0^*(N)$ will return thresholds below the quantile based upper bound following the policy $\pi_0^*(N)$. For this reason, the result is indeed an exercise band.

This exercise band (see also Figure 3.11) provides a straight-forward decision support for the option holder. Translated to our situation with the generation department and the trading unit, the trading unit is willing to pay a higher price to the generation unit for the electricity if both sides can agree on this exercise band as a production plan for the generation department. The produced energy is exposed to less price fluctuation (by basically skipping hours with high volatility) and therefore trading asks for a smaller premium for managing the price risk. At the opposite side (see Figure 3.7) the trading unit could sell the swing option to a retail customer and declare the imposed exercise strategy based as a barrier option or *dynamic swing cap* whose upper bound varies with the remaining delivery hours and with larger market movements. In practice these caps would be much coarser. In case of our monthly option, for example, every week the issuer could set new exercise bands for the upcoming week. Then the upper bound would be simplified to a step function with four steps.

Finally we want to remark that our stopping problem in equation 3.77 does not directly approximate our EaR definition $q_{1-\beta}(\epsilon)$ from equation 3.54. It does not look at the quantile of the loss distribution after a Forward hedge, but on the ACF directly (V_0 instead of ϵ). In reality energy markets provide a so called *Balance of Month* contract that enables a trader to hedge the remaining delivery period of a month. Even though this product is rarely liquid it could be used to hedge the swing option during delivery. We ignore this hedge for we will show in case of an American option that merely controlling the quantile of the non-hedged position results in the desired EaR mitigation as well. Let us therefore return to our swing option example.

In section 3.4.2 we decided to use a quadratic approximation for $P^{1-\beta}(X_t, b^*)$. We also keep using the same basis functions for approximating the continuation value as in the last chapter. So we get

$$\begin{aligned} R = 2 &\Rightarrow Y_{t+1}(X_t, 1) = \alpha_{0,t} + \alpha_{1,t}X_t + \alpha_{2,t}X_t^2 \\ \tilde{R} = 2 &\Rightarrow \pi\tilde{Y}_{t+1}(X_t, 1) = \tilde{\alpha}_{0,t} + \tilde{\alpha}_{1,t}X_t + \tilde{\alpha}_{2,t}X_t^2 \\ K = 2 &\Rightarrow P^{1-\beta}(X_t, b^*) = b_{0,t}^* + b_{1,t}^*X_t + b_{2,t}^*X_t^2. \end{aligned} \tag{3.82}$$

Table 3.13 presents the results of our heuristic for the American option. The table shows the total option value for all three strikes and three quantiles. Column 3 and 4 present the option values for the risk neutral ($C_0 := C_0(x_0, 1)$) vs. the risk adjusted policy ($\tilde{C}_0 := \pi\tilde{C}_0(x_0, 1)$). As assumed the risk adjusted policy returns smaller numbers. If our heuristic works well, then this reduction should be more than compensated by a shrinking quantile. Translated into our total option values, the risk sensitive buyer's option \tilde{C}_β^B should nevertheless become more valuable than the risk neutral one C_β^B where $\tilde{C}_\beta^{B/S}$ is defined in equation 3.58, but using our risk sensitive figures $\pi\tilde{C}_0$ and $\tilde{\epsilon}$, the latter calculated after applying the best Forward hedge. Also recall that we use normalized prices according to equation 3.39. The seller's option on the other hand should become cheaper by more than double of the fair value reduction $C_0 - \tilde{C}_0$ (see also equation 3.60). Columns 5 and 6 present the buyer's and column

7 and 8 the seller's option. Column 3, 5 and 7 are taken from Tables 3.5 and 3.9 for direct comparison. Let us first look at the buyer's option. \tilde{C}_β^B is equal or higher than C_β^B for the

β	K	C_0	\tilde{C}_0	C_β^B	\tilde{C}_β^B	\tilde{C}_β^S	C_β^S
0.01	0	4.011	3.882	1.954	1.998	5.677	6.364
0.01	1	3.014	2.899	0.919	0.919	4.969	5.364
0.01	2.5	1.604	1.490	0.000	0.000	3.549	3.981
0.05	0	4.011	3.802	2.689	2.717	4.859	5.438
0.05	1	3.014	2.812	1.749	1.761	3.866	4.453
0.05	2.5	1.604	1.407	0.233	0.260	2.462	3.092
0.3	0	4.011	3.460	3.635	3.316	3.656	4.352
0.3	1	3.014	2.459	2.633	2.309	2.658	3.356
0.3	2.5	1.604	1.060	1.185	0.903	1.264	1.953

Table 3.13.: Impact of risk adjusted policy on total option value

1 % and 5 % quantile. For $K = 0$ and $\beta = 0.01$ we observe a fair value of $C_0 = 4.0114$. The option buyer identifies a possible loss of $q_{0.01} = (1.954 - 4.0114) = -2.057$ in 1% of all scenarios and he asks for a discount of exactly that number on the fair value. Our quantile sensitive policy results in a fair value of 3.882. Nevertheless the option buyer is willing to pay a higher price, namely 1.998. Obviously the new policy reduced the potential loss even more ($C_0 - \tilde{C}_0 = 0.129 < q_\beta^B - \tilde{q}_\beta^B = 0.173$). That is exactly what our EaR efficiency according to definition 3.54 demands. Recall from the same definition that the quantile $q_\beta(\epsilon)$ is computed from the loss distribution *after* a Forward/Future hedge. Our heuristic, however, is actually only based on the non-hedged position. Still, the heuristic provides EaR efficient buyer options. Translated to our business case we can state that the trading unit accepts to pay a higher price, if the generation department commits to the risk sensitive production policy. However, the performance for the buyer's option decreases with larger probabilities and strikes. The 0 values for $K = 2.5$ and $\beta = 0.01$ stand out. They do not indicate a zero production as the option values \tilde{C}_0 and C_0 are above 0. In Table 3.9 we saw that the hedge with a Future failed in this case. In 1 % of all scenarios there is simply no exercise. Then the loss is identical to the fair value and the total option value is simply 0. The risk adjusted policy cannot improve this situation. For $\beta = 0.3$ all risk adjusted buyer's options fall below the results of the regular option valuation (e.g. for $K = 0$ we observe $\tilde{C}_{0.3}^B = 3.316$ as opposed to $C_{0.3}^B = 3.635$). A large loss probability means a small quantile in absolute terms. The table reveals that our heuristic provides weak results for this case. Recall that our heuristic implicitly focuses on the seller's option by looking at the upper tail of the cash distribution. Cash flows resulting from prices beyond the fair value plus the quantile will be penalized. If this threshold is low due to a small quantile, then too many high prices will be ignored and the option value decreases too quickly.

Let us turn to the seller's option in columns 7 and 8. All risk adjusted option values \tilde{C}_β^S are below the regular option values C_β^S . The trading department can ask for less compensation of the replacement risk and can launch a more competitive offer to retail customers. However, the retail customer will only accept the cheaper price if less than half of the reduction will come from a profit cut (see also equation 3.60). For $K = 1$ and $\beta = 5\%$ the risk adjusted policy makes the total option cheaper by $4.453 - 3.866 = 0.587$ and only $3.014 - 2.812 = 0.202$ i.e. less than 50 % are due to a decline in fair value. So, this new option is more beneficial for the retail customers. Like for the buyer's option the heuristic produces EaR efficient option values for $\beta = 1\%$ and 5% . In fact the seller's options are more efficient than the buyer's option. For $K = 0$ and $\beta = 5\%$ for instance, the excess of the quantile reduction

over the profit cut is $\tilde{C}_\beta^B - C_\beta^B = 0.028$ for the buyer's option and $C_\beta^S - \tilde{C}_\beta^S - 2(C_0 - \tilde{C}_0) = 5.438 - 4.859 - 8.022 + 7.604 = 0.161$ for the seller's option. This can be explained by the fact that our heuristic is based on the seller's option and thus directly controls the right tail. Again, we observe that the heuristic fails for a loss probability of 30 %. The penalty price of our heuristic simply becomes too low for high loss probabilities.

So far, our option valuation relied on price scenarios according to equation 2.7 with constant volatility $\sigma = 0.5$. Our heuristic should perform even better for price scenarios with changing risk profile. Then we would expect that the risk sensitive policy identifies and picks less risky exercise hours in order to mitigate EaR and improve the total option values. Hence, we generate a second set of price scenarios where the underlying price process only differs from equation 2.7 by replacing the constant volatility σ with a time-dependent σ_t

$$\begin{aligned} \ln X_{t+1} &= (1 - \kappa) \ln X_t \Delta t + \sigma_t \epsilon_t & \epsilon_t &\sim N(0, 1) \\ \sigma_t &= \mathbb{I}_{t \in \mathbb{O}} \sigma_1 + (1 - \mathbb{I}_{t \in \mathbb{O}}) \sigma_2, \end{aligned} \tag{3.83}$$

where ϵ_t are i.i.d, $\Delta t = 1$ and $\mathbb{O} = \{1, 3, 5, \dots\}$ is the set of all odd hours in our delivery period and \mathbb{I} is an indicator function. Hence, we keep all parameters the same and only change every second hour the volatility from $\sigma_1 = 0.5$ to $\sigma_2 = 0.7$. We also normalized the prices again according to equation 3.39. Table 3.14 presents the results for the 1 % loss probability. Again, the table lists the risk-adjusted and non risk-adjusted option values in

K	C_0	\tilde{C}_0	C_β^B	\tilde{C}_β^B	C_β^S	\tilde{C}_β^S
0	5.93	5.65	1.83	2.21	9.76	11.50
1	4.94	4.64	1.09	1.40	8.43	10.69
2.5	3.53	3.18	0.00	0.00	7.53	9.19

Table 3.14.: Impact of risk adjusted policy on price scenarios with altering volatility ($\beta = 1$ %)

column 2 and 3 as well as the buyer's and seller's option in columns 4 to 7. In deed, our heuristic produces more EaR-efficient option values compared to the single volatility case. Let us compare the values for $K = 0$. The excess of the quantile reduction over the profit decline for the buyer's option is $\tilde{C}_\beta^B - C_\beta^B = 2.21 - 1.83 = 0.38$ compared to $1.998 - 1.954 = 0.044$ for the constant volatility. In relative terms this is 6 % vs. 1 % of the initial fair value C_0 and \tilde{C}_0 . For the seller's option we compare the case with altering volatility $C_\beta^S - \tilde{C}_\beta^S - 2(C_0 - \tilde{C}_0) = 11.5 - 9.76 - 11.86 + 11.3 = 1.18$ to the case with constant volatility $6.364 - 5.677 - 8.022 + 7.764 = 0.429$ or in relative terms 25 % vs. 14 % of the initial fair value C_0 and \tilde{C}_0 . Hence, we can roughly observe an improvement in efficiency by at least factor 2 for the itm and atm option. The fact that the EaR efficiency is higher for the seller's option is illustrated in Figure 3.10 which relates to Figure 3.9. We see the distribution for the situation of altering volatility and strike of 0. The risk sensitive distribution is tighter i.e. the gap between the right tails has more than the double size of the gap between the expectations. Also, the left tail of the risk adjusted distribution moved more to the right than the expectation shifted to the left. The former is relevant for the seller's option, the latter for the buyer's option (see equations 3.59 and 3.60). Note that for better readability we plotted the distributions with the same number of buckets instead of fixed bucket borders. Hence, a higher frequency of observations does not result in taller, but more narrow bars.

We also want to visualize the risk adjusted exercise strategy that leads to this distribution. The optimal policy of a regular American option valuation relates today's cash flow and continuation value to today's price. At each stage it allows for calculating the equilibrium

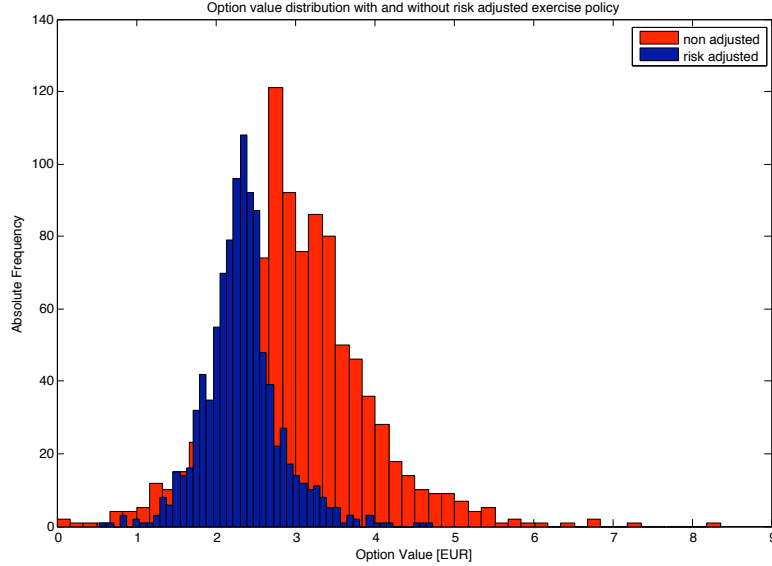


Figure 3.10.: Cash flow histogram for single exercise (risk and non-risk adjusted)

price where both the current cash flow and tomorrow's option value coincide. Lining up these values along all stages in a price/time diagram defines the exercise border. If we observe a price below that border, then we should keep the option and continue until we eventually observe a price above the border. Then, we will exercise immediately. Now, our quantile regression framework relates today's price to the quantile of tomorrow's option value. In our analysis we used a linear equation which enables us to solve immediately for the equilibrium. We receive a new threshold that we can also chain along all stages. This new line lies above the exercise border and therefore is an upper bound. Our risk policy states that the very first time we observe a price between these two borders, we will exercise the option. Consequently the former exercise region transformed to an exercise *band*. Figure 3.11 shows this band for the American option we analyzed in Table 3.13. We can see that the upper border fluctuates much stronger than the lower one which is an indication of instability of the associated risk adjusted policy.

Now, let us move from the American option to the more general case of the swing option. The main difficulty of the swing option is that we suddenly have multiple cash events per single scenario $V_0^*(x_0, N) = \sum_{n=1}^N Z_{\tau_n^*}$ with $\tau_n^* := \tau_n^*(0, N)$. Hence, we face correlation effects within a single path between separate $Z_{\tau_n^*}$ and $Z_{\tau_m^*}$, $n \neq m$. In general this will make the impact of a single exercise on the overall distribution smaller or, the other way around, allow for higher marginal quantiles. An evident approach is therefore to look at the marginal distribution $\Delta V_{t+1}^*(n) := V_{t+1}^*(X_{t+1}, n) - V_{t+1}^*(X_{t+1}, n-1)$ between the n -th and $(n-1)$ -th option exercise. This is consistent with the regular swing option valuation where we exercise the n -th swing if its cash flow exceeds the difference between tomorrow's expected n -th and $(n-1)$ -th option value. Hence, we take the swing option definition of equation 2.3, but apply our modified cash flow¹⁵

$$\pi \tilde{C}_0^*(x_0, N) = \sup_{\tilde{\pi}_0(N) \in \Pi_0(N)} \mathbb{E}^{(\tilde{\pi}_0(N))} \left[\sum_{n=1}^N \pi \tilde{Z}_{\tau_n} \mid X_0 = x_0 \right], \quad (3.84)$$

¹⁵Note that the risk neutral and risk sensitive policy both belong to the same set of admissible policies $\Pi_0(N)$.

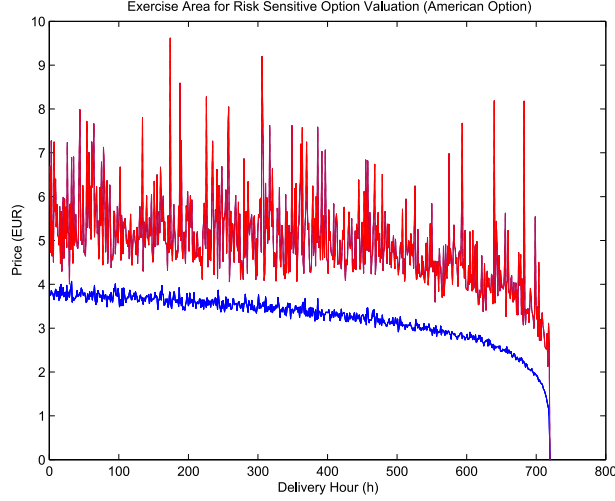


Figure 3.11.: Upper and lower price threshold for each stage

with the new cash flow ${}^n\tilde{Z}_{\tau_n}$ defined as follows

$${}^n\tilde{Z}_{\tau_n}^\beta := \begin{cases} Z_{\tilde{\tau}_n} & \text{if } Z_{\tilde{\tau}_n} \leq q^{1-\beta}(Z_{\tau_n^*}, X_{\tilde{\tau}_n}), \\ -c & \text{else,} \end{cases} \quad (3.85)$$

where $\tilde{\tau}_n := \tilde{\tau}_n(0, N)$, $\tau_n^* := \tau_n^*(\tilde{\tau}_n + 1, N)$ and $Z_{\tilde{\tau}_n} := (X_{\tilde{\tau}_n} - K)^+$. The penalty c must be high enough to make the sum $\sum_{n=1}^N Z_{\tau_n}$ always negative. As our price process fluctuates around 1 with standard deviation of 0.5 and $N = 720$, $c = 10000$ is sufficient. Note that $q^{1-\beta}(Z_{\tau_n^*}, X_{\tilde{\tau}_n})$ is the quantile of the n -th exercise. In context of our ACF this translates to the n -th conditional marginal quantile $q^{1-\beta}(\Delta V_{t+1}^*(n), X_t)$

$$\begin{aligned} \beta &\approx \text{Prob} \left(Z_{\tau_n^*(t+1,1)} \leq q^{1-\beta}(Z_{\tau_n^*(t+1,1)}, X_t) \mid X_t \right) \\ \beta &\approx \text{Prob} \left(\Delta V_{t+1}^*(n) \leq q^{1-\beta}(\Delta V_{t+1}^*(n), X_t) \mid X_t \right). \end{aligned} \quad (3.86)$$

For the approximation of the conditional quantile $P^{1-\beta}(X_t, {}_n b^*) \approx q^{1-\beta}(\Delta V_{t+1}^*(n), X_t)$ we use again our quantile regression approach. This time we regress on the marginal cash flow $(X_t, \Delta V_{t+1}^*(n))$ in order to relate the current price to the marginal quantile of the ACF of the next hour. Again, we apply equation 3.66

$$P^{1-\beta}(X_t, {}_n b^*) := \sum_{k=0}^K {}_n b_k^*(X_t)^k, \quad (3.87)$$

where vector ${}_n b^* := ({}_n b_0^* \dots {}_n b_K^*)'$ is the minimizer of

$$\min_{{}_n b \in \mathfrak{R}^{K+1}} \sum_{i=1}^I \rho_{1-\beta} \left(\Delta v_{t+1}^i(n) - P^{1-\beta}(x_t^i, {}_n b) \right). \quad (3.88)$$

Then, we can also express the modified cash flow in terms of the ACF

$${}^n\tilde{Z}_t^\beta(X_t, \tilde{a}) := \begin{cases} \tilde{a}Z_t & \text{if } Z_t \leq P^{1-\beta}(\Delta V_{t+1}^*(n), X_t), \\ -c & \text{else,} \end{cases} \quad (3.89)$$

with $Z_t := (X_t - K)^+$. Note that like for the American option we compute the approximated quantiles from the marginal values of the risk neutral swing option model ($P^{1-\beta}(\Delta V_{t+1}^*(n), X_t)$ not $P^{1-\beta}(\Delta_\pi \tilde{V}_{t+1}(n), X_t)$!). Then the dynamic program is identical to equation 3.80 except that we replace the modified cash flow ${}_\pi\tilde{Z}_t^\beta$ by ${}^n\tilde{Z}_t^\beta$ and do not restrict n to 0,1, but $n = 0,1,\dots,N$. The solution method via Longstaff-Schwartz regression stays the same.

Let us now continue with our numerical example. The parameter settings for the swing option are identical to our previous example for the American option (see equation 3.82). Table 3.15 compares the swing option with different swing rights that are derived from both policies, risk and non-risk sensitive. The table content is similar to the previous tables. This time we only arranged the columns separately by risk and non-risk adjusted policy. Table 3.16 adds the numbers for the price scenarios with altering volatility. A direct comparison of the

Swings	K	C	$C_{0.05}^B$	$C_{0.05}^S$	\tilde{C}	$\tilde{C}_{0.05}^B$	$\tilde{C}_{0.05}^S$
10	0.0	31.235	27.321	35.419	27.983	25.539	30.346
10	1.0	21.245	17.362	25.440	17.993	15.540	20.371
10	2.5	6.771	3.259	10.942	3.743	1.312	6.423
50	0.0	116.903	110.189	123.444	95.903	92.398	99.315
50	1.0	66.952	60.275	73.559	46.012	42.266	49.596
50	2.5	7.595	3.592	12.425	7.386	3.541	12.151
360	0.0	497.506	491.609	503.567	359.804	346.986	372.290
360	1.0	142.982	136.460	149.711	137.507	130.269	145.043
360	2.5	7.595	3.592	12.425	7.386	3.541	12.151
720	0.0	720.000	720.000	720.000	720.000	720.000	720.000
720	1.0	142.982	136.460	149.711	137.507	130.269	145.043
720	2.5	7.595	3.592	12.425	7.386	3.541	12.151

Table 3.15.: Buyer's and seller's total option value (risk and non-risk adjusted)

two tables shows that different to the American option example we cannot observe a stronger impact of the risk policy if the underlying price has an altering volatility. Furthermore, both price scenarios reveal separate, but identical values for the otm option and $N = 50, 360$ and 720 . Obviously the otm option will exercise less than 50, but still more than 10 swings (an in-depth analysis reveals 27 swings for our price scenarios with flat volatility and 45 swings for the prices with flipping volatility). We have a similar situation for the atm option with 360 and 720 swing rights. A further analysis shows that the atm option exercises 323 swings for underlying prices with flat volatility and 341 swings for underlying prices with flipping volatility.

In general, we must observe that our heuristic does not return EaR efficient swing option values in terms of our definition in 3.54. Our objective states that the loss in fair value should be overcompensated by the reduction in the quantile (see also equation 3.56). In Table 3.15 we see that this comparison already fails for 10 swings. Again, we calculate the risk adjusted buyer's and seller's option $\tilde{C}_\beta^{B/S}$ from equation 3.58 and use $\tilde{C}_0^*(x_0, N)$ and residuals $\tilde{\epsilon}$ instead, the latter calculated after applying the best Forward hedge. None of the risk adjusted buyer's options \tilde{C}_β^B is more valuable than C_β^B as we would expect. Likewise the seller's option \tilde{C}_β^S is only cheaper due to a loss in fair value rather than a decline in risk premium (e.g. in

Swings	K	C	$C_{0.05}^B$	$C_{0.05}^S$	\tilde{C}	$\tilde{C}_{0.05}^B$	$\tilde{C}_{0.05}^S$
10	0.0	41.887	35.059	50.156	35.517	31.517	39.788
10	1.0	31.905	24.951	40.582	25.624	21.625	30.037
10	2.5	17.363	10.534	25.661	11.282	7.242	15.947
50	0.0	140.698	130.486	151.454	107.391	101.940	113.189
50	1.0	90.783	80.763	101.496	57.434	52.257	62.997
50	2.5	23.909	15.302	33.982	23.403	14.677	33.448
360	0.0	522.978	516.282	529.489	359.619	342.820	376.438
360	1.0	172.313	164.338	180.541	167.145	157.716	176.206
360	2.5	23.909	15.302	33.982	23.403	14.677	33.448
720	0.0	720.000	720.000	720.000	720.000	720.000	720.000
720	1.0	172.313	164.338	180.541	167.145	157.716	176.206
720	2.5	23.909	15.302	33.982	23.403	14.677	33.448

Table 3.16.: As Table 3.15 but based on price scenarios with altering volatility

Table 3.15 for $K = 0$ and $N = 10$ we receive a loss in fair value of $C - \tilde{C} = 3.25$, but a reduction in risk premium of only $C_{0.05}^S - \tilde{C}_{0.05}^S - (C_0 - \tilde{C}_0) = 1.817$ which ought to be higher than 3.25). However, we can still argue that the reduction holds in relative terms i.e. 10 % cut in fair value entailed a 43 % reduction in EaR. Our objective significantly fails for the itm option with a large number of swing rights (e.g. 360 swings and $K = 0$ in Table 3.15: fair value reduction of $C_0 - \tilde{C}_0 = 137.70$ opposed to risk *increase* from $C_\beta^S - C_0 = 503.567 - 497.506 = 6.061$ to $\tilde{C}_{0.05}^S - \tilde{C}_0 = 12.486$), but improves with higher strikes or less swings (e.g. $K = 2.5$ and 50 swings: fair value reduction of $C_0 - \tilde{C}_0 = 0.209$ compared to a risk mitigation of $C_{0.05}^S - \tilde{C}_{0.05}^S - (C_0 - \tilde{C}_0) = 0.065$). The more swing rights are available and the more the option is in the money, the closer the swing option resembles a regular Forward contract and the worse the performance of the risk policy gets. This is due to the fact that the Forward hedge can cover more and more of the risk exposure. In Table 3.16, for instance, we can compare the relative loss for $K = 0$ and 10 itm swings as opposed to 360 itm swings (i.e. half a Forward contract): $(C_{0.05}^S - C_0)/C_0 \approx 19\%$ reduces to 1.2%. Once the hedging effect strongly applies it outperforms our extended risk adjusted exercise policy. In short, our heuristic is specifically designed for incomplete markets with very limited hedging opportunities (i.e number of swing rights is significantly smaller than number of delivery hours or very high strikes, e.g. gas fired power plants).

An exception is the perfect hedge. This is the itm option with 720 swings. It stands out against the rest of the rows. The fact that the total option value for the non risk policy is identical to the fair value is not new to us. The itm option with 720 swings behaves identically to a Forward contract and can therefore be perfectly hedged with a Forward. Thus, there is no risk and hence no additional spread. However, we get the same result for the risk sensitive policy which is correct, but surprising on the first glance. Recall that our heuristic is based on the non-hedged position and should therefore consider a non-zero risk premium during the valuation. To understand the reason for the correct result, recall from equations 3.73 and 3.75 that the penalty term for the cash flow at stage t will be computed from the marginal distribution of the subsequent stage $P^{1-\beta}(\Delta V_{t+1}(X_{t+1}, n), X_t)$. For every swing right beyond the remaining number of delivery hours, i.e. $n > T-t$, this marginal value is zero as all swing options with more swing rights than exercise opportunities have the same value as the swing option with as many swing rights as remaining delivery hours ($n = T-t$), i.e. $V_{t+1}(X_{t+1}, T) = V_{t+1}(X_{t+1}, T-1) = \dots = V_{t+1}(X_{t+1}, T-t)$. In particular in case of $N = T+1$ all for the penalty term relevant marginal value functions are zero, i.e.

$\Delta V_1(T+1) = \Delta V_2(T), \dots, \Delta V_T(2) = 0$. Consequently in case of 720 swings and 720 delivery hours the penalty never applies as there is no marginal distribution and we receive again the non-risk adjusted result i.e. 720.

3.5. Directions for Further Research

In this chapter we introduced the notion of a replacement risk adjusted total option value penalizing the fair value with the EaR figure that we defined as an adequate measure for spot price risk in electricity markets. In particular we were interested in EaR efficient option values. Our benchmark of compressing the distribution to a larger extent than loosing in expectation turned out to be a difficult target. However, this is a realistic objective since compromising on a likely (i.e. the expectation) for an unlikely result (i.e. EaR) is hard to accept in practice. We presented a heuristic of controlling the quantile directly using quantile regression that can generate these efficient option values in case of a single exercise right. We observed that our heuristic failed for large loss probabilities β . Then, the quantile $q_\beta(\epsilon)$ and thus the risk premium is small. At the same time our heuristic imposes a smaller upper bound that forces to exercise small cash flows and reduces the fair value. A large loss probability, however, stands for a less risk averse option holder and should rather relax the upper bound. Obviously, using the β -quantile as the threshold can be too strict. One should therefore investigate a new relation between the loss probability β and the quantile that defines the upper exercise bound.

In addition the hedging aspect is not sufficiently covered in our proposed heuristic (recall that EaR is calculated from a hedged position). Currently the quantile regression runs on the pairs (X_t, V_{t+1}) i.e. current spot price and the accumulated cash flow of the next stage. The latter represents the uncovered option value for the remaining delivery period and we explained that the Balance-of-Month Forward contract F_0^{BOM} allows for hedging this remaining delivery period. In a first extension one could therefore try to run the regression on the hedged ACF $(X_t, (V_{t+1} - \Delta^F F_0^{\text{BOM}}))$ with Δ^F being the Forward delta (see also section 3.3.2). This would lead to a new exercise band. This modification might require a different set of basis functions other than our polynomials as the hedge portfolio $(V_{t+1} - \Delta^F F_0^{\text{BOM}})$ certainly features a new pay-off structure. In general, the analysis of different basis functions in conjunction with possibly non-linear quantile regression schemes as mentioned in section 3.4.2 is another direction for further investigation. In this context one could also review the poor performance of the R_t^1 statistic that did not reflect the comparably good quantile projection. An investigation of the stability of the R_t^1 statistic across different quantiles could be added, too.

The observation that our risk-adjusted policy was less successful for swing options should be addressed as well. In our opinion the reason is twofold. First, it is difficult to assess the impact of the n -th exercise of a single path on the overall option distribution. In case of the American option the conditional distribution of the next stage's value function is a good representative for the overall distribution because it reflects a similar American option that would be issued tomorrow. This is different for the swing option. The intermediate marginal ACFs $\Delta V_t(X_t, n)$ could be interpreted as a portfolio of linked American options where the portfolio value would relate to the total option value $V_0(X_0, N)$. Within this context the risk analysis of the swing option could be translated into a portfolio VaR problem. In the literature there is the notion of *component VaR* which decomposes the portfolio VaR into its individual assets such that the sum of all components returns again the overall VaR. In our case this would be the decomposition of the VaR for the total swing option into its individual swing rights. The method requires the estimation of VaR sensitivities i.e. the change in

overall VaR with a change in individual swings. A good overview of the method is provided in [31]. We think that this is a promising direction for further research.

Second, we observed that the impact of a successful hedge prevails any risk sensitive exercise policy. The more the number of swings approaches the total amount of delivery hours the better a Forward hedge reduces the quantile. A further analysis should try to find the minimum number of exercise rights that are at least necessary for a successful hedge of the swing option with a Forward contract. This analysis should be run for different strikes (itm, atm, otm) and underlyings (base, peak, off-peak price). Then, we know that any swing option with less exercise rights should rather apply our proposed dynamic cap in order to prevent large potential losses. A real world example for a peak swing option with weekly adjusted caps could conclude the analysis of our heuristic. Recall that we based our heuristic on the direct comparison of the risk with the non-risk adjusted policy according to equations 3.59 and 3.60. Any new solution scheme should rather focus on the objective function in equation 3.58 directly.

In the next chapter we will also look at hedging strategies. We will move away from the mere swing option analysis and investigate the combination of a swing option and a power generation asset as an appropriate hedge portfolio. In this context we will return to our synthetic spot delta definition that will help us to find the right portfolio structure.

4. Power Generation Assets

In this chapter we want to extend our basis model of chapter 2 to value power plants, so called *power generation assets*. To be precise we want to provide a short-term value of the plant that can be reflected by the value of its generated output for the near future (usually a year). Swing options, that we investigated so far, are one approach to price a power plant contract. They model a power plant as an asset that can produce electricity for a fixed fuel cost (strike) and considers an extra energy constraint via its limited number of exercise rights. Every hour the power plant owner can decide whether to generate electricity or not. In reality, however, especially thermal power plants cannot be turned on and off every hour. Operational constraints limit its flexibility. The actual generation schedule is determined by numerous technical restrictions. In particular within the context of risk management real option models often rely on Monte-Carlo techniques to compute sensitivities and value distributions and therefore rely on short calculation times. For this reason, a valuation model needs to incorporate only those physical limitations that mainly define the production value.

The literature on generation asset valuation is large and therefore we only want to present the most recent articles and cover different valuation approaches as well as different power plant characteristics. Tables 4.1 and 4.2 provide a summary of selected papers. It is helpful to categorize the different power plant models by fuel type as this usually drives the kind and number of underlying prices as well as the specific technical characteristics. Consequently, we want to differentiate between hydro and thermal power plants. Another important criteria is the granularity of the models. The short-term valuation of a generation asset is usually based on an optimization of the production schedule to define the future projected cash flow and the real option is defined by the expectation of this cash flow. In practice a power plant owner needs to send his planned production schedule to the grid operator on a quarterly hour granularity. From a valuation point of view electricity prices are only traded on an hourly basis, therefore the smallest decision stage should be an hour. However, for the standard time horizon of a year this can be computationally expensive. Therefore power plant models work with daily and weekly granularities or a mixture of both more granular for the near and less granular for the far end of the delivery period.

Let us first look at hydro plants. The main complexity of hydro plants originates from the water reservoir which translates to an overall energy constraint. The level of available water determines the amount of electricity that the plant can produce over a certain demand period. As we will later in this chapter discuss in detail, an energy constraint introduces a new dimension to the decision domain and hence significantly increases the computational burden. Frauendorfer and Vinarski [28] try to reduce the complexity by saving decision steps. They apply a multistage stochastic program where they separate a production year into six stages which they optimize separately using only a reduced set of schedule candidates. They compromise on the technical constraints as they are mainly interested in a risk analysis. They focus on the electricity price and use a two factor model to describe the spot and Forward price component of the electricity price. It allows them to compute Forward deltas and a PnL distribution. Lüthi and Doege [48] also investigate the distribution of a hydro power plant, but additionally introduce the water inflow as a risk factor. They also go down to an hourly granularity. Lüthi simplifies the operational constraints via weighted step functions

Paper	Plant Characteristics	Price Modelling	Valuation Approach	Risk Analysis
Carmona	<ul style="list-style-type: none"> Fuel switching power plant Start-up and shut down costs Ramping cost Ramping time 	<ul style="list-style-type: none"> Monte Carlo simulation: <ul style="list-style-type: none"> Electricity/spot price Gas spot price Oil spot price 	<ul style="list-style-type: none"> Stochastic Dynamic Programming <ul style="list-style-type: none"> LS regression Daily stages 	—
Deng	<ul style="list-style-type: none"> Thermal power plant Max number of start-ups Min and max capacity Start-up time start-up and shut-down cost lower and upper heat rate 	<ul style="list-style-type: none"> Monte-Carlo simulation: <ul style="list-style-type: none"> Electricity/spot price Gas Forward price 	<ul style="list-style-type: none"> Stochastic dynamic programming <ul style="list-style-type: none"> LS Regression Daily stages by price band 	<ul style="list-style-type: none"> Dynamic Forward Hedge via synthetic spark spread option deltas
Fraundorfer	<ul style="list-style-type: none"> Hydro power plant max energy(water reservoir) Min and max capacity Ramping time 	<ul style="list-style-type: none"> Scenario Trees: <ul style="list-style-type: none"> Electricity/spot price Electricity/Forward price 	<ul style="list-style-type: none"> Multistage stochastic programming: <ul style="list-style-type: none"> 6 stages (first week + 5 intervals) Reduced set of schedule candidates ratchet constraint between stages are disregarded 	<ul style="list-style-type: none"> PnL distribution via forward iteration Base/Peak Delta (finite difference method) Comparison with det. optimization (full information)
Lüthi	<ul style="list-style-type: none"> Hydro power plant Max energy(water reservoir) Fixed marginal cost 	<ul style="list-style-type: none"> Monte-Carlo simulation: <ul style="list-style-type: none"> Electricity/Price Electricity/Demand Water Inflow 	<ul style="list-style-type: none"> Linear Optimization: <ul style="list-style-type: none"> Hourly decision variables Approximation of schedules via weighted step functions 	<ul style="list-style-type: none"> Conditional VaR Parametric Analysis: <ul style="list-style-type: none"> calculation of a mean-cVaR efficient frontier shadow price (slope of frontier) interpreted as "hedge value of flexibility" Marginal Value of Flexibility
Porchet	<ul style="list-style-type: none"> Thermal power plant Min off/on time Start-up/shut down costs Ramp rate 	<ul style="list-style-type: none"> Monte Carlo simulation <ul style="list-style-type: none"> Electricity/spot price Coal spot price 	<ul style="list-style-type: none"> Reflected Backward Stochastic Differential Equation: <ul style="list-style-type: none"> Cash flow as SDE with regime switching continuous model (no stages) 	<ul style="list-style-type: none"> Comparison of power plant value for complete and incomplete market

Table 4.1.: Selected generation asset valuation literature (Part 1)

Paper	Plant Characteristics	Price Modelling	Valuation Approach	Risk Analysis
Römisch	Combined Heat and Power <ul style="list-style-type: none"> • Ramping time • Min/max capacity • Fixed heat rate 	Pruned Scenario Trees: <ul style="list-style-type: none"> • Electricity spot price • Electricity demand • Heat demand 	Multistage stochastic optimization: <ul style="list-style-type: none"> • Daily stages • (non integer) LP at each stage 	Mean-risk objective function with polyhedral risk measures (see section)
Tseng	Thermal power plant <ul style="list-style-type: none"> • Start-up/shut-down time • Min on/off time • Min/max capacity 	2-dim trinomial lattices: <ul style="list-style-type: none"> • Electricity spot price • Gas spot price 	Stochastic dynamic programming: <ul style="list-style-type: none"> • Hourly stages 	—
Weber	Combined Heat and Power <ul style="list-style-type: none"> • Min and max heat demand • Fixed heat rate 	Monte-Carlo simulation: <ul style="list-style-type: none"> • Electricity spot price • Gas and Coal price 	Combination of spark spread option and analytical dispatch decision <ul style="list-style-type: none"> • Hourly stages • Dimensionality reduction via spark spread ratios 	<ul style="list-style-type: none"> • PnL Distribution via Delta-Gamma-VaR • Integral Earnings-at-Risk (see also section) • Conditional-VaR • Volumetric hedge • Forward delta hedge (finite difference method)

Table 4.2.: Selected generation asset valuation literature (Part 2)

that allow him to run a linear optimization. Furthermore he introduces a figure for comparing different power plant investments that he calls *value of flexibility*. It is the difference between VaR figures of two profit and loss distributions arising from different technologies. This value should allow to evaluate the benefit of new technologies in terms of faster reaction on market changes and hence in risk mitigation.

Different to hydro plants thermal power plant models need to capture the fuel price as a second price component. In addition, thermal plants are less flexible due to the required warm-up and cool off phases as well as the necessary injections for the start-up of the turbines. Tseng and Lin [62] look at a gas fired power plant with start-up and shut-down as well as minimal on- and off-times. Following the classical forest approach for swing options (see Kaminiski et al. [40]) they define a stochastic dynamic program on a two dimensional tree representing the hourly gas and electricity price. The different trees stand for the different operational modes of the power plant. Deng and Xia [23] also look at a gas fired power plant and value the real option via stochastic dynamic programming. Instead of a lattice they rely on Monte-Carlo simulation and therefore use the Longstaff-Schwarz regression method to run the backward iteration. They consider a large set of operational constraints including a max number of start ups and a lower and upper heat rate. The latter reflects the fact that power plants are designed for max electricity production. The heat rate goes down if the generation runs below the max level and hence the power plant is less efficient. Due to the complex set of technical constraints Deng and Xia compromise on the price granularity by simulating only daily prices by price band rather than hours. They also examine hedging strategies with power and gas Forwards. As they cannot compute the relevant sensitivities directly for their complex power plant model, they replicate the generation asset first via a strip of spark spread options. Ignoring any technical restrictions the spark spread option is the simplest instrument to value a power plant (a swing option can at least cover one constraint i.e. a maximal energy production). Barz [5] was one of the first who investigated this idea based on gas and power Forward contracts. A spark spread option looks at the difference between the electricity and the fuel price. In order to make both comparable the gas price will be translated in MW via the heat rate (this is where the term *spark* comes from). From a cash flow perspective a power plant in deed converts a negative fuel cash flow into a positive electricity cash flow. The power plant will only produce if the spread is positive which motivates to use this spread for the option's underlying. For these spark spread options Deng and Xia can compute more easily the power and gas Forward delta. Now, Deng and Xia use these deltas to define a hedge portfolio consisting of gas and electricity Forward contracts and a bond. The Forward deltas calculated from the spread options are their vehicle to dynamically find and adjust the actual Forward positions in the hedge portfolio for their power plant. Following the spark spread approach Castellacci, Siclari et al. [17] investigated spark spread basket options where the contingent claim is defined on the price difference between the electricity price and a basket of two fuel prices. In this way they want to model fuel switching power plants. Fuel switching introduces a second fuel price as yet another risk factor. The owner of a fuel-switching power plant can usually decide whether to produce with gas or oil. Castellacci and Siclari use factor reduction and fast simulation techniques like stratified sampling to reduce the valuation complexity of their basket option.

Carmona [15] goes one step further. He also investigates fuel switching options, but even introduces technical constraints like ramping time and several cost components. Due to the three correlated risk factors he applies Monte-Carlo simulation in conjunction with Longstaff-Schwarz regression based backward iteration. He benchmarks his results against an alternative numerical method called reflected backward stochastic differential equations (BSDE). Porchet et al. [55] use this method to value a coal-fired power plant. BSDE is a continuous version of stochastic dynamic programming. The conditional expectation within the Bellman equation is

described as a continuous stochastic process. Then the Bellman equation becomes a stochastic differential equation (SDE) that will be solved via variational inequalities. They consider different operational modes of the plant like min off- and on- times via regime switching which adds further equations to the system of BSDE's. Porchet et al. also study the impact of market incompleteness inherent to electricity markets (see also our discussion in section 3.54). They compensate the lack of a risk-free numeraire by looking at a utility function that reflects the risk aversion of the power plant owner. Then, they show that the power plant value is dependent on the risk aversion of the owner in an incomplete market.

Römisch and Eichhorn [25] also investigate the impact of risk aversion on the power plant value. They define a mean-risk objective function to value a combined heat and power plant (CHP) where a weighting factor between profit and risk reflects the risk aversion. They use polyhedral risk measures as discussed in section 3.4 to value the risk component in their objective. CHP facilities produce not only electricity, but heat as well. They are usually obliged to fully supply the surrounding households with heat. So the optimization needs to take into account the uncertain heat demand which also impacts the electricity production. Römisch and Eichhorn therefore introduce heat and electricity demand as two additional risk factors and neglect the fuel price instead. As their risk analysis requires extensive computation time they introduce a pruning technique for scenario trees that allows to reduce the number of price trajectories to few representative paths. In addition they look at daily decision stages and ignore start-up and shut-down times to avoid integer constraints. In this way they are able to translate their multistage stochastic optimization problem into linear programs. Weber [67] also investigates a CHP facility and considers a large set of physical restrictions. He even looks at the fuel price as well. In particular he examines a coal and gas fired CHP. For his risk analysis, however, he is also forced to simplify his model to a combination of spark spread options with fixed heat rate and analytical dispatch decisions that can only consider min and max heat demand. Then, he reduces the risk dimension even further by introducing spark spread ratios that allow to compute the fuel component directly from the random electricity price. With this simplification he is able to compute Forward deltas and gammas that he inserts into a Taylor series expansion. He computes a delta-gamma profit and loss distribution to examine his Integral Earnings-at-Risk approach (see also section 3.4).

All the presented models need to compromise between accuracy and valuation time that are mainly defined by the power plant profile. Hence, in the first section we introduce our type of power plant with its technical characteristics that we want to value. Throughout this chapter we will work with one basic example that we will modify step by step. Different to the last two chapters this time we want to provide a real world business case. Consequently we need to move from our simple price trajectories that served well for our illustrations in the last two chapters to a set of scenarios that reflect true price fluctuations. We will stick to our known mean-reverting price process and describe in section 2 the calibration of the price process to actual market data. In the third section we will use those prices to value our power plant without an energy constraint. We will also provide lower and upper bounds. In the fourth section we will repeat this analysis with an additional energy constraint. In the fifth section we will look at hedging strategies for our power plant and conclude this chapter with suggestions for further research.

4.1. Power Plant Characteristics

Every day the power plant owner needs to register tomorrow's generation schedule to the grid operator (so called *nomination*) until noon. This is briefly before the energy exchange settles the spot prices for tomorrow. Hence, we can assume that the dispatcher knows tomorrow's

prices almost surely when he makes his dispatching decision as prices will not deviate that much any more after he performed his nomination. Our dispatcher runs a thermal power plant with the following profile:

- minimal capacity L_{\min} (= 240 MW)
- maximal capacity L_{\max} (= 530 MW)
- minimal runtime t_{on} (= 12 h)
- minimal off-time t_{off} (= 8h)
- start-up and shut-down costs K_u, K_o (= 3000 EUR, 0 EUR)
- variable production costs K (50 EUR, 70 EUR, 90 EUR)
- (maximal energy production \mathcal{W}_0)

In parenthesis you see the actual values that we will use for our example throughout this chapter. Min and max capacity define the electricity band for the power production per hour. A thermal power plant cannot produce any capacity from zero level upwards. It first needs to be warmed up such that the turbines run on a minimum spin before the power plant can produce the first power. The start-up cost are the charge for the fuel injection to kick off the turbines. Once they are running they cannot be stopped abruptly but rather need to run a minimum number of t_{on} hours. We have the opposite situation when the power plant will be turned off. It has to cool down for at least t_{off} hours before another start can be performed. Variable costs are mainly yearly maintenance fees that are spread equally across the production hours.

The maximum energy constraint is a technical feature of so called combined heat and power plants (CHP). They do not only produce power, but also provide heating for the neighboring cities. Electric heating can be translated into an energy constraint which would be a lower bound in this case. Furthermore environmental obligations can lead to energy constraints as well. Governments assign CO2 emission certificates to power plant owners. These certificates deliberately do not last for the maximum energy production and are meant as an incentive to improve generation efficiency. An upper energy constraint can reflect the border beyond which the power plant needs to buy CO2 certificates on the market to cover the extra pollution which results in higher costs. Then, the power plant owner can compare if it is more profitable to produce at maximum level regardless of the CO2 emissions and accept the cost for additional CO2 certificates or produce only up to the certificate free limit. Finally, an energy constraint can help to calculate the marginal profit on produced energy which can serve as a basis to define the merit order for options on spinning reserve energy. The merit order is a list of price-quantity pairs that a trader sends to the auction of the exchange. It states for which price the trader is willing to pay or sell what amount of electricity, in this particular case spinning reserve energy. Utilities are obliged to produce a certain amount below their total potential production. This extra energy buffer is called spinning reserve energy and is meant for emergency to stabilize the grid in case of a sudden outage or fallout of another power plant within the national grid. Instead of saving that amount of energy power plant owners can buy options on spinning reserve energy from other utilities. If the dispatcher knows the characteristic profit/energy line of his power plant then he can easily assign prices for various energy amounts that he is willing to pay. Imposing an energy constraint will allow him to compute this line.

In the following sections we will provide a short-term value of the power plant via the calculation of the expected net present value of a certain production period, in our example

this will be one month (March 08). An evaluation model for such a real option should cover three areas. First, it should provide a fair value of the produced electricity. Second, it should deliver a concrete schedule for the nomination of the following day. Third, it should provide sensitivities for hedging. We will address all three objectives in the subsequent sections. But first we will review our price process in order to generate realistic price scenarios for our intended analysis.

4.2. Electricity Prices: A Real World Example

In section 3.2 we gave an introduction to Forward curve engineering in electricity markets. We explained that our price process in equation 2.7 can be understood as an idealized spot price fluctuation around a flat Forward curve with a single price equal to 1. We used this setup to stay consistent with an example from Meinshausen et al. [50]. This time we want to rather generate prices that resemble actual EEX (European Energy Exchange) spot prices. We will introduce two different descriptions of the price dynamics. Both processes have in common that instead of a single dimensional price process they treat the 24 hourly prices of a day as individual price processes summarized in a vector X_d . The former mean-reversion parameter is now a vector with 24 components $\kappa \in \mathbb{R}^{24}$. In this section we use small letters with index t for vector components. The first model extends our existing mean-reverting process by a time dependent mean, i.e. the hourly PFC. Recall from equation 3.31 that the hourly PFC $h_d := h_d(g_0)$ reflects the expected hourly price conditional on the current Future price g_0 . In this setup it is a vector with 24 components $h_d^t, t = 1, \dots, 24$. Again we look at a discrete model, this time written with vectors

$$\begin{aligned} \text{P1: } \ln X_d &= \ln h_d + S_d \\ S_{d+1} &= (1 - \kappa) * S_d + \Sigma \epsilon_d, \quad \epsilon_d^t \sim N(0, 1), \end{aligned} \quad (4.1)$$

where the individual random factors ϵ_d^t are i.i.d and Σ is the variance-covariance matrix of the 24 hours and the symbol $*$ stands for the multiplication of each vector component. Note that we obtain the same price process as in equation 2.7 if we make the former single mean m time dependent as follows $m_d^t = \frac{1}{\kappa^t} \frac{\partial h_d^t}{\partial t} + h_d^t$. The second price process P2 is a special case of P1 with $\kappa^t = 0$. It models the (log) price directly instead of the log returns like in the first model

$$\begin{aligned} \text{P2: } \ln X_d &= \ln h_d + S_d \\ S_d &\sim N(0, \Sigma), \end{aligned} \quad (4.2)$$

where individual vector components between days $S_{d_1}^t, S_{d_2}^t$ with $d_1 \neq d_2$ are independent. The second model also uses the log in order to prevent negative prices during the price generation. In both price models the variance-covariance matrix Σ covers the interaction between hours as well as price spikes by higher volatility in certain hours. This is consistent with the market view where each hour is treated as a separate product and the observation that jumps cluster around certain hours only (e.g. hour 12). Both price processes separate strictly between a deterministic drift h_d and random variations S_d . In this way we are able to extract the seasonality first and handle the stochastic component afterwards.

The two price processes mainly differ in their price generation. In P1 a new price still relies on the previous one. P2 shifts the seasonal shape every day independently and thus generates independent daily prices. Therefore it does not require any mean reversion to control the deviation from the mean as fluctuations cannot accrue from day to day. We also want to stress again the distinction between S_d and X_d . As explained in the previous chapter, S_d

stands for the individual hourly random behavior (spot price component) of the overall spot price X_d . The next two sub sections explain the parameter estimation from historical prices and the calibration of those parameters to the current Forward curve.

4.2.1. Parameter Estimation

The seasonality of electricity prices is a complex mixture of different patterns. Yearly, weekly and daily shapes overlap and form the underlying time dependent mean of the price dynamics. The time series of electricity prices generally reveals large spikes, which distort the underlying seasonal behavior and make a proper estimation of the shapes difficult. Therefore, we extract those outliers in a preprocess by applying *repeated filtering* introduced by Clewlow and Strickland [19]. We compute the mean m and standard deviation s for the log prices of our time series and identify all data points beyond $m \pm 3s$ and replace them by the value of the previous day. We repeat these two steps on the filtered prices until no more outliers can be identified. Instead of replacing an outlier by the value of the previous day one could interpolate the neighboring values. In an unstable situation, however, jumps often occur in a row. Then, interpolation will not erase outliers immediately. An alternative strategy replaces an outlier by the previous price of the same hour and day type or simply by the price of the previous hour. Once we have filtered out these outliers we obtain a clearer picture of the seasonality which leads us to the concept of day types.

Day types reduce all 365 days of a year to a certain number of representatives. Weekdays for instance reveal a common intra-day profile which differs from a typical weekend shape. Thus, we could define two day types called "Weekday" and "Weekend" and assign a characteristic behavior. A further separation would distinguish between each day of the week. This would result in 7 day types from Monday to Sunday. Both approaches would cover the weekly seasonality between the day types and the intra-day patterns within the day types. In order to take into account the yearly pattern one could furthermore differentiate between the four seasons of a year or even between each month of the year. Hence, one would have for instance a "Monday - summer" or a "Tuesday - February" profile. Holidays could be treated accordingly (Monday - holiday, ...).

Those day types should not be absolute price levels but rather weighting factors to the corresponding $i = 1, \dots, I$ monthly price band prices. One differs between "peak" (9h to 20h on weekdays) and "off-peak" prices ($m = 1, 2$). Monthly price band prices change in absolute terms throughout the years, but the quality of the day type shapes stays the same (e.g. higher prices in winter than in summer due to heating demand). Therefore day types ($k = 1, \dots, K$) are better represented by shaping factors rather than absolute price patterns. Since we investigate log prices, those factors become spreads to the monthly log price band prices. Hence, we decompose the time series in monthly price band prices with $m=1, 2$ price bands and $i = 1, \dots, I$ months i.e. historical Future prices ${}_m G^i$ plus day type adjustment factors α_{kl} also known as *hourly curve adjustments*

$$\ln h_d^t = \sum_{i=1}^I \sum_{m=1}^2 (\ln {}_m G^i) D_t^{(im)} + \sum_{k=1}^2 \sum_{l=1}^{24} (\ln \alpha_{kl}) I_t^{(kl)} \quad (4.3)$$

$$I_t^{(kl)} = \begin{cases} 1, & \text{if hour } t \text{ belongs to the } l\text{-th hour of the day type } k \\ 0, & \text{otherwise} \end{cases}$$

$$D_t^{(im)} = \begin{cases} 1, & \text{if hour } t \text{ belongs to price band } m \text{ of month } i \\ 0, & \text{otherwise,} \end{cases}$$

where $m = 1$ stands for peak and $m= 2$ for off-peak, $i = 1, \dots, I$ are all months in the time

series, $k = 1, \dots, 2$ our two day types and $l = 1, \dots, 24$ are the individual hours of a day type. While we look at every price band of every month separately throughout the entire historical time series we apply always the same day type/pattern α_{kl} to its associated calendar month (e.g. while we compute a separate mG^i for every January offpeak and peak price in the time series we will still apply the same day type "Weekday-January" α_{kl} on those months). First, we compute mG^i by averaging the corresponding price band hours per month. Having extracted those monthly averages we group the deseasonalized prices by hour and day type. Applying again the sample mean for these groups separately results in α_{kl} .

For our concrete example we will apply a monthly granularity with the simple categories of "Weekday" and "Weekend" i.e. "Weekday March", "Weekend July", etc. We use the EEX prices from 2003 to 2007 to estimate the shapes according to equation 4.3. Figure 4.1 illustrates the overall fit of our seasonal shape across the entire price history. We can observe an adequate coverage of the main price dynamics, but also need to admit the uncovered spikiness of the prices. While positive jumps with prices beyond 200 EUR are most apparent in the first place, it is actually the number of price drops often down to 0 that are even more frequent (this observation would actually motivate a model using semi-absolute deviation which looks at separate up and down volatility). Figure 4.2 presents a typical summer shape with the

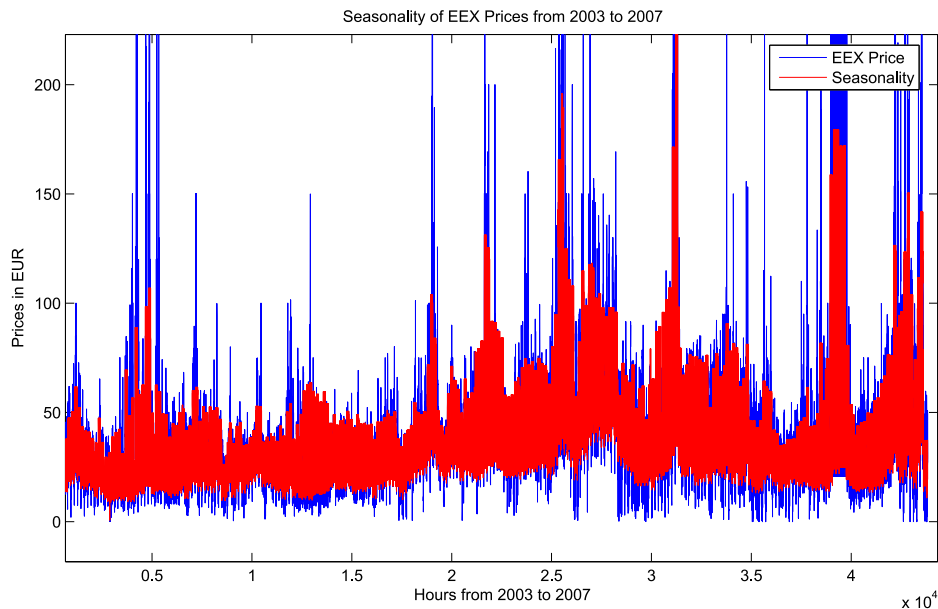


Figure 4.1.: Seasonal patterns vs. actual electricity prices in 2003 to 2007

characteristic peak around noon that in reality is often a spike as indicated by the actual historical price from July 07 that we have overlaid. Figure 4.3 compares our winter shape with an actual price in October. The winter shape reveals the typical double peak pattern during lunch and dinner time. Having identified the seasonal pattern we deseasonalize the original (i.e. non-preprocessed) prices to obtain the remaining pure spot price dynamics S_d including the spikes. So far the estimation of both price process models P1 and P2 is identical. The first price process needs to further extract the mean reversion vector κ . From equation 4.1 we know

$$S_d = (1 - \kappa) * S_{d-1} + \Sigma \epsilon_d, \quad (4.4)$$

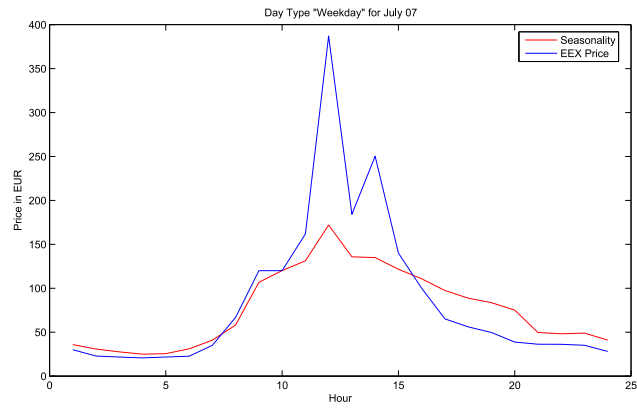


Figure 4.2.: Seasonal pattern vs. historical price for a weekday in July 2007

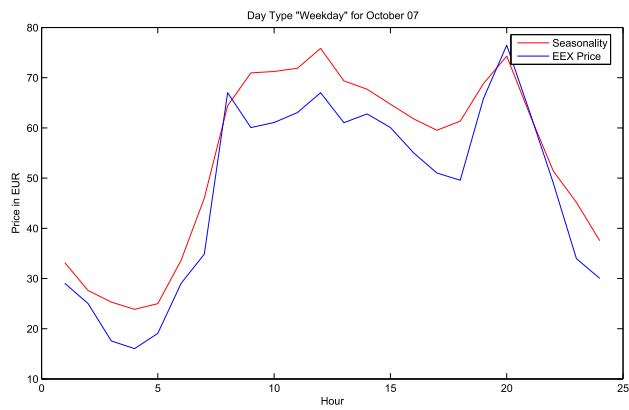


Figure 4.3.: Seasonal pattern vs. historical price for a weekday in October 2007

where the symbol $*$ stands for the multiplication of each vector component. Then we apply a linear regression to extract κ for each vector component. The residuals ϵ_d are the daily returns calibrated by the mean reversion parameter (recall that S_d is in fact a log price and therefore $S_d - (1 - \kappa) * S_{d-1}$ is a return). We assume the same mean reversion parameters for weekdays and weekends. Table 4.3 shows the result for the vector κ . We can see a general

H1	H2	H3	H4	H5	H6	H7	H8	H9	H10	H11	H12
0.77	0.77	0.73	0.71	0.76	0.84	0.82	0.89	0.95	0.99	0.94	0.65
H13	H14	H15	H16	H17	H18	H19	H20	H21	H22	H23	H24
0.85	0.79	0.96	1.02	1.00	0.85	0.87	0.73	0.68	0.66	0.62	0.65

Table 4.3.: Mean-reversion vector κ

high mean reversion speed with more than 0.6 across all hours. The higher the value the smaller the impact of the previous price and the stronger the price will be pulled back to the mean. Then the shape stands out for that hour more clearly. Hence, it is no surprise that hour 12 has a small value since this is the most spiky hour that tends to deviate far from the mean whereas hour 15 to 17 are mainly driven by the seasonal pattern.

The last step of the parameter estimation focuses on the variance-covariance structure Σ of the log returns ϵ_d (P1) and log prices S_d (P2) respectively. There are basically two approaches for calculating the volatility. We either assume a seasonal volatility to acknowledge for different fluctuations in winter and in summer months (heating demand introduces an additional uncertainty and thus higher volatility on the price during winter months). Alternatively, one could rather prefer to rely on most recent market behavior. The former would require to group ϵ_d and S_d by month and compute the variance and correlation for these time buckets, the latter would simply calculate the variance covariance matrix from the most recent data (usually 60 days). In particular if one wants to investigate larger time horizons a combination of both is advisable (a GARCH model, for instance, allows for differentiating between a short term and long term volatility). We will focus on a delivery period for the single month of March 2008 and will therefore compute the variance and correlation from the last 60 days in 2007. Figure 4.4 and 4.5 compare the volatilities for both price processes separately for weekends and weekdays. We can see that both price processes reveal almost identical volatilities.

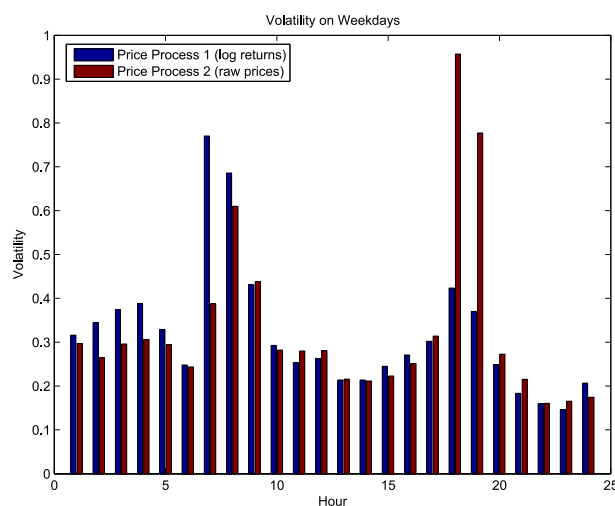


Figure 4.4.: Volatility on weekdays from log returns (P1) vs. prices (P2)

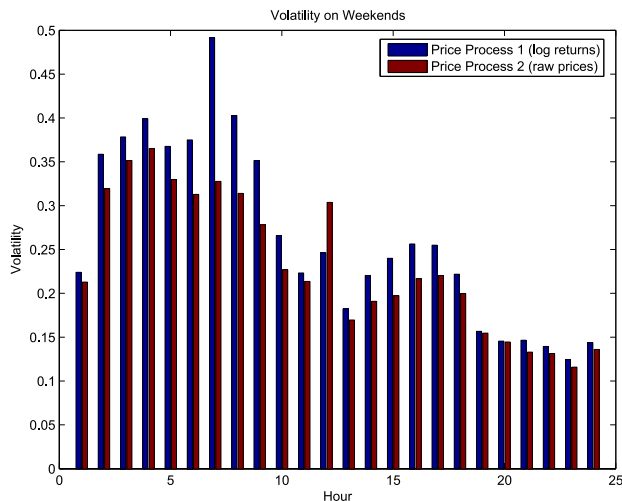


Figure 4.5.: Volatility on weekends from log returns (P1) vs. prices (P2)

An exception are hours 7, 8, 18 and 19 for the weekday volatilities. These hours are borders of the off-peak to the peak price band. In reality hour 7 often flips between an off-peak and a peak-like price which explains the high volatility. Market participants seem to regard hour 7 rather like a peak than an off-peak hour. The fact that the volatility for hour 18 and 19 is more than double for the prices compared to the log returns can be explained by huge jumps during these hours that specifically occurred in December, a month that is usually very volatile due to the Christmas holiday season. Jumps have an immediate impact on the mere price based volatility (P2). Remember that our log returns, instead, are adjusted by the mean reversion parameter κ according to equation 4.4 which compensates part of the fluctuation and makes the final volatility result smaller. But also in terms of the log returns hour 18 and 19 have a high volatility (even higher than hour 12). Recall from Figure 4.3 the second peak during the evening hours for winter shapes. Apparently, this second peak does not clearly stand out and makes these hours more volatile. As expected, on weekends the volatility is generally smaller. The higher volatility in morning hours can be explained by large negative jumps almost down to 0 that tend to happen mainly during early morning hours on weekends. This is where the EEX even published negative prices the first time in 2008. Figure 4.6 and Figure 4.7 present the correlation between neighboring hours. To be precise, a correlation at hour i in the graph stands for the correlation between hour i and $i + 1$. Consequently we only have 23 observations. As assumed we can detect a generally high correlation throughout weekdays and weekends that again only drops at the border between peak and offpeak hours. By definition prices between price bands should be less correlated than within a price band. While this is properly the case in the evening (the correlation between hour 19 and 20 as well as hour 20 and 21 is significantly smaller) this characteristic is shifted in the morning by one hour. The correlation between hour 7 and 8 is more than 90% and underlines another time that hour 7 is treated like a peak hour by the market. Instead hour 5 to 6 and 6 to 7 show the expected behavior of a weaker correlation. On weekends where we have only off-peak hours the correlation profile is fairly stable.

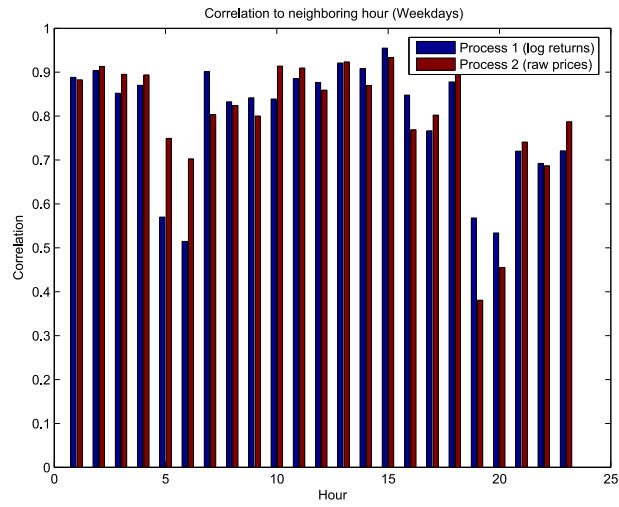


Figure 4.6.: Correlation on weekdays between neighboring prices

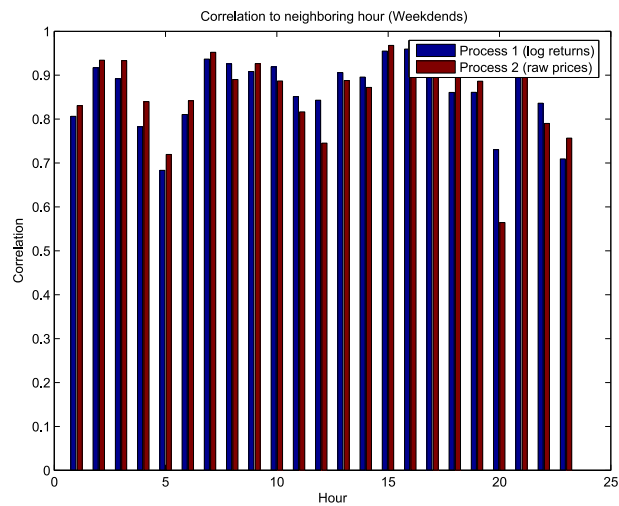


Figure 4.7.: Correlation on weekends between neighboring prices

4.2.2. Price Generation

Now that we have calculated all relevant parameters, we will generate new price scenarios. In particular we want to calibrate the price process to the current term structure of the Forward curve. The calibration consists of two steps. First we normalize the hourly curve adjustments such that the average of all factors for the same price band m and month i is 1. The relevant first normalization factor $\eta_{im}^{[1]}$ is

$$\begin{aligned} \tilde{\alpha}_t &= \eta_{im}^{[1]} \alpha_t, & t \in \mathbb{T}_{im} \\ \eta_{im}^{[1]} &= \left(\frac{1}{|\mathbb{T}_{im}|} \sum_{t \in \mathbb{T}_{im}} \alpha_t \right)^{-1}, \end{aligned} \quad (4.5)$$

where \mathbb{T}_{im} is the set of hours that belong to month i and price band m and $|\mathbb{T}_{im}|$ is the total number of hours in this set (see also equation 3.32). Then we replace in equation 4.3 the historical Future prices ${}_m G^i$ by the current Future prices ${}_m \hat{G}^i$ and apply $\tilde{\alpha}_t$ instead of α . The resulting \tilde{h}_d^t constitutes the new PFC according to our definition from section 3.2. Then we add the correlated random spot price component S_d that we either generate directly from the variance covariance matrix of the prices (P2) or implicitly via the log return process ξ_d (P1). The random log prices are also automatically normalized in average as the mean of $\ln S_d$ is zero. However, the actual prices are not. These N scenarios will therefore also be normalized to make sure that the average of the random prices of the same price band and month across all scenarios returns again the initial Forward price. This leads to the second normalization factor $\eta_{im}^{[2]}$

$$\begin{aligned} x_d^t &= \eta_{im}^{[2]} e^{\tilde{h}_d^t} e^{s_d^t}, & t \in \mathbb{T}_{im} \\ \eta_{im}^{[2]} &= \frac{{}_m G^i}{\frac{1}{N} \frac{1}{|\mathbb{T}_{im}|} \sum_{n=1}^N \sum_{t \in \mathbb{T}_{im}} x_t^n}. \end{aligned} \quad (4.6)$$

The normalization requires that the price band hours do not overlap. For this reason we work with peak and off-peak prices. In reality, the German energy exchange quotes peak and base prices instead. However, the off-peak price can be derived directly from the other two through the following relation

$${}_B T^i {}_B G^i = {}_P T^i {}_P G^i + {}_O T^i {}_O G^i, \quad (4.7)$$

where B, P and O stand for Base, Peak and Off-Peak and T^i are the total number of hours that belong to the corresponding price band B, P, O and month i . Figure 4.8 illustrates how a single trajectory contains information of both the Forward prices and the seasonality. Note that the seasonal shape taken from historical prices reflects the market view of hour 7 being another peak price (hour 7 already reaches the level of the Forward peak price). All examples in this chapter will use 1000 price scenarios that are generated based on price process P2. Appendix C provides further sample paths of this price process.

4.3. Valuation without Energy Constraints

Our first valuation approach will ignore the energy constraint W_0 . In practice, the power plant owner needs to register a day schedule one day in advance and hence needs to make his dispatching decision on a daily basis. As spot prices are traded day ahead and consequently settle daily as well, we will apply a daily price filtration and decision process. Then, the

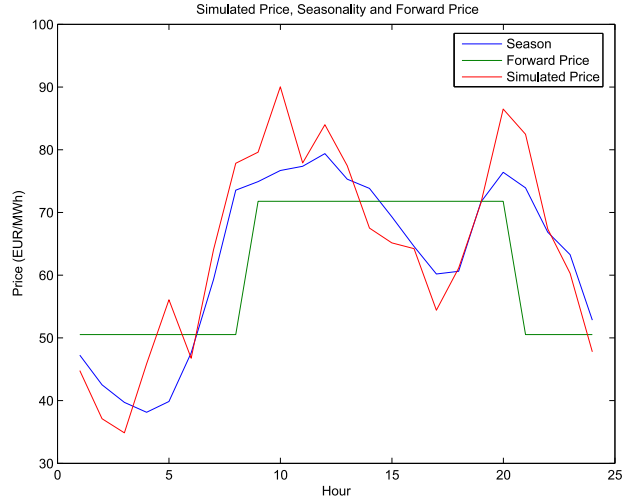


Figure 4.8.: The simulated price on top of the season and Forward price

power plant owner will run his power plant to maximize the cash flow Z_d for today's given price. This daily cash flow is the difference between the 24 hourly electricity prices of a day d summarized in a vector X_d and the variable production cost K . Note that different to our swing option model in the previous two chapters a negative cash flow has to be accepted in case one of the price vector components X_d^t falls below K , but the power plant has not yet passed the minimum runtime. Like X_d the daily schedule L_d is also a vector containing the actual quantity profile (24 different capacities in MW) for each hour of a day. Furthermore, we introduce the auxiliary binary vectors β_d^o and β_d^u that trigger the shut-down and start-up costs K_o and K_u at each hour where the schedule switches the power plant on and off. As in our previous chapters we ignore discounting. Then the cash flow can be written as

$$Z_d := (X_d - KI)'L_d - (K_o I)' \beta_d^o - (K_u I)' \beta_d^u, \quad (4.8)$$

with I being the unity vector. The value of the entire power plant production is the sum of these daily cash flows that are linked by the on- and off-times. Without an energy constraint the dispatcher only needs to make sure that the plant's operating states will not be violated from one day to the next. To ensure a valid new schedule for day d we only need to know the off-line hours m or running hours k until midnight of the previous day which we declare as the start state $U_d := (U_d^{(1)}, U_d^{(2)}) := (m, k)$ of a day with $m \in \{0, \dots, t_{\text{off}}\}$ and $k \in \{0, \dots, t_{\text{on}}\}$ with $m \cdot k = 0$ and $m + k > 0$. In order to simplify the notation we denote with $\mathbb{L}_{\text{on,off}}(U_d)$ all schedules L_d at a fixed day $d = 0, \dots, D$ that meet the on- and off-times t_{on} and t_{off} as well as the min and max capacity $L_{\min}, L_{\max} > 0$ based on start state U_d . Each vector component L_d^t , $1 \leq t \leq 24$, stands for an hourly production capacity in MW. Furthermore, we denote $L_d^{s_1, s_2} := L_{d-1}^{24+s_1, s_2}$ for $s_1, s_2 \leq 0$, in particular $\mathbb{L}_{L_{d-1}^{24+s_1}} := 0$ for $s_1 := -U_d^{(1)} + 1, \dots, 0$ and $\mathbb{L}_{L_{d-1}^{24+s_2}} := 1$ for $s_2 = -U_d^{(2)} + 1, \dots, 0$ with \mathbb{I} being the indicator function. Finally we assign $L_{-1}^t := 0, 1 \leq t \leq 24$, if $U_0^{(1)} > 0$ and $L_{-1}^t := 1, 1 \leq t \leq 24$, if $U_0^{(2)} > 0$. Then, we can write

the feasible production schedules as

$$\mathbb{L}_{\text{on,off}}(U_d) := \left\{ \left(L_d^t \right)_{1 \leq t \leq 24} \left| \begin{array}{l} \forall t = 1, \dots, 24 : L_{\min} \leq L_d^t \leq L_{\max}, \quad L_d \in \mathbb{R}^{24}, \\ \forall s_1, s_2 = -\max\{t_{\text{on}}, t_{\text{off}}\} + 2, \dots, 0, 1, \dots, 24 : \\ -1 - \mathbb{I}_{L_d^{s_1} > 0} + \mathbb{I}_{L_d^{s_1-1} > 0} + \mathbb{I}_{L_d^t \leq 0}, \quad \tau = s_1 + 1, \dots, \min\{s_1 + t_{\text{off}} - 1, 24\}, \\ \mathbb{I}_{L_d^{s_2} > 0} - \mathbb{I}_{L_d^{s_2-1} > 0} - \mathbb{I}_{L_d^t > 0} \leq 0, \quad \tau = s_2 + 1, \dots, \min\{s_2 + t_{\text{on}} - 1, 24\}, \end{array} \right. \right\}. \quad (4.9)$$

Thus, today's dispatch decision L_d will define tomorrow's start state U_{d+1} and thus impact the set of admissible schedules for tomorrow. It also automatically determines the auxiliary vectors β_d^o, β_d^u that trigger the start-up and shut-down costs. Formally $(L_d, \beta_d^o, \beta_d^u)$ build the relevant action space

$$A(U_d) := \left\{ (L_d, \beta_d^o, \beta_d^u) \left| \begin{array}{l} L_d \in \mathbb{L}_{\text{on,off}}(U_d), \\ \forall s = 0, 1, \dots, 24 : \\ \mathbb{I}_{L_d^{s-1} > 0} - \mathbb{I}_{L_d^s > 0} - \beta_d^{o,s} \leq 0, \quad \beta_d^{o,s} \in \{0, 1\}, \\ -\mathbb{I}_{L_d^{s-1} > 0} + \mathbb{I}_{L_d^s > 0} - \beta_d^{u,s} \leq 0, \quad \beta_d^{u,s} \in \{0, 1\} \end{array} \right. \right\}, \quad (4.10)$$

with $L_d^s := L_{d-1}^{24}$ for $s = 0$ and $L_{-1}^t := 0, 1 \leq t \leq 24$, if $U_0^{(1)} > 0$ and $L_{-1}^t := 1, 1 \leq t \leq 24$, if $U_0^{(2)} > 0$. Now, we investigate rules f_d that pick an action out of $A(U_d)$ for a given price vector X_d and start operating state U_d , i.e. $(X_d, U_d) \xrightarrow{f_d} (L_d, \beta_d^o, \beta_d^u) \in A(U_d)$. We are mainly interested in the optimal sequence of these rules denoted as the policy $\pi_d^* := \{f_d^*, \dots, f_D^*\}$ that maximizes the expected cash flow of the entire remaining production period. In particular we are interested in the policy starting at $d = 0$, i.e. π_0^* which we can find by solving

$$C_0(x_0, u_0) := \sup_{\pi_0 \in \Pi_0} \mathbb{E}^{(\pi_0)} \left[\sum_{d=0}^D Z_d | X_0 = x_0, U_0 = u_0 \right], \quad (4.11)$$

where Π_0 is the set of all admissible policies starting at $d = 0$ and given start price $X_0 = x_0$ and start operating state $U_0 = u_0$. Again, $\mathbb{E}^{(\pi_0)}[\dots]$ stands for the expectation under the Markov chain that follows the policy π_0 . Next, we want to express this dynamic program via a Bellman iteration. First we simplify the action domain and define it only by the end state $J_d := (J_d^{(1)}, J_d^{(2)}) := (m', k')$ (e.g. (4,0) means shut-down after the last peak hour i.e. 20:00 hrs). It does not only determine the start state and thus the set of allowed schedule candidates for tomorrow (in this example the power plant needs to stay off at least $(t_{\text{off}} - 4)$ more hours), but we can also immediately derive the production schedule and auxiliary variables $(L_d, \beta_d^o, \beta_d^u)$, i.e. the original action space, given today's start state U_d and price vector X_d .

For this purpose we first introduce a nested mixed integer problem (MIP)

$$\begin{aligned}
 Z_d(X_d, U_d, J_d) &= \max_{L_d, \xi_d, \beta_d^u, \beta_d^o} \{(X_d - KI)'L_d - K_u I' \beta_d^u - K_o I' \beta_d^o\} \\
 &\text{subject to:} \\
 L_{\min} \xi_d - L_d &\leq 0 \\
 -L_{\max} \xi_d + L_d &\leq 0 \\
 \Lambda \xi_d &\leq 0 \\
 -I - B \xi_d &\leq 0 \\
 E \xi_d - \beta_d^u &\leq 0 \\
 -E \xi_d - \beta_d^o &\leq 0 \\
 L_d^t &\in \{0\} \cup [L_{\min}, L_{\max}] \\
 \xi_d &:= \xi_d(U_d, J_d) \\
 \xi_d^t, \beta_d^{o,t}, \beta_d^{u,t} &\in \{0, 1\} \\
 t &= -\max\{t_{\text{on}}, t_{\text{off}}\} + 1, \dots, -1, 0, 1, \dots, 24.
 \end{aligned} \tag{4.12}$$

Thus, the daily schedules are linked via the operating state at the beginning U_d and end of the day J_d . Recall that the hourly dispatch L_d is a vector with 24 capacities l_d^t in MW while $Z_d, U_d, L_{\min}, L_{\max}, K, K_u, K_o$ and J_d are scalars, all other variables are vectors. The auxiliary binary variables ξ_d^t encode the operating state of the power plant for each hour (0 not running, 1 running). Note from equation 4.9 that the running index t goes below the 24 hours of a day. Variables ξ_d^t with $t \leq 0$ describe the last operating states of the previous day. In addition the domain of ξ_d is predefined by the start and end states U_d and J_d . For example, if $U_d = (4, 0)$ then $\xi_d^t = 0$ for $t = -3, \dots, 0$. Likewise the hours at the end of the day are preset by J_d

$$\begin{aligned}
 \xi_d^t &\leq 0, & -U_d^{(1)} < t \leq 0 \\
 1 - \xi_d^t &\leq 0, & -U_d^{(2)} < t \leq 0 \\
 \xi_d^t &\leq 0, & 24 - J_d^{(1)} < t \leq 24 \\
 1 - \xi_d^t &\leq 0, & 24 - J_d^{(2)} < t \leq 24.
 \end{aligned} \tag{4.13}$$

The first two constraints in equation 4.12 ensure that the power plant production stays in between the min and max capacities per hour L_{\min} and L_{\max} . An individual row t of the two vector equations looks as follows

$$\begin{aligned}
 L_{\min} \xi_d^t - L_d^t &\leq 0 \\
 -L_{\max} \xi_d^t + L_d^t &\leq 0.
 \end{aligned} \tag{4.14}$$

The third and fourth constraint in equation 4.12 guarantee that the sequence of on and off hours meets the minimum shut-down and running times

$$\begin{aligned}
 \xi_d^t - \xi_d^{t-1} - \xi_d^\tau &\leq 0, & \tau = t + 1, \dots, \min\{t + t_{\text{on}} - 1, T\}, \\
 -1 - \xi_d^t + \xi_d^{t-1} + \xi_d^\tau &\leq 0, & \tau = t + 1, \dots, \min\{t + t_{\text{off}} - 1, T\}, \\
 t &= -\max\{t_{\text{on}}, t_{\text{off}}\} + 2, \dots, 0, 1, \dots, 24.
 \end{aligned} \tag{4.15}$$

Obviously, matrix Λ contains mainly zero values and exactly (-1) twice and (+1) once per row. Figure 4.9 shows the sub matrix of Λ for $t = -10$ and $t_{\text{on}} = 12$. The sub matrix scans the

11 hours after $t = -10$ and forces the associated ξ_d^t to be set to 1 if the prior hour $t-1 = -11$ is set to 0 and the current hour t is set to 1. In this way the minimum running time of 12 hours holds true.

$$\text{Col index: } \mathbf{-11 \ -10 \ 9 \ \dots \ 0 \ 1 \ \dots \ 24}$$

$$\begin{pmatrix} -1 & 1 & -1 & 0 & \dots & 0 \\ \vdots & \vdots & \vdots & \vdots & \vdots & \vdots \\ -1 & 1 & 0 & \dots & 0 & -1 & \dots & 0 \end{pmatrix}$$

Figure 4.9.: Sub matrix of Λ for $t_{\text{on}} = 12$ and $t = -10$

Matrix B has the same structure. The signs are only flipped and the left outermost 1 starts at -7 instead of -11 as $t_{\text{off}} = 8$. The last two constraints in equation 4.12 trigger the start-up and shut-down cost whenever the running state ξ_d^t flips from 0 to 1 (start-up) and vice versa (shut-down)

$$\begin{aligned} \xi_d^t - \xi_d^{t-1} - \beta_d^{u,t} &\leq 0 \\ -\xi_d^t + \xi_d^{t-1} - \beta_d^{o,t} &\leq 0 \\ t &= 1, \dots, 24. \end{aligned} \quad (4.16)$$

Figure 4.10 shows the structure of matrix E for our example with $t_{\text{on}} = 12$ and $t_{\text{off}} = 8$. It

$$\text{Col index: } \mathbf{-11 \ -10 \ 9 \ \dots \ 0 \ 1 \ \dots \ 24}$$

$$\begin{pmatrix} 0 & \dots & 0 & -1 & 1 & \dots & 0 \\ \vdots & \vdots & \vdots & \vdots & \vdots & \vdots & \vdots \\ 0 & \dots & \dots & \dots & 0 & -1 & 1 \end{pmatrix}$$

Figure 4.10.: Matrix E

only contains 0 values and exactly one (-1,1) pair per row.

4.3.1. MIP Reformulation

Let N_s and N_e be the number of operating states at the start and the end of a day, I^1 the number of price scenarios and D the number of production days. Then we need to solve the MIP at maximum $(N_s \times N_e \times I \times D)$ times. This large amount of payoff calculations motivates for a more efficient reformulation of the MIP. Recall from equation 4.12 that the auxiliary vector ξ represents the running mode of the power plant and L_d is the associated volume profile on top of it. For a given operating sequence ξ we can specify the profit maximizing volume profile right away if no energy constraints will be imposed. Operating hours l_d^t that are out of the money will certainly produce at minimum capacity L_{min} whereas in the money hours produce at maximum capacity L_{max} . The start-up and shut-down costs of an individual schedule can therefore be directly derived from M by simply counting the triggers α and β from equation 4.16 multiplied with the corresponding single cost. If we enumerate all possible

¹Do not confuse the max number of scenarios I with the unity vector I .

operation sequences ξ_d as rows in a matrix M , then we can compute the payoff of each schedule via a matrix calculation. We denote with \hat{X}_d not the single price vector X_d , but a matrix that contains *all* scenarios for the same day d in its columns (\hat{X}_d has the size $(24 \times I)$). Then $\hat{X}_d^{(+)}$ sets all negative hours to zero and $\hat{X}_d^{(-)}$ sets all positive hours to zero. Consequently, we can solve all scenarios at the same time with the following equation

$$R_d = M(\hat{X}_d^{(+)} - KI) L_{\max} + M(\hat{X}_d^{(-)} - KI) L_{\min} - (K_u I)' \alpha - (K_o I)' \beta, \quad (4.17)$$

where matrix M is of size $(N \times 24)$ with N being the total number of allowed schedules for a given U_d and J_d (as explained in equation 4.13 the individual operating sequences ξ_d and thus $M := M(U_d, J_d)$ are dependent on the fixed start and end state). Hence, the resulting matrix R_d is of size $(N \times I)$. The maximum vector component r_d^{ni} of column vector R_d^i is the optimal cash flow $Z_d(x_d^i, u_d^i, j_d^i)$ for scenario i and we can write for every i

$$Z_d(x_d^i, u_d^i, j_d^i) = \max_{1 \leq n \leq N} \{r_d^{ni}\}. \quad (4.18)$$

The corresponding row index n determines the row in matrix M that holds the associated best schedule. Running this matrix calculation $(N_s \times N_e)$ -times for all scenarios at once is significantly faster than performing the Simplex algorithm of a solver for every scenario separately.

4.3.2. Bellman Iteration

Now, let us translate equation 4.11 into a Bellman iteration. The generation days $d = 0, \dots, D$ become the decision stages of the program. The states of each stage have two dimensions: the start operating state U_d with m off-line or k running hours until midnight of yesterday and the known price vector X_d . The action set contains all possible end states J_d for the given start state with m' off-line or k' running hours until midnight of today with $m, m' \in \{0, 1, \dots, t_{\text{off}}\}$ and $k, k' \in \{0, 1, \dots, t_{\text{on}}\}$. Again, the value function $C_d^*(X_d, U_d)$ is the value of an option that is newly issued at day d given today's price X_d and the power plant start state U_d . Whereas the continuation value $Q_{d+1}^*(X_d, U_{d+1})$ is the expected option value at $d + 1$ given today's price X_d and tomorrow's start state U_{d+1} . This expectation for the future days is important for the dispatching decision. The dispatcher might accept a lower profit today if this enables him to benefit more from potential profits tomorrow or vice versa to prevent losses. If he expects for instances low prices (e.g. from Friday to the off-peak day Saturday) then today's generation schedule should not end up in an operating state that will force him to produce the next day as well. The transition rule is fairly simple as tomorrow's start state U_{d+1} is identical to today's end state J_d . Then, the dispatcher has to find the sequence of operating *end* states that will maximize his total expected profit. The set of end states \mathbb{J}_d can depend on the start state U_d , in particular for long on- and off-times. In our specific example with $t_{\text{on}} = 12$ and $t_{\text{off}} = 8$, this is not the case. The marginal profit is today's cash flow Z_d whose calculation we discussed in detail in the previous section. Thus, we can express the value

function via the following Bellman iteration

$$\begin{aligned}
 C_d^*(X_d, U_d) &= \max_{J_d} \{ Z_d(X_d, U_d, J_d) + \mathbb{E} [C_{d+1}^*(X_{d+1}, J_d) | X_d] \} \quad 0 \leq d \leq D \\
 \text{state : } (X_d, U_d) \quad U_d &:= (U_d^{(1)}, U_d^{(2)}) := (m, k) \\
 \text{action : } J_d \in \mathbb{J}(U_d) &= \{(1, 0), \dots, (m', 0), (0, 1), \dots, (0, k')\} \\
 J_d &:= (J_d^{(1)}, J_d^{(2)}) := (m', k'), \quad m' := m'(U_d) \quad k' := k'(U_d) \\
 \text{transition : } \{X_d, U_d\} &\longrightarrow \{X_{d+1}, J_d\} \quad \text{i.e. } U_{d+1} = J_d \\
 \text{marginal profit : } &Z_d(X_d, U_d, J_d) \\
 \text{value function : } &C_d^*(X_d, U_d) \\
 \text{continuation value : } &Q_{d+1}^*(X_d, U_{d+1}) := \mathbb{E} [C_{d+1}^*(X_{d+1}, U_{d+1}) | X_d],
 \end{aligned} \tag{4.19}$$

with $C_{D+1}^*(X_{D+1}, U_{D+1}) := 0$. In order to compute the expectation conditional on today's price we also need to define the transition probability. Recall from section 4.2 that our definition of our price process consists of 24 correlated mean reverting prices

$$\begin{aligned}
 \ln x_d^t &= \ln h_d^t + s_d^t \\
 s_d^t &= (1 - \kappa^t) s_{d-1}^t + \sigma_d^t \epsilon, \quad \epsilon \sim N(0, 1),
 \end{aligned} \tag{4.20}$$

with S_d being the vector of the spot price component of the electricity price and s_d^t a single hour within that price vector. h_d^t is the deterministic seasonal shape for hour t at day d and κ^t is the mean reversion rate for hour t . σ_d^t is the volatility for hour t at day d with correlation $\rho_d^{t,\tau}$ to all other $\tau \in \{1, \dots, 24\} \setminus t$ hours in d . For this kind of price process Lucia and Schwartz [47] showed that the random log price components follow conditionally correlated Normal distributions

$$\ln x_{d+1}^t \sim \mathbb{N} \left(\ln h_{d+1}^t + (\ln x_d^t - \ln h_d^t) e^{-\kappa^t}, \frac{(\sigma_d^t)^2}{2\kappa^t} (1 - e^{-2\kappa^t}) \right), \tag{4.21}$$

with $\Delta t = 1$. Like in our basis model for the swing option we need to approximate the continuation value. Again, we apply the Longstaff-Schwartz regression technique and rely on the ACFs which is the sum of all daily cash flows for a single price path following the optimal exercise policy $\{J_s^*\}_{s \geq d}$

$$V_d^*(X_d, U_d) := \sum_{s=d}^D Z_s(X_s, J_{s-1}^*, J_s^*), \tag{4.22}$$

with $J_{d-1}^* := U_d$. According to Longstaff and Schwartz an individual realization of the continuation value $Q_{d+1}^*(x_d^i, u_{d+1}^i)$ is close to the average of all ACFs $v_{d+1}^{*,j}(u_{d+1}^i) := V_{d+1}^*(x_{d+1}^j, u_{d+1}^i)^2$ with realized prices x_{d+1}^j generated from x_d^i according to equation 4.20

$$Q_{d+1}^*(x_d^i, u_{d+1}^i) \approx \frac{1}{J} \sum_{j=1}^J v_{d+1}^{*,j}(u_{d+1}^i). \tag{4.23}$$

The numerical procedure can only approximate from below the optimal continuation value $Q_{d+1}^*(X_d, U_{d+1})$ by $Y_{d+1}(X_d, U_{d+1})$ and the ACF $V_d^*(X_d, U_d)$ by $V_d(X_d, U_d)$. The continuation

²Recall our convention from section 2.1 to use small letters with exponent i for realization of random variables.

value will be approximated with a linear combination of basis functions

$$Y_{d+1}(X_d, J_d) := Y_{d+1}(X_d, J_d^{(n)}) := \Psi_{n,d+1}(X_d)' \alpha_{n,d+1}, \quad (4.24)$$

with $n = 1, \dots, N$ valid end states $J_d^{(n)}$ and vectors $\Psi_{n,d+1}$ and $\alpha_{n,d+1}$ have length R . The relevant coefficients $\alpha_{n,d+1,r}$ for the basis functions $\Psi_{n,d+1,r}$ with $r = 1, \dots, R$ will be computed by regressing the pairs $(X_d, V_{d+1}(X_{d+1}, U_{d+1}))$. Note that at each stage d the regression needs to be performed N -times (i.e. for each possible end state separately). This is similar to our swing option where we have to run the regression separately for each exercise right and day (see equation 2.6). Once, we have approximated the continuation value with a functional description Y_{d+1} we are able to approximate the best action J_d^* via \hat{J}_d^* which we then use to update $V_d(X_d, U_d)$ from $V_{d+1}(X_{d+1}, U_{d+1})$

$$\begin{aligned} \hat{J}_d^* &:= \arg \max_{J_d} \{Z_d(X_d, U_d, J_d) + Y_{d+1}(X_d, J_d)\} \\ V_d(X_d, U_d) &\approx Z_d(X_d, U_d, \hat{J}_d^*) + V_{d+1}(X_{d+1}, \hat{J}_d^*). \end{aligned} \quad (4.25)$$

We iterate until the first stage ($d=0$) and then can approximate the actual option value $C_0^*(x_0, u_0)$ by $C_0(x_0, u_0)$ with the average over $i = 1, \dots, I$ realizations of the approximated ACF

$$C_0(x_0, u_0) \approx \frac{1}{I} v_0^i(u_0). \quad (4.26)$$

The analysis of appropriate basis functions $\Psi_{n,d+1,r}(X_d, J_d)$ is more complex compared to our previous swing option model. We cannot simply set again the basis function identical to the price, e.g. $\Psi_{n,d+1,r}(X_d, J_d) = X_d$, and look at polynomials of different degrees. X_d is not a single price any more, but a price vector with 24 components. Already a quadratic approximation would result in more than 48 parameters to estimate if we used all vector components for the regression. This is certainly not feasible and instead requires a simpler representation of the price vector that would suit well for the regression. A popular method is the principal component analysis (PCA) which, generally speaking, aggregates the characteristics of original observations into artificial new factors by preserving the original information represented by its variance-covariance structure. In the following section we will use this tool in order to define our vector of basis functions $\Psi_{n,d+1,r}$.

4.3.3. Principal Component Analysis

The principal component analysis is a sub field of factor analysis whose main objective is to reduce the dimensionality of a multi-scale data set. In our case there are price vectors with 24 components. The principal component analysis achieves the reduction by combining the different dimensions $t = 1, \dots, T = 24$ of the original data set via a linear combination to new artificial factors a_1, a_2, \dots, a_M (for readability we use capital letters for vectors X , small letters for vector components x_t and small letters with a sub-index represent realizations of a random component x_t^i). For instance, hour t of our first realization of price vector X_d (from now on we skip the sub index d indicating the day) would be translated to

$$x_t^1 := \gamma_{1t} a_1^1 + \gamma_{2t} a_2^1 + \dots + \gamma_{Mt} a_M^1. \quad (4.27)$$

The previous equation is always true for $M = T$. In matrix form we can also write

$$X := A \cdot \Gamma'$$

$$\begin{pmatrix} x_1^1 & \dots & x_T^1 \\ \vdots & & \vdots \\ x_1^N & \dots & x_T^N \end{pmatrix} := \begin{pmatrix} a_1^1 & \dots & a_T^1 \\ \vdots & & \vdots \\ a_1^N & \dots & a_T^N \end{pmatrix} \cdot \begin{pmatrix} \gamma_{11} & \dots & \gamma_{M1} \\ \vdots & & \vdots \\ \gamma_{1T} & \dots & \gamma_{MT} \end{pmatrix}', \quad (4.28)$$

with $X_t = (x_t^1 \dots x_t^N)'$ being a column vector representing all realizations for component m . A is called the factor matrix while F contains the so called *factor loadings* with $\Gamma_m = (\gamma_{m1} \dots \gamma_{mT})'$ being the loading vector for hour t . Technically Γ is a rotation matrix that twists the coordinate system such that the expansion of data points X concentrates on a smaller number of axes (dimensions). A is then the representation of X with respect to the new coordinate system. Finding the best rotation matrix Γ leads to an Eigenvalue calculation which we do not want to derive here in detail. We refer to Überla [64] for a detailed derivation. It is important to note that the information content is the same before and after the rotation as the trace of both variance-covariance matrices for Ω_X and Ω_A match

$$\text{trace}(\Omega_X) = \text{trace}(\Omega_A)$$

$$\text{trace}\left(\frac{1}{N}(X - \bar{X})'(X - \bar{X})\right) = \text{trace}\left(\frac{1}{N}(A - \bar{A})'(A - \bar{A})\right). \quad (4.29)$$

While the diagonal of Ω_X contains the volatilities of the individual hours, the diagonal of Ω_A represents the volatilities of the new synthetic factors. If the PCA is successful then trace of Ω_A will have a lot of values close to 0 that carry no more information. Hence, the best rotation matrix will have the smallest amount of non-zero components in the diagonal to make up the trace. These remaining volatilities represent the highest density of information and make the remaining factors negligible. Table 4.4 provides the results for our PCA analysis. We analyzed three different representations of our electricity price separately for weekday and

$\epsilon_d (WD)$	A_1	A_2	A_3	A_4	A_5	A_6	A_7	A_8	A_9	A_{10}	A_{11}	A_{12}
$S_d (WD)$	0.45	0.64	0.82	0.87	0.89	0.91	0.93	0.94	0.95	0.96	0.97	0.98
$X_d (WD)$	0.51	0.74	0.82	0.88	0.91	0.93	0.95	0.96	0.97	0.97	0.98	0.98
$\epsilon_d (WE)$	0.74	0.92	0.95	0.97	0.98	0.99	0.99	0.99	0.99	1	1	1
$S_d (WE)$	0.64	0.79	0.84	0.88	0.91	0.93	0.95	0.96	0.97	0.97	0.98	0.98
$X_d (WE)$	0.63	0.77	0.83	0.88	0.91	0.93	0.95	0.96	0.97	0.97	0.98	0.98
	0.83	0.89	0.94	0.95	0.96	0.97	0.98	0.98	0.99	0.99	0.99	0.99
$\epsilon_d (WD)$	A_{13}	A_{14}	A_{15}	A_{16}	A_{17}	A_{18}	A_{19}	A_{20}	A_{21}	A_{22}	A_{23}	A_{24}
$S_d (WD)$	0.98	0.98	0.99	0.99	0.99	0.99	1	1	1	1	1	1
$X_d (WD)$	0.99	0.99	0.99	0.99	0.99	1	1	1	1	1	1	1
$\epsilon_d (WE)$	1	1	1	1	1	1	1	1	1	1	1	1
$S_d (WE)$	0.99	0.99	0.99	0.99	1	1	1	1	1	1	1	1
$X_d (WE)$	0.99	1	1	1	1	1	1	1	1	1	1	1

Table 4.4.: Percentage of the total variance explained by the new factors.

weekend prices which make up the six rows of the table. The columns represent the synthetic factors (the table is split after 12 factors). The first row investigates the log returns ϵ_d on weekdays. Recall from equation 4.1 that these are the log returns after extracting the mean reversion factor κ . The second row looks at the same matrix for the de-seasonalised (log)

prices S_d according to equation 4.2. The third row works directly with the weekday price X_d . The remaining three rows repeat the same analysis for weekend prices. We look at the last 60 weekdays and 30 weekends respectively as this time frame is agreed by practitioners to be an adequate horizon for the volatility calculation. The actual table cells contain the cumulative sum of the diagonal of matrix Ω_A up to m divided by the entire trace

$$A_m := \frac{\sum_{t=1}^m \sigma_{tt}^2}{\sum_{t=1}^{24} \sigma_{tt}^2}, \quad (4.30)$$

with σ_{tt}^2 being the t -th entry of the diagonal of Ω_A . Hence, the table cells show us the percentage of the total volatility covered until factor A_m . For instance, column "A1" states that the first principal component covers between 45 % to 74% of the total variance of the weekday price vector if we rely on either ϵ_d, S_d or X_d . In general we can state that the first five factors cover already 90 % of the entire information. Even more surprising is the fact that the PCA performs best on the full price X_d including the seasonality. While the seasonal pattern is an explained deterministic deviation and therefore formally must not enter the actual volatility calculation it obviously helps to describe the characteristic of each price component and hence to find an alternative condensed representation. The first principal component based on X_d covers already 74 % respectively 83 % of the entire fluctuation. An astonishing result that we will make use of in a later section.

The PCA framework enables us to drill down even further and explain the amount of information that the new factors A_m carry of each original price component. We can represent the covariance of pairwise price dimensions by the sum of the product of appropriately standardized factor loadings $\tilde{\Gamma}$ (so called *fundamental theorem of factor analysis*)

$$\Omega_X = \Gamma \Omega_A \Gamma' = \tilde{\Gamma} \tilde{\Gamma}', \quad (4.31)$$

with $\tilde{\Gamma} = \Gamma \sqrt{\Omega_A}$. The columns of $\tilde{\Gamma}$ represent the initial price components and the rows stand for the new artificial factors. For z -transformed prices ($\tilde{X}_d^t = (X_d^t - \bar{X}_d^t) / S_d^t$) with \bar{X}_d^t being the average of all price scenarios of hour t at day d and S_d^t the associated standard deviation, the sum of the squares along a column in $\tilde{\Gamma}$ is the variance of the corresponding price component which by definition is 1. Hence, cutting this sum after M factors returns a number k_{Mt}

$$k_{Mt} := \sum_{m=1}^M \tilde{\gamma}_{mt}^2 \quad t = 1, \dots, T \quad (4.32)$$

which is between 0 and 1 and can be interpreted as the percentage of the total information of the price at hour t that is passed on to the first M principal components a_1, \dots, a_M . Alternatively, we can look at the correlation r_{mt} between a factor a_m and the individual price hour x_d^t to assess the contribution of an individual hour to a specific principal component (again we neglect index d)

$$r_{mt} := \tilde{\gamma}_{mt} := \frac{\frac{1}{N} \sum_{n=1}^N (x_t^n - \bar{x}_t)(a_m^n - \bar{a}_m)}{\sigma_X \sigma_A} \quad t = 1, \dots, T \quad m = 1, \dots, M, \quad (4.33)$$

with σ_X, σ_A respectively, being the square root of the diagonal of the variance-covariance matrix Ω_X and Ω_A . The previous equation states that the factor loadings $\tilde{\gamma}_{mt}$ for z -transformed input data are identical to these correlations. Table 4.5 presents the correlations and their squares for the first three principal components of the factor loadings that we derived from the price X_d directly. The first six columns show the results for weekday, the last six columns for weekend prices ($\nu := \gamma(WE)$). The squared numbers allow for computing k_{t1} to

H	γ_{1t}	γ_{2t}	γ_{3t}	γ_{1t}^2	γ_{2t}^2	γ_{3t}^2	ν_{1t}	ν_{2t}	ν_{3t}	ν_{1t}^2	ν_{2t}^2	ν_{3t}^2
1	0.79	-0.49	0.25	0.63	0.24	0.06	-0.76	-0.48	0.16	0.58	0.23	0.02
2	0.80	-0.52	0.12	0.64	0.27	0.02	-0.76	-0.57	0.19	0.57	0.33	0.04
3	0.74	-0.57	0.19	0.55	0.32	0.03	-0.71	-0.64	0.17	0.50	0.41	0.03
4	0.69	-0.60	0.22	0.48	0.36	0.05	-0.71	-0.64	0.17	0.50	0.41	0.03
5	0.74	-0.49	0.19	0.55	0.24	0.04	-0.76	-0.52	0.19	0.58	0.27	0.04
6	0.88	-0.29	0.03	0.78	0.09	0.00	-0.91	-0.04	0.30	0.82	0.00	0.09
7	0.85	-0.13	-0.20	0.73	0.02	0.04	-0.90	0.25	0.24	0.81	0.06	0.06
8	0.92	-0.07	-0.12	0.85	0.00	0.01	-0.88	0.36	0.21	0.78	0.13	0.04
9	0.90	-0.03	-0.26	0.82	0.00	0.07	-0.92	0.29	0.15	0.85	0.09	0.02
10	0.94	0.16	-0.15	0.88	0.03	0.02	-0.93	0.26	0.06	0.86	0.07	0.00
11	0.94	0.14	-0.11	0.88	0.02	0.01	-0.92	0.26	-0.01	0.84	0.07	0.00
12	0.92	0.17	-0.16	0.85	0.03	0.03	-0.86	0.32	-0.04	0.73	0.10	0.00
13	0.94	0.26	-0.03	0.89	0.07	0.00	-0.93	0.23	-0.10	0.86	0.05	0.01
14	0.95	0.23	-0.09	0.90	0.05	0.01	-0.91	0.28	-0.02	0.83	0.08	0.00
15	0.89	0.24	-0.20	0.80	0.06	0.04	-0.93	0.31	0.04	0.87	0.09	0.00
16	0.90	0.34	-0.16	0.82	0.12	0.03	-0.93	0.31	0.10	0.86	0.10	0.01
17	0.77	0.55	0.30	0.59	0.30	0.09	-0.93	0.27	0.06	0.87	0.07	0.00
18	0.57	0.57	0.59	0.32	0.32	0.35	-0.94	0.19	-0.03	0.89	0.03	0.00
19	0.68	0.50	0.51	0.47	0.25	0.26	-0.76	-0.04	-0.45	0.58	0.00	0.20
20	0.88	0.01	-0.26	0.78	0.00	0.07	-0.77	-0.09	-0.49	0.59	0.01	0.24
21	0.93	0.15	-0.14	0.86	0.02	0.02	-0.91	-0.07	-0.23	0.82	0.01	0.05
22	0.85	0.03	-0.16	0.72	0.00	0.02	-0.86	-0.13	-0.23	0.74	0.02	0.05
23	0.88	-0.08	0.10	0.78	0.01	0.01	-0.74	-0.39	-0.33	0.54	0.15	0.11
24	0.78	-0.22	0.12	0.60	0.05	0.01	-0.79	-0.42	-0.18	0.62	0.17	0.03

Table 4.5.: Contained information and correlation of the first three principal components with respect to each individual hour by weekday and weekend

k_{t3} according to equation 4.32. Hence, summing up columns 5 to 7 or 10 to 12 for the same row tells us the percentage of the total information of hour t that is covered by the first up to the third principal component. For example, we see that factor 1 covers 63 % of hour 1 of a weekday, factor 1 and 2 together explain already 87 % and factor 3 adds another 6 % to the overall deviation of hour 1. Analyzing the entire column of γ_{1t}^2 we see that the first component covers best hours 8 to 16 on weekdays and 6 to 18 on weekends with more than 80 % contribution. The second factor mainly describes the morning hours with more than 24 % contribution while factor 3 captures hour 18 and 19 on weekdays (35 % and 26 %) and hour 19 and 20 on weekends (20 % and 24 %). If we move on to the correlations we observe that the first principal component is highly positively correlated with all weekday hours and highly negatively correlated with all weekend hours. The second component already reveals a far less strong correlation and flips the sign during off-peak hours on weekdays and peak hours on weekends. If we recall the relationship between base, peak and off-peak hours from equation 4.7 then we could interpret factor 1 as a base price and factor 2 as a peak, respectively off-peak price representation.

4.3.4. Numerical Results

Now, let us continue with our Bellman iteration from section 4.3.2. We stopped at the description of the basis functions for the Longstaff-Schwartz regression. The PCA results allow us to replace our 24 dimensional price vector X_d with a small number of principal components (PC) a_m . To be precise we use their rotation functions to define our basis functions in vector $\Psi_{n,d}(X_d, J_d)$. In a first step we want to find the exact number of necessary PC for our specific power plant example from section 4.1. We run a quadratic approximation for the first 4 principal components. Let us illustrate the approximation for the first two PC (for readability we skip the day index d on the right side of the equations: e.g. $a_1^i := a_{d,1}^i$ and $\alpha_{0,n} := \alpha_{d+1,0,n}$)

$$\begin{aligned} \Psi'_{n,d+1}(X_d, J_d) &= \Psi'_{n,d+1}(X_d) = (1 \ a_1 \ a_2 \ a_1^2 \ a_1 a_2 \ a_2^2) \\ Y_{d+1}(X_d, J_d) &= \Psi'_{n,d+1}(X_d) \alpha_{d+1} \\ &= \alpha_{0,n} + \alpha_{1,n} a_1 + \alpha_{2,n} a_2 + \alpha_{11,n} (a_1)^2 + \alpha_{12,n} a_1 a_2 + \alpha_{22,n} (a_2)^2 \quad (4.34) \\ a_m &= \sum_{t=1}^{24} \gamma_{mt} X_d^t \quad m = 1, 2 \end{aligned}$$

with X_d^t being the t -th hour of random vector X_d . We use the factor loadings γ_{mt} that we derived directly from the prices (see Table 4.5) as they reduced the dimensionality most efficiently. Dependent on whether d is a weekday or weekend we apply the corresponding factor loadings γ_{mt} or ν_{mt} . Again, the sub index n of parameters $\alpha_{.,n}$ stands for the currently selected end operating state $J_d^{(n)}$. We find the α_{d+1} -parameters by regressing on the pairs $(X_d, V_{d+1}(X_d, J_d^{(n)}))$ separately for each $J_d^{(n)}$. Table 4.6 presents the valuation results for our power plant with the parameter profile presented in section 4.1. Similar to our swing option examples in the previous chapter we want to compute the real option value for an itm, atm and otm situation. The off-peak and peak Forward price for March 08 is 50.59 EUR and 71.85 EUR respectively. Hence, we choose the strikes $K = 50, 70$ and 90 EUR to reflect the three different scenarios. For each strike we run the LS quadratic approximation according to equation 4.34 for the very first and up to the first four PC separately. Hence, every four rows in Table 4.6 build one block where each block represents an itm, atm or otm situation. We assume that the power plant was already running at least 12 hours at midnight on 1-Mar-08 i.e. the start state is $(0,12)$. The first column presents the value $C_0 := C_0(x_0, u_0)$ for the

stochastic optimization as outlined in equation 4.11. The fact that the option values are so

C_0	C_0^s	$C_0^{0.95}$	C_0^f	C_0^{PFC}	C_0^F	$C_0^{(L622)}$	$C_0^{(L723)}$	$C_0^{(L024)}$
4.406	4.760	4.405	4.492	3.968	3.072	4.019	4.053	4.251
4.407	4.760	4.406						
4.407	4.761	4.401						
4.408	4.761	4.407						
1.188	1.423	1.185	1.203	0.463	0.184	1.156	1.143	0.139
1.188	1.423	1.185						
1.188	1.423	1.185						
1.188	1.423	1.185						
0.209	0.336	0.205	0.210	0	0	0.205	0.203	<0
0.209	0.336	0.205						
0.209	0.336	0.205						
0.209	0.336	0.205						

Table 4.6.: Value of the Power Generation for March 08 in mio EUR.

close to each other no matter whether we use one or four PCs is remarkable. Even when changing the strike which will change the shape of the ACF the values almost match for all four PC settings. From Table 4.4 we know that the first PC explains 74 % of the weekday and 83 % of the weekend deviations and apparently that is sufficient for the LS regression. Recall that the LS regression only provides a lower bound of the real option value. In order to assess the quality of this lower bound, we provide an upper bound as well. Due to the complexity of the real option model we cannot present a primal-dual approach as discussed in chapter 1 and rather rely on the option value based on the full information $C_0^f := C_0^f(x_0, u_0)$ i.e. all prices are known in advance. Hence, there is no uncertainty about the future any more and we can adjust the generation schedule such that it takes advantage of every price situation. Formally, the continuation value will be replaced by the actual subsequent ACF for the specific price path (path-wise optimization). Hence, the stochastic optimization becomes deterministic. In equation 4.19 we can remove the continuation value and replace the Bellman equation with

$$\begin{aligned}
 V_d^f(X_d, U_d) &:= \max_{J_d} \left\{ Z_d(X_d, U_d, J_d) + V_{d+1}^f(X_{d+1}, J_d) \right\}, \\
 C_0^f(x_0, u_0) &\approx \frac{1}{I} \sum_{i=1}^I v_0^{f,i}(u_0).
 \end{aligned} \tag{4.35}$$

In particular, no more principal components are required. Like for C_0 we compute the option value for the operating state at the first delivery day $u_0 = (0, 12)$. Then the option value $C_0^f := C_0^f(x_0, u_0)$ is the average of the individual ACFs $v_0^{f,i}(u_0)$ that all start from the same initial price x_0 and start state u_0 . The figures for C_0^f in Table 4.6 are only slightly higher than the stochastic option values C_0 . The difference is almost negligible. This observation in conjunction with our previous statement about the small impact of the number of PCs lets us assume that our stochastic model achieves already good results with the first PC only. At least in average $V_d(X_d, U_d)$ and $V_d^f(X_d, U_d)$ are close to each other. We will investigate in sections 4.5 whether that is also true for the individual scenario values when we will take a closer look at the distributions. The itm situation for $K = 50$ EUR can give us a first indication. The power plant is always profitable and produces a flat schedule. Then the value fluctuation of $V_d(X_d, U_d)$ is only driven by the price. Recall that the price scenarios are normalized and mean-reverting. Both effects should keep the price scenarios close to the Forward price. If that is true then the option value should not differ much from a deterministic valuation

with the Forward price and hourly adjusted Forward price only. We find those values in the 4th and 5th column of Table 4.6. The valuation is identical to equation 4.35 except for the simplification that we have only one single price path, either the PFC $\{h_d\}_d$ with its day type patterns (see equation 4.3) or the mere Future price $G_0 = g_0$

$$\begin{aligned}
 V_d^G &:= V_d^G(g_0, U_d) := \max_{J_d} \left\{ Z_d(g_0, U_d, J_d) + V_{d+1}^G(g_0, J_d) \right\} \\
 C_0^G &:= C_0^G(g_0, u_0) := V_0^G(g_0, u_0) \\
 V_d^{PFC} &:= V_d^{PFC}(h_d, U_d) := \max_{J_d} \left\{ Z_d(h_d, U_d, J_d) + V_{d+1}^{PFC}(h_{d+1}, J_d) \right\} \\
 C_0^{PFC} &:= C_0^{PFC}(h_0, u_0) := V_0^{PFC}(h_0, u_0).
 \end{aligned} \tag{4.36}$$

Both values C_0^G and C_0^{PFC} are deterministic and represent the intrinsic value of the option. The difference $(C_0 - C_0^{PFC})$ is therefore the time value of the real option. It is only about 10 % of the intrinsic value for the itm situation which underlines that the normalization and mean-reversion keeps the price scenarios close to the Forward price. The time value becomes larger for the other two strikes since the flexibility in the schedules will additionally contribute to the option value C_0 . The following two figures illustrate these schedule variations. Figure 4.11 shows the production based on the Forward price g_0 and the PFC $\{h_d\}_d$ for the first week in March 08. The off-peak price is 51.59 EUR and therefore the power plant will always

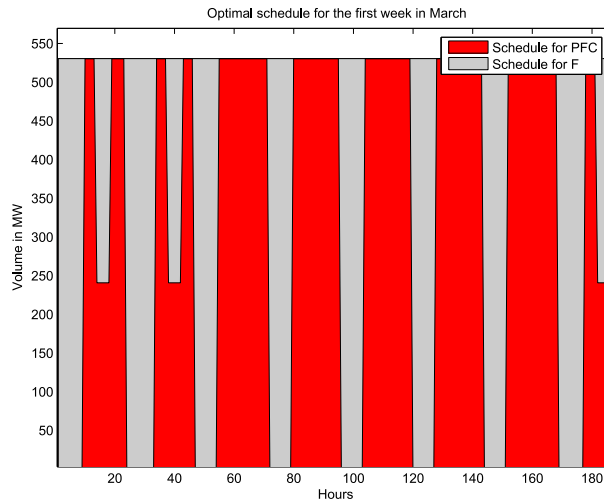


Figure 4.11.: The optimal schedules for the Future price and hourly PFC

produce for a strike of 50 EUR and indeed the grey production area shows full capacity of 530 MW for all hours. The red area shows the optimal schedule for the PFC. Recall from Figure 4.8 that the shaped price usually goes below the off-peak price in morning hours and thus below our strike of 50 EUR. We can see that the power plant turns off during those early morning hours and create 7 production blocks representing the 7 days of the week. The first two blocks stand out with their double-peak structure. 01-March 08 is a Saturday. Obviously, there are some afternoon hours during the weekend that go below the strike. But as the power plant is not able to turn off due to the minimal run-time it can only minimize the loss by running on minimum capacity. The other hours over-compensate that loss which explains why the power plant does not shut-down completely. Overall the hourly PFC returns a 30 % higher production value than the valuation with the flat price band curve (3 mio vs. 3.9 mio

EUR).

Figure 4.12 illustrates the impact of the power plant's flexibility even better. We see the optimal schedules for two selected price scenarios. The timeline is trimmed to the actual production hours for these two price scenarios. The figure shows how itm hours trigger the

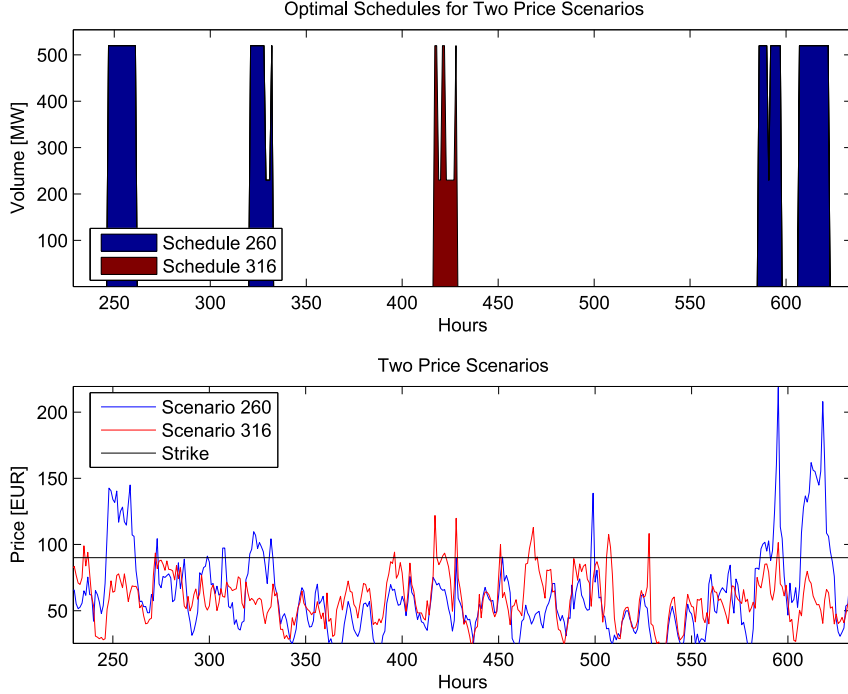


Figure 4.12.: The optimal schedules for two specific price scenarios.

production. Apparently only the double peak structure around hour 425 is long enough above the strike to turn on the plant at least once for scenario 316. For scenario 260 this is more often the case. Figure 4.12 also demonstrates that even though the schedules vary in their quantity profile and thus total energy generation, single generation blocks look similar (in this example 12 hours on-time during peak hours). They are only pieced together in various different ways. For this reason it is no surprise that a comparison of the schedules underlying each cash flow $V_0(x_0, u_0)$ reveal only a limited number of relevant actions J_d . A classical peak schedule for instance will always pick $J_d = (4, 0)$ i.e. shutting down after the last peak hour 20:00. So, across all D days and I scenarios we counted the number of schedules for each \hat{J}_d^* . We ordered them in declining sequence and took as many J_d^* until 95 % of all $I \cdot D = 30000$ schedules were covered. Equation 4.37 shows the resulting sets $\mathbb{J}^{0.95}$ for each strike. The corresponding option values are presented in column 3 of Table 4.6. Note that $C_0^{0.95}(x_0, u_0)$ is still a stochastic optimization problem according to equation 4.19, but with a significantly reduced action set

$$\begin{aligned}
 C_d^{0.95}(X_d, U_d) &:= \max_{J_d \in \mathbb{J}^{0.95}(K)} \left\{ Z_d(X_d, U_d, J_d) + \mathbb{E}[C_{d+1}^{0.95}(X_{d+1}, J_d) | X_d] \right\} \\
 \mathbb{J}^{0.95}(K = 50) &:= \{(2, 0), (3, 0), (4, 0), (8, 0), (0, 6), (0, 12)\} \\
 \mathbb{J}^{0.95}(K = 70) &:= \{(1, 0), (2, 0), (3, 0), (4, 0), (8, 0), (0, 12)\} \\
 \mathbb{J}^{0.95}(K = 90) &:= \{(3, 0), (4, 0), (8, 0)\}.
 \end{aligned} \tag{4.37}$$

For $K = 50$ and $K = 70$ $\mathbb{J}^{0.95}$ contains only 5 and 6 actions respectively, for $K = 90$ we even observe only 3 relevant actions. The resulting error $C_0 - C_0^{0.95}$ of this simplification is almost negligible throughout all three strikes. The performance improvement on the other hand is significant considering that the computation time increases nearly linearly with the number of states. Hence, reducing the number of states to less than a quarter means the same reduction in computation time.

This small approximation error motivates an even stronger simplification. If we compare the three reduced action sets $\mathbb{J}^{0.95}(K)$, $K = 50, 70, 90$, we recognize that they share the actions $\{(3,0),(4,0),(8,0)\}$. $J_d = (8,0)$ indicates that the power plant is turned-off for at least 8 hours. If the power plant is turned off at the latest at 16:00 then it is more than likely that the price scenario for the entire day is otm and thus we can assume that end state (8,0) stands for no production during the whole day. $J_d = (3,0)$ and $(4,0)$ represent schedules that end at hour 20:00 or 21:00. Not surprisingly this is exactly the border between peak and off-peak. Obviously, peak schedules (starting around 8:00 and ending around 20:00) are relevant as well. For atm and itm situations $J_d = (0,12)$ is also an important schedule. This end state represents a full production day. If the plant runs for at least 12 hours until midnight, then it is very likely that it runs already the whole day. (0,12) and (8,0), i.e. full/no production, are especially important for weekends where there are no extra peak prices. Then, we usually have full production if the off-peak price is above K . Otherwise there is no production at all. If we recall from section 4.3.1 the notion of separating a schedule in its operating sequence (0 = off, 1 = on) and volume profile then on-time during peak hours, complete shut-down and full run-time are the most likely candidates that make up an optimal (close to optimal) production policy. If we define a group of those schedule candidates, i.e. 0-1 row vectors with 24 components, $\mathbb{L} = \{(0\dots01\dots10000), (0\dots01\dots1000), \dots\}$ that can be mutually concatenated in all variations without violating t_{on} and t_{off} , then we can eliminate completely the operating states U_d and J_d . Consequently we can simplify our MIP from $Z_d(X_d, U_d, J_d)$ to $\mathbb{L}Z_d(X_d)$. The new optimization problem is identical to equation 4.12 except for a single change where we replace $\xi_d := \xi_d(U_d, J_d)$ by $\xi_d \in \mathbb{L}$

$$\begin{aligned} \mathbb{L}Z_d(X_d) &= \max_{L_d, \xi_d, \beta_d^u, \beta_d^o} \{(X_d - KI)'L_d - K_u I' \beta_d^u - K_o I' \beta_d^o\} \\ \text{subject to:} \\ L_{\min} \xi_d - L_d &\leq 0 \\ -L_{\max} \xi_d + L_d &\leq 0 \\ E\xi_d - \beta_d^u &\leq 0 \\ -E\xi_d - \beta_d^o &\leq 0 \\ L_d^t &\in \{0\} \cup [L_{\min}, L_{\max}] \\ \xi_d &\in \mathbb{L} \\ \xi_d^t, \beta_d^{o,t}, \beta_d^{u,t} &\in \{0, 1\} \\ t &= 1, \dots, 24. \end{aligned} \tag{4.38}$$

By restricting ξ_d to be a member of \mathbb{L} we can skip the constraints with matrix Λ and B in equation 4.15 that verify the on- and off-times. Likewise we can reduce the running index t to the 24 hours of the current day. Furthermore the dynamic program including the estimation of the continuation value will be replaced by a sequence of daily MIPs. The sum of these local optima is the overall optimal solution for a single price path and we average all price

paths to receive the actual real option value

$$\begin{aligned}\mathbb{L}V_0(x_0) &:= \sum_{d=0}^D \mathbb{L}Z_d(X_d) \\ \mathbb{L}C_0(x_0) &:= \mathbb{E}[\mathbb{L}V_0(X_0)|X_0 = x_0].\end{aligned}\tag{4.39}$$

Column 7 to 9 of Table 4.6 provide the asset values for this approach using three different schedule sets. The label $\mathbb{L} = L622$ stands for all schedules that start at 6 in the morning and end at the latest at 22:00 in the night. Likewise $L723$ contains all schedules between 7:00 and 23:00 and $L024$ consists of only two schedules that are full or no production. All schedules within each of the three subsets can be combined arbitrarily since the minimum off-time of 8 hours is always guaranteed. For the itm scenario full production is certainly a frequently used schedule. For this reason $L024$ returns the smallest error for $K = 50$ ($C_0(L024) = 4.2$ mio EUR vs. $C_0 = 4.4$) mio EUR). The situation changes for $K = 70$ and $K = 90$. Once turned on $L024$ forces to run the power plant the entire day i.e. also during the off-peak hours after 20:00. These hours are usually below the strike which let the other two sets prevail over $L024$. Hence, making the preselection of schedule candidates dependent on the strike (using $L024$ for $K = 50$ and $L622$, $L723$ for $K = 70$ and $K = 90$) is important in order to receive good results. Then, at least in our example, the heuristic produces only an error of less than 5 % compared to the proper stochastic real option value C_0 (for $K = 70$ and $K = 90$ it is even only around 1 %). At the same time it is several times faster than the stochastic program as it reduces the state space by one dimension (J_d) and allows for a local optimization. We will therefore rely on this heuristic in the next section when we introduce an energy constraint to our model. Finally, we want to mention the option value C_0^s which represents a swing option with 744 hourly exercise rights, one for each delivery hour (see our basic model in section 2.6 for the exact definition). Obviously this column returns the highest asset value since it ignores any physical constraint. The difference ($C_0^s - C_0 \approx 0.36$ mio EUR) represents the financial gain through additional technical flexibility. In our example the additional value of flexibility stands for 6 %, 16 % and 38 % of the power plant value C_0 with $K = 50, 70$ and 90 EUR. Hence, the higher the initial marginal production costs K of the power plant the more beneficial a technical upgrade of a power plant will be and the sooner such an investment will amortize.

4.4. Valuation with Energy Constraint

In this section we want to additionally introduce a maximum production of W_0 to our power plant model. Compared to our model in equation 4.11 we therefore introduce the constraint W_d to our definition of the action space in equation 4.10. It stands for the remaining energy from the current day d to the end of the production period D

$$A(U_d, W_d) := \left\{ (L_d, \beta_d^o, \beta_d^u) \left| \begin{array}{l} \sum_{s=d}^D I' L_s \leq W_d, \\ L_d \in \mathbb{L}_{\text{on,off}}(U_d), \\ \mathbb{I}_{L_d^{t-1} > 0} - \mathbb{I}_{L_d^t > 0} - \beta_d^{o,t} \leq 0, \quad \beta_d^{o,t} \in \{0, 1\}, \\ -\mathbb{I}_{L_d^{t-1} > 0} + \mathbb{I}_{L_d^t > 0} - \beta_d^{u,t} \leq 0, \quad \beta_d^{u,t} \in \{0, 1\} \end{array} \right. \right\}, \tag{4.40}$$

with I being the unity vector, i.e. $(1, 1, \dots, 1)'$, and \mathbb{I} being the indicator function. We also need to extend our state space by the energy amount W_d . Consequently our decision rule will be extended as well to $(X_d, U_d, W_d) \xrightarrow{f_d} (L_d, \beta_d^u, \beta_d^o) \in A(U_d, W_d)$. We define an admissible policy as a sequence of valid decision rules $\pi_d := \{f_d, \dots, f_D\}$. Again, we look for the optimal

policy π_0^* that maximizes the expected profit for the entire production period

$$C_0(x_0, u_0, \mathcal{W}_0) = \sup_{\pi_0 \in \Pi_0} \mathbb{E}^{(\pi_0)} \left[\sum_{d=0}^D Z_d \left| \begin{array}{l} X_0 = x_0, \\ U_0 = u_0, \\ W_0 = \mathcal{W}_0 \end{array} \right. \right], \quad (4.41)$$

with Z_d as defined in equation 4.8 and Π_0 is the set of all valid policies at the beginning of the production period. As before $\mathbb{E}^{(\pi_0)}[\dots]$ stands for the expectation under the Markov chain that follows the policy π_0 . Again, we want to translate this dynamic program into a Bellman iteration. In our previous model without energy constraints we were able to reduce the action set to the end operating state J_d only and could still find the relevant daily production schedule L_d . Now, our additional energy constraint requires to track the energy contribution of the daily schedule as well that we denote with w_d . Note that w_d is the *actual* day production whereas W_d ³ is the maximum total *available* energy amount for the remaining period d to D . Then the extended model resembles a storage optimization problem. Similar to a storage or gold mine where the manager needs to extract the resource according to the fluctuating market price, our dispatcher also needs to allocate his limited energy amount across the production days in order to maximize the overall profit. But different to a storage problem we still have to additionally consider the intra-day production plan, i.e. the daily schedules are still linked by the daily running end states J_d . Hence, for a given start state U_d and price X_d we can retrieve L_d for any chosen pairs (J_d, w_d) . Also note that W_d is a continuous variable. Thus w_d is also continuous and the daily maximum profit becomes a continuous function Z_d as well. A straightforward approach would discretize w_d^* and W_d . The domain space of W_d , however, can be large, especially for longer production periods like a year. This would require to compromise on the grid size for W_d to keep the model numerically tractable. On the other hand this can lead to imprecise results. With EEX peak prices of up to 100 EUR/MWh only small inaccuracies in the generation amount can already lead to significant changes in the production value. Therefore we rather decide to keep the energy amount continuous and approximate the continuous function. We still calculate Z_d at fixed energy grid points w^r , $r = 1, \dots, R$, but fit those points to a polynomial continuous function.

This is where we want to reuse our MIP from equation 4.12. Formally, we need to extend the search domain of our MIP in equation 4.12 by another dimension for the energy amount which we denote with w , i.e. $Z_d(X_d, U_d, J_d, w)$. As we want w_d^* to be the optimal *actual* energy usage we could define w to be a *mandatory* energy production. However, this can lead to less profitable cash flows. For instance we could force to produce during otm hours only for meeting the fixed energy production. Instead, we want to focus on the maximum cash flow. For this reason we define w only as the *upper* daily energy constraint. At the same time we reduce again the search domain by eliminating the start and end operating state U_d and J_d . As we have seen in the previous section, a baseload power plant like the one in our example in combination with the general peak/ off-peak price pattern does not vary its (0,1)-operating states that often. In fact, Table 4.6 illustrated that a set of schedule candidates \mathbb{L} specifically adjusted for a concrete market environment (otm/atm/itm) leads to a close approximation of the actual optimal cash flow. Recall that all schedules in this set can be linked together without violating the on- and off-times. In equation 4.38 we introduced the corresponding modified MIP that we now extend by the upper energy constraint $I'L_d \leq w$ at the top of the

³This definition is an exception to our general convention of large letters for random variables and small ones for their realizations.

constraint list

$$\begin{aligned}
 \mathbb{L}Z_d(X_d, w) &= \max_{L_d, \xi_d, \beta_d^u, \beta_d^o} \{(X_d - KI)'L_d - K_u I' \beta_d^u - K_o I' \beta_d^o\} \\
 &\text{subject to:} \\
 &I' L_d \leq w \\
 &L_{\min} \xi_d - L_d \leq 0 \\
 &-L_{\max} \xi_d + L_d \leq 0 \\
 &E \xi_d - \beta_d^u \leq 0 \\
 &-E \xi_d - \beta_d^o \leq 0 \\
 &L_d^t \in \{0\} \cup [L_{\min}, L_{\max}] \\
 &\xi_d \in \mathbb{L} \\
 &\xi_d^t, \beta_d^{o,t}, \beta_d^{u,t} \in \{0, 1\} \\
 &t = 1, \dots, 24.
 \end{aligned} \tag{4.42}$$

Hence, we use this new MIP to calculate the optimal cash flow for all relevant grid points by setting $w := w^r$. The valid grid points fall into the interval $[w_{\min}, w_{\max}]$ where w_{\min}, w_{\max} are the the minimum and maximum possible energy production per day defined by the schedule with the shortest and longest running hours in \mathbb{L} . If \mathbb{L} contains enough schedules to cover all possible intermediate running hours, then this interval is a closed line, otherwise it is the union of smaller intervals. The MIP does not only return the maximum profit, but also returns the corresponding optimal schedule L_d^* and thus the optimal energy w_d^*

$$w_d^* := \sum_{t=1}^{24} L_d^{t,*}, \tag{4.43}$$

by simply summing up the individual 24 hourly capacities $L_d^{t,*}$. In situations where the price vector X_d is mainly itm, w_d^* will match w and w^r , respectively, otherwise $0 \leq w_d^* < w$. We use the pairs $(w_d^*, \mathbb{L}Z_d^*(X_d, w^r))$ (not (!) $(w^r, \mathbb{L}Z_d^*(X_d, w^r))$) as the input for a polynomial fit to receive a cash flow curve $\mathbb{L}\hat{Z}_d(x_d^i, w_d)$ in w_d for a fixed price vector x_d^i ⁴

$$\mathbb{L}\hat{Z}_d(x_d^i, w_d) := \mathbb{L}\hat{z}_d^i(w_d) \approx \sum_{n=0}^N b_{d,n}^i w_d^n. \tag{4.44}$$

Each individual cash flow curve $\mathbb{L}\hat{z}_d^i(w_d)$ is only valid in $[\underline{w}_d^i, \bar{w}_d^i] \in [w_{\min}, w_{\max}]$ where \underline{w}_d^i and \bar{w}_d^i are the shortest and longest production amount with maximum profitability for price scenario i. \underline{w}_d^i , for instance, will never be 0 if \mathbb{L} does not contain a zero production schedule. \bar{w}_d^i is mainly driven by the price scenario. The itm hours define the number of hours with maximum capacity L_{\max} and thus the maximum energy amount. For an otm price scenario, for instance, it is not beneficial to have long production hours even if available in \mathbb{L} and hence $\bar{w}_d^i < w_{\max}$. The entire procedure to receive $\mathbb{L}\hat{z}_d^i(w_d)$ requires MIP solutions for each price vector i and grid point $W^r \in [w_{\min}, w_{\max}]$. Therefore we investigated again a faster alternative matrix calculation. Due to the new energy constraint we cannot use any longer our MIP reformulation from section 4.3.1. For this reason we will introduce yet another fast implementation approach.

⁴From now on we use a hat to label variables that stand for approximated continuous functions.

4.4.1. MIP Reformulation

Different to section 4.3.1 the solution of the MIP via complete enumeration of all $\{0,1\}$ schedules becomes more difficult with an additional upper energy bound w . Then we cannot apply a digital volume profile on top of the operating states like in section 4.3 in order to quickly generate the entire schedule. Instead we have to introduce a profile matrix \mathcal{L} that holds the actual MW for each hour of a given $(0,1)$ schedule and price vector

$$R_d := (M * \mathcal{L})(X_d - KI) - (K_u I)' \alpha - (K_o I)' \beta, \quad (4.45)$$

where $*$ indicates the component-wise multiplication and I is the unity matrix. \mathcal{L} is of size $(J \times 24)$ with J being the number of schedule candidates in the set \mathbb{L} . Each row of \mathcal{L} represents the volume profile in MW for the corresponding operating sequence of the same row in M and given price vector X_d . Each profile hour can take four different values $\{0, L_{\min}, l, L_{\max}\}$, where $L_{\min} \leq l \leq L_{\max}$. The intermediate value l differs from row to row and can only appear once or not at all in one single row. Either the best digital schedule is automatically below w . Then there is only $0, L_{\min}$ and L_{\max} . Otherwise the energy of the schedule goes up to the limit. Then the most profitable hours run on max capacity and only one of these max capacities has to be reduced to l to match exactly the upper bound. A new algorithm should therefore rearrange the hours in descending order of their profit $(x_d^t - K)$ and assign max capacity to each hour until the first hour that exceeds w . This very single hour will be reduced to an intermediate value l in order to mach w . The following procedure defines in detail the algorithm for setting up each row $j = 1, \dots, \hat{J}$ in \mathcal{L} :

1. Compute all digital schedules according to equation 4.17 and select the sub set where the generated energy is below w . Pick the one with the highest profit ("best value from below"). Remove all schedule rows j from M and \mathcal{L} whose profit is smaller. Then M and \mathcal{L} is of new size $(\hat{J} \times 24)$
2. For the remaining schedules fill all hours with L_{\min} .
3. Sort the schedule prices $(X_d - KI)$ in descending order and bring the columns of $M * \mathcal{L}$ in the same order.
4. Iterate from the top through this sorted list of hours $t = 1, \dots, T$ and replace L_{\min} with L_{\max} in the corresponding column in $M * \mathcal{L}$ until $(x_d^t - K) < 0$ or stop at hour $t = t_{\max}$ where the energy bound is exceeded the first time for row j . In the latter case reduce the volume $l_j^{t_{\max}}$ to $l = w - \sum_{t \in T \setminus t_{\max}} l_j^t$ in order to meet w and continue the iteration with the next row $j+1$.

Note that compared to equation 4.17 we use X_d instead of \hat{X}_d as we need to set up \mathcal{L} for each price scenario X_d individually and therefore cannot compute all scenarios at once with a single matrix calculation as before. Consequently the new R_d is not a matrix, but only a vector of length \hat{J} . The row index \hat{j} of the maximum component in R_d defines the row in \mathcal{L} that holds the optimal schedule

$$\mathbb{L}Z_d(X_d, w) := \max_{1 \leq \hat{j} \leq \hat{J}} \{R_d^{\hat{j}}\}. \quad (4.46)$$

Hence, we have to run this matrix calculation for all I price scenarios. For this reason the whole procedure will only be faster than a MIP solver if the size of M can be kept small. This is in particular the case for power plants with long minimum on- and off-times. Step 1 is therefore designed as a filter and especially reduces the number of candidates efficiently for

large upper bounds w . Then the best schedule from below will have a high profit that will allow to exclude most of the schedules and keep \hat{J} small. In our specific example with $t_{\text{on}} = 12$ and $t_{\text{off}} = 8$ the matrix implementation of a single day dispatch optimization runs 10 to 25 times faster than the corresponding CPLEX implementation of the MIP getting faster with increasing energy. As a further step recall that we introduced in equation 4.42 a preselection of candidate schedules \mathbb{L} that will keep M small independently of the available energy.

4.4.2. Bellman Iteration

So far we looked at the daily cash flow curve $\mathbb{L}\hat{z}_d^i(w_d)$ (see equation 4.42) that we will now use as an input for our Bellman expression to describe the cash flows between the days. We start again from the situation without energy constraint, in particular from our Bellman equation 4.19. Our new state space is not only continuous with respect to the spot price vector X_d , but also with respect to the remaining total energy W_d at the beginning of day d that will become another dimension of the state space. For computational feasibility we do not extend the state space, but rather replace the power plant running mode J_d with W_d by focusing on a smaller class of optimization problems that is restricted to a preselection of candidate schedules \mathbb{L} . As discussed in context of equation 4.37 this set can vary with strike K . We will label all figures relying on this set with \mathbb{L} as a prefix. This preselection fits very well to our definition of the daily cash flow curve $\mathbb{L}\hat{z}_d^i(w_d)$ for which we will use the same set of schedule candidates. This daily cash flow curve becomes the marginal profit of our dynamic program. As explained in context of equation 4.44 the daily cash flow will have lower and upper energy bounds that depend on individual price realizations x_d^i , i.e. $(\underline{w}_d^i, \bar{w}_d^i)$ or in general terms $(\underline{w}_d(X_d), \bar{w}_d(X_d))$, for the *actual* production dependent on the price scenarios ($i=1, \dots, I$) and schedule set \mathbb{L} . This interval defines the action set A_d for the current stage d . We also introduced the interval $[w_{\min}, w_{\max}]$ where w_{\min} and w_{\max} are computed from the schedule with the shortest and longest running hours multiplied by L_{\min} and L_{\max} respectively. All individual intervals $[\underline{w}_d^i, \bar{w}_d^i]$ fall into this larger one. As the overall *actual* production is a concatenation of the daily ones, there will also be an individual lower and upper bound of the *actual* overall production which we denote with $(\underline{W}_d^i, \bar{W}_d^i)$. The latter must not be confused with the overall *available* production W_d . Since we use the same price process as in the previous chapters we can describe the transition from X_d to X_{d+1} via our conditional normal distribution from equation 4.21. The new transition rule also needs to describe how the remaining energy evolves over time. The remaining energy of the next stage W_{d+1} is simply the current one W_d reduced by the current generation amount w_d . As usual the value function $\mathbb{L}C_d^*(X_d, W_d)$ is the value of an option that would be newly issued at day d observing the current price X_d and available energy W_d . Whereas the continuation value $\mathbb{L}Q_{d+1}^*(X_d, W_{d+1})$ is the expectation of the option value at $d+1$ conditional on today's price X_d and tomorrow's remaining energy W_{d+1} . Hence, we can express the value function with

the following Bellman equation

$$\begin{aligned}
 \mathbb{L}C_d^*(X_d, W_d) &= \max_{w_d} \{ \mathbb{L}Z_d(X_d, w_d) + \mathbb{E} [\mathbb{L}C_{d+1}^*(X_{d+1}, W_d - w_d) | X_d] \} \quad 0 \leq d \leq D \\
 \text{state : } (X_d, W_d) & \quad X_d : \text{current price, } W_d : \text{remaining available energy} \\
 \text{action : } w_d \in A_d & := [w_d(X_d), \min[\bar{w}_d(X_d), W_d]] \quad \text{actual production at day } d \\
 \text{transition : } \{X_d, W_d\} & \longrightarrow \{X_{d+1}, W_d - w_d\} \\
 \text{marginal profit : } \mathbb{L}Z_d(X_d, w_d) & \quad \text{cash flow for actual production} \\
 \text{value function : } \mathbb{L}C_d^*(X_d, W_d) & \\
 \text{continuation value : } \mathbb{L}Q_{d+1}^*(X_d, W_{d+1}) & := \mathbb{E} [\mathbb{L}C_{d+1}^*(X_{d+1}, W_{d+1}) | X_d],
 \end{aligned} \tag{4.47}$$

with $\mathbb{L}C_{D+1}^*(X_{D+1}, W_{D+1}) := 0$. The implementation of the backward iteration needs to consider that $\mathbb{L}Z_d(X_d, w_d)$, respectively $\mathbb{L}C_d^*(X_d, W_d)$ and $\mathbb{L}Q_{d+1}^*(X_d, W_{d+1})$ are continuous functions with respect to two dimensions, X_d, w_d and X_d, W_d respectively. As we will apply the Longstaff-Schwartz approach again we furthermore introduce the ACF $\mathbb{L}V^*(X_d, W_d)$ as another continuous function with two dimensions

$$\mathbb{L}V_d^*(X_d, W_d) := \sum_{s=d}^D \mathbb{L}Z_s(X_s, w_s^*), \tag{4.48}$$

with $\sum_{s=d}^D w_s^* \leq W_d$. Following the Longstaff-Schwartz regression, we approximate an individual realization of the continuation value $\mathbb{L}Q_{d+1}^*(x_d^i, W_{d+1})$ by the average of all individual path-wise ACFs starting from the next stage with future prices x_{d+1}^j generated from the observed price x_d^i such that

$$\mathbb{L}Q_{d+1}^*(x_d^i, W_{d+1}) \approx \frac{1}{J} \sum_{j=1}^J \mathbb{L}V_{d+1}^*(x_{d+1}^j, W_{d+1}). \tag{4.49}$$

Formally, $\mathbb{L}Z_d(X_d, w_d)$ and $V_d^*(X_d, W_d)$ are functions with two dimensions. Similar to the approximation of $\mathbb{L}Z_d^*(X_d, w_d)$ with $\mathbb{L}\hat{z}_d^i(w_d)$ our numerical procedure will only approximate the *two* dimensional function for the ACF by $i=1, \dots, I$ *one* dimensional curves. i.e. $\mathbb{L}\hat{v}_d^i(W_d) := \mathbb{L}\hat{V}_d(x_d^i, W_d)$

$$\mathbb{L}\hat{v}_d^i(W_d) := \sum_{m=0}^M \alpha_{d,m}^i W_d^m \approx \mathbb{L}v_d^{*,i}(W_d), \tag{4.50}$$

or in general terms

$$\mathbb{L}\hat{V}_d(X_d, W_d) := \sum_{m=0}^M \alpha_{d,m}(X_d) W_d^m \approx \mathbb{L}V_d^*(X_d, W_d). \tag{4.51}$$

In order to calculate these individual ACF curve we first need sample points $v_d^{i,*}(W^r)$ on the fixed grid $W^r \in [0, W_0]$, $r = 1, \dots, R$, for each price scenario i that we fit to a polynomial curve similar to the approximation of the marginal profit $\mathbb{L}\hat{z}_d^i(w_d)$ (see discussion around equation 4.44). Hence, we need to solve the Bellman equation for each grid point and price scenario which requires an approximation of the continuation value $\mathbb{L}Q_{d+1}^*(X_d, W_{d+1})$. Recall that the Longstaff-Schwartz regression is based on the pairs $(x_d^i, \mathbb{L}\hat{v}_{d+1}^i(W_{d+1}))$. The ACF $\mathbb{L}\hat{v}_{d+1}^i(W_{d+1})$, however, is not a single value any more, but a *curve* with respect to the re-

maintaining energy W_{d+1} (on the very last stage it is identical to the marginal profit curve i.e. $\mathbb{L}\hat{v}_D^i(W_D) = \mathbb{L}\hat{z}_D^i(w_D)$). Consequently the approximated continuation value $\mathbb{L}\hat{Y}_{d+1}(X_d, W_{d+1})$ cannot be any longer a function of the current price only, but will also be a curve with respect to the remaining energy W_{d+1} . For this reason we do not regress the current price to a single value, but to an entire curve. Note that we use a polynomial approximation for each ACF curve (see equation 4.50) which we therefore can represent by their parameters $\alpha_{d+1,m}^i$, i.e. one parameter set $\alpha_{d+1,m}$ for each price scenario i separately. We therefore only run a regression on these parameters i.e. on the pairs $(x_d^i, \alpha_{d+1,m}^i)$. The resulting regression vector $\lambda_{d+1,m}$ of length R allows us to describe the set of parameters $\bar{\alpha}_{d+1,m}(X_d)$

$$\bar{\alpha}_{d+1,m}(X_d) \approx \Psi'_{d,m}(X_d) \lambda_{d+1,m}, \quad (4.52)$$

where $\Psi_{d,m}(X_d)$ is a vector of basis functions that transform the price vector into a scalar. $\bar{\alpha}_{d+1,m}(X_d)$ enables us in a second step to define the approximated continuation value curve for any given price X_d and remaining energy W_{d+1}

$$\mathbb{L}\hat{Y}_{d+1}(X_d, W_{d+1}) = \sum_{m=0}^M \bar{\alpha}_{d+1,m}(X_d) W_{d+1}^m \approx \mathbb{L}Q_{d+1}^*(X_d, W_{d+1}). \quad (4.53)$$

As the Bellman equation is now a sum of two functions we can find the optimal current energy production per scenario i and grid point W^r via the first derivative

$$w_d^{i,r,*} = \arg \left\{ \frac{\partial}{\partial w_d} \mathbb{L}\hat{z}_d^i(w_d) + \frac{\partial}{\partial w_d} \mathbb{L}\hat{y}_{d+1}^i(W^r - w_d) = 0 \right\}. \quad (4.54)$$

The relevant grid points W^r to investigate need to belong to the individual interval of the remaining *actual* generation from day d onwards, i.e. $W^r \in [\underline{W}_d^i, \bar{W}_d^i]$. We determine this interval iteratively. The new lower bound is simply the minimum of the lower bound of today's production and the remaining production from tomorrow onwards. The new upper bound is the sum of the upper bound of today's and the remaining production, i.e.

$$\begin{aligned} \underline{W}_d^i &:= \min\{\underline{w}_d^i, \underline{W}_{d+1}^i\} \\ \bar{W}_d^i &:= \bar{w}_d^i + \bar{W}_{d+1}^i, \end{aligned} \quad (4.55)$$

where $\bar{W}_D^i := \bar{w}_D^i$ and $\underline{W}_D^i := \underline{w}_D^i$. We need to verify that $w_d^{i,r,*} \in [\underline{w}_d^i, \bar{w}_d^i]$ and $W^r - w_d^{i,r,*} \in [\underline{W}_{d+1}^i, \bar{W}_{d+1}^i]$. Otherwise we need to adjust $w_d^{i,r,*}$ to $\tilde{w}_d^{i,r,*}$ (see discussion in context of equation 4.59). Then we can compute the corresponding ACF value for each grid point

$$\mathbb{L}v_d^i(W^r) \approx \mathbb{L}\hat{z}_d^i(\tilde{w}_d^{i,r,*}) + \mathbb{L}\hat{y}_{d+1}^i(W^r - \tilde{w}_d^{i,r,*}). \quad (4.56)$$

We fit the pairs $(W^r, \mathbb{L}v_d^i(W^r))$ to a polynomial curve according to equation 4.50. Now, we can start the next iteration step by computing the continuation value curve $Y_d(X_{d-1}, W_d)$. We repeat this entire iteration until $t=0$. Finally we obtain the option value curve by averaging all individual ACFs for any initial available energy \mathcal{W}_0 and fixed x_0

$$\mathbb{L}C_0(x_0, \mathcal{W}_0) \approx \frac{1}{I} \sum_{i=1}^I \mathbb{L}\hat{v}_0^i(x_0, \mathcal{W}_0). \quad (4.57)$$

Let us conclude with a summary of all relevant steps of the backward iteration

1. For each stage $d = D, D-1, \dots, 0$

- a) For each price scenario $i = 1, \dots, I$
 - i. Calculate the marginal profit function $\mathbb{L}\hat{z}_d^i(w_d)$ by solving equation 4.42 for all grid points W^r falling into $[w_{\min}, w_{\max}]$ and fit them to a curve (e.g. polynomial fit). We receive the actual production interval $[\underline{w}_d^i, \bar{w}_d^i]$ and the curve parameters $b_{d,n}^i$ of equation 4.44.
 - ii. Calculate the new overall actual production interval $[\underline{W}_D^i, \bar{W}_D^i]$ according to equation 4.55 where $\bar{W}_D^i := \bar{w}_D^i$ and $\underline{W}_D^i := \underline{w}_D^i$.
 - b) Calculate the continuation value curve $\mathbb{L}\hat{Y}_{d+1}(X_d, W_{d+1})$ by regressing the parameters $(x_d^i, \alpha_{d+1,m}^i)$ where $\alpha_{D+1,m}^i := 0$ and $\alpha_{D,m}^i = b_{D,m}^i$ (i.e. $\mathbb{L}\hat{v}_D^i(W_D) = \mathbb{L}\hat{z}_D^i(w_D)$). We receive a vector $\lambda_{d+1,m}$ for each parameter $\bar{\alpha}_{d+1,m}$ according to equation 4.52.
 - c) For each grid point $W^r \in [\underline{W}_D^i, \bar{W}_D^i]$ and price scenario $i = 1, \dots, I$
 - i. Solve the Bellman equation via classical calculus according to equation 4.54. We receive the optimal day production $w_d^{i,r,*}$.
 - ii. Check that $w_d^{i,r,*} \in [\underline{w}_d^i, \bar{w}_d^i]$ and $W^r - w_d^{i,r,*} \in [\underline{W}_{d+1}^i, \bar{W}_{d+1}^i]$. Otherwise adjust the optimal day production to $\tilde{w}_d^{r,i,*}$ (see also discussion in context of equation 4.59).
 - iii. Calculate the value function value $\mathbb{L}v_d^i(W^r)$ using $\tilde{w}_d^{r,i,*}$ according to equation 4.56.
 - d) Fit the pairs $(W^r, \mathbb{L}v_d^i(W^r))$ to the new curve $\mathbb{L}\hat{v}_d^i(W_d)$. We receive the parameters $\alpha_{d,m}$ of equation 4.50.
2. For a given initial available energy \mathcal{W}_0 we average the corresponding figures on the individual ACF curves $\mathbb{L}\hat{v}_0^i(\mathcal{W}_0)$, $i = 1, \dots, I$, according to equation 4.57 to receive the real option value $\mathbb{L}C_0(x_0, \mathcal{W}_0)$.

Finally, we would like to emphasize that tracking the production intervals $[\underline{W}_D^i, \bar{W}_D^i]$ for each price scenario $i = 1, \dots, I$ separately allowed for applying a simple quadratic approximation of the cash flow curves $\hat{z}_d^*(w^i)$, $\hat{v}_d^i(W_d)$ and thus a simple analytical solution of the Bellman equation via the first derivative (see equation 4.54) since only within these intervals even for long production horizons like a year the cash flow curves expose a parabolic pattern.

4.4.3. Numerical Results

We continue with our previous example from section 4.3.4, but now impose different upper energy bounds W_0 to our power plant. The technical constraints stay the same as listed in section 4.1. First, we look at the daily production $\mathbb{L}\hat{Z}_d(X_d, w_d)$ and need to find the appropriate degree N for our polynomial $b_{d,n}$, $n = 0, \dots, N$. For this purpose we select an arbitrary weekday in March-08. We choose a grid distance of $\Delta W^r = 1000$ MWh and compute the marginal profit $Z_d(X_d, W^r)$ for all grid points $w_{\min} \leq W^r \leq w_{\max}$. This interval is driven by the set \mathbb{L} of (0,1) candidate schedules for which we choose L622 since we look at a weekday i.e. we allow running hours between 6:00 and 22:00. Hence, we added ± 2 hours to a classical peak schedule. Recall from section 4.2.1 that hour 6,7,20 and 21 often reveal peak price levels. Therefore we want to allow a production during these hours as well. The smallest energy amount once the power plant is up and running is the minimum up-time multiplied with the minimum capacity i.e. $w_{\min} = 12\text{h} \times 240 \text{ MW} = 2880$ MWh. All curves need to start from that value and are zero beforehand. The largest possible energy production is a flat schedule with max capacity i.e. $w_{\max} = 16\text{h} \times 530 \text{ MW} = 8480$ MWh. All individual

intervals $[w_d^i, \bar{w}_d^i]$ fall into this maximum range. As illustrated in Figure 4.13, we retrieve already good results for a quadratic fit. The figure presents the curves for the first 50 price vectors. The graph shows that not all curves will really produce up to w_{\max} . If the price

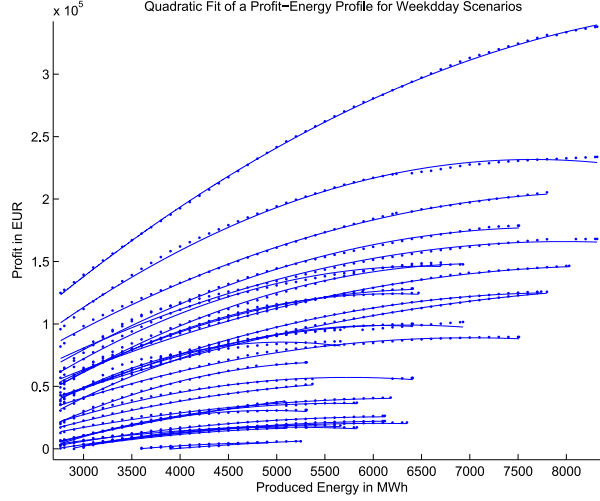


Figure 4.13.: Profit-energy curve $\mathbb{L}\hat{z}_d^i$ for a single weekday in March 08 ($K=70$) with fixed grid and quadratic approximation

vector has too many otm hours (in this example we used $K = 70$) then the power plant will not make use of the extra energy for the profit would decrease otherwise. Hence all curves are only plotted up to the energy amount with the highest cash flow \bar{w}_d^i and actually need to be extrapolated from that peak value with a flat line parallel to the x-axis until 8480 MWh. For better readability we skipped this extrapolation in Figure 4.13 likewise we skipped the zero values for $w_d < 2880$ MWh. As we observed a parabolic shape for the daily profit-energy line the sum of all these days will reveal a quadratic pattern as well. For this reason we use the quadratic approximation for the ACF $\hat{V}_d(X_d, W_d)$ as well. Next, we look at the approximation of the continuation value. Let us illustrate the procedure for the last stage where $\mathbb{L}\hat{v}_D^i(W_D) := \mathbb{L}\hat{z}_D^i(w_D) := \alpha_{D,0}^i + \alpha_{D,1}^i W_D + \alpha_{D,2}^i W_D^2$. In this situation the interval for the global and local production are the same: $w_D^i = \bar{W}_D^i$ and $\bar{w}_D^i = \bar{W}_D^i$. First, we run a regression on the pairs $(X_{D-1}, \alpha_{D,0/1/2})$ to find the polynomial coefficients $\bar{\alpha}_{D,m}(X_{D-1})$ of the continuation value curve. Like in section 4.3.4 we replace the price vector X_{D-1} by the principal components. From our numerical analysis in Table 4.6 we know that we can focus on the first PC only, i.e. $a_{1,D-1}$. Formally, we use the rotation functions of our principal component analysis as our basis functions $\Psi_{D-1,m}(X_{D-1}) = a_{1,D-1}^m$. Figures 4.14 to 4.16 plot the parameters $\alpha_{D,0}$, $\alpha_{D,1}$ and $\alpha_{D,2}$ of the last delivery day $\mathbb{L}\hat{v}_D^i(W_D) = \mathbb{L}\hat{z}_D^i(W_D)$ for all three strikes $K = 50, 70$ and 90 against the first PC $a_{1,D-1}$. All graphs resemble the payoff profile of a sold (Figure 4.14 and 4.15) or bought (Figure 4.15) call option. Zero parameter values indicate a zero continuation value (no production is also a valid schedule of our candidate set L622). This band of zero parameters moves to the right with increasing strike for all three parameters $\alpha_{D,0}$, $\alpha_{D,1}$ and $\alpha_{D,2}$. A higher strike requires a higher price vector X_D and hence a higher first PC $a_{1,D}$ in order to afford a power plant start-up. The option like curve shape motivates yet another quadratic approximation to find the parameters $\bar{\alpha}_{D,m}$. This leads to

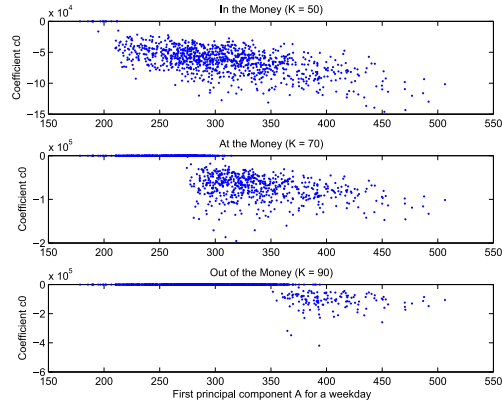


Figure 4.14.: Parameter pairs $(a_{1,D-1}, \alpha_{D,0})$ for all three strikes at $D = 30$

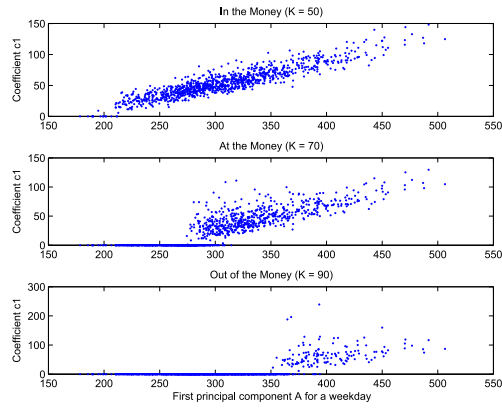


Figure 4.15.: Parameter pairs $(a_{1,D-1}, \alpha_{D,1})$ for all three strikes at $D = 30$

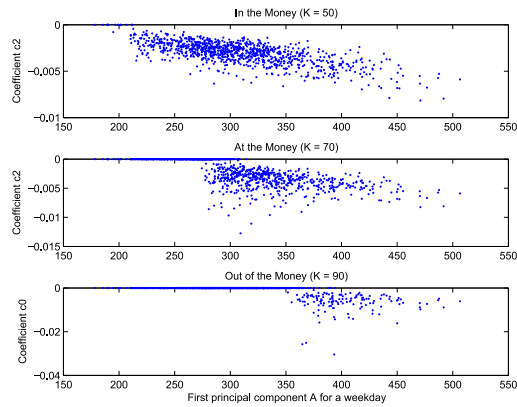


Figure 4.16.: Parameter pairs $(a_{1,D-1}, \alpha_{D,2})$ for all three strikes at $D = 30$

the following concrete representation of our basis functions

$$\begin{aligned}
 N = 2 &\Rightarrow \mathbb{L}\hat{z}_d^i(w_d) = b_{d,0}^i + b_{d,1}^i w_d + b_{d,2}^i w_d^2 \\
 M = 2 &\Rightarrow \mathbb{L}\hat{v}_d^i(W_d) = \alpha_{d,0}^i + \alpha_{d,1}^i W_d + \alpha_{d,2}^i W_d^2 \\
 &\Rightarrow \mathbb{L}\hat{Y}_{d+1}(X_d, W_{d+1}) \\
 &= \bar{\alpha}_{d+1,0}(X_d) + \bar{\alpha}_{d+1,1}(X_d)W_{d+1} + \bar{\alpha}_{d+1,2}(X_d)W_{d+1}^2 \\
 \Psi_{d,m,j}(X_d) := (a_{1,d})^j, J = 2 &\Rightarrow \bar{\alpha}_{d+1,m}(X_d) = \lambda_{d+1,m,0} + \lambda_{d+1,m,1} a_{1,d} + \lambda_{d+1,m,2} a_{1,d}^2,
 \end{aligned} \tag{4.58}$$

with $a_{1,d} = \sum_{t=1}^{24} \gamma_{1t} x_d^t$ (see also equation 4.27). For quadratic functions we can easily calculate the first derivative with classical calculus and are able to solve the Bellman equation directly for any grid values W^r

$$w_d^{r,*,i} = \frac{2 \bar{\alpha}_{d+1,2}^i W^r + \bar{\alpha}_{d+1,1}^i - b_{d,1}^i}{2(b_{d,2}^i + \bar{\alpha}_{d+1,2}^i)}. \tag{4.59}$$

Recall from Figure 4.13 that the parabolic behavior of energy vs. profit is only valid within individual production intervals $[w_d^i, \bar{w}_d^i]$ for each scenario i . As we use the same quadratic approach for the ACFs $\mathbb{L}\hat{v}_d^i(W_d)$ and approximated continuation value $\mathbb{L}\hat{Y}_d(X_d, W_{d+1})$ we likewise receive intervals $[\underline{W}_d^i, \bar{W}_d^i]$ and $[\underline{W}_{d+1}^{[y]}, \bar{W}_{d+1}^{[y]}]$. As explained in equation 4.55 the intervals for W_d are not only the remaining energy values, but represent the *actual* energy usage. However, for the continuation value we cannot apply these individual upper and lower bounds as the continuation values is a conditional average of *all* next step ACFs $\mathbb{L}\hat{v}_{d+1}^i(W_{d+1})$. Therefore there is only a common interval $[\underline{W}_d^{[y]}, \bar{W}_d^{[y]}]$ as it is an average across all scenarios. We can only rely on our set of candidate schedules \mathbb{L} as well as L_{\min} and L_{\max} to define these borders. The lower bound $\underline{W}_d^{[y]}$ is the shortest number of running hours of a single day that we can find in \mathbb{L} . Recall that we use schedule candidates with running hours between 6:00 and 22:00. Then the shortest running time is in fact the minimum runtime and we receive $\underline{W}_d^{[y]} = t_{\text{on}} L_{\min} = 2880$ MWh. The upper bound is the largest number of running hours in \mathbb{L} multiplied by the number of remaining days and L_{\max} . In our case \mathbb{L} allows a production of 16 hours, hence $\bar{W}_d^{[y]} = 16 \cdot (D - d + 1) \cdot L_{\max}$.

We need to check the validity of $w_d^{r,*,i}$ not only against $[w_d, \bar{w}_d]$, but also $W^r - w_d^{r,*}$ against the energy interval of the ACF $[\underline{W}_{d+1}^i, \bar{W}_{d+1}^i]$ and the continuation value $[\underline{W}_{d+1}^{[y]}, \bar{W}_{d+1}^{[y]}]$. First, for each scenario i we compare $w_d^{r,*,i}$ with today's energy interval $[w_d^i, \bar{w}_d^i]$. If $w_d^{r,*,i}$ is below the minimum border, then our schedules in \mathbb{L} do not allow to produce such a small amount and we need to replace $w_d^{r,*,i}$ by 0 meaning no production today. If $W^r - w_d^{r,*,i} < \underline{W}_{d+1}^{[y]}$ i.e. the remaining energy after today's production is below the required minimum energy interval, then today's energy allocation will be reduced to $\tilde{w}_d^{r,*,i} = W^r - \underline{W}_{d+1}^{[y]}$. However, if the adjusted generation amount falls below the minimum possible day production, i.e. $\tilde{w}_d^{r,*,i} < w_d^i$, then we set $\tilde{w}_d^{r,*,i} = 0$ meaning no production today. If $w_d^{r,*,i}$ exceeds the upper bound of today's possible production, i.e. $w_d^{r,*,i} > \bar{w}_d^i$ we reduce it to $\tilde{w}_d^* := \bar{w}_d^i$. It would not make sense to claim a higher energy amount if we can attain the same profit with less energy. If $W^r - w_d^{r,*,i} > \bar{W}_{d+1}^i$, we do not need to adjust w_d^* , but compute the ACF at \bar{W}_{d+1}^i since we said that $\mathbb{L}\hat{V}(W_d^i) := \mathbb{L}\hat{V}_d(\bar{W}_d^i)$ for all $W_d^i > \bar{W}_d^i$. If no production is a valid candidate we also need to compare the adjusted volume with zero production: $\mathbb{L}\hat{z}_d^i(w_d^{r,*,i}) + \mathbb{L}\hat{y}_{d+1}^i(W^r - w_d^{r,*,i})$ vs. $\mathbb{L}\hat{y}_{d+1}^i(W^r)$. After this correction the adjusted optimal production $\tilde{w}_d^{r,*,i}$ will be used to compute the ACF $\mathbb{L}\hat{v}_d^i(W^r)$ at the specific grid point r according to equation 4.56. Note that

all these adjustments implicitly assume that \mathbb{L} allows any production amount in $[\underline{w}_d^i, \bar{w}_d^i]$. In our example this is indeed the case as L622 allows any production between 8 and 16 hours, hence the interval is a continuous line. Figure 4.17 plots the optimal policy $\tilde{w}_d^{r,*i}$ for $d = 26$ March 08. The 3D plot shows the first PC a_1 on the x-axis and the total available production

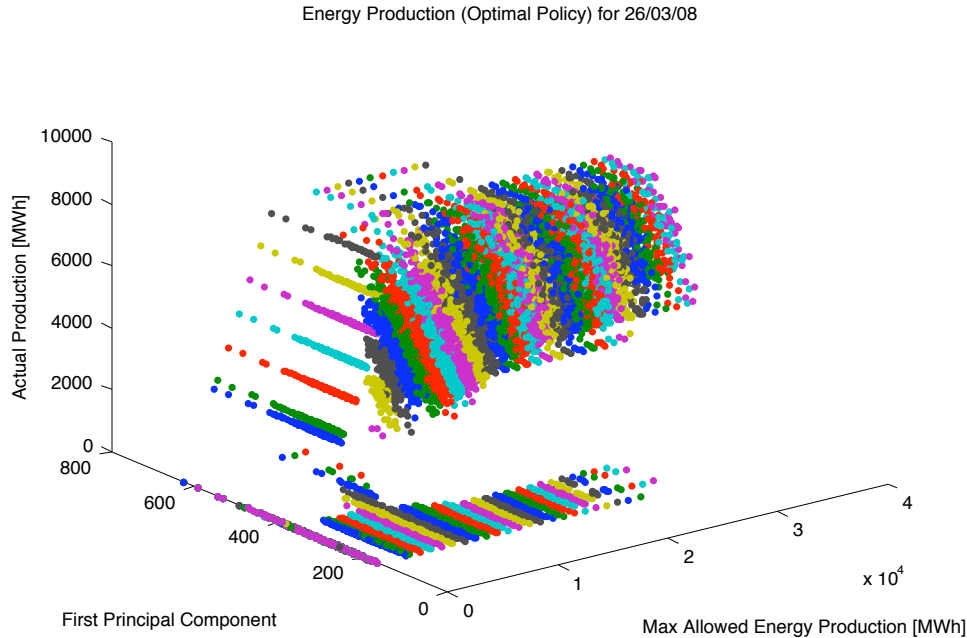


Figure 4.17.: Production as a function of the first PC a_1 and available energy W_d

W_d on the y-axis. Dependent on these two variables we see today's production w_d on the z-axis. The flat roof of the mountain-like surface is at $w_{\max} = 8480$ MWh which is the total possible day production. The colors intend to emphasize the grid structure where identical colors stand for policy values of the same energy grid point W^r but different price scenarios. We can identify two regions separated on the W_d axis at value 8480 MWh (we can envision a parallel line to the a_1 -axis going through $W_d = w_{\max} = 8480$ MWh). If the remaining total energy can be entirely produced the same day ($W_d \leq w_{\max}$) then this will be done once the price exceeds a specific threshold ($a_1 > 350$). This threshold is similar to the exercise line in Figure 2.3 that triggers an option exercise for any observed price above that line. This rule explains the ramp in the $(w_d - W_d)$ -layer which raises in the w_d -dimension until $W_d = w_d = 8480$ MWh. For larger remaining energy amounts (i.e. the area beyond the imaginary line: $W_d > w_{\max}$) we observe another ramp in the $(w_d - a_1)$ -layer. The ramp becomes steeper and starts earlier (i.e. smaller a_1) the more energy is available (i.e. the more we shift the $(w_d - a_1)$ -layer along the W_d dimension. A steeper ramp translates into a larger day production and that for even smaller price vectors/smaller a_1). On 26 March there are only five days left until the end of the production period. Before leaving large available energy unused the power plant can afford to produce more even at a smaller price as long as the resulting cash flow is still positive. That's why the floor of the graph indicating no production ($w_d = 0$) gets more narrow and less dense in a_1 dimension with increasing W_d .

Once we have iteratively solved equation 4.59 we finally are able to represent the option

value as an average of I contingent cash flows $\mathbb{L}\hat{v}_0^i(\mathcal{W}_0)$

$$\begin{aligned} C_0(x_0, \mathcal{W}_0) &\approx \mathbb{E}[\mathbb{L}\hat{V}_0(X_0, W_0)|X_0 = x_0, W_0 = \mathcal{W}_0] \\ &\approx \frac{1}{I} \sum_{i=1}^I \left[\mathbb{I}_{\underline{W}_0^i \leq \mathcal{W}_0 \leq \overline{W}_0^i} \left(\alpha_{0,0}^i + \alpha_{0,1}^i \mathcal{W}_0 + \alpha_{0,2}^i \mathcal{W}_0^2 \right) \right. \\ &\quad \left. + \mathbb{I}_{\mathcal{W}_0 > \overline{W}_0^i} \left(\alpha_{0,0}^i + \alpha_{0,1}^i \overline{W}_0^i + \alpha_{0,2}^i (\overline{W}_0^i)^2 \right) \right]. \end{aligned} \quad (4.60)$$

The indicator function \mathbb{I} restricts the profit-energy curve to the individual true production interval $[\underline{W}_0^i, \overline{W}_0^i]$. The ACF is 0 for $(\mathcal{W}_0 < \underline{W}_0^i)$ and stays at the cash flow for \overline{W}_0^i if $\mathcal{W}_0 > \overline{W}_0^i$. Hence, there will be no more production than \overline{W}_0^i even if available. Figure 4.18 shows those individual cash flows for strike $K = 70$ and the schedule candidate set $\mathbb{L} = \text{L622}$. Like in Figure 4.13 we skipped the extrapolation with the parallel line to the x-axis at $\hat{v}_0^i(\overline{W}_0^i)$ for $\mathcal{W}_0 > \overline{W}_0^i$. Again, \mathcal{W}_0 in $\hat{v}_0^i(\mathcal{W}_0)$ is the remaining available energy which is identical to the actual energy usage for $\mathcal{W}_0 < \overline{W}_0^i$.

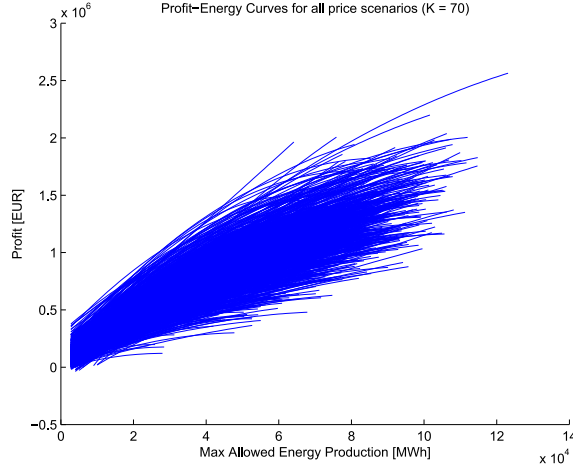


Figure 4.18.: Profit Energy Curves for all price scenarios.

While equation 4.60 is a lower bound of the option curve we added the calculation with full price information as well to provide an upper bound. Then the ACF becomes a contingent function on the known price $\mathbb{L}\hat{v}_d^{f,i}(W_d^i)$ and we can run a deterministic dynamic program by price scenario. Our current model in equation 4.47 stays the same except for a new objective function:

$$\mathbb{L}\hat{v}_d^{f,i}(W_d) := \max_{w_d} \left\{ \mathbb{L}\hat{z}_d^i(w_d) + \mathbb{L}\hat{v}_{d+1}^{f,i}(W_d - w_d) \right\}. \quad (4.61)$$

The former continuation value is replaced by the subsequent contingent ACF $\hat{v}_{d+1}^{f,i}(W_d - w_d)$ and thus we can skip the extra estimation of the parameters $\bar{\alpha}_{d+1,m}$ as prices are known. In equation 4.59 we only need to replace $\bar{\alpha}_{d,m}$ with $\alpha_{d,m}$ and verify that the calculated optimal energy amount w_d^* falls into the valid energy intervals. This time we can directly rely on the individual bounds $[\underline{W}_{d+1}^i, \overline{W}_{d+1}^i]$ rather than the shared interval from the continuation value $[\underline{W}_{d+1}^{[y]}, \overline{W}_{d+1}^{[y]}]$

$$w_d^{*,i} := \arg \max_{w_d} \left\{ \mathbb{L}\hat{z}_d^i(w_d) + \mathbb{L}\hat{v}_{d+1}^{f,i}(W_d - w_d) \right\} \quad (4.62)$$

In this way the estimation of the parameters $\alpha_{d,m}$ and thus the description of the contingent cash flow curves $\mathbb{L}\hat{v}_0^{f,i}(W_0)$ becomes more accurate and the energy allocation is more efficient than $\mathbb{L}\hat{v}_0^i(W_0)$

$$\begin{aligned} \mathbb{L}\hat{v}_d^{f,i}(W_d) &= \mathbb{I}_{\underline{W}_d^i \leq W_d \leq \overline{W}_d^i} \left(\alpha_d^i + \alpha_1^i W_d + \alpha_2^i W_d^2 \right) + \mathbb{I}_{W_d > \overline{W}_d^i} \left(\alpha_d^i + \alpha_1^i \overline{W}_d^i + \alpha_2^i (\overline{W}_d^i)^2 \right) \\ \mathbb{L}C_0^f(x_0, \mathcal{W}_0) &\approx \frac{1}{I} \sum_{i=1}^I \mathbb{L}\hat{v}_0^{f,i}(\mathcal{W}_0). \end{aligned} \tag{4.63}$$

Thus, we approximate the contingent ACFs $\mathbb{L}\hat{v}_d^{f,i}(W_d)$ for each price scenario i separately by sampling the W_d -domain i.e. calculate analytically the best action per grid point W^r . The rest of the algorithm is identical to the lower bound calculation. Computing equations 4.60 and 4.62 for several different initial energy amounts \mathcal{W}_0 and interpolating the results leads to Figure 4.19. It plots the lower bound $\mathbb{L}C_0(x_0, W_0)$ and upper bound $\mathbb{L}C_0^f(x_0, W_0)$ of the

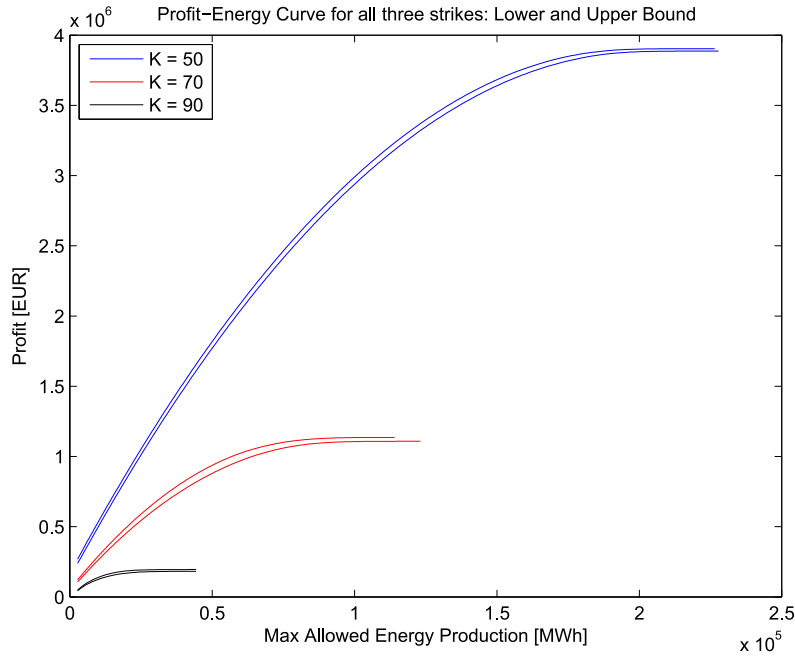


Figure 4.19.: Upper and lower bound option values, C_0^f and C_0 for all three strikes.

power plant for all three strikes and only those W_0 where all curves $\mathbb{L}\hat{v}_0^i(W_0)$ and $\mathbb{L}\hat{v}_0^{f,i}(W_0)$ still increase with more energy across *all* scenarios i.e. $W_0 \in [\underline{W}_0, \overline{W}_0]$ with

$$\begin{aligned} \underline{W}_0 &= \max\{\underline{W}_0^i\} \\ \overline{W}_0 &= \min\{\overline{W}_0^i\}. \end{aligned} \tag{4.64}$$

Hence, the graph shows the profit-energy line for the *core production* of the power plant. Any individual curve with $W_0^i > \overline{W}_0$ might still grow due to the contribution of higher cash flows of some scenarios. However, W_0 would then only represent the cash flow for the *available* energy amount. As expected all curves have a parabolic shape. With increasing strike the saturation is achieved much earlier. Table 4.7 provides actual lower bound values from these

K	\overline{W}_0 [MWh]	$\mathbb{L}C_0$ [EUR]	$\mathbb{L}c$ [EUR/MWh]	$\mathbb{L}c_0^{0.75}$ [EUR/MWh]	$\mathbb{L}c_0^{0.5}$ [EUR/MWh]	$\mathbb{L}c_0^{0.25}$ [EUR/MWh]
50	227,867	3,886,316	17.0	22.20	27.91	34.42
70	123,118	1,028,493	12.41	10.87	12.55	30.30
90	44,380	182,480	4.11	5.34	7.61	11.53

Table 4.7.: Option values in EUR and EUR/MWh for different max energy levels (Backward Iteration)

three curves for a selection of initial energy amounts. Column 2 and 3 present \overline{W}_0 and the corresponding option value $\mathbb{L}C_0 := \mathbb{L}C_0(x_0, \overline{W}_0)$. An increase of the strike from 50 EUR to 90 EUR entails a cut in \overline{W}_0 to less than 20 % (from 227867 MWh down to 44380 MWh). The decrease in the associated option value C_0 is even more dramatic. $\mathbb{L}C_0$ for K=90 goes down to 5 % of the itm value $\mathbb{L}C_0$ for K=50. The values in column $\mathbb{L}C_0$ do not match those of column $C_0(L622)$ in Table 4.6 (recall that we set $\mathbb{L} = L622$). We need to recognize that our option model with energy constraint returns smaller values. For instance for K = 50 we identify a gap of $4.406 - 3.886 = 0.52$ mio EUR (compare Table 4.6 with Table 4.7). The difference indicates a loss in accuracy due to the more complex approximation of the continuous ACF and related continuation functions. The gap can be partially explained by the fact that $\mathbb{L}C_0$ in Table 4.7 is computed for \overline{W}_0 . Different to $C_0(L622)$ in Table 4.6 $\mathbb{L}C_0$ does not contain the highest cash flows $\mathbb{L}v_0^i$ for all scenarios, but only those where $W_0 \leq \overline{W}_0$. For this reason $C(L622)$ is larger in general. The last four columns present option values per MWh indicated with a small c

$$\mathbb{L}c_0^{0.25} = \frac{\mathbb{L}C_0(0.25x_0, \overline{W}_0)}{0.25\overline{W}_0} \quad \mathbb{L}c_0^{0.5} = \frac{\mathbb{L}C_0(x_0, 0.5\overline{W}_0)}{0.5\overline{W}_0} \quad \mathbb{L}c_0^{0.75} = \frac{\mathbb{L}C_0(x_0, 0.75\overline{W}_0)}{0.75\overline{W}_0}. \quad (4.65)$$

The superscript indicates the initial available energy W_0 amount relative to \overline{W}_0 e.g. $W_0^{0.25} = 0.25 \overline{W}_0$. Not surprisingly, the price per MWh goes down with more energy available. The power plant will pick the most profitable hours first which explains the concave form of the option curves in Figure 4.19.

Let us finally describe the algorithm for the forward iteration used for an out-of-sample data set. It relies on the approximation of the continuation value at each stage / generation day represented by the parameters $\overline{\alpha}_{d,m}$ that we computed during the backward iteration. For a given initial upper energy amount $W_0 = \mathcal{W}_0$ we can calculate the option value by running through the following steps

1. For each price scenario $i = 1, \dots, I$
 - a) For each day $d = 0, \dots, D$
 - i. We compute the profit energy curve $\mathbb{L}\hat{z}_d^i(w_d)$ by solving equation 4.42 for selected sampling points $W^r \in [w_d^i, \overline{w}_d^i]$ (for $d = 0$ choose $W^r \in [w_{\min}, w_{\max}]$) and then perform a quadratic fit. We receive the function: $\mathbb{L}\hat{z}_d^i(w_d) = b_{d,0}^i + b_{d,1}^i w_d + b_{d,2}^i w_d^2$.
 - ii. For the remaining total energy amount W_d^i (with initial value $W_0^i := \mathcal{W}_0$) we compute today's generation amount $w_d^{*,i}$ by solving equation 4.59 with $W^r = W_d^i$.⁵

⁵The relevant parameters $\overline{\alpha}_{d,0}^i$, $\overline{\alpha}_{d,1}^i$ and $\overline{\alpha}_{d,2}^i$ were calculated beforehand from our stored parameter set $\lambda_{d,m,j}$ and the rotation function of the first PC $a_{1,d}$ according to equation 4.58.

- iii. We check the solution $w_d^{*,i}$ against the intervals $[\underline{w}_d^i, \min\{W_d^i, \bar{w}_d^i\}]$ and possibly adjust the value to $\tilde{w}_d^{*,i}$ as discussed in context of equation 4.59.
- iv. We update the production value $\mathbb{L}v_{d+1}^i(W_d^i - \tilde{w}_d^{*,i}) := \mathbb{L}v_d^i(W_d^i) + \mathbb{L}z_{d+1}^i(\tilde{w}_d^{*,i})$ with $\mathbb{L}v_0^i(\mathcal{W}_0) = 0$ and $W_{d+1}^i := W_d^i - \tilde{w}_d^{*,i}$.
- v. We repeat steps (i.) to (iv.) with the next day $d + 1$ until we reach D or $W_d^i = 0$.

2. We average all production values to approximate the option value $\mathbb{L}C_0(x_0, \mathcal{W}_0) \approx \frac{1}{N} \sum_{i=1}^N \mathbb{L}\hat{v}_D^i(W_D^i)$.

Note that in step 1.a.(iv.) we only track a single overall production value $v_d^i(W_d)$ per scenario and do not approximate the entire ACF curve $\hat{v}_d^i(W_d^i)$. But we can nevertheless regain the entire profit-energy curve $\mathbb{L}C_0(x_0, W_0)$ by repeating the algorithm for several different upper bounds $\mathcal{W}_0^{(m)}$ with $m = 1, \dots, M$ and either interpolate the values $\mathbb{L}C_0(x_0, \mathcal{W}_0^{(m)})$ as done in Figure 4.20 or run another curve fitting⁶. Figure 4.20 shows the result of the forward iteration $\mathbb{L}C_0(x_0, W_0)$ for $K = 70$ EUR and three new price scenario sets with 1000 price trajectories each, normalized to the fixed base and peak Future price of 50.59 EUR and 71.85 EUR in March 08. We can see that forward iteration results are fairly close to each other. As indicated by the second sub graph the largest discrepancy between all three sets is less than 10000 EUR compared to corresponding real option value of 0.9 mio EUR which is around 1.1 %. A proper stability test would apply the forward iteration on further sets of price scenarios (e.g. 20) assuming the same Forward price for base and peak. Based on these results we could compute the confidence interval for our estimator of the option value C_0 as a stability measure.

4.4.4. Heuristic Solution

Next, we want to benchmark our valuation model against an energy allocation that is based on a heuristic approach. Recall from equation 4.47 that today's generation amount is dependent on our expectation of the value of the remaining energy from tomorrow onwards (continuation value). This expectation is again dependent on the price we observe today. We described this expectation as a function of the remaining energy and today's price $\mathbb{L}\hat{Y}_{d+1}(X_d, W_{d+1})$ (see equation 4.53). We also computed the value-energy profile for today's generation $\mathbb{L}\hat{Z}_d(X_d, w_d)$ (see equation 4.44) and by comparing both curves we found the best energy allocation for today w_d^* . A heuristic should prevent the complex approximation of the continuation values and assess the dependency between today and the rest of the delivery period with easier rules. For this reason we want to define a simple policy that is based on the following principles

1. Today's maximum energy production w_d (see equation 4.71) can take three different values: (i) enough energy to produce the entire day ($24 \times L_{\max}$) or (ii) only for peak ($12 \times L_{\max}$) hours or (iii) not at all.
2. We extend our MIP from equation 4.12 by an upper energy bound and apply w_d from 1. We reduce the list of available generation schedules by limiting the end states J_d such that an immediate shut down on the next day is always possible (i.e. the power plant was off or runs already for at least 12 hours at midnight on the prior day, see also equation 4.75).

⁶Alternatively we could ignore steps 1.a.(iii) and (iv) and instead run the MIP another time with $w := w_d^{*,i}$ from 1.a.(ii). Then we would use the resulting optimal cash flow $\mathbb{L}z_d^i(w_d^{*,i})$ (see equation 4.42) and new optimal energy allocation w_d^* (see equation 4.43) to update the value function and remaining energy, i.e. $\mathbb{L}v_{d+1}^i(W_d^i - w_d^{*,i}) := \mathbb{L}v_d^i(W_d^i) + \mathbb{L}z_{d+1}^i(\tilde{w}_d^{*,i})$ and $W_{d+1}^i := W_d^i - w_d^{*,i}$.

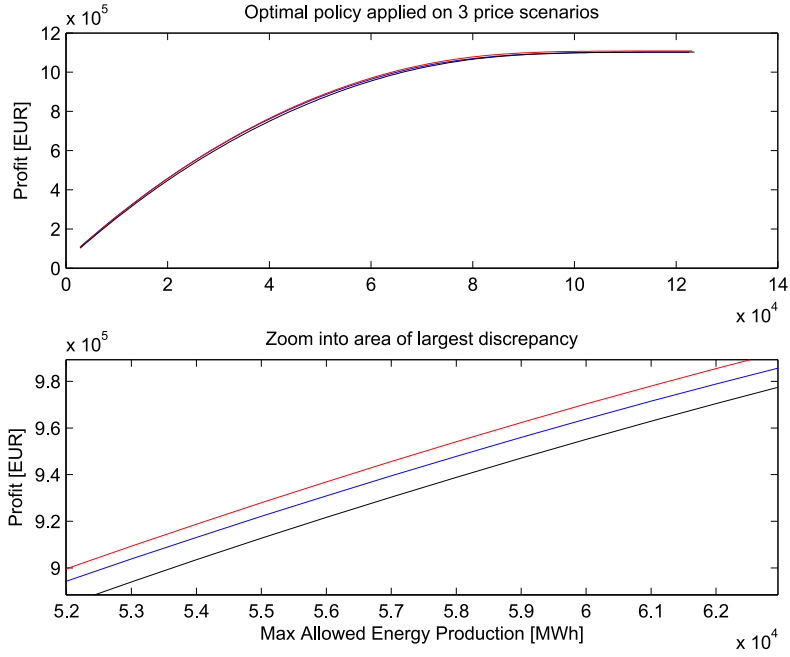


Figure 4.20.: Forward iteration with 3 out-of-sample data sets.

3. We assess the likelihood of today's observed price $X_d^{O/P}$ (see equation 4.67) by relying on the distribution of the average delivery price for the remaining production period $\bar{X}_d^{O/P}$ (see equation 4.68).

4. We relate the percentage that our remaining energy W_d (see equation 4.72) covers of the total potential production for the entire remaining delivery period \bar{W}_d (see equation 4.69) to the likelihood of the price that we observe today. If W_d , for instance, only holds for 10 % of \bar{W}_d , then we will nevertheless produce today if today's price belongs to 10 % of the highest prices that we could have observed today. In other words, the less energy is available, the better the current price scenario has to be before we reduce the available energy even more by producing today.

The heuristic is not dependent on any estimation of the conditional expectation. Instead it runs a local optimization i.e. finds every day's maximum payoff $Z_d := Z_d(X_d, U_d, J_d, w_d)$. This new cash flow definition is based on our initial MIP from equation 4.12 to which we refer for all other variable declarations. We extend the MIP by the energy constraint $I'L_d \leq w_d$

and specific sub sets of start states \mathbb{J}_{off} (see equation 4.75)

$$\begin{aligned}
 Z_d(X_d, U_d, J_d, w_d) &= \max_{L_d, \xi_d, \beta_d^u, \beta_d^o} \{(X_d - KI)'L_d - K_u I' \beta_d^u - K_o I' \beta_d^o\} \\
 &\text{subject to:} \\
 &\quad I' L_d \leq w_d \\
 &\quad L_{\min} \xi_d - L_d \leq 0 \\
 &\quad -L_{\max} \xi_d + L_d \leq 0 \\
 &\quad \Lambda \xi_d \leq 0 \\
 &\quad -I - B \xi_d \leq 0 \\
 &\quad E \xi_d - \beta_d^u \leq 0 \\
 &\quad -E \xi_d - \beta_d^o \leq 0 \\
 &\quad L_d^t \in \{0\} \cup [L_{\min}, L_{\max}] \\
 &\quad \xi_d := \xi_d(U_d, J_d) \\
 &\quad J_d \in \mathbb{J}_{\text{off}} \\
 &\quad \xi_d^t, \beta_d^{o,t}, \beta_d^{u,t} \in \{0, 1\} \\
 &\quad t = -\max\{t_{\text{on}}, t_{\text{off}}\} + 1, \dots, -1, 0, 1, \dots, 24.
 \end{aligned} \tag{4.66}$$

Note that w_d in equation 4.66 is an upper daily energy constraint that we specify according to rule 3 and 4. Hence, we first separate the initial available energy amount W_0 into its peak and off-peak parts $W_0^{O/P}$. We allow a peak production for today, i.e. $w_d = 12L_{\max}$, only if the average of today's peak hour prices X_d^P

$$X_d^{O/P} = \frac{1}{|\mathbb{T}_d^{O/P}|} \sum_{t \in \mathbb{T}_d^{O/P}} x_d^t, \tag{4.67}$$

is above the relevant quantile $q_\beta(\bar{X}_d^P)$, $\beta > 0.5$, of the distribution of the average peak prices for the remaining generation period \bar{X}_d^P

$$\bar{X}_d^{O/P} = \frac{1}{\sum_{n=d}^D |\mathbb{T}_n^{O/P}|} \sum_{n=d}^D \sum_{t \in \mathbb{T}_n^{O/P}} x_n^t, \tag{4.68}$$

where $\mathbb{T}_d^{O/P}$ is the set of peak and off-peak hours respectively at day d and $|\mathbb{T}_d^{O/P}|$ is the number of hours in set $\mathbb{T}_d^{O/P}$. We allow for a full day production $w_d = 24L_{\max}$ only if additionally the same criteria holds true for the off-peak hours X_d^O . These quantiles and hence the threshold for today's production will be higher the less energy is available for the rest of the production period as rule 4 derives the corresponding probability β from the ratio of the remaining available energy at the current stage $W_d^{O/P}$ and the max energy $\bar{W}_d^{P/O}$ that could be potentially produced until the end of the delivery period separated for peak and off-peak hours, i.e.

$$\bar{W}_d^{O/P} = \sum_{n=d}^D |\mathbb{T}_n^{O/P}| L_{\max}. \tag{4.69}$$

Assigning the complementary percentage to β ensures that the corresponding quantile increases the less energy is available (recall that we look at the upper tail of the distribution,

i.e. $\beta > 0.5$)

$$\beta := \beta_d^{O/P} = 1 - \frac{W_d^{O/P}}{\overline{W}_d^{O/P}}. \quad (4.70)$$

In short, w_d is defined as follows

$$w_d := w_d(W_d^O, W_d^P) = \begin{cases} \min\{12 L_{\max}, W_d^P\} & \text{if } X_d^P \geq q_\beta(\overline{X}_d^P), X_d^O < q_\beta(\overline{X}_d^O), \\ \min\{24 L_{\max}, W_d^P + W_d^O\} & \text{if } X_d^P \geq q_\beta(\overline{X}_d^P), X_d^O \geq q_\beta(\overline{X}_d^O), \\ 0 & \text{else.} \end{cases} \quad (4.71)$$

Basically, the current price needs to belong to the best $(1 - \beta)$ percent of all prices in order to allow an energy production for today. For a baseload production both, today's peak and off-peak price $X_d^{O/P}$, need to exceed the quantiles $q_\beta(\overline{X}_d^{O/P})$ of the distribution for both peak and off-peak price band prices of the remaining delivery period. The local maximization searches for the optimal end state J_d^* that maximizes the current cash flow Z_d . It also returns the best schedule L_d^* and thus the remaining energy from tomorrow onwards, i.e. W_{d+1} implicitly defines w_{d+1} (see equation 4.71) and henceforth the optimization problem of the next stage Z_{d+1} with $U_{d+1} = J_d^*$

$$W_{d+1}^{O/P} := W_{d+1}^{O/P}(L_d^*) = W_d^{O/P} - \sum_{t \in \mathbb{T}_d^{O/P}} l_d^{t,*}. \quad (4.72)$$

Recall that w_d is today's upper energy bound whereas the schedule L_d^* describes the *actual* energy production resulting from our local maximization. Thus, the heuristic only determines the *available* production at day d and calculates an optimal *actual* production for it. We solve this MIP in a forward iteration separately for every day $d=0, \dots, D$ and price scenario $i = 1, \dots, I$ starting from the same initial known price $X_0 = x_0$. Hence, for each price scenario we receive the ACF

$$V_0^h(x_0, u_0, \mathcal{W}_0^O, \mathcal{W}_0^P) = \sum_{d=0}^D \max_{J_d} Z_d(X_d, U_d, J_d, w_d), \quad (4.73)$$

whose average is our approximation of the real option value

$$C_0^h(x_0, u_0, \mathcal{W}_0^O, \mathcal{W}_0^P) \approx \frac{1}{I} \sum_{i=1}^I v_0^{h,i}(u_0, \mathcal{W}_0^O, \mathcal{W}_0^P). \quad (4.74)$$

Recall that similar to our model without an energy constraint in equation 4.19 the daily production schedules L_d are linked via the start and end operating state $U_{d+1} := J_d^*$. The main difference is that we ignore the impact of today's end state on tomorrow's admissible schedule candidates when we optimize for Z_d . For this reason we restricted \mathbb{J}_{off} to end operating states that force the power plant to shut-down at least one hour before midnight or to run long enough that it can shut-down the very first hour on the next day, i.e.

$$J_d \in \mathbb{J}_{\text{off}} = \{(1, 0), \dots, (t_{\text{off}}, 0), (0, t_{\text{on}})\}. \quad (4.75)$$

In this way we always ensure a potential immediate shut-down on the next day. This preselection improved the heuristic otherwise the policy often failed on Friday's when the next day

is an entire off-peak day. The resulting smaller set of candidate schedules does still require to track the start operating state U_d since not all combinations of candidate schedules meet the time constraints. Start states (4,0) or (3,0), for instance, guarantee a zero start the next day, but also determine the earliest start hour, in this case 8 or 9 o'clock on the next morning. This is different to our continuous SDP where the set of candidate schedules is even more restricted to schedules that can be freely concatenated.

In order to compare the results with our previous two models we run our heuristic for several initial energy values W_0 and interpolate the results. Table 4.8 summarizes and Figure 4.21 visualizes the numbers for our three models (stochastic C_0 , deterministic/full information C_0^f , heuristic C_0^h) and three different strikes. The columns stand for different upper energy bounds as a percentage of the energy amount \overline{W}_0 from Table 4.7. The results help us to assess the quality of our stochastic dynamic program (SDP). We can see that our SDP performs better than the heuristic only for the itm situation. For the atm and otm case where only fewer hours are in the money the flexibility of the power plant i.e. the optimal dispatch contributes most to the valuation. Obviously the dispatch policy of the heuristic leads to higher cash flows than the SDP⁷. Consequently our set of schedule candidates for the SDP does not cover all relevant dispatches. Recall that our set L622 allows for a production between hour 6 and 22. This is obviously too restricted. In order to show that our SDP is able to return good results even for more flexible power plants if the right schedule set is in place we repeat the same example with half of the on- and off-times, i.e. $t_{\text{on}} = 6$ and $t_{\text{off}} = 4$. In addition we alter our candidate schedules to L723 that contains all schedules between hour 7 and hour 23. Figure 4.22 presents the results. First of all we can observe that in general all three valuation

K		10%	20 %	30%	40%	50 %	60 %	70 %	80 %	90 %	100 %
50	C_0^f	1.047	1.741	2.339	2.8415	3.2489	3.5610	3.7778	3.8997	3.9382	3.9410
	C_0^h	0.948	1.560	2.120	2.6192	3.0376	3.4044	3.6721	3.8184	3.8877	3.9305
	C_0	0.972	1.664	2.263	2.7688	3.1811	3.5001	3.7261	3.8607	3.9129	3.9188
70	C_0^f	0.376	0.614	0.804	0.9477	1.0451	1.1009	1.1257	1.1336	1.1350	1.1352
	C_0^h	0.372	0.580	0.769	0.9150	1.0136	1.0745	1.1086	1.1242	1.1303	1.1330
	C_0	0.335	0.553	0.729	0.8661	0.9675	1.0365	1.0779	1.0971	1.1024	1.1029
90	C_0^f	0	0.097	0.125	0.1478	0.1650	0.1777	0.1867	0.1927	0.1967	0.1991
	C_0^h	0	0	0.118	0.1349	0.1533	0.1688	0.1805	0.1885	0.1939	0.1970
	C_0	0	0.077	0.103	0.1240	0.1403	0.1530	0.1628	0.1701	0.1756	0.1796

Table 4.8.: Option values in mio EUR relative to \overline{W}_0 (forward iteration with new price scenarios)

models return higher option values than in our initial example due to the higher flexibility of the power plant. In particular the shorter run-times allow for intra-day shut-downs during non-profitable hours and thus generate larger cash flows. This time our SDP returns higher option values than the heuristic model throughout the entire energy interval and all strikes. With increasing available energy the simple energy allocation of the heuristic model becomes more and more a weakness. The power plant in this second example has a faster reaction time and therefore can run in smaller time intervals i.e. can generate smaller energy buckets. While the SDP model by design can allocate energy continuously, the heuristic model tends to allocate too much energy on days where smaller energy buckets would be sufficient. Recall that the heuristic only differs between peak, base and no energy allocation. In this way there is less energy left for more beneficial future delivery days. This effect is most apparent for

⁷In Figure 4.12 we put this result into a different perspective when we look at the associated risk of the different dispatch policies. The heuristic turns out to generate also a much higher risk profile.

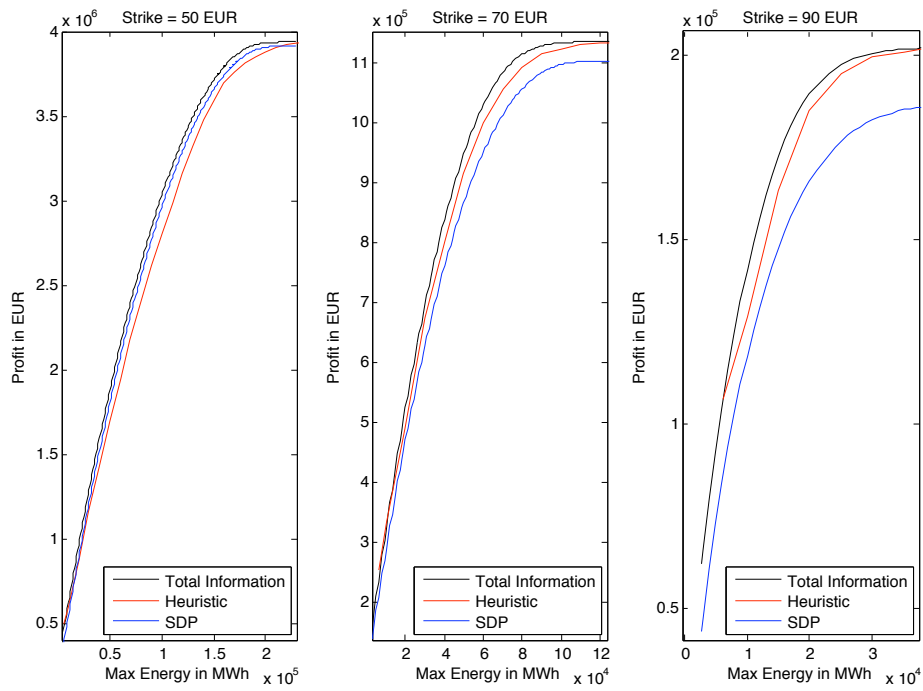


Figure 4.21.: Power plant valuation with $t_{\text{on}} = 12$ and $t_{\text{off}} = 8$ and L622 for the SDP.

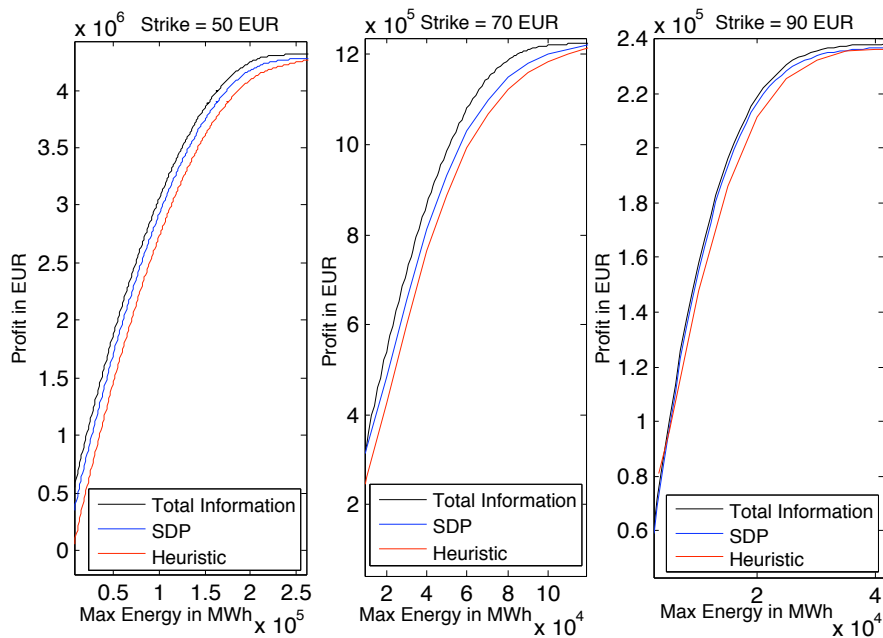


Figure 4.22.: Power plant valuation with $t_{\text{on}} = 6$ and $t_{\text{off}} = 4$ and L723 for the SDP.

the atm situation where hourly prices fluctuate around the strike and dispatching becomes very important. This is where all three models deviate most. As soon as full energy is available the optimization does not need to consider future delivery days any longer and the local optimization of the heuristic model will approximate the results of the model with full information. Thus we observe the largest value deviation among the three models for initial energy bounds between 70 % to 90 % of the total energy.

As an immediate next step for further research we would suggest to investigate different basis functions for the approximation of the continuation value curve in order to address the inaccuracy of our SDP in our first example. Instead of using one set of basis function across all strikes one could rather have different sets. For the itm case, for instance, one could work with linear functions as the power plant is always running and thus the ACF and continuation value are linear with respect to the price. For the atm and otm situation this is not true any longer and one would need to apply a different set. The two examples also illustrated the importance of the candidate schedules. Like for the basis functions one should investigate as well different candidate schedules dependent on the strike.

4.5. Hedge Analysis

Next, we want to apply our discussion about risk controlling from chapter 3 for our power plant model. In particular we want to investigate several hedging alternatives. First, we want to look at a Forward and volumetric hedge before we try to find an appropriate swing contract that will help us to cover the spot price risk. The former requires the calculation of Forward deltas and the latter the computation of spot deltas. For this reason we will focus first on the computation of these sensitivities (see section 3.3.2 and 3.3.4 for a detailed description of the relevant figures). Let us first look at the Forward deltas. We focus on peak prices and thus the peak Forward delta since dispatching will mainly fall into peak hours especially for two (atm, otm) of our three scenarios (recall that the peak Futures price in our example is $g_0 = 70.85$ EUR). We apply equation 3.45, where $C_0^*(x_0, g_0, \delta)$ will be replaced by our three valuation models, i.e. stochastic $C_0 := C_0(x_0, W_0)$, deterministic $C_0^f := C_0^f(x_0, W_0)$ and heuristic approach $C_0^h(x_0, u_0, \mathcal{W}_0^O, \mathcal{W}_0^P)$ and we calculate Δ^F for all grid points W^r . Figure 4.23 visualizes the interpolated results and Tables 4.9 to 4.11 show the actual figures for dedicated energy values and all three strikes in column 4. All sub graphs are trimmed to the core generation domain $[\underline{W}_0, \overline{W}_0]$ (see also equation 4.64). Hence, the most right energy value on each curve refers to the 100 % available energy \overline{W}_0 in Tables 4.9 to 4.11. Beyond that value all curves will still slightly grow due to some (but not any more all) scenarios that still provide a higher cash flow through a larger production. To be precise, the graphs show the MWDelta

$$\Delta_{\text{MW}}^F := \frac{\Delta^F}{|\mathbb{T}_F|}, \quad (4.76)$$

i.e. the Forward delta divided by the delivery hours $|\mathbb{T}_F|$ of the Forward (see also section 3.3.1 for a detailed discussion). Recall that the MWDelta can be interpreted as the capacity in MW that the Forward will provide every hour during delivery. This figure allows for a direct comparison with the maximum capacity of our power plant which is $L_{\max} = 530$ MW. Most apparent in Figure 4.23 is the almost linear relation of the Forward MWDelta with respect to the available energy W_0 across all option models and strikes except for W_0 close to \overline{W}_0 where by definition the cash flows and thus the delta will not change any longer. This linear behavior is mainly caused by the mean reversion. It ensures that the electricity prices

are mainly driven by the seasonal daily shapes. In our example all shapes are identical on weekdays. Thus, all weekday schedules will look similar and resemble flat peak schedules. With increasing available energy, more of these daily peak schedules will be concatenated. As prices are similar between weekdays due to the normalization, the power plant value is mainly a linear function of the available energy as long as there are still unused weekdays and so is the Forward delta. The blue line indicates the delta based on the model with full information

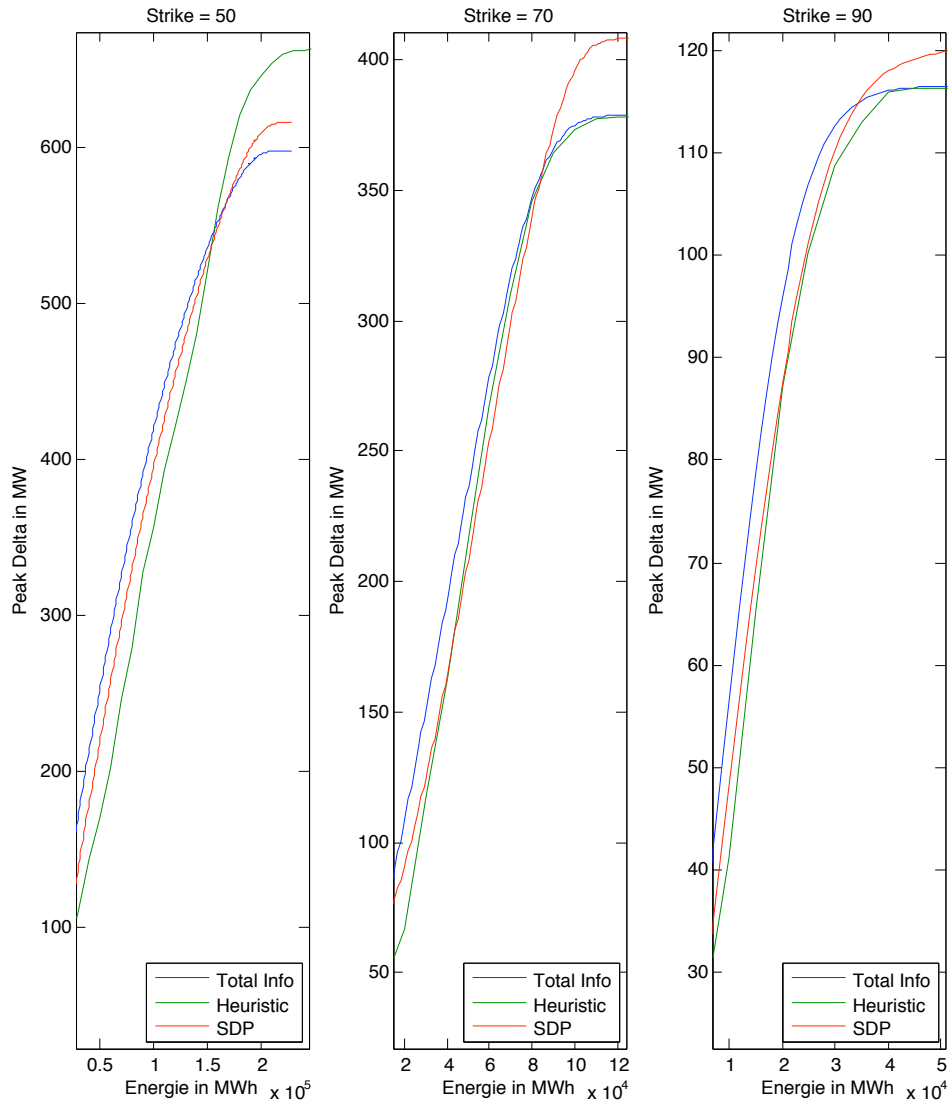


Figure 4.23.: Forward deltas for all three valuation models and strikes

about future prices C_0^f . We can see that our stochastic model (from now on we abbreviate it with SDP) is below this line until full energy is available. Then it is significantly above the blue line. Recall that the Forward delta is a value hedge. High deltas stand for large value changes which usually result from large energy amounts (the larger the energy amount the more small price shifts change the asset value) or high production flexibility (small price shifts suddenly lead to entirely new dispatch profiles and thus different energy amounts). In this sense the small delta of our SDP before full production indicates that our SDP tends to produce not enough for the given initial energy amount. This observation lets us assume

that the approximated continuation values are rather too high and prevent more variability in the production. On the other hand, the SDP Forward delta is too high in case of nearly full energy availability ($W_0 = \overline{\overline{W}}_0$). This becomes most obvious in direct comparison with the Forward delta based on the power plant model without energy constraints $C_0^r := C_0(x_0, u_0)$ with $C_0 := C_0(x_0, u_0)$ from equation 4.26 and values in Table 4.6. The figure can only serve as an upper reference value as by definition we cannot restrict C_0^r to $\overline{\overline{W}}_0$. For $K = 70$ MW and full energy amount we observe Δ^F for $C_0 = 409$ MW that is even larger than Δ^F for C_0^r with 384 MW. Evidently, our SDP requires more energy, but nevertheless returns a smaller real option value. Thus, the introduction of an energy constraint and the related approximation schemes entail a loss in accuracy and energy efficiency. For $K = 50$ MW we see that all Forward deltas clearly exceed the maximum hourly capacity of $L_{\max} = 530$ MW. Recall from section 3.3.2 that different to the volumetric hedge the Forward delta as a value hedge can indeed be higher than the max capacity of the power plant to compensate for the flexibility and thus the non-linearity of the option value (a contract with fixed delivery will instead always have a delta that matches the delivery schedule). The fact that for $K = 50$ and $W_0 = \overline{\overline{W}}_0$ the Forward delta for our heuristic is even higher than our SDP (Δ^F for C_0 is 606 MW and Δ^F for C_0^h is 670 MW) stands for a small energy efficiency and corresponds to our observation from Table 4.8 that the heuristic performs worst of all models for $K = 50$. In general the delta results are consistent with the option values. For instance we see that the deltas of our heuristic and full information match for high W_0 . Likewise we observe similar option values C_0^h and C_0^f .

K	W_0		Δ_{MW}^F	$\Delta_{\text{MW}}^{9-11}$	Δ_{MW}^{12}	$\Delta_{\text{MW}}^{13-16}$	$\Delta_{\text{MW}}^{17-20}$
50	30 %	C_0^f	207	181	306	124	260
		C_0^h	176	160	47	67	298
		C_0	173	132	210	109	236
		C_0^s	206	230	480	19	263
	50 %	C_0^f	310	293	438	203	369
		C_0^h	321	234	406	248	408
		C_0	279	248	366	189	342
		C_0^s	300	338	607	105	346
	70 %	C_0^f	395	389	534	269	459
		C_0^h	402	335	576	297	478
		C_0	369	353	480	258	434
		C_0^s	378	421	702	183	416
	100 %	C_0^f	597	513	617	351	567
		C_0^h	670	552	579	405	597
		C_0	606	498	584	347	549
		C_0^s	570	526	760	286	503
		C_0^r	643	749	756	447	696

Table 4.9.: MW deltas for different upper energy bounds relative to $\overline{\overline{W}}_0$ and strike $K = 50$ EUR

Next, we proceed with the spot delta. As motivated in section 3.3.4 we are not interested in the sensitivity with respect to today's spot price only and therefore introduced the notion of the synthetic spot delta in equation 3.53. Consequently, we need to aggregate neighboring spot prices to new artificial products p . We decided to group the individual peak spot prices into four blocks $p \in \{9 - 11, 12, 13 - 16, 17 - 20\}$. We grouped those hours together that are highly correlated. From our correlation analysis of the weekday prices in Figure 4.6 we saw that the noon price stands out, but the remaining peak prices can be bundled together.

K	W_0		Δ_{MW}^F	Δ_{MW}^{9-11}	Δ_{MW}^{12}	Δ_{MW}^{13-16}	Δ_{MW}^{17-20}
70	30 %	C_0^f	189	155	339	90	246
		C_0^h	163	121	355	53	224
		C_0	160	118	288	81	213
		C_0^s	204	228	472	17	263
	50 %	C_0^f	302	289	469	179	361
		C_0^h	310	256	517	199	375
		C_0	281	234	484	180	335
		C_0^s	293	337	589	95	340
	70 %	C_0^f	368	387	495	234	425
		C_0^h	364	374	472	246	420
		C_0	379	351	622	252	430
		C_0^s	357	417	639	158	400
	100 %	C_0^f	379	406	500	239	435
		C_0^h	379	407	501	238	435
		C_0	409	405	638	269	459
		C_0^s	387	473	616	184	429
C_0^r		384	411	520	245	437	

Table 4.10.: MW deltas for different upper energy bounds relative to \overline{W}_0 and strike K = 70 EUR

K	W_0		Δ_{MW}^F	Δ_{MW}^{9-11}	Δ_{MW}^{12}	Δ_{MW}^{13-16}	Δ_{MW}^{17-20}
90	30 %	C_0^f	116	92	217	34	167
		C_0^h	116	93	214	34	167
		C_0	118	85	227	40	169
		C_0^s	141	156	333	-12	200
	50 %	C_0^f	116	93	216	34	168
		C_0^h	116	93	214	34	168
		C_0	120	91	222	40	173
		C_0^s	144	161	331	-12	204
	70 %	C_0^f	116	93	216	34	168
		C_0^h	116	93	214	34	168
		C_0	120	91	222	40	173
		C_0^s	144	161	331	-12	204
	100 %	C_0^f	116	93	216	34	168
		C_0^h	116	93	214	34	168
		C_0	120	91	222	40	173
		C_0^s	144	161	331	-12	204
		C_0^r	117	90	230	34	167

Table 4.11.: MW deltas for different upper energy bounds relative to \overline{W}_0 and strikes K = 90 EUR

Hence, the resulting Taylor series representation looks as follows

$$\begin{aligned}
 V_0^*(x_0, g_0, \delta) &:= C_0^*(x_0, g_0, \delta) + \Delta^{9-11}(X_{9-11} - h_{9-11}) + \Delta^{12}(X_{12} - h_{12}) \\
 &\quad + \Delta^{13-16}(X_{13-16} - h_{13-16}) + \Delta^{17-20}(X_{17-20} - h_{17-20}) + \epsilon
 \end{aligned} \tag{4.77}$$

Note that we are interested in the MWDelta (see section 3.3.1) and therefore divide the sensitivity by the associated number of delivery hours $|\mathbb{T}_p|$ and we abbreviate

$$\Delta_{\text{MW}}^p := \frac{\Delta^p}{|\mathbb{T}_p|}, \tag{4.78}$$

where \mathbb{T}_p is the set of all hours of the delivery period that belong to product p . We compute these MWDeltas for all our models and replace $V_0^*(x_0, g_0, \delta)$ and $C_0^*(x_0, g_0, \delta)$ in equation 3.53 accordingly: for our power plant with full information by $V_0^f(x_0, \mathcal{W}_0)$ and $C_0^f(x_0, \mathcal{W}_0)$, for our heuristic by $V_0^h(x_0, u_0, \mathcal{W}_0^O, \mathcal{W}_0^P)$ and $C_0^h(x_0, u_0, \mathcal{W}_0^O, \mathcal{W}_0^P)$, for our SDP with and without energy constraint, by $V_0(x_0, \mathcal{W}_0)$, $C_0(x_0, \mathcal{W}_0)$, $V_0^r(x_0, u_0)$ and $C_0^r(x_0, u_0)$, and for a swing option with the same hourly capacity as our power plant i.e. $L_{\max} = 530$ MW by $V_0^s := V_0(x_0, N)$ and $C_0^s := C_0(x_0, N)$ (see equations 2.3 and 2.9). We ran the calculation for all three strikes and ten different upper energy bounds W_0 starting from 10 % to 100 % of \overline{W}_0 . For the swing option we translate the different upper energy bounds into different number of swing rights via $N = W_0/L_{\max}$. Only for $W_0 = \overline{W}_0$, i.e. full available energy, we compute the MWDelta for our real option model without energy constraint C_0^r . Tables 4.9 to 4.11 present and Figure 4.24 visualizes the results for the three different strikes. For readability we only plotted two option models: our SDP vs. our deterministic model (full information). The deterministic model is always the line of the same color pair that starts more to the left. Each color stands for one of the synthetic products. Thus, for small energy amounts W_0 the synthetic spot delta of our SDP is always smaller throughout all price blocks and strikes. We interpret the spot MWDelta as the average capacity in MW during the associated product hours. The deltas of the deterministic model represent the best allocation. For large W_0 and $K = 70$ and $K = 90$ the SDP returns higher deltas than the deterministic model except for the first block (9-11). This is an indication of an inefficient energy allocation of our SDP for these blocks. In general, the shape for all curves is similar to the ones of the Forward delta in Figure 4.23 and can be explained analogously by the mean reversion character and the identical weekend and weekday patterns of the prices. With increasing available energy W_0 there are more production days (i.e. less 0 MW days) and consequently the average hourly capacity increases. However, the fact that the spot MWDeltas for different price blocks drift apart with increasing strike shows that the average capacity does not increase equally across all hours. Especially the outstanding delta curve for hour 12 underlines its particular value contribution to the daily production schedule. The high delta also indicates large value changes due to high volatility and spikiness of hour 12. It is also the only curve that does not increase monotonously, but briefly falls before it converges to a fixed delta value. Apparently its contribution to the overall asset value will be partially compensated by the other price blocks as soon as the full or almost entire energy amount is available.

In general we can state that the more distinct the spot deltas mutually differ the better is the classification of the corresponding price blocks. For the itm situation the power plant produces a baseload schedule and the deltas of the different blocks are close to each other. The small difference is only originated in the different price variations. With rising strike the dispatch decision becomes more important and we can see that the delta and hence average production varies between blocks. Block 13-16 for instance has always the smallest delta which can be explained best by the seasonal shape. Reviewing Figure 4.3 we see that the

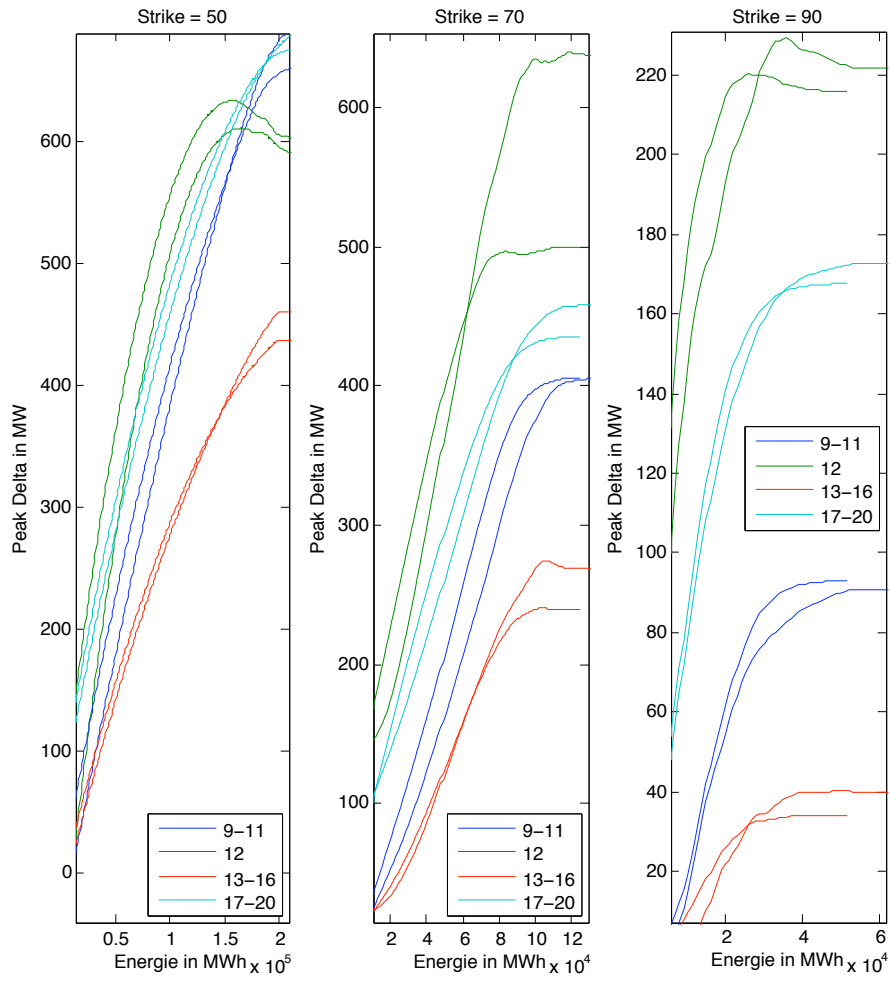


Figure 4.24.: Spot deltas calculated via SDP and total information.

price usually goes down after noon and will only go up again in the evening. Consequently there is less production during these hours and hence a smaller delta.

Next, we want to use these spot deltas to specify a swing option contract that a power plant owner can sell to other market participants in order to offset the spot price risk of his generation asset. We denote the swing option with $C_0^{s,*} := C_0^{s,*}(x_0, N, L)$ (see also equation 2.3 with L implicitly set to 1) where x_0 is the current spot price, N the number and L the size of the swing rights. First, we will work with a general description of the power plant $C_0^*(x_0, \mathcal{W}_0, \delta)$ where \mathcal{W}_0 is the initial energy amount and δ is a parameter vector covering all technical constraints of the specific power plant. We will soon replace this general description with our different implementation models. We set up a hedge portfolio C_0^H consisting of a long position in the power plant and a short position in the swing option

$$C_0^{H,*}(x_0, \mathcal{W}_0, N, L, \delta) := C_0^*(x_0, \mathcal{W}_0, \delta) - C_0^{s,*}(x_0, N, L). \quad (4.79)$$

In particular, we are interested in the number of swing rights N and swing size L that the swing option should carry. As a measure for the risk mitigation we want to use our definition of EaR. Recall that EaR is based on the distribution of the difference of the potential, i.e. ACF, versus the expected cash flow of an option value after a Forward hedge. For this purpose we first need the definition of the ACF for our hedge portfolio which is the difference of the ACFs of the two underlying contracts

$$V_0^{H,*}(x_0, \mathcal{W}_0, N, L, \delta) := V_0^*(x_0, \mathcal{W}_0, \delta) - V_0^{s,*}(x_0, L, N), \quad (4.80)$$

with $V_0^{s,*} := V_0^{s,*}(x_0, L, N)$ as defined in equation 2.9 with $L = 1$ and $V_0^*(x_0, \mathcal{W}_0, \delta)$ being a general description of the ACF of a power plant with energy constraint that we will replace with our different implementation models (see for instance equation 4.48). Then EaR of our hedge portfolio is the β -quantile of the remaining spot price exposure ϵ^H after a Forward hedge

$$\epsilon_H(x_0, g_0, \mathcal{W}_0, N, L, \delta) := V_0^{H,*}(x_0, \mathcal{W}_0, N, L, \delta) - C_0^{H,*}(x_0, \mathcal{W}_0, N, L, \delta) - \Delta^F(F_0 - g_0), \quad (4.81)$$

with Δ^F as the Forward delta according to equation 3.45. In short, the objective is to find the number of swing rights N and swing size L for a hedge portfolio with given initial energy amount \mathcal{W}_0 that will minimize respectively maximize the EaR figure dependent on whether we look at a buyer's or seller's situation i.e. whether β is greater or smaller than 0.5

$$\begin{aligned} \max_{N,L} q_\beta^B &:= \max_{N,L} q_\beta(\epsilon_H(x_0, g_0, \mathcal{W}_0, N, L, \delta)), \quad \beta < 0.5 \\ \min_{N,L} q_\beta^S &:= \min_{N,L} q_\beta(\epsilon_H(x_0, g_0, \mathcal{W}_0, N, L, \delta)), \quad \beta > 0.5. \end{aligned} \quad (4.82)$$

Different to the last chapter we are not interested in a dynamic strategy that looks for appropriate dispatch decisions during delivery as we want to sell the swing contract in advance of the actual production period (see also the distinction between *before* and *in* delivery in our introductory example in section 3.1). Note that the objective focuses on the risk measure only. A further consideration of the expected value of the portfolio in terms of a mean-risk analysis is not necessary. The reduction of the real option value through selling the power plant production via the swing option is compensated by the cash of the same amount that we earn for the sale. So only the deviation from this option premium i.e. expected value $C_0^{*,s}$ implies a potential loss and therefore is only relevant for this investigation. This is exactly

represented by ϵ_H . We want to introduce a heuristic to solve equation 4.81 that will be useful for a comparison once a proper solution becomes available. The straightforward approach uses a combination of a Forward and swing contract. We will call this approach a *volumetric* hedge as it follows the basic idea in section 3.3.3. The Forward contract would cover the minimum capacity L_{\min} once the power plant is running. The corresponding volume delta (see also equation 3.50) is then simply the number of the Forward contract delivery hours T^F multiplied by L_{\min}

$$\Delta^w := T^F L_{\min}. \quad (4.83)$$

In our case this is a peak Forward as our power plant mainly runs during peak hours in the atm ($K=70$) and otm case ($K = 90$). The further schedule profile above L_{\min} will be covered by a swing option with swing size $L^{vol} := L_{\max} - L_{\min}$. The relevant number of swings will be derived from the remaining energy amount after subtracting the energy of the Forward contract Δ^w from the initially available energy \mathcal{W}_0

$$N^{vol} := \lfloor \frac{\mathcal{W}_0 - \Delta^w}{L^{vol}} \rfloor, \quad (4.84)$$

where the symbol $\lfloor \cdot \rfloor$ stands for rounding to the closest lower integer. Then the relevant residual for computing the quantile according to equation 4.81 looks as follows

$$\begin{aligned} \epsilon_H^{vol}(x_0, \mathcal{W}_0, g_0, N^{vol}, L^{vol}, \delta) &:= V_0^{H,*}(x_0, \mathcal{W}_0, L^{vol}, N^{vol}) - C_0^{H,*}(x_0, \mathcal{W}_0, N^{vol}, L^{vol}, \delta) \\ &\quad - \Delta^w(F_0 - g_0). \end{aligned} \quad (4.85)$$

You will find the corresponding figures in column 4 and 5 of Table 4.12. The technical constraints of a power plant, however, make it less flexible than a swing option with the same amount of producible energy and therefore the volumetric hedge is not the most efficient hedge. We want to rather account for the inflexibility by reducing the number of swing rights below the total available energy. This is where our synthetic spot delta comes into play. The idea is to compare the spot deltas for both the power plant $\Delta_{\mathcal{W}_0}^p$ and the swing option Δ_N^p and find the number of exercise rights and size where both spot deltas fit best. The figures $\Delta_{\mathcal{W}_0}^p$ and Δ_N^p will be calculated according to equation 3.53 by replacing $V_0^*(x_0, g_0, \delta)$ with $V_0^*(x_0, \mathcal{W}_0)$ and $V_0^{s,*}(x_0, 1, N)$ respectively for each artificial product p. Note that we calculate the spot delta for the swing option with size $L=1$. By adjusting the swing size after the delta calculation we can make the swing spot delta fit the power plant spot delta

$$L^p(\mathcal{W}_0, N) := \frac{\Delta_{\mathcal{W}_0}^p}{\Delta_N^p}. \quad (4.86)$$

Note that we adjust the swing size for each artificial product p individually. Next we look for the common swing size across all artificial products that has the smallest absolute difference from the individual spot deltas. This is exactly the definition of the median

$$\bar{L}(\mathcal{W}_0, N) := \arg \min_x \sum_{p=1}^P |L^p(\mathcal{W}_0, N) - x|. \quad (4.87)$$

Finally we look for the number of swing rights whose median fits all P spot deltas best. This

is the approximated optimal swing number

$$\hat{N}^*(\mathcal{W}_0) := \arg \min_N \sum_{p=1}^P \left| L^p(\mathcal{W}_0, N) - \bar{L}(\mathcal{W}_0, N) \right|. \quad (4.88)$$

The optimal swing size can then be directly derived as

$$\hat{L}^* := \bar{L}(\mathcal{W}_0, \hat{N}^*). \quad (4.89)$$

The underlying rationale is that a close match of the spot delta positions between the power plant and the swing option should indicate a good hedge of the spot risk and thus of EaR. The algorithm runs as follows

1. Compute synthetic spot deltas $\Delta_{\mathcal{W}_0}^p$ according to equation 3.53.
2. For each swing option $N = 1, \dots, T$ with T being the maximum number of production hours
 - a) Compute synthetic spot deltas Δ_N^p with fixed swing size $L_{\max} = 1$ according to equation 3.53.
 - b) Divide each spot delta Δ_N^p , $p = 1, \dots, P$, by the power plant's spot delta $\Delta_{\mathcal{W}_0}^p$ of the same product p according to equation 4.86.
 - c) Compute the median $\bar{L}(\mathcal{W}_0, N)$ of the adjusted spot deltas according to equation 4.87.
3. Out of all T swing options pick the one whose median has the smallest total absolute differences to its individual spot deltas (see equation 4.88). This is $\hat{N}^*(\mathcal{W}_0)$. The corresponding median is \hat{L}^* (see equation 4.89).

We apply this algorithm for four initial energy bounds (\mathcal{W}_0 is 30 %, 50 %, 70 % and 100 % of \bar{W}_0) and all three strikes ($K = 50, 70, 90$) and receive the corresponding quantiles \hat{q}_β^* . We also compute the quantiles for the volumetric hedge q_β^{vol} with N^{vol} and L^{vol} . Finally we compare both with the quantile q_β^* based on the optimal hedge

$$\begin{aligned} q_\beta^{vol} &:= q_\beta(\epsilon_H^{vol}, x_0, g_0, \mathcal{W}_0, N^{vol}, L^{vol}, \delta) \\ \hat{q}_\beta^* &:= q_\beta(\epsilon_H, x_0, g_0, \mathcal{W}_0, \hat{N}^*, \hat{L}^*, \delta) \\ q_\beta^* &:= q_\beta(\epsilon_H, x_0, g_0, \mathcal{W}_0, N^*, L^*, \delta). \end{aligned} \quad (4.90)$$

We compute the optimal hedge via full enumeration, i.e. we generate the distribution of the hedge portfolio for all $N = 1, \dots, T$ and all L and look for the smallest quantile that defines N^* and L^* . This can become cumbersome for large N and in particular for large L . Recall from Figure 4.24 and our introductory example in section 3.1 that the spot delta can exceed the maximum capacity of the power plant L_{\max} . The analysis of our particular example revealed that none of the spot deltas exceeds twice the maximum capacity. Therefore the full enumeration runs on the interval $L \in [1, 2 \cdot L_{\max}]$. If we apply a granularity of $\Delta N = 1$ and $\Delta L = 1$ MW, then the full enumeration requires $T \times 2L_{\max} \times I$ revaluations of the hedge portfolio to receive the optimal quantile with I being the number of price trajectories. Our heuristic instead finds L directly and therefore can prevent the additional enumeration over $2L_{\max}$. In order to understand how much the gain in computation time results in a lack of accuracy we introduce the approximation error R as the relative deviation of the approximated

from the optimal quantile

$$R := \frac{|\hat{q}_\beta^* - q_\beta^*|}{|q_\beta^*|}, \quad (4.91)$$

and we denote with m_R and s_R the sample mean and standard deviation of the estimation error. We retrieve the relevant sample points using 100 out-of-sample price paths. We apply our heuristic to find the (\hat{N}^*, \hat{L}^*) pairs that define the relevant swing contract and the corresponding \hat{q}_β^* . Then we compute the optimal pair (N^*, L^*) and related quantile q_β^* via full enumeration over N and L . We run this calculation separately for our three different valuation models, So we replace $V_0^*(x_0, \mathcal{W}_0, \delta)$ with the true stochastic program $C_0(x_0, \mathcal{W}_0)$, the heuristic model $C_0^h(x_0, u_0, \mathcal{W}_0^O, \mathcal{W}_0^P)$ and the deterministic valuation $C_0^f(x_0, \mathcal{W}_0)$. Table 4.12 summarizes the results.

K	W_0	Model	$q_{0.05}^{\text{vol}}$	$q_{0.95}^{\text{vol}}$	$q_{0.05}^*$	$q_{0.95}^*$	$\hat{q}_{0.05}^*$	$\hat{q}_{0.95}^*$	m_R	s_R
50	30%	C_0^f	-2.650	2.674	-1.233	1.035	-1.263	1.061	2.9%	0.41%
		C_0^h	-4.433	4.344	-3.929	3.782	-4.045	3.894		
		C_0	-2.516	2.520	-1.388	1.336	-1.426	1.371		
	50%	C_0^f	-2.460	2.284	-1.683	1.697	-1.725	1.742	2.7%	0.35%
		C_0^h	-3.586	3.068	-2.938	3.062	-3.017	3.151		
		C_0	-2.391	2.184	-1.679	1.632	-1.725	1.689		
	70%	C_0^f	-2.601	2.251	-2.044	1.870	-2.09	1.907	2.2%	0.29%
		C_0^h	-3.254	3.026	-3.023	2.405	-3.087	2.451		
		C_0	-2.556	2.289	-2.231	1.997	-2.278	2.033		
	100%	C_0^f	-2.534	2.404	-2.136	1.954	-2.182	1.991	2.0%	0.25%
		C_0^h	-2.793	2.823	-2.644	2.791	-2.694	3.046		
		C_0	-2.752	2.541	-2.261	2.025	-2.315	2.067		
70	30%	C_0^f	-1.154	1.323	-1.169	1.321	-1.201	1.356	2.7%	0.22%
		C_0^h	-2.054	1.939	-1.799	1.848	-1.844	1.894		
		C_0	-1.490	1.492	-1.427	1.337	-1.463	1.371		
	50%	C_0^f	-2.866	2.903	-1.224	1.147	-1.264	1.18	2.9%	0.27%
		C_0^h	-3.123	3.001	-1.822	1.711	-1.872	1.759		
		C_0	-2.924	2.757	-1.714	1.326	-1.764	1.364		
	70%	C_0^f	-2.168	2.231	-1.240	0.911	-1.273	0.942	3.1%	0.32%
		C_0^h	-2.766	2.312	-2.325	1.371	-2.394	1.407		
		C_0	-2.638	2.192	-1.873	1.263	-1.932	1.304		
	100%	C_0^f	-1.855	1.712	-1.234	0.891	-1.272	0.923	3.4%	0.35%
		C_0^h	-2.825	2.131	-1.944	1.204	-2.015	1.246		
		C_0	-2.438	1.955	-1.762	1.127	-1.832	1.169		
90	30%	C_0^f	-0.605	0.707	-0.516	0.605	-0.622	0.731	3.1%	0.29%
		C_0^h	-0.992	1.042	-0.861	1.002	-0.882	1.136		
		C_0	-0.711	0.739	-0.632	0.661	-0.733	0.758		
	50%	C_0^f	-0.711	0.843	-0.666	0.803	-0.736	0.831	3.5%	0.35%
		C_0^h	-0.941	1.260	-0.930	1.067	-0.974	1.305		
		C_0	-0.918	0.843	-0.867	0.830	-0.954	0.872		
	70%	C_0^f	-0.763	0.955	-0.737	0.926	-0.789	0.959	3.6%	0.41%
		C_0^h	-1.296	1.135	-1.228	1.105	-1.269	1.176		
		C_0	-1.006	1.023	-0.993	0.995	-1.025	1.027		
	100%	C_0^f	-0.829	1.141	-0.811	1.106	-0.861	1.184	3.8%	0.45%
		C_0^h	-1.303	1.358	-1.296	1.212	-1.342	1.416		
		C_0	-1.108	1.189	-1.062	1.122	-1.101	1.163		

Table 4.12.: EaR values in multiples of 100,000 EUR

Before we look at the effect of the different hedge portfolios, let us first start a direct comparison of the valuation models across all computed quantiles. The quantiles of the heuristic valuation approach C_0^h clearly stand out with the worst performance throughout all strikes, hedge type and available energy amount. The left and right quantile are always the highest in absolute terms. This is most obvious for $K = 50$ and $\mathcal{W}_0 = 0.3\overline{\overline{W}}_0$ with $q_{0.05}^{vol}(C_0^h) = 0.44$ mio EUR for the heuristic vs. $q_{0.05}^{vol}(C_0^f) = 0.26$ mio EUR for the deterministic vs. $q_{0.05}^{vol}(C_0) = 0.25$ mio EUR for the stochastic model. In this case the heuristic policy produces a 75 % higher risk than the other two models. This observation tarnishes the good results we received in the previous section in terms of the expected value (see Table 4.8 and Figure 4.21). We assume that the heuristic's simple energy allocation rule assigns daily energy less cautious and therefore results in more extreme cash flows. Comparing the cash flows of identical price trajectories among the different valuation models should help to verify this assumption, but was beyond the scope of our analysis. Comparing the hedge types we can see that the swing

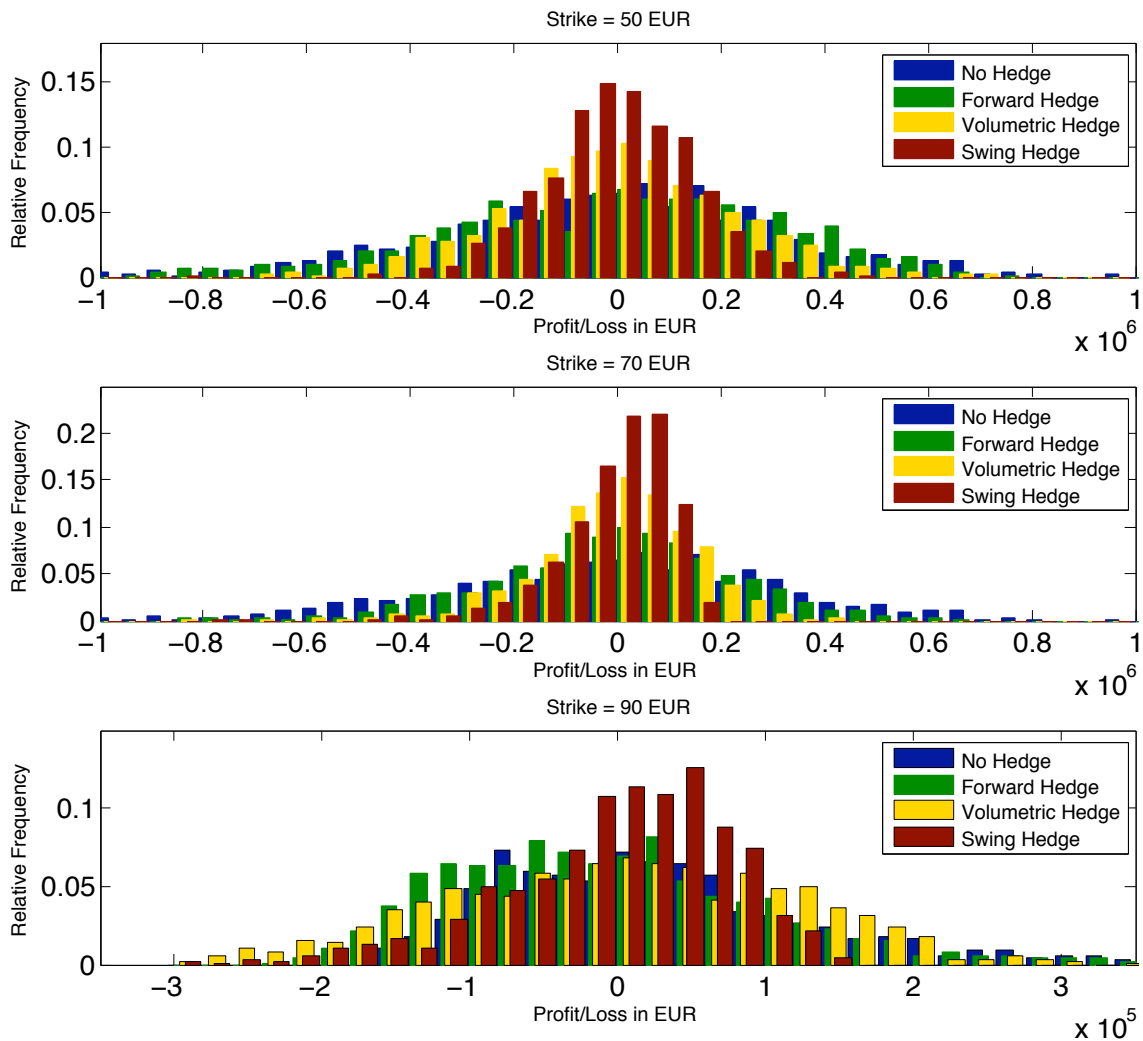


Figure 4.25.: Profit and loss histogram for 70 % of total energy $\overline{\overline{W}}_0$

hedge q_β^* and \hat{q}_β^* respectively clearly prevails the volumetric hedge q_β^{vol} across all strikes and different energy restrictions. Figure 4.25 illustrates this effect by a further comparison with the non-hedged and Forward hedged position. We see the hedge portfolio distributions for 70

% of the total energy amount \overline{W}_0 and all three strikes (recall from Table 4.8 and Figure 4.21 that energy amounts between 50 % and 70 % of the total possible production \overline{W}_0 benefit most from the power plant flexibility). The distributions were generated with our SDP model⁸. Not surprisingly, all hedges significantly reduce the quantile compared to the non-hedged position. For $K = 70$ EUR, for instance, the unprotected power plant value returns a quantile of - 0.571 mio EUR. Already the Forward delta hedge reduces the potential loss by 30 % to -0.397 mio EUR. This figure will be again reduced by 33 % to -0.2638 mio EUR through the volumetric hedge. The swing hedge allows yet another reduction of the potential loss by nearly 30 % to - 0.183 mio EUR. The graphs show that this effect is actually smaller for itm ($K=50$) and otm ($K=90$) power plants. The reason is that for $K = 50$ EUR the optimal (N^*, L^*) pair for the swing hedge is close to (T, L_{\max}) as the power plant will produce almost every hour at full capacity. In this situation of almost no change in produced energy the volumetric hedge is very efficient. The swing hedge still returns a slightly smaller quantile as our set of candidate schedules $L622$ allows for a production during non-peak hours (hour 6,7,21 and 22) that is not covered by the peak Forward contract of the volumetric hedge. We observe a similar situation for $K = 90$ EUR. A swing option with full exercise rights will only exercise at few itm hours. Again, the produced energy amount hardly varies and therefore the volumetric hedge already returns good results and the swing hedge can only provide a minor improvement.

Finally let us look at the swing hedge only and compare the quantiles based on the heuristic (\hat{N}^*, \hat{L}^*) versus the optimal selection (N^*, L^*) . The last two columns in Table 4.25 provide the estimation error of our heuristic according to equation 4.91 based on 100 out of sample price sets with 1000 trajectories each. We can see that the average estimation error m_R and standard deviation s_R becomes worse with increasing strike. The range is between $m_R = 2\%$, $s_R = 0.25\%$ for $K = 50$ and $m_R = 3.8\%$, $s_R = 0.45\%$ for $K= 90$ and is originated in the nature of our numerical approach. Recall that the input data to the Longstaff-Schwartz regression are only itm(!) price-cash flow pairs (X_d, V_d) , i.e. X_d has to be larger than the strike. For high strikes like $K = 90$ there are not many price-cash flow pairs left (our in depth analysis revealed situations with not more than 20 data pairs) which makes the regression less accurate. The average estimation error also increases with more available energy W_0 except for $K = 50$ where we observe the opposite. For $K = 50$ and 100 % available energy we observe the smallest approximation error and standard deviation. Recall that we need to find the (N^*, L^*) pair for the swing option that reduces the hedge portfolio's quantile best. For $K = 50$ both, the power plant and the swing option are deep in the money and thus we observe full production i.e. $N^* = T$. Analyzing the actual pairs (N^*, L^*) and (\hat{N}^*, \hat{L}^*) we indeed observe $N^* = \hat{N}^* = T$ and only see variability in L^* and \hat{L}^* which makes the approximation of our heuristic more accurate. We have a similar situation for small energy amounts like $W_0 = 30\% \overline{W}_0$. The available energy is so small that only few itm hours are used for the production. So again, there is not a large variation in the number of hours N and we only see changes in L^* and \hat{L}^* which keeps m_R and s_R small. However, with increasing available energy and especially increasing strike the actual production will vary more and therefore we see more variations in N^* as well which makes the approximation \hat{N}^* more difficult. Still with an approximation error of less than 4 % overall the heuristic performs very well. The main reason is that different (N, L) combinations still lead to similar quantiles q_β . Therefore (\hat{N}^*, \hat{L}^*) do not need to match exactly (N^*, L^*) to get \hat{q}_β^* close to q_β^* . Finally, we want to remark that the approximation error does not vary between the different valuation models that's why we did not provide m_R, s_R figures by valuation model. The reason is that the heuristic tries to match the spot deltas between the power plant and the swing option and does not care based on which model these deltas were calculated. As a summary we can

⁸In Appendix D you will find an alternative representation of the same histograms.

state that our heuristic based on matching synthetic spot deltas allows for a fast and close approximation of the optimal hedge of a power plant with a swing contract. Recall that the complete enumeration for finding the optimal swing option parameters instead requires at least $(N \times 2L_{\max} \times I)$ revaluations of the hedge portfolio opposed to $(N \times I)$ revaluations, but the optimal result improves i.e. minimizes the risk only by not more than 4 %.

4.6. Directions for Further Research

In our first power plant model that ignored an energy threshold we introduced the idea to split a daily schedule into its operational mode (on/off sequence) and its volume profile. This idea helped us to replace the MIP for the calculation of the marginal profit by a faster matrix computation to compute the daily production schedule and marginal profit. So far, we illustrated the small error of this simplification on the option value for one runtime/off-time setting (12 and 8 hours). A further investigation with different shorter and longer runtime/off-time constraints would be necessary to underline the effectiveness in terms of the small approximation error compared to the performance improvement. The main difficulty in particular with shorter minimal run- and off-times is that the number of candidate schedules increases which will slow down the matrix calculation (recall that the matrix calculation requires the complete enumeration of schedules). For this reason we started to look into cluster analysis that would help us to associate a small subset of schedules with a representative price vector. For any new price scenario we would detect the schedule cluster with the best fitting price representation. In this way we could pick a small subset of schedules that we would use in the matrix calculation. Our first results were promising, but a complete error analysis of such a cluster approach is still an open task.

Recall that we had to modify the matrix calculation when we added an energy constraint (see section 4.4.1). The schedule profile linked to an on-off-switching sequence did not follow a simple hourly min/max capacity any longer, but required a filling logic of the individual hours. We introduced one possible implementation of this filling logic, but think that further investigations into faster algorithms is beneficial for the overall performance of the power plant valuation. In particular, we think that a separate design for short and long run-/off-times might be helpful.

The separation of a schedule in its volume profile and switching sequence also allowed us to define a small subset of schedule candidates in terms of the switching sequence only that helped us to eliminate the start operating mode from the state space. In this way we were able to set up our continuous stochastic dynamic program in section 4.4. We used our candidate schedule set L622 for the entire subsequent numerical analysis. However, in Table 4.6 we already pointed out that the candidate set should rather vary with different strikes. In other words the impact of different schedule candidate sets on the continuous real option value should be reviewed and a smarter selection (e.g. separate subsets for weekdays and weekends) will very likely improve the current results.

As we have seen in Table 4.8 our comparison of the three implementation approaches for power plants with energy constraint revealed a lack of accuracy of our stochastic optimization model. Our stochastic models with and without energy constraint should have coincided in case of no energy constraint. Instead, we had to observe a significant gap i.e. a reduced efficiency of our stochastic model with energy constraint in terms of profit compared to allocated energy. One reason is the aforementioned focus on a single set of schedule candidates. Another reason are two specific approximation errors that accumulate with every decision stage: the appropriate definition of the basis functions on one hand and the identification of the relevant energy domain on the other hand. So far we used the same quadratic approach

to describe the marginal profit function, continuation value and the overall cash flow. A separation into different sets of basis functions is advisable. For the marginal profit as a function of the daily allocated energy one could replace the quadratic by a rational function. Especially the asymptotic behavior of the profit-energy curve towards the total available energy (right end of the curve) cannot be covered well by a parabolic curve. A rational function can adjust better to variations in the curve shape. Regarding the approximated function for the continuation values recall that we used the quadratic function first with respect to the energy amount and then approximated the corresponding function parameters $\bar{c}_{d,m}$ again as a quadratic function of the current price. A combined rather than a separate approximation of the price and energy dimension might improve the accuracy. We think that the latter, in particular the quadratic approximation of $\bar{c}_{d,m}$, caused the main inaccuracy. An analysis of different basis functions should therefore also include a new sequential versus a simultaneous approximation with respect to price and energy. We recommend to reuse our factor analysis as it turned out to efficiently reduce the price dimension from 24 to a single factor. This will help to keep the number of variables small for the regression. However, we also want to point out that the success of the factor analysis could mainly be explained by the strong mean-reversion and hence clear seasonality of the prices. The analysis should therefore be reviewed with different parameter settings for the price process.

The second main approximation error of our continuous stochastic program is the difficulty of defining a common valid energy domain space $[W_d^{[y]}, \bar{W}_d^{[y]}]$ for the continuation value as it is approximated from ACFs with varying energy intervals (see discussion around equation 4.59). If the interval for the remaining energy of the continuation value is larger than most of the related individual cash flows, then the dispatch policy will tend to spend too much daily energy too early in the delivery period and vice versa for too small energy intervals. In particular this error accumulates with every stage and therefore requires special attention. The efficiency of profit compared to allocated energy decreases if the interval tends to be too large. This is the case in our implementation where the real option value with energy constraint is smaller than the option value without energy constraint in case of no energy restriction ($W_0 = \bar{W}_0$). New interval definitions should be investigated and also be tested for larger production periods. A year compared to a one month delivery will reveal the accumulation error even better and thus allow for a proper comparison.

The surprisingly good result of our heuristic is also worth a further investigation. Translating the remaining available energy into a quantile based price threshold for the exercise decision was the key for the good results. The long on and off-times of our power plant allowed to consider only three type of schedules (base hours, peak hours, no production). In a next step one should therefore stress-test the heuristic against different run- and off-times which will increase the number of potential schedule candidates and will make the link between allocated energy and price threshold more complex. It will be interesting to see if the heuristic will still return good results in particular for short operating times.

Finally, we want to review our hedge analysis. We were able to show that a swing option can hedge a power plant more effectively than a Forward or Futures hedge. So far the analysis focused on the loss function only i.e. we looked for an appropriate swing option with size N^* that will reduce the Earnings-at-Risk figure best (see equation 4.81). We could extend the analysis by including the profit as well and hence define a mean risk function similar to our investigations in chapter 2. One could also investigate a combination of a Forward and a swing option as the hedging product where the Forward covers the minimum production level of the power plant and the swing option compensates the additional generation variability. This is potentially the cheaper hedge as the Forward hedge part does not entail any cost and additionally reduces the swing size and thus the option premium.

In addition several applications of our stochastic power plant model with volume constraints should be investigated. It can be used to price options on spinning reserve energy. Large utilities are obliged to hold a daily back log of a certain energy amount that is meant to stabilize the electricity grid in case of a sudden outage. Alternatively, a power plant owner can buy an option on this reserve energy from another utility. By valuing the power plant once with a free energy allocation and then with a capped amount due to the spinning reserve provides an indication of the spinning reserve value and hence the price of an appropriate option. The power plant owner can repeat this valuation for several different spinning reserve amounts and in this way create his merit order (option prices for different reserve energy amounts) if he wants to participate in an auction. The same procedure is applicable to find the fair CO₂ prices for a specific power plant portfolio of a utility company. Governments deliberately granted less CO₂ certificates than necessary for the full production. This can be translated into an upper energy border beyond which extra CO₂ prices apply. As for the spinning reserve the real option value with and without the extra energy constraint can be computed. The valuation difference allows to derive a fair CO₂ price for the own generation asset. These kind of scenarios should be investigated in a real world business case.

A rather long-term project would extend the characteristics of our thermal power plant. A first important extension should introduce the fuel and possibly the CO₂ price. The appropriate swing option for hedging would then be a spark spread basket swing option. Its payoff function is the difference between the power price and the sum of the fuel and CO₂ price calculated at the exercise hours. The increasing complexity through additional random price processes could be handled via further dimension reduction tools other than principal component analysis. Siclari and Castellacci [17] or Weber [67] used the spark spread or basket price instead of each individual price component. Furthermore the impact of unforeseen outages on the production value should be investigated. Outages occur quite frequently and are the main source for jumps of the spot price. Power plant owners have statistics about outages which should allow for defining an appropriate stochastic process. The outage process will be imposed after a generation decision. A power plant owner registers tomorrow's generation schedule today. Then the outage suddenly occurs the next day which will impact the generation decision for the day after tomorrow. One could investigate whether there are smart dispatch policies that allow to reduce the average loss caused by sudden outages.

A. Selected Source Code

You will find the entire source code for all the models of this thesis on the enclosed CD. We separated the source code that represents a closed topic of its own into different folders. Each folder contains a readme.txt file that presents the relevant function calls in the right sequence. We also added one further folder covering the cluster analysis that we suggested as a further improvement or our MIP reformulation of the daily schedule optimization (see section 4.4.1). In this Appendix we want to focus on some key implementation aspects. Each listing is limited to those code sections that illustrate the main steps of the corresponding algorithm. We begin each listing with a brief introduction where we refer to particular code statements with the label {n} that can be found again in the corresponding listing marked with ***** n *****.

A.1. Volumetric Swing Option

The following algorithm is the implementation of the upper bound for a volumetric swing option according to see section 2.4). It consists of two large nested loops, each treating all outer price paths simultaneously. The first one iterates over every additional marginal swing right n . At the beginning of each iteration the function `forwarditerationMult` (see {1}) determines the stopping times for the entire delivery period. Two aspects are important: First, these stopping times will be calculated only once for each marginal swing right using the policy at the *initial* stage (hence, there are no recalculations for every delivery hour). Second, the total number of stopping times is always one swing right below the marginal swing currently under investigation. In this way we model the fact that $\tau_k \in \pi(n-1, t=0)$ in equation 2.30. The second loop computes the marginal martingale M for each hour. It requires the calculation of the lower bound value L at each stage h as well as the expected continuation value EL_h . The latter requires to verify whether there was an exercise at the previous stage. This check runs differently for a single versus many remaining swing rights only because of a mere technical reason. `forwarditerationMult` is not defined for a single exercise ($n=1$). So, in case of a single exercise we compute the exercise decision directly via the optimal policy at the previous hour (see {2}). In all other cases (see {3}) we can rely on the stopping times we already calculated in {1}. In case of no exercise the expected continuation value is identical to the lower bound value at the previous stage. Otherwise we need to generate new prices (`generateMR`) for the current hour starting from the price of the previous hour. We use the Bellman equation to quickly approximate the new marginal lower bound value (see {4} and equation 2.23). After we found all hourly marginal martingales we remove all exercised hours (see {5}) and compute the maximum cash difference according to equation 2.43 for each price path separately. Their average is finally the approximation of the marginal upper bound. Then we move to the next swing right.

```
function Cu = multupperbound(S,S0,alpha,K,NN,Uh,mu,sigma,kappa)
% S (N,H) N price scenarios for H hours
% S0 start price
% alpha (M+1,n+1,H) polynomial parameters for each hour and exercise right
% K strike price
% NN number of scenarios for nested loop
```

```

% Uh (1,H) number of exercises per stage
% mu mean of nested MC
% sigma sigma of nested MC
% kappa mean reversion speed of nested MC
%
% return
% Cu(M) upper bound for marginal swing right m

% initialization of variables
[...]

% Sh, Sh1: price of current/previous hour
% Yh, Yh_1, Yh_2: current continuation value with all, less than 1 and less
    than 2 swing rights
% Yh_h1, Yh_1_h1, Yh_2_h1: continuation value of previous hour

% for each swing n
for n=2:M % n = 1 stands for 0 swings
    [...]

    *** 1 ***
    % get stopping times through forward iteration at initial(!) stage
    [Cf,tau] = forwarditerationMult(S,n-1,Uh,alpha);

    % martingale for hour 1 will be calculated differently (!)
    h = 1;
    % first single exercise (m = 2)
    [...]

    % simplified lower bound calculation via continuation value
    dLh(I) = max(Sh(I),Yh);

    % then more than one exercise (m > 2)
    if (n>2)
        [...]

        % simplified lower bound calculation via continuation value
        dLh(I) = max(Sh(I) + Yh_1, Yh) - max(Sh(I) + Yh_2,Yh_1);
    end

    % in hour 1 martingale = lower bound value
    Ma(:,h) = dLh;

    % hour > 1
    for h=2:H

        % first single exercise
        [...]

        % lower bound value
        dLh(I) = max(Sh(I),Yh);
        [...]

        *** 2 ***
        % check exercise at previous stage
        [MM, II] = max([Sh1(I) Yh_h1], [], 2);

        % no exercise at previous stage
        [...]

        % exercise at previous stage => nested loop

```

```

for j = 1:length(III)
    Sht = generateMR(Sh1(I(III(j))),NN,1,1,mu,sigma,kappa);
    Yh = polyval(a,Sht); % continuation value
    dELh(I(III(j))) = mean(max(Sht,Yh));
end
[...]

% more than one exercise
for k = 3:n
    [...]

    %lower bound value
    dLh(I) = max(Sh(I) + Yh_1,Yh) - max(Sh(I) + Yh_2,Yh_1);
    [...]

    *** 3 ***
    % check exercise at previous stage
    X = tau(I,h-1) - tau(I,h);
    III = find(X == 0);

    % no exercise at previous stage
    if (length(III)>0)
        dELh(I(III)) = Yh_h1(III) - Yh_1_h1(III);
    end

    % exercise at previous stage => nested loop
    III = find(X>0);
    if (length(III) >0)
        for j = 1:length(III)
            Sht = generateMR(Sh1(I(III(j))),NN,1,1,mu,sigma,kappa);
            Yh = polyval(a,Sht); % continuation value
            Yh_1 = polyval(a_1,Sht); % continuation value
            Yh_2 = polyval(a_2,Sht); % continuation value

            *** 4 ***
            dELh(I(III(j))) = mean(max(Sht + Yh_1,Yh)- max(Sht + Yh_2, Yh_1))
                ;
        end
    end
    %%% expected continuation value (end) %%%
    [...]
end
end

% compute martingale
Ma(:,h) = Ma(:,h-1) + dLh - dELh;
end

% remove all exercised hour
D = zeros(N,H);
DD = diff(tau,1,2);
D(:,1:H-1) = tau(:,1:H-1).*DD.*(-1);

*** 5 ***
% outer loop
for i=1:N
    X = (D(i,:) == 0) ;
    I = find(X==1);
    % compute max(Z - M)
    [U(i),MM] = max(S(i,I)-Ma(i,I),[],2);
end

```

```

% average all individual results
Cu(n) = mean(U);
end

```

Listing 1: Upper bound computation for multiple exercises at the same stage

A.2. Risk adjusted Option Exercise

The following algorithm implements the valuation of an American option using a risk adjusted exercise strategy (see section 3.4.3). The main structure of the code is identical to our implementation of the regular American/swing option. The outer loop represents the backward iteration and makes use of several CompEcon library functions [52]. In addition to the regular swing option with value function `Vopt` we run a second iteration in parallel for the risk adjusted value function `V`. As emphasized in equation 3.73 we compute the quantile `Qopt` for the regular value function only (see {1}). But we penalize cash flows exceeding this quantile (see {2}) when we calculate the new risk adjusted value function according to the Bellmann equation. The quantile regression is based on a linear optimization and we rely on a library by Roger Koenker (<http://www.econ.uiuc.edu/~roger/research/>). The listing also contains our implementation of the Longstaff-Schwartz regression (sub function `lsm`) where we want to point out the important pre-selection of only in-the-money price/value function pairs (see {3}) before starting the regression via `polyfit`.

```

function V = dpborders(S,K,r,n,q,iscall)
% S price scenarios (N,H)
% K strike
% r interest rate
% n degree of polynomial used for quantile regression
% q (Lq,1) quantiles to investigate
% iscall 1 if call, else 0
%
%
% return
%
% V (N,1) value function per scenario with risk restriction

[...]
% init last Stage
[...]

% backward iteration
for h=H-1:-1:1

    Sh = S(:,h);
    Z = payoff(Sh,K,iscall);

    % Run least square approximation and quantile regression
    % for risk-adjusted AND(!) regular value function

    Copt = lsm(Vopt*exp(-r),Sh,K,1,iscall);

    *** 1 ***
    [Qopt,beta] = qreg(Vopt,Sh,n,q);
    [C,alpha] = lsm(V*exp(-r),Sh,K,1,iscall);

% loop through scenarios

```

```

for i =1:N
    % fetch associated reward function
    Zi = Z(i,:);
    f = Zi(ones(M,1),:);
    f(ID) = penalty;

    % find policy pi for no risk restriction situation
    % Bellmann equation
    [c, pi] = valmax(Copt(:,i),f,P,1);
    IND = sub2ind(size(f),(1:M)',pi);
    Vopt(:,i) = f(IND)+Vopt(TRANS(IND),i)*exp(-r);

    *** 2 ***
    % find policy for risk adjusted situation
    % do not allow exercises above quantile
    f(:,2) = f(:,2) + penalty*(f(:,2)> Qopt(i));
    % Bellmann equation
    [c, pi] = valmax(C(:,i),f,P,1);
    IND = sub2ind(size(f),(1:M)',pi);
    V(:,i) = f(IND)+V(TRANS(IND),i)*exp(-r);
end
end

function [C,alpha] = lsm(V,S,K,n,iscall)
% Longstaff-Schwartz regression
%
% V (M,N) value function of next stage and all N paths
% S (N,1) price paths for current stage
% K strike
% n max degree of polyfit function
% iscall 1 if call, 0 else
%
% return
% C (M,N) continuation values for each state and price path
% alpha (M,n+1) indices of itm prices

[...]

if(iscall == 1)
    dS = S-K*ones(N,1);
else
    dS = K*ones(N,1)-S;
end
I = find(dS>0)
[...]

*** 3 ***
% consider only itm price/value pairs
S = S(I);
CC = C(:,I)
VV = V(:,I)

% compute coefficients for cond. expectation via polyfit
for i=2:M
    Vi = VV(i,:);
    alpha(i,:) = polyfit(S,Vi,n);
    CC(i,:) = polyval(alpha(i,:),S);
end
C(:,I) = CC;

```

Listing 2: Quantile Based Option Exercise

A.3. MIP Reformulation

Our real option model in chapter 4 requires the calculation of an optimal dispatch schedule with every decision stage and state. This dispatch decision can be described as a mixed integer problem (MIP). In section 4.3.1 and 4.4.1 we replaced the MIP by a fast matrix calculation whose implementation we present in this section. The method requires a complete enumeration of all relevant schedules that we present in the first sub section. The second sub section outlines the code for the actual matrix calculation.

A.3.1. Schedule Enumeration

As we need to run as many schedule enumerations as matrix calculations we had to rely on a fast implementation. The enumeration requires several nested loops which in general have a poor performance in Matlab. For this reason we decided to implement the schedule enumeration logic in c and exposed it to matlab via the Matlab interface API. The code below ignores the interface logic and focuses on the actual enumeration. The algorithm lists all schedules for a given start state encoded by `offset0` and `offset1` which stand for the number of off- and on-hours before midnight of the previous day. `enumerateSchedules` iterates over each hour of the delivery period. It first fills the minimum number of 0 or 1 values to meet the minimum on- and off-time according to `offset0` and `offset1`. From this new start position the function loops through the hours and subsequently adds a 1 and `toff` 0 values in case the prior value was 1. Otherwise a single 0 value will be added. Then, in both cases the inner `fill` function will be called recursively (see {1}). In this way the `fill` function adds and iteratively extends a new running block in a double nested loop until all schedules are enumerated.

```
double** enumerateSchedules(int ton, int toff, int T, int *rows, int offset0,
    int offset1)
/* This function enumerates all valid schedules based on an offset of either 0
   s (offset0) or 1s
   * (offset1).
*/
{
    double **S;
    double *s;
    int t,t1,t2,i;
    int N; // number of rows in S

    /* create first row in S and s */

    S = (double **) calloc(1, sizeof(double*));
    s = (double*) calloc(T, sizeof(double));
    N = 0;

    /* first determine type and length of offset */

    if(offset0 > 0)
    {
        t1 = toff - offset0 - 1; // new position, subtract 1 since loop (*) starts with
                               t1, hence is adding another t1+1 0
        /* start recursion */

        for(t= t1; t<T;t++) //(*)
        {
            N = fill(t,T,ton, toff, &S, s, N);
        }
    }
}
```



```

    }
}
else
{
    /* init s with (ton-offset1) 1s */

    t1 = ton-offset1 -1; ///// new position , subtract 1 since loop (*) starts
        with t1

    for (t=0;t<t1;t++)
        s[t] = 1;

    for(t= t1; t<T;t++) //(*)
    {
        if(t>=0)
            s[t] = 1;

        t2 = t+toff;

        if(t2 > T-1)
            N = fill(t2,T,ton, toff,&S,s,N);
        else
        {
            for(i= t2; i<T;i++)
            {
                N = fill(i,T,ton, toff,&S,s,N);
            }
        }
    }
}

/* free memory */
free(s);
*rows = N;
return S;
}

int fill(int t0, int T, int ton, int toff, double ***S, double *s0, int rows)
/* This function will be called recursively. It copies the current vector s
and adds ton 1s. In
* a following nested loop it adds further 1s up to the end. With every
additional 1
* it adds toff 0s and adds further 0s within the inner loop. With every
additional 0 the
* function calls itself.
*
* param
*
* t0    the last filled position in s
* T    total length
* ton   getMin number of 1s
* toff  getMin number of 0s
* **S   (NxT) schedule matrix
* *s    last row in matrix
* rows  current number of rows in S
*
* return
*
* int   updated number of rows in S
*/

```

```

{
  int t,t1,t2,i;
  double *s;
  int N1; // minimum number of 1s
  int N0; // minimum number of 0s

  /*copy vector s0 */
  s = (double *) calloc(T, sizeof(double));
  for (t=0;t<T;t++)
    s[t] = s0[t];

  if (t0 < T-1)
  {
    N1 = getMin(ton-1,(T-1)-t0); // (T-1) => indexing starts with 0, (ton-1) =>
      we start loop (*) with setting another 1

    // now fill N1 1s

    for (t=t0+1;t<=t0+N1;t++)
      s[t] = 1;

    t1 = t0+N1; // new index position
    if(t1 == T-1)
    {
      /* add s to S */
      rows = rows + 1;
      *S = (double **) realloc(*S, sizeof(double*)*rows);
      (*S)[rows-1] = s;
    }
    else
    {
      for (t=t1+1;t<T;t++) // (*)
      {
        s[t] = 1; //for t=t1+1 => the last 1 of ton

        N0 = getMin(toff,(T-1)-t); // (T-1) => indexing starts with 0,

        // leave N0 0s

        t2 = t+N0; // new index position

        // now set another 0 and call fill again
        for (i=t2;i<T;i++) // (**)
        {
          *** 1 ***
          rows = fill(i,T,ton, toff,S,s,rows);
        }
      }
      free(s);
    }
  }
}
else
{
  /* add s to S */
  rows = rows + 1;
  *S = (double **) realloc(*S, sizeof(double*)*rows);
  (*S)[rows-1] = s;
}
return rows;
}

```

Listing 3: Schedule Enumeration

A.3.2. Matrix Representation

The two main ideas that allowed to translate the MIP into a matrix calculation are first the separation of a schedule into its hourly operation mode (on/off- hours) plus the actual volume profile (MW per hour) and second, that the profile itself can only take three different quantities per running hour. This is either the minimum capacity v_{\min} , the maximum capacity v_{\max} or at most one hour with a capacity in between. The latter only occurs if the entire available energy will be used and the actual amount varies with the individual observed price vector. Therefore we need to treat each price scenario separately in a loop (see `FillPerScenario`). In order to keep this loop small we try to reduce the list of all possible schedules. We do so by first computing the schedules without an energy constraint. In this case the schedules only feature two states v_{\min} and v_{\max} what we refer to as a 'bang-bang' or digital schedule (see {1}). These schedules can be computed even faster because they can be calculated for all price trajectories simultaneously without any extra loop. In case of a generation asset valuation without an energy constraint (see section 4.3.1) this fast bang-bang calculation is sufficient. With an energy constraint, though, we pick from these schedules only a subset that has an energy production below the predefined max energy and select the one with the highest cash flow. All schedules below this benchmark will be excluded (see {2}). For the remaining schedules we fill the running hours in descending price sequence with v_{\max} (see in particular {3} for the compact and very efficient implementation) and adjust the very last filling hour to the intermediate quantity L if necessary.

```

function [Copt,Eopt,Sopt] = findOptSchedule(S,Pd,Xud, vmin, vmax, emax)
% This function finds the optimal schedule based on an enumeration of all basis
% solutions.
%
% param:
%
% S:      (K,T) enumeration of all basis solution (i.e. valid schedules)
% Pd:     (T,N) price scenarios P-K
% Xud:    (K,1) start-up and shut-down costs associated with each basis solution.
% vmin   min capacity
% vmax   max capacity
% emax   max energy
%
% return:
%
% Copt   (N,1) optimal values
% Eopt   (N,1) optimal energy
% Sopt   (N,1) index of optimal schedule in schedule set

vdiff = vmax - vmin;
[T,N] = size(Pd);
[...]

% remove all schedules where sum(S,2)*vmin > emax

I = find(sum(S,2)*vmin<=emax);
[...]
S = S(I,:);
Xud = Xud(I);

K = size(S,1);

```

```

% compute best with bang-bang

Ip = Pd>0; %itm hours
Im = 1-Ip;
Vmax = Ip*vmax;
Vmin = Im*vmin;
Vminmax= Vmax+Vmin;

*** [1] ***
% matrix calculation to compute the cash flow
C = S*(Pd.*Ip)*vmax+S*(Pd.*Im)*vmin-repmat(Xud,1,N);
[Copt,Ic] = max(C,[],1);
Vopt = S(Ic,:).*Vminmax';
Eopt = sum(Vopt,2);
Sopt = S(Ic,:);

% check whether bang-bang violates emax, we are done if that is never the
% case

Ix = find(Eopt > emax);
[...]

% compute best from below for those scenarios that exceed emax as a benchmark
% for the filling algorithm

Ex = S*Vminmax(:,Ix);
Cx = C(:,Ix);
[K,M] = size(Ex);
Ib = find(Ex<=emax);
[...]
Cb = ones(K,M)*(-100000);
Cb(Ib) = Cx(Ib);
[Cbm, Ibm] = max(Cb,[],1);
Ebm = Ex(Ibm + (0:K:(M-1)*K));

% extract price scenarios that violated emax and run filling algorithm

P = Pd(:,Ix);
for i = 1:N
    [c, v] = fillerScenario(Pd(:,i),Xud,Cbm(1,i),S,vmin,vmax,vdiff,emax);
    Cf(1,i) = c;
    Ef(1,i) = sum(v,2);
    Sf(i,:) = v>0;
end

% now compare best from below with filling

n = length(Ix);
Cc = zeros(2,n);
Cc(1,:) = Cbm;
Cc(2,:) = Cf;
[...]
[C,I] = max(Cc,[],1);
Copt(Ix) = C;
[...]

function [c, v] = fillPerScenario(Pi,Xud,emax,S,vmin,vmax,vdiff,emax)

T = size(Pi,1);

```

```

v = zeros(1,T);

% get pos., neg. and cum price matrix Pn,Pp,Pc and number of pos prices Np

Pn = min(Pi,0); % only pos prices
Pp = max(Pi,0); % only neg prices
Ps = sort(Pi,1,'descend');
Pc = cumsum(Ps);
Np = sum(Pi>0);

% compute filling hours, i.e. hours that can be > vmin

H = sum(S,2); % sum of on-hours
E = emax - H*vmin; % available energy
Ef = floor(E/vdiff); % number of potential on hours
F = min(Ef,H); % in case S has a small number of running hours
Ec = ceil(E/vdiff); %max number of hours that can be filled up
F1 = min(Ec,H);
L = rem(E,vdiff); % remaining energy amount < vdiff
L = L + (Ef == Ec)*vdiff; % if ceil = floor, then L = vdiff
I = find(Ec ==0);
if (length(I) >0)
    L(I) = L(I) - vdiff; %account for emax = vmin*H
end

% identify relevant schedules

R = vmin*(S*Pp);
X = (-1)*vmin*(S*Pn);
% fill as much hours as hours with pos prices Np or valid filling hours F1
M = min(Np,F1);
M = max(M,1);
R1 = vdiff*Pc(M); % value of filling hours
Rmax = R + R1; % total value fo schedule

*** [2] ***
% extract those schedules whose value > best from below
I = find(Rmax - X - Xud > cmax);

% now filling logic for remaining schedules

if (size(I,1) > 0)

    % extract relevant schedules

    SS = S([I],:);
    XXud = Xud(I);
    LL = L(I);

    % determine new filling threshold

    [SP,Is] = sort(SS*diag(Pi),2,'descend');
    Nsp = sum(SP>0,2); % itm hours that are on-hours at the same time
    FF1 = min(F1(I),Nsp); %filling only for itm hours
    FF1 = max(FF1,1);
    FF = min(F(I),Nsp);
    % fill up to FF with vmax

    mmax = max(FF); % largest number of itm-on-hours across all schedules

    V = ~(SP==0);

```

```

V = V *vmin;

*** [3] ***
% fill all schedules with vmax according to individual itm-on-hours
for j=1:mmax
    idx = FF>0;
    V(idx,j) = (FF(idx)>0)*vmax;
    FF = FF-idx;
end

% remainder for FF1

[K,T] = size(SS);
R = [1:K]';
% in case FF1 = FF = Nsp then the filling will be wrong, but bang-bang will
    take over
IND = sub2ind(size(V),R,FF1);
% this will prevent that a non schedule hour will be filled-up
V(IND) = (LL+vmin).*(V(IND)>0);

% now compute optimum

C = sum(V.*SP,2)-XXud;
[c, ii] = max(C);
v(:,[Is(ii,:),:]) = V(ii,:);

else
    c = -1000000;
    v(1,:) = 0;
end

```

Listing 4: MIP Reformulation

A.4. Power Plant Valuation

Our power generation asset model is a direct extension of our basic swing valuation in section 2.1. The basic code structure of the dynamic program is therefore similar to Listing 2. The next two subsections present the relevant modifications for the power plant model first without and then with an additional energy constraint. The former is a discrete and the latter a continuous model.

A.4.1. No Energy Constraint - Discrete Model

Compared to the swing option code in Listing 2 the discrete real option model requires three main extensions: new state space (power plant running mode at midnight rather than remaining swing rights), new payoff function (value of optimal daily dispatch instead of standard contingent claim) and multi- vs. single dimensional price process. The operation mode is encoded via an integer between 1 and (`ton` + `toff`). The first `toff` numbers represent the amount of hours before midnight since the last shut-down. The remaining integers are the number of hours before midnight since the last start-up (see {3}). For each of these start states we enumerate all relevant schedules via `enumerateSchedules` (see Listing 3) and separate them by end state (see {4}) as we need to compute the payoff by start/end state pair for each day. Then we calculate the associated continuation values for these pairs. In order to be able to apply the Longstaff-Schwartz regression we replace the daily price vector `Sd` by the first `m` principal components `Fd` via multiplication with the rotation matrices `FLWD` and `FLWE`

for weekday and weekend prices respectively (see {1}). As m can be larger than 1 we can only rely on `polyfit` for $m = 1$. Otherwise we use the Matlab operator for a multi-dimensional regression which requires all variables and product of variables as separate columns in the input matrix X (see {2}). After the regression in `lsm` we calculate the Bellmann equation by price scenario similar to Listing 2.

```

function [V,Pi] = dprealopt(S,K,r,n,vmin,vmax,c_su,c_sd,toff,ton,DT,FLWD,FLWE,m
)
% S (N,H) N price paths for H hours
% K strike
% r one stage interest rate
% n (Ln,1) max degree of polynomials to consider in Longstaff
% vmin min capacity
% vmax max capacity
% c_su start-up cost
% c_sd shut-down cost
% toff off time
% ton on time
% DT (D,3) year month weekday
% FLWD (24,24) factor loadings weekdays
% FLWE (24,24) factor loadings weekends
% m number of factors
%
% return
%
% V (M,N) value function per scenario with risk restriction
% Pi (M,N,D) end state per start state and scenario

[...]

% backward iteration

for d=D-1:-1:1

    d
    Sd = SS(:, :, d);
    % calculate daily schedules
    Z = payoff(Sd,K,toff,ton,vmin,vmax,c_su,c_sd);

    *** 1 ***
    % apply principal components separate for peak and off-peak

    dt = DT(d,3);
    if((dt>1) & (dt<7))
        Fd = Sd*FLWD;
    else
        Fd = Sd*FLWE;
    end
    Fd = Fd(:, 1:m);

    % Run least square approximation

    C = lsm(V*exp(-r),Fd,n);

    Pid = Pi(:, :, d);
    % loop through scenarios

    for i =1:N
        % fetch associated reward function
        Zi = Z(:, i);
        Zi = reshape(Zi,M,M)';

```

```

    f = Zi;
    %f(ID) = penalty;

    % calculate Bellmann equation

    [c, pi] = valmax(C(:, i), f, P, 1);
    IND = sub2ind(size(f), (1:M)', pi);
    V(:, i) = f(IND) + V(TRANS(IND), i) * exp(-r);
    Pid(:, i) = pi;
end
Pi(:, :, d) = Pid;
end

function Z = payoff(S, K, toff, ton, vmin, vmax, c_su, c_sd)
%     S      (N,24) scenarios for a day
%     K      strike
%
% return
%
%     Z      (M*M,N) first M rows are start state 1, second M rows are start
%             state 2

M = toff + ton;
N = size(S, 1);
Z = zeros(M*M, N);
for t = 1:M
    Z((t-1)*M+1:t*M, :) = solveOptimal(vmin, vmax, ton, toff, t, S', K, c_su, c_sd);
end

function C = lsm(V, S, n)
%     V      (M,N) value function of next stage and all N paths
%     S      (N,H) price vectors for current stage
%     K      strike
%     n      max degree of polyfit function
% iscall    1 if call, 0 else
%
% return
%     C      (M,N) continuation values for each state and price path
%     I      indices of itm prices

% init dimensions
[M, N] = size(V);
C = zeros(M, N);
H = size(S, 2);

% if more than 1 independent variable
if (H > 1)
    X = zeros(N, 1 + n * H + n * nchoosek(H, 2));

    *** 2 ***
    % set up vector for linear regression x y x^2 xy y^2 ...
    m = 1;
    X(:, 1) = ones(N, 1);
    for h = 1:H
        for i = h:H
            A = S(:, i) .* S(:, h);
            for j = 1:n
                X(:, m+j) = A;
                A = A .* A;
            end
        end
    end
end

```



```

        m = m + n;
    end
end

% compute coefficients for cond expectation

    for i=1:M
        Vi = V(i,:)';
        alpha = X\Vi; % run linear regression
        C(i,:) = X*alpha;
    end
else
% for single variable run polyfit
    for i=1:M
        Vi = V(i,:)';
        alpha = polyfit(S,Vi,n);
        C(i,:) = polyval(alpha,S);
    end
end
end

function Copt = solveOptimal(vmin,vmax,ton,toff,t0,P,X,c_su,c_sd)
% vmin: min capacity per hour
% vmax: max capacity per hour
% ton: min running time
% toff: min cooling time
% t0: vector holding the relevant operating states
% P: (T,N) price scenarios
% X: strike
% c_su: start-up costs
% c_sd: shut-down costs
%
% return:
% Copt: (toff+ton,N) profit distribution for each end state

penalty = - 1000000;
N = size(P,2);
Pd = P-X;
T = size(Pd,1);

*** 3 ***
% determine operating state at the beginning of the day

if (t0>toff)
    offset1 = t0-toff;
    offset0 = 0;
else
    offset0 = t0;
    offset1 = 0;
end

SS = enumerateSchedules(ton,toff,T,offset0,offset1);

tm = max(ton,toff);
A = cast(SS(:,[T-tm+1:T]),'double');
A = fliplr(A);
N1 = sum(cumprod(A,2),2);
N0 = sum(cumprod(1-A,2),2);
Copt = zeros(ton+toff,N);

*** 4 ***

```

```

% separate schedules by end state
for t=1:(toff+ton)

    if(t<=toff)
        if(t==toff)
            I = find(N0>= toff);
        else
            I = find(N0 == t);
        end
    else
        if(t==(toff+ton))
            I = find(N1 >=ton);
        else
            I = find(N1== t-toff);
        end
    end
    [...]
    S = SS(I, :);
    [...]
    [Copt(t, :), Lopt] = findOptSchedule(S, Pd, Xud, vmin, vmax);
end
end

```

Listing 5: Discrete Stochastic Dynamic Programming

A.4.2. Energy Constraint - Continuous Model

With the introduction of an energy constraint to the power plant we decided to move towards a continuous stochastic dynamic program. The general structure of the backward iteration is similar to Listing 5. The switch to a continuous model, however, required a new variable declarations. Now, variables for the marginal profit `alpha`, the value function `V` and continuation value `C` stand for functions rather than actual values. As we use parabolic functions ($f(x) = p_0 + p_1x + p_2x^2$) only, the variables store the three polynomial parameters p_0, p_1, p_2 that describe the entire curve. There is a curve for each price scenario $i = 1, \dots, I$ separately. In addition the variables store the valid domain space of each curve as we are only interested in the positive monotonously increasing (concave) part of the curve. Thus the two variables `V` and `alpha` are of size $(I, 5)$. The In section 4.4.3 we discussed the different energy intervals in detail and we assign them to the variables as follows: $V(:, 4) = \underline{W}_d^i$, $V(:, 5) = \overline{W}_d^i$, $\alpha(:, 4) = \underline{w}_d^i$, $\alpha(:, 5) = \overline{w}_d^i$, $wmin = \underline{W}^y_{,d}$ and $wmax = \overline{W}^y$ (see {1}, {2} and {7}). The individual function parameters for `alpha`, `V` and `C` will be calculated from a grid of value/energy pairs via `polyfit`. The function `payoff` runs the regressions to gain the marginal profit functions stored in `alpha`. First, we generate the energy grid based on the schedule candidates `L` that we have chosen beforehand and are an input to `dprealoptcont` (see also Table 4.6). Then we compute the optimal dispatch for each grid point and price scenario using `solveOptimal` from Listing 4 before we fit the energy/profit pairs to a parabolic curve and save the resulting parameters in `alpha`. For the continuation value, following the Longstaff-Schwartz regression, we need to additionally regress the function parameters of `V` (i.e. $c_{0/1/2}$) over all itm price scenarios (see {6} in function `lsm`). We obtain the parameters $\alpha_{0/1/2}$ (see also equation 4.58). We use these parameters to calculate the best energy allocation `x`. First we define the interval of the total remaining energy based on the energy domain of the current marginal profit function and the energy domain of the previous value function (see {2}). For each grid point and price scenario we calculate the Bellmann equation via the first derivative ({3}) following equation 4.54. As discussed in section 4.4.3 the resulting best energy allocation $w_d^{*,r,i}$ has to fit into the valid energy domain and if not will be adjusted.

The function `computeX` performs all relevant checks (see detailed comments in the code) and adjusts $w_d^{*,i,r}$ to $\tilde{w}_d^{*,i,r}$. The auxiliary variable `W` tracks modifications of $\tilde{w}_d^{*,i,r}$ to 0 as only for non-zero energy allocations we need to compute new value functions. We apply the best non-zero energy allocation to each individual price scenario to compute the new value function by energy grid point (see {4}). Finally, we regress these new value function/energy pairs (see {5}) to obtain the new value function curve parameters `V(:,1:3)` and again restrict the individual energy domain to the concave part of the parabola (see {7}) before we start the next iteration.

```

function [V,Pi] = dprealoptcont(S,K,r,vmin,vmax,c_su,c_sd,toff,ton,DT,FLWD,FLWE
,L,dE,n)
% S (N,H) N price paths for H hours
% K strike
% r one stage interest rate
% vmin min capacity
% vmax max capacity
% c_su start-up cost
% c_sd shut-down cost
% toff off time
% ton on time
% DT (D,3) year month weekday
% FLWD (24,24) factor loadings weekdays
% FLWE (24,24) factor loadings weekends
% L (M,24) schedule candidates
% dE grid distance
% n polynomial degree for approximation of c0,c1 and c2
%
% return
%
% V (N,5) a0,a1,a2,Wmin,Wmax
% Pi (3,n,D) coefficients for c0,c1 and c2 for each day d in D (number of
coefficients dependent on polynomial degree n)

[...]

% backward iteration

for d=D-1:-1:1

    wmin = zeros(N,1);
    wmax = zeros(N,1);
    Sd = SS(:, :, d);
    [...]

    % new payoff function returns function parameters instead of actual values
    alpha = payoff(Sd,K,toff,ton,vmin,vmax,c_su,c_sd,L,dE);

    % replace price vector by first principal component (see Listing 5)
    [...]

    % Run least square approximation

    [C,Fmin,pi] = lsm(V,exp(-r),Fd,2);
    [...]

    % determine energy grid across all scenarios

    A = (alpha(:,4)>0).*(V(:,4)>0);
    I = find(A==1);

```

```

wmin(I) = min(alpha(I,4),V(I,4));
I = find(A == 0);

*** 2 ***
wmin(I) = max(alpha(I,4),V(I,4));
wmax = alpha(:,5) + V(:,5);
I = find(wmin>0);
emin = min(wmin(I));
emax = max(wmax);
M = floor((emax-emin)/dE);
U = ceil(emin/dE);
M = floor((emax-U*dE)/dE);
E = [emin (U*dE:dE:U*dE+M*dE) emax];
M = length(E);

% loop through grid points

Y = zeros(N,M); % intermediate value function by scenario and grid point
W = zeros(N,M); % current remaining energy by scenario and grid point
X = zeros(N,M); % optimal current energy allocation by scenario and grid
    point

for m=1:M

    w = E(m); % energy at grid point m
    *** 3 ***
    % compute Bellman equation via first derivative
    % W identical to w if w is valid for a specific scenario, else W = 0
    [x,W(:,m)] = computeX(alpha,w,C,Fd,Fmin,wmin,wmax);
    X(:,m) = x;

    % check validity of the computed result
    I = find(W(:,m)>0);
    for ii=1:length(I)
        i = I(ii);
        % no energy allocation
        if(x(i) == 0)
            Y(i,m) = polyval(V(i,1:3),w);
        else
            % full energy allocation
            if(x(i) == w)
                Y(i,m) = polyval(alpha(i,1:3),w);
            else
                *** 4 ***
                % regular case
                Y(i,m) = polyval(alpha(i,1:3),x(i)) + polyval(V(i,1:3),w-x(i));
            end
        end
    end
end

% calculate new value function curve
for i=1:N
    Yi = Y(i,:);
    Wi = W(i,:);
    I = find(Yi > 0);
    if(length(I) >2)
        Wi = Wi(I);
        Yi = Yi(I);
    end
    *** 5 ***
end

```

```

        V(i,1:3) = polyfit(Wi',Yi',2);
        % define energy domain per scenario
        wmin(i) = min(Wi); % start with smallest energy
        [M, II] = max(Yi); % end at maximum profit
        wmax(i) = Wi(II);
    end
end

% add new wmin and wmax
*** 7 ***
V(:,4) = wmin;
V(:,5) = wmax;
end

function alpha = payoff(S,K,toff ,ton ,vmin ,vmax ,c_su ,c_sd ,L,dE)
%      S      (N,24) scenarios for a day
%      K      strike
% toff min off-time
% ton min on-time
% vmin min capacity
% vmax max capacity
% c_su start-up cost
% c_sd shut-down cost
% L (SL,24) schedule candidates
% dE grid distance
%
% return
%
%      R      (N,5) a0, a1, a2, wmin, wmax

% set up energy grid points

N = size(S,1);
emin = ton*vmin;
emax = max(sum(L,2))*vmax;
M = floor((emax-emin)/dE);
C = ceil(emin/dE);
M = floor((emax-C*dE)/dE);
E = [emin (C*dE:dE:C*dE+M*dE) emax];
M = length(E);
Zopt = zeros(M+1,N); % account for 0 production
Eopt = zeros(M+1,N);

% compute schedule by grid point

for m=1:M
    [Zopt(m+1,:),Eopt(m+1,:)] = solveOptimal(E(m),L,vmin,vmax,ton ,toff ,S',K,
        c_su,c_sd);
end

E = Eopt;
Z = Zopt;

alpha = zeros(N,5);

% regress by grid point

for i=1:N
    X = [E(:,i) Z(:,i)];
    [U] = unique(X,'rows');

```

```

I = find(U(:,1) >0);
if(length(I) >2)
    U = U(I,:);
    a = polyfit(U(:,1),U(:,2),2);
    alpha(i,1:3) =a;
    % now get w domain
    W = (min(U(:,1)):1:max(U(:,1)))';
    Y = polyval(a,W);

    *** 1 ***
    % store Wmin, Wmax
    I = find(Y>0,1);
    alpha(i,4) = W(I);
    [M,I] = max(Y);
    alpha(i,5) = W(I);
end
end

function [C,Smin,pi] = lsm(V,r,S0,n)
% V (N,5) a0,a1,a2, wmin,wmax
% r interest
% S0 (N,1) price for current stage
% n polynomial degree to approximate c0,c1 and c2
%
% return
% C (N,3) function parameters per price scenario that describe a
% quadratic function  $V = a_0 + a_1 E + a_2 E^2$ 
% Smin all PCAs below Smin will result in C = 0
% pi (3,n+1) polynomial coefficients for c0,c1,c2

% init dimensions
[N] = size(V,1);
C = zeros(N,5);
pi = zeros(3,n+1);

% regress on parameters c0,c1,c2

F0 = S0;

% second, linear fit for a0
*** 6 ***
a0 = V(:,3);
alpha = polyfit(F0,a0,n);
pi(1,:) = alpha;
c0 = polyval(alpha,F0);
C(:,3) = c0;

% third linear fit for a1
*** 6 ***
a1 = V(:,2);
alpha = polyfit(F0,a1,n);
pi(2,:) = alpha;
c1 = polyval(alpha,F0);
C(:,2) = c1;

% third linear fit for a2
*** 6 ***
a2 = V(:,1);
alpha = polyfit(F0,a2,n);

```

```

pi(3,:) = alpha;
c2 = polyval(alpha,F0);
C(:,1) = c2;

Smin = 0;

function [x,ww] = computeX(alpha,w,C,F,Fmin,wmin,wmax)
%   alpha   (N,5)   a0, a1, a2, xmin, xmax per scenario
%   w       (N,1)   current max energy
%   C       (N,3)   c0,c1,c2 per scenario
%   F       (N,1)   current principal component
%   Fmin    (N,1)   threshold for 0 continuation values
%   wmin    (N,1)   min energy for continuation values
%   wmax    (N,1)   max energy for continuation values
%
%   return
%
%   x       (N,1)   today's optimal production
%   ww      (N,1)   w if w is valid for scenario i, 0 else

xmin = alpha(:,4);
xmax = alpha(:,5);
N = size(C,1);
x = zeros(size(C,1),1);
ww = ones(N,1)*w;           % set to 0 if w is not valid for scenario i

% first extract non zero coefficients

II = find(alpha(:,3)~=0);
xx = x(II);
aa = alpha(II,:);
CC = C(II,:);
FF = F(II);

I = find((C(:,3) == 0) & (alpha(:,3) == 0));
ww(I) = 0;

% compute x via the derivative of the Bellmann function assuming a quadratic
% equation

% first continuation value non zero
I = find(FF>=Fmin);
*** 3 ***
xx(I) = (2*CC(I,1).*w+CC(I,2)-aa(I,2))./(2*(aa(I,1)+CC(I,1)));

% second continuation value zero
I = find(FF<Fmin);
xx(I) = (-1)*aa(I,2)./(2*aa(I,1));
x(II) = xx;
xold = x;

% if w < min(wmin,xmin) then w = 0

I = find(w<min(wmin,xmin));
if (length(I) > 0)
    ww(I) = 0;
end

% if w > (wmax +xmax) then w = 0

I = find(w> wmax + xmax);

```

```

if (length(I) > 0)
    ww(I) = 0;
end

% if x < xmin then x = 0

A = (x<xmin);
I = find(A == 1);
if(length(I) >0)
    x(I) = 0;
end

% if x > min(xmax,w) then x = min(xmax,w)

W = min(xmax,w);
A = (x>W);
I = find(A == 1);
if(length(I) >0)
    x(I) = W(I);
end

% if w-x < wmin then x = 0 (if w < wmin or w > wmax) then ww = 0 as well

A = (w-x<wmin);
I = find(A == 1);
if(length(I) >0)
    x(I) = 0;
    A = ((w >wmax(I)) | (w <wmin(I)));
    II = find(A ==1);
    if(length(A) >0)
        ww(I(II)) = 0;
    end
end

% if w-x > wmax then x = ww = 0

A = (w-x>wmax);
I = find(A == 1);
if(length(I) >0)
    x(I) = 0;
    ww(I) = 0;
end

% compare xopt with x = 0 and x = w for w in [wmin,wmax] and w in [xmin,xmax]
]

I = find((w>=wmin) & (w<=wmax) & (w>=xmin) & (w<=xmax) );
for ii=1:length(I)
    i = I(ii);
    R = polyval(alpha(i,1:3),x(i))+ polyval(C(i,1:3),w-x(i));
    R0 = polyval(C(i,1:3),w);
    Rw = polyval(alpha(i,1:3),w);
    xx = [x(i) 0 w];
    [M,m] = max([R R0 Rw]);
    x(i) = xx(m);
end

% compare xopt with x = 0 where w only in [wmin,wmax] or w = 0

I = find((w>=wmin) & (w<=wmax) & ((w<xmin) | (w>xmax)));
for ii=1:length(I)

```



```
    i = I(ii);
    R = polyval(alpha(i,1:3),x(i))+ polyval(C(i,1:3),w-x(i));
    R0 = polyval(C(i,1:3),w);
    if (R0 >R)
        x(i) = 0;
    end
end

% compare xopt with x = w where w only in [xmin,xmax]

I = find((w>=xmin) & (w<=xmax) & ((w<wmin) | (w>wmax)));
for ii=1:length(I)
    i = I(ii);
    R = polyval(alpha(i,1:3),x(i))+ polyval(C(i,1:3),w-x(i));
    Rw = polyval(alpha(i,1:3),w);
    if (Rw >R)
        x(i) = w;
    end
end
```

Listing 6: Continuous Stochastic Dynamic Programming

B. Volumetric Swing Option - Further Examples

The following two tables present two more upper bound calculations for the volume constraint case in addition to Table 2.4 with the parameter settings as in section 2.5, but with drift $\mu = 0.1$ and strike $K = 1$.

n	$\underline{C}_0(n)$	$\Delta D_0(n)$	$[\underline{C}_0^{(99\%)}(n), \overline{C}_0^{(99\%)}(n)]$
1	5.300	0.007	[5.221 , 5.368]
2	10.197	0.020	[10.071 , 10.553]
3	14.753	0.103	[14.596 , 15.227]
4	19.097	0.214	[18.914 , 19.856]
5	23.319	0.192	[23.111 , 24.165]
10	42.804	0.123	[42.505 , 44.067]
15	60.595	0.154	[60.233 , 62.626]
20	77.288	0.009	[76.877 , 79.552]
30	108.400	0.035	[107.913 , 111.063]
40	137.432	0.021	[136.880 , 140.595]
50	164.875	0.062	[164.269 , 168.600]
60	191.047	0.013	[190.397 , 195.373]
70	216.176	0.066	[215.482 , 221.232]
80	240.402	0.100	[239.668 , 246.148]
90	263.903	0.122	[263.129 , 270.541]
100	286.762	0.011	[285.949 , 293.905]

Table B.1.: Swing Option with Volume Constraint ($\mu = 0.1$)

n	$\underline{C}_0(n)$	$\Delta D_0(n)$	$[\underline{C}_0^{(99\%)}(n), \overline{C}_0^{(99\%)}(n)]$
1	4.230	0.006	[4.174, 4.291]
2	8.042	0.018	[7.951, 8.073]
3	11.625	0.141	[11.513, 12.039]
4	15.016	0.193	[14.887, 15.822]
5	18.221	0.221	[18.074, 19.023]
10	32.727	0.043	[32.519, 33.934]
15	45.516	0.163	[45.266, 47.711]
20	57.214	0.054	[56.928, 59.446]
30	78.291	0.242	[77.953, 80.933]
40	97.264	0.113	[96.875, 100.377]
50	114.694	0.099	[114.262, 118.356]
60	130.873	0.023	[130.403, 135.197]
70	146.087	0.292	[145.586, 151.200]
80	160.373	0.045	[159.842, 166.055]
90	173.897	0.036	[173.339, 180.577]
100	186.773	0.193	[186.188, 194.002]

Table B.2.: Swing Option with Volume Constraint ($\mu = 0.1$, $K = 1$)

C. Price Path Samples

The following two figures show a subset of the price scenarios that we used throughout this entire thesis. Figure C.1 shows the trajectories that we used in chapter 1 and 2. They were generated with the price process and parameter settings suggested in the example by Meinshausen and Hambly [50]. See equation 2.7 for the price process definition and section 2.5 for the actual parameter settings. Figure C.2 shows sample paths of our hourly electricity spot prices that we used in our real world example for pricing power generation assets in chapter 3.

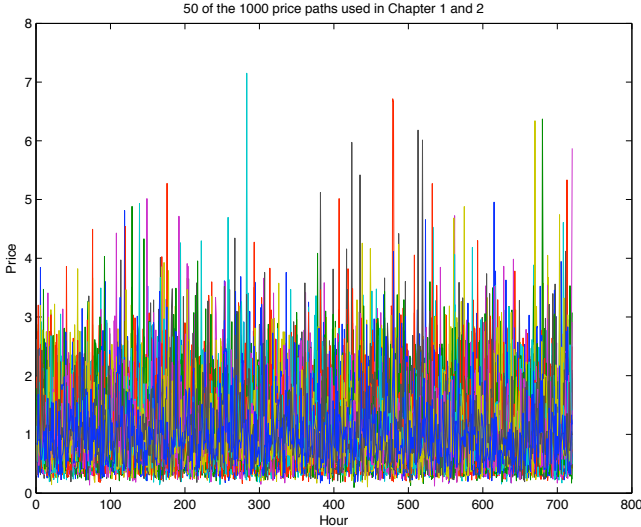


Figure C.1.: Mean reverting prices around $x_0 = 1$

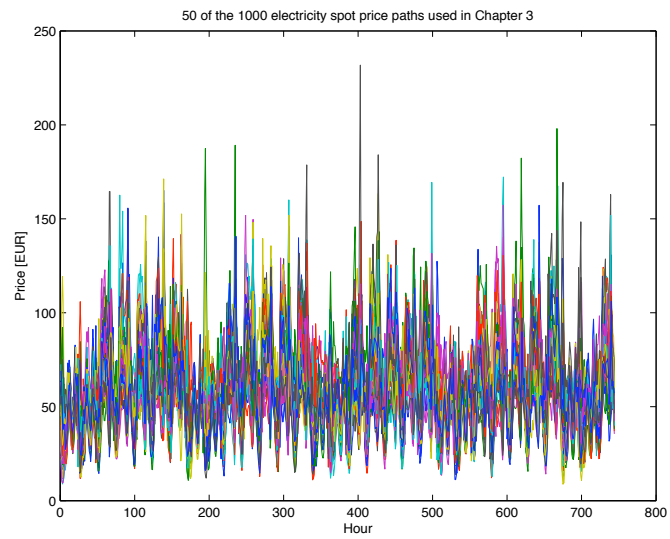


Figure C.2.: Hourly electricity prices for March 08 with weekend and weekday day types

D. Profit and Loss Distribution of Hedged Power Plant

The following graph is an alternative representation of Figure 4.25. It shows the same histograms, but plotted with identical number of buckets instead of fixed bucket borders. Hence, a higher frequency of observations does not result in taller, but more narrow bars. In this way the histograms do not overlay each other too much and simplify a direct comparison.

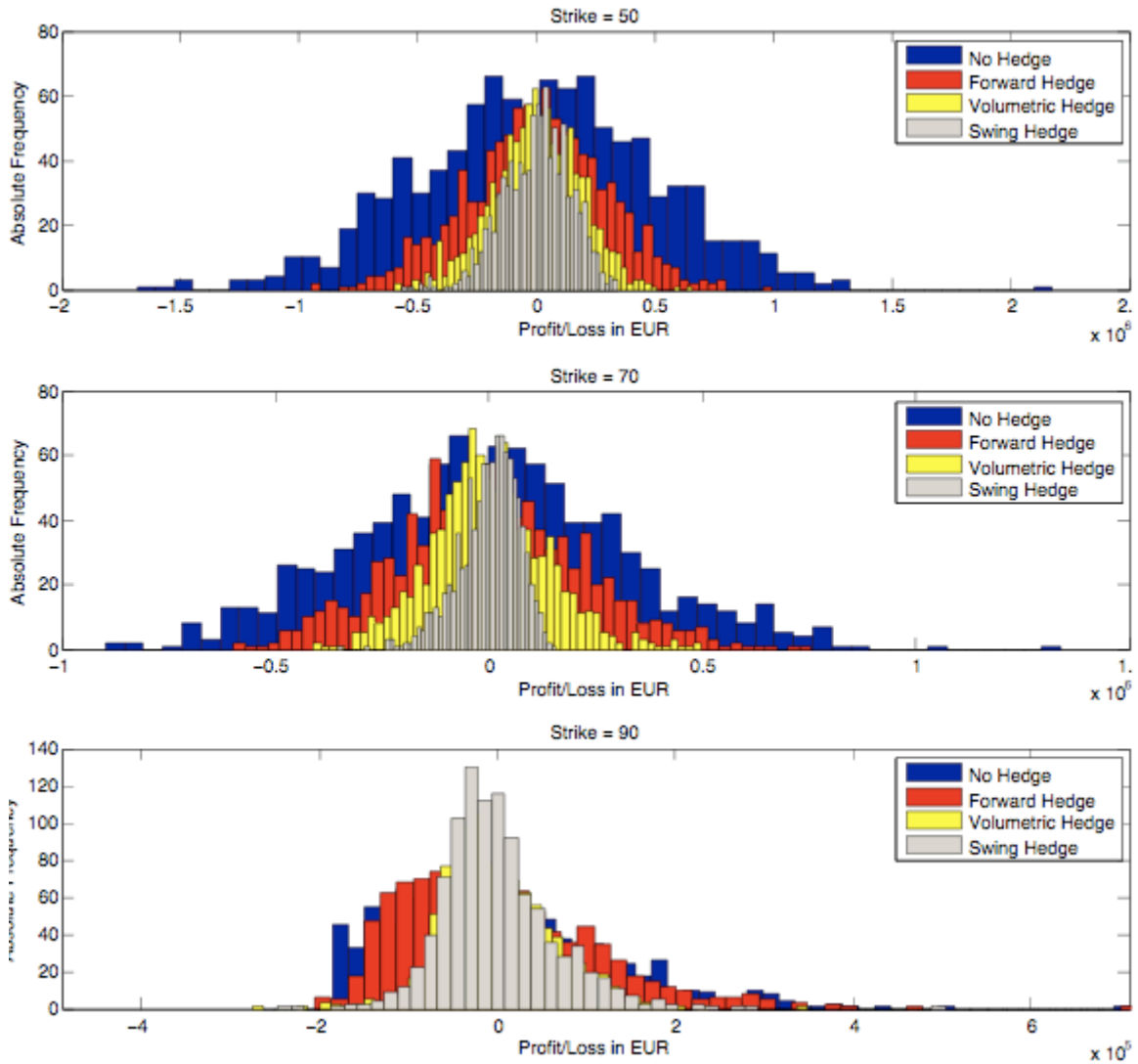


Figure D.1.: Profit and loss histogram for 70 % of total energy \overline{W}_0

Bibliography

- [1] ALEKSANDROV, N. ; HAMBLY, B. M.: *A dual approach to some multiple exercise option problems*. 2008
- [2] ANDERSEN, L ; BROADIE, M: Primal-Dual Simulation Algorithm for Pricing Multidimensional American Options. In: *Management Science* 50 (2004), Sep, Nr. 9, S. 1222–1234
- [3] ARTZNER, P. ; DELBAEN, F. ; EBER, J.-M. ; HEATH, D.: Coherent measures of risk. In: *Mathematical Finance* 9 (1999), S. 203–228
- [4] BALLY, V. ; PAGER, G. ; PRINTEMS, J.: A quantization method for pricing and hedging multi-dimensional American style options. In: *Working paper* (2002)
- [5] BARZ, G.: *Stochastic financial models for electricity derivatives*, Stanford University, Diss., 1999
- [6] BELOMESTNY, D. ; BENDER, C. ; SCHOENMAKERS, J.: *True Upper Bounds for Bermudan products via non-nested Monte-Carlo*. 2007
- [7] BELOMESTNY, D. ; MILSTEIN, G. N. ; SPOKOINY, V.: *Regression methods in pricing American and Bermudian options using consumption processes*. 2007
- [8] BENDER, C.: *A dual pricing formula for multi-exercise options under volume constraints*. 2008
- [9] BENDER, C. ; SCHOENMAKERS, J.: An iterative method for multiple stopping: convergence and stability. In: *Advanced Applied Probability* 38 (2006), S. 729–749
- [10] BENDER, C. ; WANG, X.: *Zur Bewertung mehrfach ausübbarer Optionen mittels Dualität und Monte-Carlo Simulation*. 2008
- [11] BIERBRAUER, M. ; TRÜCK, S. ; WERON, R.: Modelling Electricity Prices with Regime Switching models. In: *Lecture Notes in Computer Science* 3039 (2000)
- [12] BROADIE, M. ; CAO, M.: *Improved lower and upper bound algorithms for pricing options by simulation*. 2007
- [13] BROADIE, M. ; GLASSERMAN, P.: A stochastic mesh method for pricing high dimensional American options. In: *Journal of Computational Finance* 7 (2004), S. 35–72
- [14] BURGER, M. ; KLAR, B. ; MÜLLER, A. ; SCHINDLMAYER, G.: A Spot Market Model for Pricing Derivatives in Electricity Markets. In: *Journal of Quantitative Finance* 4 (2004), S. 109–122
- [15] CARMONA, R. ; LUDKOVSKI, M.: *Optimal Switching with Applications to Energy Tolling Agreements*. 2005
- [16] CARRIERE, J.F.: Valuation of the early-exercise price of options using simulations and nonparametric regression. In: *Insurance: Mathematics and Economics* 19 (1996), S. 19–30

- [17] CASTELLACCI, G. ; SICLARI, M. J. ; ROSS, S. ; LIAO, W.: Real Option Valuation of Power Generation Assets and Spread-Switching Options. In: *Proceedings of Forecasting Financial Markets* (2004)
- [18] CHEN, N. ; GLASSERMAN, P.: *Additive and multiplicative duals for American option pricing*. 2005
- [19] CLEWLOW, L. ; STRICKLAND, C.: *Energy Derivatives: Pricing and Risk Management*. In: *Lacima Publications* (2000)
- [20] COX, J. ; ROSS, S. ; RUBINSTEIN, M.: Option pricing: A simplified approach. In: *Financial Econom.* 7 (1979), S. 229–263
- [21] DAHLGREN, M.: A continuous time model to price commodity based swing options. In: *Review of Derivatives Research* 8 (2005), S. 27–47
- [22] DENG, S.: Stochastic Models of Energy Commodity Prices and Their Applications: Mean-Reversion with Jumps and Spikes. In: *Working Paper* 3 (2000), S. 859–867
- [23] DENG, S. J. ; XIA, Z.: *Pricing and Hedging Electricity Supply Contracts: a Case with Tolling Agreements*. 2005
- [24] EICHHORN, A. ; RÖMISCH, W.: Polyhedral risk measures in stochastic programming. In: *SIAM Journal of Optimization* 16 (2005), S. 69–95
- [25] EICHHORN, A. ; RÖMISCH, W.: *Dynamisches Risikomanagement in der Energiewirtschaft*. 2008
- [26] FÖLLMER, H. ; SCHIED, A.: Convex Measures of Risk and Trading Constraints. In: *Finance and Stochastics* 6 (2002), Apr
- [27] FORTIN, I ; FUSS, S. ; HLOUSKOVA, J. ; KHABAROV, N. ; OBERSTEINER, M. ; SZLOGAYOVA, J.: *An Integrated cVaR and Real Options Approach to Investments in the Energy Sector*. 2007
- [28] FRAUENDORFER, K. ; VINARSKI, A.: *Risk Measurement in Electricity Markets*. 2007
- [29] GLASSERMAN, P.: Smoking Adjoints: Fast Monte-Carlo Greeks. In: *Risk Magazine* (2006), Jan, S. 88–92
- [30] GLASSERMAN, P. ; YU, B.: Simulation of American options: Regression Now or Regression Later ? In: NIEDERREITER, H. (Hrsg.): *Monte Carlo and Quasi Monte Carlo Methods*. 2. Springer, 2002, S. 213–226
- [31] HALLERBACH, G.: *Discussion Paper: Decomposing Portfolio Value-at-Risk: A General Analysis*. 1999
- [32] HAMBLY, B. ; HOWISON, S. ; KLUGE, T.: *Modelling spikes and pricing swing options in electricity markets*. 2007
- [33] HAUGH, M.B. ; KOGAN, L.: Pricing American Options: A Duality Approach. In: *Operations Research* 52 (2004), March-April, Nr. 2, S. 258–270
- [34] HULL, J.C.: *Options Futures and Other Derivatives*. 6th. Prentice Hall International Editions, 2005

- [35] HUNTER, D.R. ; LANGE, K.: Quantile Regression via an MM algorithm. In: *Journal of Computational and Graphical Statistics* 9 (2000), S. 60–77
- [36] IBANEZ, A.: Valuation by simulation of contingent claims with multiple early exercise opportunities. In: *Mathematical Finance* 14(2) (2004), S. 223–248
- [37] JAILLET, P. ; RONN, E. ; TOMPAIDIS, S.: Valuation of commodity based swing options. In: *Management Science* 7 (2004), S. 909–921
- [38] JAMSHIDIAN, F.: *The duality of optimal exercise and domineering claims: A Doob-Meyer decomposition approach to the Snell envelope*. 2006
- [39] JOSHI, M. S.: A simple derivation of and improvements to Jamshidian’s and Rogers’ upper bound methods for Bermudan options. In: *Applied Mathematical Finance* 14(3) (2007), S. 197–205
- [40] KAMINSKI, Gibner Vince S. Vince Stinson: *Managing Energy Price Risk*. Risk Publications, London, 1995
- [41] KLEINDORFER, P.R.: *Multi-Period VaR-Constrained Portfolio Optimization with Applications to the Electric Power Sector*. 2004
- [42] KNITTEL, C ; ROBERTS, M: An Empirical Examination of Deregulated Electricity Prices. In: *POWER WP 087* (2001)
- [43] KOENKER, R. ; BASSETT, G.: Regression Quantiles. In: *Econometrica* 46 (1978), S. 33–50
- [44] KOENKER, R. ; MACHADO, A. F.: Goodness of Fit and Related Inference Processes for Quantile Regression. In: *Journal of the American Statistical Association* 94 (1999), Dec, S. 1296–1310
- [45] KOENKER, R. ; PARK, B.J.: An interior point method for nonlinear quantile regression. In: *J. Econometrics* 71 (1999), S. 265–283
- [46] KOLODKO, A ; SCHOENMAKERS, J.: Upper bounds for Bermudian style derivatives. In: *Monte-Carlo methods and Appl.* 10 (2004), S. 331–343
- [47] LONGSTAFF, F.A. ; SCHWARTZ, E.S.: Valuing American Options by Simulation: A Simple Least-Squares Approach. In: *The Review of Financial Studies* 14 (2001), Nr. 1, S. 113–147
- [48] LÜTHI, H.J. ; DOEGE, J.: *Convex Risk Measures for Portfolio Optimization and the Concept of Flexibility*. 2005
- [49] MARKOWITZ, H.M.: *Mean-Variance Analysis in Portfolio Choice and Capital Markets*. Blackwell, Oxford, 1987
- [50] MEINSHAUSEN, N. ; HAMBLY, B.M.: Monte Carlo methods for the valuation of multiple exercise options. In: *Mathematical Finance* 14 (2004), Oktober, Nr. 4, S. 557–583
- [51] MERTON, R. C.: Option Pricing When Underlying Stock Returns are Discontinuous. In: *Journal of Financial Economics* 3 (2001), Mar, S. 125–144
- [52] MIRANDA, M. (Hrsg.) ; FACKLER, P. (Hrsg.): *Applied Computational Economics and Finance*. MIT Press, 2002

- [53] NEUMANN, J. von ; MORGENSTERN, O.: *Theory of Games and Economic Behavior*. Princeton University Press, Princeton, 1947
- [54] PFLUG, G.Ch. ; URYASEV, S. (Hrsg.): *Some Remarks on the Value-at-Risk and the conditional Value-at-Risk*. Kluwer Academic Publishers, 2000
- [55] PORCHET, A. ; TOUZI, N. ; WARIN, X.: *Valuation of a power plant under production constraints and market incompleteness*. 2005
- [56] ROCKAFELLAR, R.T. ; URYASEV, S.: Optimization of conditional value-at-risk. In: *The Journal of Risk* 2 (2000), S. 21–41
- [57] ROGERS, L. C. G.: Monte Carlo valuation of American options. In: *Mathematical Finance* 12 (2002), S. 271–286
- [58] RÖMISCH, W. ; WEGNER SPECHT, I.: *Modellierung der Spotpreise - Literaturüberblick*. 2005
- [59] RUSZCZYNSKI, A. ; SHAPIRO, A.: *Optimization of Risk Measures*. 2005
- [60] SPRINGER, M.D. (Hrsg.): *The Algebra of Random Variables*. Wiley, New York, 1979
- [61] TOMPAIDIS, S. ; YANG, C.: *Pricing American Style Options by MC Simulation: Alternatives to Ordinary Least Square*. 2007
- [62] TSENG, C. L. ; LIN, K. Y.: A Framework Using Two-Factor Price Lattices for Generation Asset Valuation. In: *Operations Research* 55(2) (2007), S. 234–251
- [63] TSITSIKLIS, J.N. ; ROY, B. van: Regression Methods for Pricing Complex American-Style Options. In: *IEEE Transactions on Neural Networks* 12 (2001), S. 694–703
- [64] ÜBERLA.: *Faktorenanalyse*. Springer, 1971
- [65] UNGER, G.: *Hedging Strategy and Electricity Contract Engineering*, Swiss Federal Institute of Technology, Zurich, Diss., 2002
- [66] WAGNER, M.R. ; SKANTZE, P. ; ILLIC, M.: Hedging Optimization Algorithms for Deregulated Electricity Marketst. In: *Proceedings of the 12th Conference on Intelligent Systems Application to Power Systems*, 2003
- [67] WEBER, C. (Hrsg.): *Models for decision support under uncertainty in the electricity industry*. Kluwer Academic Publishers, 2004

Selbständigkeitserklärung

Neben der in der Dissertation angeführten Literatur und Zusammenarbeit mit Prof. Dr. Bender (TU Braunschweig) habe ich keine weiteren Hilfsmittel benutzt.

Ich bezeuge durch meine Unterschrift, dass meine Angaben über die bei der Abfassung meiner Dissertation benutzten Hilfsmittel, über die mir zuteil gewordene Hilfe sowie über frühere Begutachtungen meiner Dissertation in jeder Hinsicht der Wahrheit entsprechen.

Berlin, den 20.10.2010

Thomas Enge